Zebrafish (*Danio rerio*) Leukocyte Immune-Type Receptor (DrLITR) Variable Control of the Phagocytic Response

by

Rikus Rudolph Niemand

A thesis submitted in partial fulfillment of the requirements for the degree of

Master of Science

in
Physiology, Cell, and Developmental Biology

Department of Biological Sciences
University of Alberta

ABSTRACT

To combat microbial invaders, immune cells elicit a range of potent antimicrobial effector responses coordinated by complex intracellular signalling events. These events are initiated by the engagement of cell surface-expressed proteins, termed immunoregulatory receptors, that bind to and recognize foreign bodies. The transduction of extracellular events across the cell membrane by immune receptors allows for fine-tuning of immunological responses against microbes and for the resolution of tissue injury.

Leukocyte immune-type receptors (LITRs) are a polymorphic and polygenic group of immunoregulatory proteins originally discovered in channel catfish (*Ictalurus punctatus*; IpLITRs) that share structural and phylogenetic similarities with mammalian members of the immunoglobulin superfamily (IgSF). IpLITRs contain both putative stimulatory and inhibitory receptor-types that regulate innate immune cellular functions through their cytoplasmic tail (CYT) regions, inducing both classical and unique intracellular signalling networks. Previous characterization of IpLITR-types has allowed our lab to examine how immune receptors associate with adaptor signalling molecules and form homo- and heterodimers, inhibit cellular cytotoxicity through classical and non-classical inhibitory components, induce differing modes of target capture and engulfment through an inhibitory receptor-type, as well as cross-inhibiting the phagocytic response using novel CYT signalling network mechanisms.

Our lab has identified new LITR-types within the zebrafish genome (*Danio rerio*; DrLITRs) that have been shown to be ubiquitously expressed during embryogenic development and zebrafish adulthood. While some of these DrLITR-types are indicative of classical stimulatory or inhibitory receptors, DrLITR 1.2 was discovered to contain both activating and inhibitory motifs (i.e.,

immunoreceptor tyrosine-based activation motif; ITAM and immunoreceptor tyrosine-based inhibitory motif; ITIM) within the same receptor CYT. This arrangement is unusual as these motifs typically exist on separate stimulatory (i.e., ITAM-containing) or inhibitory (i.e., ITIM-containing) immunoregulatory receptors that co-engage to fine-tune cellular signalling and effector responses. My overall objective in this thesis was to examine the role both an ITAM and an ITIM play in controlling DrLITR-mediated signalling. My research aims were, i) to create DrLITR 1.2 as well as motif dysfunctional receptor constructs to generate DrLITR-expressing AD-293 cells, ii) to use these newly created construct-expressing cells to examine the phagocytic capacity of DrLITR 1.2 using a flow cytometric phagocytosis assay, and iii) to examine the novel ITIM-dependent augmentation of DrLITR 1.2-mediated phagocytosis.

My results show that engagement of DrLITR 1.2-expressing cells with phagocytic targets resulted in a robust phagocytic response dependent on the presence of a functional ITAM within the receptor CYT. In addition, I also show that the ITIM motif surprisingly enhances the overall phagocytic response of the receptor while simultaneously decreasing the receptor's ability to bind to targets. Utilizing confocal fluorescence microscopy, I show that the ITIM-associated inhibitory signalling molecule SHP-2 is localized to the bead-cell interface during the phagocytic engulfment of targets relying on the presence of a functional ITIM within the receptor CYT. Similarly, the ITAM-associated stimulatory signalling molecule Syk was also shown to be recruited to the phagocytic synapse and was dependent on a functional ITAM. Using pharmacological inhibition profiling, I also show that DrLITR 1.2 uses signalling molecules indicative of other ITAM-containing receptors and that the ITIM may play a role in protecting DrLITR 1.2 from crosstalk inhibition. Overall, the data presented in this thesis provides the first functional characterization of teleost immune receptors containing both an ITAM as well as an ITIM within the same receptor CYT. This thesis uncovers

new information of how immunoreceptor tyrosine-based motifs fine-tune immunoregulatory receptor-mediated signalling responses.

PREFACE

This thesis was the original work of Rikus Rudolph Niemand. No animals were used during the completion of this research; therefore, no ethics committee approval was required. I was responsible for data collection and analysis, as well as writing this manuscript. Dr. James Stafford contributed philosophical, conceptual, and technical guidance and edited this manuscript. I supervised three undergraduate students: Jeiel Iyawe (BIOL 298), Casey Wong (BIOL 398), and Nishi Patel (BIOL 499).

DEDICATED

Vir my Oupi

March 19th, 1944 – October 24th, 2019

“No one can take away your education from you. It is with you forever!”

Vir al die liefde en ondersteuning

Dankie

ACKNOWLEDGEMENTS

I first would like to say thank you to my supervisor Dr. James Stafford. From the undergraduate student who used a tank to describe immune cells all the way to a graduate student that understands a little bit more about phagocytosis. Thank you for inspiring me to pursue science. I don't think there is another supervisor out there as great as you. I truly am fortunate. Hopefully, so are the Oilers next season!

I would also like to thank Dr. Patrick Hanington for being on my committee and for giving me great advice and motivation to keep going with my research. To Dr. Lisa Willis for being a part of the defence. A special thanks to Dr. Aja Rieger. Not only did you help me with training and advice for experiments, but you also made the flow core feel not that far away (Except in the winter).

To all the people in the Stafford lab, past and present, you guys are some of the best people I had the pleasure of being around. Harry; thank you for trusting me with your babies. I hope I made you proud of all the work that I did. Your words still inspire me "blame everyone but yourself". Hima; thank you for helping me and forcing me to do crosswords. I still taste the Korean food! Yemaya; thank you for being my partner in crime against Dustin in the back part of the lab when I stole Hima's spot. Jacob; my LITR brother. Thank you for being a wealth of knowledge. I really did hate bleeding all those carp. Sunanda; thank you for always being so sweet and kind. Mike's class wasn't that bad. Right? Nora; for listening to me rant, enabling my Filistix addiction, and corrupting me with the spook, thank you. Hussain; I never had a younger brother, but you were the closest to one. Thank you for helping me solve issues with my assays. Kendra; thank you for being bright and cheerful even when experiments were not working. Kareem; thanks for all the advice about industry and for all the stories. I'll make you proud with all the games I'll be playing. Najia; just like how Harry passed on the AD-293 system to me, I pass it on to you. You'll do great! Dustin; thank you for taking on that undergraduate student who used agarose to make agar plates, who broke so many coverslips, and who truly admired you as a scientist and a friend.

To the friends I have made outside of my lab: Ximena, Lee, Michelle, Adam, Danyel, Mirzabek, Enezi, Farah, and Amro. You all made me laugh and thoroughly enjoy my time at the university.

To my parents and Ouma: thank you for being my number 1 fan and for supporting me all the way through school. I wouldn't have made it this far if it wasn't for you and for all the food I stole. Thank you for all the love and guidance. Baie dankie!

Thank you, Ilani, Hannah, and Lauren, for being three of the most amazing women in my life. All the love and support you have shown me have kept me going.

TABLE OF CONTENTS

CHAPTER III

MATERIALS AND METHODS

CHAPTER IV

EXAMINATION OF DRLITR-MEDIATED CONTROL OF THE PHAGOCYTIC RESPONSE

CHATER V

EXAMINING RECRUITMENT OF PSHP-2 AND STIMULATORY SIGNALLING EFFECTORS DURING DRLITR 1.2-MEDIATED PHAGOCYTOSIS

CHAPTER VI

GENERAL DISCUSSION AND FUTURE DIRECTIONS

LIST OF TABLES

LIST OF FIGURES

LIST OF ABBREVIATIONS

- aa — Amino acid
- ADCC — Antibody-dependent cellular cytotoxicity
- AF — Alexa Fluor
- Akt — AK strain transforming
- AMPs — Antimicrobial peptides
- Arp2/3 — Actin-related protein 2/3 complex
- ASB — Antibody staining buffer
- BCR — B cell receptor
- BLAST — Basic local alignment search tool
- BSA — Bovine serum albumin
- C3 — Complement component
- CBP — CREB binding protein
- Cbp — Csk binding proteins
- CD — Cluster of differentiation
- Cdc42 — Cell division control protein 42
- cDNA — Complementary DNA
- CEACAM — Carcinoembryonic antigen-related cell adhesion molecules
- CR — Complement receptors
- CREB — Cyclic-AMP response element binding protein
- CSB — Cell staining buffer
- Csk — C-terminal Src kinases
- CTLs — Cytotoxic T cells
- CYT — Cytoplasmic tail
- D — Domains
- DAG — Diacylglycerol
- DAMPs — Danger-associated molecular patterns
- DAP — DNAX-activation protein
- DISC — Death-inducing signalling complex

- DMEM Dulbecco's modified eagle media
- DMSO Dimethyl sulfoxide
- DPBS Dulbecco's phosphate-buffered saline
- dpf Days post fertilization
- DrLITR *Danio rerio* leukocyte immune-type receptor
- dsRNA Double-stranded RNA
- EAT-2 EWS/FLI1 activated transcript 2
- EDTA Ethylenediaminetetraacetic acid
- EGFR Epidermal growth factor receptor
- ERK Extracellular signal-regulated kinase
- EST Expressed sequence tag
- ETC Electron transport chain
- F Phenylalanine
- FACS Fluorescence-activated cell sorting
- F-actin Filamentous actin
- FBS Fetal bovine serum
- Fc Fragment crystallizable
- FcR Fragment crystallizable receptor
- FCRL FcR-like
- FSC Forward scatter
- Fwd Forward
- Fyn Src/Yes-related novel oncogene homolog
- G418 Geneticin
- Gab2 Grb2-associated binders
- Grb2 Growth factor receptor-bound 2
- H+L Heavy and light chain
- HA Hemagglutinin
- HD High dose
- HEK Human embryonic kidney
- hpf Hours post fertilization

- HSPs Heat-shock proteins
- Ig Immunoglobulin
- IgSF Immunoglobulin superfamily
- iITAM Inhibitory ITAM
- IL Interleukin
- IP Immunoprecipitation
- IP3 1,4,5-trisphosphate
- IpLITR Ictalurus punctatus leukocyte immune-type receptor
- IRF Interferon regulatory factors
- IRGs Immunity-related GTPases
- ITAM Immunoreceptor tyrosine-based activation motif
- ITIM Immunoreceptor tyrosine-based inhibitory motif
- ITSM Immunoreceptor tyrosine-based switch motif
- JAK Janus kinase
- JNKs C-Jun N-terminal kinases
- KIR Killer cell immunoglobulin-like receptors
- ko Knockout
- LD Low dose
- LFA-1 Lymphocyte function-associated antigen 1
- LILRs Leukocyte Ig-like receptors
- LITRs Leukocyte immune-type receptors
- LPB LPS binding protein
- LPS Lipopolysaccharides
- LRC Leukocyte receptor complex
- LSM Laser scanning confocal microscope
- Lyn Lck/Yes-related novel protein tyrosine kinase
- mAb Monoclonal antibodies
- MAC Membrane attack complex
- MAF Mean area of fluorescence
- MAPK Mitogen-activated protein kinases

- MBSU Molecular Biology Service Unit
- MD-2 Myeloid differentiation factor 2
- MEK Mitogen-activated protein kinase kinase
- MFI Mean fluorescent intensities
- MHC Major histocompatibility complex
- MPO Myeloperoxidase
- MYD88 Myeloid differentiation primary response 88
- Nck Non-catalytic region of tyrosine kinase
- NETs Neutrophil extracellular traps
- NF Non-fluorescent
- NF-κB Nuclear factor kappa B
- NITRs Novel immune-type receptors
- NK Natural killer
- pAb Polyclonal antibodies
- PAG Phosphoprotein associated with glycosphingolipid-enriched microdomains 1
- PAMPs Pathogen-associated molecular patterns
- PBLs Peripheral blood leukocytes
- PBS Phosphate-buffered saline
- PCR Polymerase chain reaction
- PD-1 Programmed death 1
- PDK Pyruvate dehydrogenase kinase
- PE Phycoerythrin
- PEACAM-1 Platelet endothelial cell adhesion molecule-1
- PFA Paraformaldehyde
- PH Pleckstrin homology
- PI(3,4,5)P2 Phosphatidylinositol 4,5-trisphosphate
- PI(4,5)P2 Phosphatidylinositol 4,5-bisphosphate
- PI3K Phosphoinositide 3-kinase
- pIgR Polymeric immunoglobulin receptor

- PKB Protein kinase B
- PKC Protein kinase C
- PLCγ Phospholipase C gamma 1
- PRRs Pattern recognition receptors
- PSGs Pregnancy-specific glycoproteins
- pSHP-2 Phosphorylated SHP-2
- PSI Position specific iterative
- pSyk Phosphorylated Syk
- pY Phosphotyrosine
- Rac Ras-related C3 botulinum toxin substrate
- RBL Rat basophilic leukemia
- ROS Reactive oxygen species
- RSK Ribosomal S6 kinase
- RTK Receptor tyrosine kinase
- RT-PCR Reverse transcriptase PCR
- Rvs Reverse
- SFK Src-family kinases
- SH2 Src-homology 2
- SH2D1A SH2 domain protein 1A
- SH3 Src-homology 3
- SHIP SH2-containing inositol 5'-phosphatase
- SHP SH2-containing protein tyrosine phosphatase
- SIgA Secretory IgA
- SIGLEC Sialic acid-binding immunoglobulin-type lectins
- SLAM Signalling lymphocytic activation molecule
- Sos Son of Sevenless
- Src Sarcoma viral oncogene homolog
- SSC Side scatter
- STAT JAK-signal transducer and activator of transcription
- Syk Spleen tyrosine kinase

- TCR T cell receptor
- TGF-β Transforming growth factor β
- TLRs Toll-like receptors
- TM Transmembrane
- TNF-α Tumor necrosis factor-α
- WAVE WASp family verprolin-homologous protein
- Wpf Weeks post fertilization
- wt Wild-type
- Y Tyrosine
- YG Yellow-green

CHAPTER I

INTRODUCTION

1.1 Overview

Innate immunity serves as a crucial first line of defence against the early stages of microbial invasion. Various innate immune cells spearhead the innate immune response by rapidly recognizing pathogen-associated molecular patterns (PAMPs) presented during infections. After binding these microbial-specific molecules using germline-encoded innate immunoregulatory receptors, immune cells are rapidly activated to execute potent effector responses (e.g., phagocytosis, degranulation, cytokine production, etc.) based on the immune cell type as well as the specific receptors that are bound (1). Recognition and binding of ligands by receptors results in the transduction of signals via intracellular recruitment and activation of various adaptor and effector molecules, which is mediated via signalling motifs contained within the cytoplasmic tail (CYT) regions of these receptors. Subsequently, signalling molecules are recruited, and a wide array of signalling networks and cascades are triggered that activate and regulate innate immune cellular effector responses. Previous characterization of immune receptors as either stimulatory or inhibitory was based on the presence of specific motifs within the receptor cytoplasmic tails. Specifically, receptors that contained an immunoreceptor tyrosine-based activation motif (ITAM) were characterized as stimulatory, while immunoreceptor tyrosine-based inhibitory motif (ITIM) containing receptors were deemed inhibitory (2).

However, there is growing evidence, including that presented in this thesis, to suggest that ITAMs are able to induce inhibition while ITIMs are able stimulate signalling, in stark contrast to what these motifs were classically described to facilitate.

Mechanisms of receptor-mediated control of innate immune cell effector responses are well-studied in mammals but less so in other animals. Fish, amphibians, birds, and many invertebrate models have all been identified to contain evolutionary conserved innate immune receptor-types and intracellular signalling molecules critical for the detection and destruction of pathogens (1,3,4). Our lab has extensively studied the leukocyte immune-type receptor (LITR) family, initially discovered in channel catfish (*Ictalurus punctatus*), as a teleost immune receptor model system for understanding the regulation and control of innate immune effector responses (5). This highly polymorphic and polygenic family shares phylogenetic similarities with various mammalian immune receptor-types including Fragment crystallizable receptors (FcRs), FcR-like (FCRLs), and immune proteins encoded in the leukocyte receptor complex (LRC) (5,6). Examination of LITRs by utilizing a heterologous expression system, whereby immune receptor-types are transfected onto the surface of cell lines, has allowed our lab to make observations on how immune receptor-types are able to regulate cellular signalling as well as innate immune effector responses. For example, the examination of the ITAM-containing receptor IpLITR 2.6b within a mammalian myeloid cell line (RBL-2H3) allowed for observations on how this receptor-type is able to recruit signalling adaptor proteins and form receptor hetero- and homodimers (7) while also inducing phagocytosis (8–11), degranulation (8) and cytokine release (12). In addition, our lab has also documented how the ITIM-containing putative inhibitory receptor IpLITR 1.1b was able to inhibit natural killer (NK)-like cell cytotoxicity both independent and dependent on the recruitment of Src-homology 2 (SH2)-containing protein

tyrosine phosphatase (SHP)-1 to the receptor ITIMs (13). Co-expression of the inhibitory receptor IpLITR 1.1b into the same non-immune cell line (AD-293) as the stimulatory receptor IpLITR 2.6b displayed IpLITR 1.1b-mediated crosstalk inhibition of cell activity by dampening the phosphorylation of signalling molecules (14). In addition, it was also observed that both the CYT proximal and distal regions of IpLITR 1.1b contributed to the recruitment of C-terminal kinase (Csk) and SHP-2, respectively, for the sustained, coordinated inhibition of cellular signalling and effector responses. In contrast to the inhibitory functions observed for this ITIM-containing receptor, when IpLITR 1.1b was transfected into a myeloid cell line (RBL-2H3), it was observed that this receptor-regulated the formation of filopodia-like protrusion form the cell membrane that helped facilitate an ITAM-independent mode of target phagocytosis, demonstrating the first characterization of functional plasticity of a teleost ITIM-containing receptor (9–12).

Recently, our lab has discovered several new teleost LITR-types within the zebrafish (*Danio rerio*) genome (15). While some of these receptor-types were reminiscent of classical putative inhibitory and stimulatory receptors, a certain subset contained non-classical arrangements of signalling motifs within their CYT region. Specifically, DrLITR 1.2 contains an unusual ITAM and ITIM combination within the same receptor tail. The presence of two bonafide classically opposing signalling motifs within the same receptor suggests that the combination of both motifs influences the signalling capabilities of the receptor. Specifically, the presence of the ITAM within the receptor suggests that possible stimulatory-associated molecules are recruited to the ITAM to induce stimulatory signalling and cellular effector responses reminiscent of other ITAM-containing receptor types (e.g., Dectin-1, CR3, and FcγR) (16,17). However, the ITIM within the same receptor CYT may also recruit inhibitory associated

signalling molecules to the ITIM, dampening the overall level of signalling, therefore inducing a weaker cellular effector response, important in the prevention of overstimulation and autoimmune diseases (18,19). Thus it was initially hypothesized that inducing DrLITR 1.2 with phagocytic targets would result in an intermediate level of target engulfment compared to ITIM-knockout mutants. To further understand the significance of receptors containing these two contrasting motifs, my thesis work focused on examining receptor-mediated signalling regulation during the induction of the phagocytic response.

1.2 Objectives

The main objective of this thesis was to examine the signalling capabilities of newly discovered DrLITR-types with a focus on understanding the purpose of tandem ITAM and ITIM motifs within the DrLITR CYT regions. The specific aims of my research were: i) generate wild-type DrLITR constructs as well as motif dysfunctional mutants for the creation of DrLITR-expressing AD-293 cell lines, ii) utilize newly created DrLITR-expressing cells to examine their phagocytic phenotype in a flow cytometric phagocytosis assay, and iii) characterize the novel ITIM-dependent augmentation of DrLITR 1.2-mediated phagocytic response.

1.3 Outline

Chapter II is an overview of literature relevant to the topics covered in this thesis. In this chapter, I initially provide information regarding the immune system with a focus on innate immunity. I then review immunoregulatory receptors in teleost fish and focus on studies characterizing IpLITRs. To conclude, I then switched my focus to zebrafish as an immune model, including information on recently discovered DrLITRs. Chapter III is a detailed

description of the research techniques, reagents, and methodologies used to complete the research described in this thesis. In chapter IV, I used a heterologous expression system as well as a flow cytometric phagocytosis assays to test the hypothesis that the ITIM motif dampens the signalling capabilities of the ITAM-containing receptor DrLITR 1.2. My results showed that not only does DrLITR 1.2 induce a potent ITAM-dependent mode of phagocytosis, but the ITIM motif enhances the overall phagocytic capacity of the teleost receptor. Chapter V uses fluorescence confocal microscopy as well as pharmacological profiling to establish the important signalling components used during DrLITR 1.2-mediated phagocytosis. My results support the hypothesis that components classically coupled with stimulatory (i.e., Src-family kinases (SFK), Spleen tyrosine kinase (Syk), phosphoinositide 3-kinase (PI3K), filamentous actin (F-actin) polymerization) and inhibitory (i.e., SHP-2) receptors are associated with DrLITR 1.2 during induction of the phagocytic response. I propose possible phosphatase-independent and phosphatase-dependent models for how SHP-2 may mechanistically enhance the signalling capabilities of DrLITR 1.2. In conclusion, chapter VI summarizes all the research findings in this thesis on how DrLITRs may expand our knowledge on immunoregulatory control of cellular effector responses, as well as future directions for this project. Chapter VII includes a bibliography of all the references used in this thesis.

Chapter II

Literature Review

2.1 Introduction to Innate Immunity

The immune system is a complex network of defence mechanisms aimed at protecting the body from microbes and helping maintain tissue homeostasis. There are two main branches of the immune system; innate immunity is composed of the intrinsic physical, cellular, and humoral components that recognize conserved features of pathogens to rapidly (within minutes to hours) activate innate immune cells and proteins for the destruction of invaders (4,20). In contrast, adaptive immunity provides long-lasting defence that organisms develop after initial pathogen infection. Adaptive immune cells (T and B cells) respond to initial invaders slower than cells of the innate immune system (1-2 weeks). However, the adaptive immune system executes rapid antimicrobial responses against secondary infections of previously encountered pathogens (20). Memory B-cells become activated upon stimulation of antigen previously encountered by their naïve progenitor, resulting in proliferation and differentiation into plasma B cells where they begin to secrete immunoglobulin (Ig) proteins (i.e., antibodies) (21). Antibodies contain a variable region that recognizes and binds to specific antigens, such as those on the surface of pathogens, while also containing a fragment crystallizable (Fc) region recognized by immune cells through receptors on their surface (22).

While adaptive immunity mounts an effective long-term immune defence against recurring infections, innate immunity serves as a crucial first line of defence against the early stages of microbial invasion while also playing a role in the activation of the adaptive arm of

immunity (23). Physical barriers such as skin and mucosal membranes block microbial invasion, while humoral and cellular components are activated upon encountering microbes that have entered the body, which engage microbial threats once the physical barriers are breached. In mammals, innate immunity and its cellular effectors (i.e., macrophages, natural killer (NK) cells, neutrophils) have been thoroughly studied and accepted to be evolutionarily conserved amongst vertebrates (24). Innate immune cells trigger potent antimicrobial responses following recognition of pathogen-associated molecular patterns (PAMPs) through germline-encoded pattern recognition receptors (PRRs), resulting in cellular activation leading to phagocytosis, degranulation, and cytokine secretion that are initiated based on the type of ligand bound and the associated immune cell(s) involved. As an example, PAMPs presented during infection with bacteria, viruses, and fungi, can be recognized by a series of PRRs called toll-like receptors (TLRs). These highly conserved immune proteins, originally discovered in *Drosophila melanogaster*, have homologues expressed in a wide range of organisms including *C. elegans*, lamprey, chickens and humans (25,26).

Ligands that induce receptor-based signalling are not always sourced directly from the invading pathogens; compartmentally segregated ligands from the host, upon cellular damage and/or cell death, can become available for the binding and induction of a specific subset of PRRs on immune cells such as macrophages (27). Endogenous danger-associated molecular patterns (DAMPS) from damaged, dead, or stressed cells can come from a verity of sources and include molecules such as heat-shock proteins (HSPs), histones, and S100 proteins, to name a few (28). DAMPS, in a similar fashion to PAMPS, can activate immune cells such as neutrophils, macrophages, and dendritic cells, resulting in the production of cytokines and chemokines, which further elicit the recruitment and activation of immune cells.

To better protect host organisms from pathogens, all innate immune cells (i.e., macrophages, neutrophils, dendritic cells, NK cells, mast cells) have been found to express immune receptors, such as TLR-types, both intracellularly and extracellularly. Endothelial cells in blood vessels and mucosal epithelial cells also express TLRs, leading to the understanding of the importance of these immune receptors in clearing infection and inducing pro-inflammatory responses in infected organisms (29,30). Their ability to serve as vital innate sensing receptors is in part due to their unique abilities to sense and activate due to ligands associated with the presence of invading pathogens. For example, TLR3 is an endosomal receptor that specifically binds to double-stranded RNA (dsRNA), a molecule associated with viruses and viral infection (25). Upon binding of dsRNA, TLR3 induces downstream activation of the transcription factor interferon regulatory factor (IRF)-3, and by extension, the poly-peptide type I interferons, which causes antimicrobial defence against viral infection (31,32). In addition to being one of the first discovered TLRs in humans, TLR4 is a plasma membrane-bound receptor that is well known to recognize and bind to lipopolysaccharides (LPS) found on the outer membrane of Gram-negative bacteria (25,33). TLR4-LPS binding and activation occur through complex formation with a series of proteins. The soluble protein MD-2 directly associates with TLR4 and is suggested to be in direct contact with LPS as MD-2 can complex with LPS in the absence of TLR4 (34,35). LPS binding protein (LPB) associates directly with LPS and facilitates interactions between LPS and the glycosylphosphatidylinositol-anchored protein CD14 (35). From there, CD14 can directly transfer LPS to TLR4/MD-2 and mitigates recognition and activation. LPS binding then leads to the induction of the MYD88 pathway, and NF- κB promoted transcription of proinflammatory cytokines (34,35). These immune proteins have been quintessential to the

survival of many organisms and highlight the importance of receptor-based recognition of insults for their rapid and efficient elimination.

One of the first physical barriers that pathogens must breach during infection is the skin. A series of stratified layers consisting of tightly packed epithelial cells connected by tight junctions form both the dermis and epidermis, whose primary role is to separate the internal and external environments, a feature shared by many vertebrates with specific changes arising from the adaption of organisms to their respective habitat (36,37). While the overall composition can differ, all vertebrates secrete a form of lubricant to help maintain the overall integrity of the external layers. In fish and amphibians, this layer takes the form of a mucosal membrane composed of glycoproteins and monosaccharides, while terrestrial animals secrete a lipid and glycolipid-based fluid (24,38). This does not imply that terrestrial organisms do not contain a mucosal barrier themselves. This vital feature conserved amongst vertebrates prevents the invasion of both ingested and air-borne pathogens from accessing entryways into the host (mouth, nasopharyngeal cavity, stomach, gills, etc.). A closer inspection of mucus reveals a wide range of characteristics that aid defences, such as antimicrobial peptides (AMPs), hydrolytic enzymes, and overall low pH (39,40). An example of AMPs is lysozyme (muramidase or N-acetylmuramichydrolase), a small secretory enzyme well characterized for its antimicrobial properties (41). This small protein is associated with a wide range of organisms, including fish, amphibians, birds, and reptiles and has also been found in a wide array of rat, mouse, and human tissues; secreted by macrophages, epithelial cells, and glandular cells. This enzyme is best known for its activity against Gram-positive bacteria, hydrolyzing the links between peptidoglycan structural units resulting in bacterial lysis (41,42).

While physical barriers in innate immunity are essential for preventing many infections, internal factors also play important roles in mitigating microbial invaders. Humoral factors make up a large section of innate immunity as soluble plasma components, helping remove apoptotic cells, pathogens and debris (43) while also acting as a bridge between the innate and adaptive arms of immunity (44). Originally named for its ability to "complement" antibodies' antimicrobial properties, the complement system is a serum and membrane-based series of proteins which help opsonize, regulate, and induce inflammatory and lytic responses against potentially pathogenic organisms (45). Complement pathways have been well studied in mammal models; however, complement activation and opsonization have been previously characterized in teleost fish such as catfish (*Ictalurus punctatus*) (3). There are three main pathways for the complement system that has been well described in mammals. In the classical pathway, complement serine protease complexes associate with antibodies (IgG1 and IgM) that are opsonized on the surface of pathogens (24,45). Through a cascade of complement cleavages, complement protein C3 is cleaved into C3b (an opsonin) and C3a, a convergence point for all three complement pathways. C3b acts to identify the opsonized target with a molecular "tag," leading to further complement cascading and assembly of a membrane-penetrating macromolecular pore (membrane attack complex; MAC), lysing the targeted pathogen. In the lectin pathway, an immunoglobulin-independent approach is used. PRRs such as mannose-binding lectin binds to and recognize carbohydrates on the surfaces of bacteria, fungi, and viruses. PRRs can then complex with serine proteases and, in a similar fashion to the classical pathway, induce complement cleavage to ultimately converge onto the induction of C3 cleavage. The proposed alternative pathway is unique in that it is initiated by the spontaneous hydrolysis of natural serum C3 into an analogue C3(H20) (45). This form binds to and cleaves other factors

resulting in the formation of an alternative convertase which cleaves C3 into C3a and C3b. C3b in this pathway can bind to serum factors and be activated into the alternative convertase form, thereby amplifying the pathway. As a result, there are a multitude of inhibitory proteins that restrict this pathway to specific contexts in order to prevent continuous complement activation in healthy organisms (46).

In this literature review, I will talk about essential aspects of innate immunology regarding both mammals and teleost fish to add important background information for my research. My focus will be on the aspects of immunoregulation of effector responses in the context of immune receptors, their functions, and the nuances of signalling dynamics. I will follow this by talking about the knowledge our lab has obtained on the immune receptor family leukocyte immune-type receptors (LITRs) on immune signalling dynamics, originally discovered in channel catfish (*Ictalurus punctatus*). To conclude, I will talk about the discovery of LITR-types in zebrafish (*Danio rerio*), the focus of my research, and their potential as a new immunoregulatory model.

2.2 Immunoregulation

In immunity, the myeloid cell lineage consists mostly of the cells from the innate immune system, including granulocytes, macrophages, monocytes, and dendritic cells (4,24). Lymphoid progenitors differentiate into cells that make up the adaptive immune system, including T and B cells and their subsets. While natural killer (NK) cells originate from the lymphoid lineage, they are classically considered as innate immune cells due to their cytokine secretion and cytotoxic functions. Regardless of origin, immune cells from both lineages contain repertoires of cell immunoregulatory receptor-types that allow cells to translate extracellular cues (i.e., ligand

binding) into intracellular signalling events controlling immune cell effector responses (47). Immunoregulatory receptors are often expressed on the plasma membrane, where they transduce extracellular signals across the cell membrane for the cell to perceive the environment around them. In general, membrane-bound immune receptors contain an extracellular region that recognizes and binds to specific ligands outside of the cell and a hydrophobic amino acid (aa)-rich transmembrane region that anchors the protein within the lipid bilayer (48). Intracellularly, immune receptors contain a cytoplasmic tail (CYT) region where various signalling molecules are recruited, typically through tyrosine-based binding events during receptor engagement, resulting in complex signalling molecule cascades that activate and regulate innate immune cellular effector responses such as degranulation, cytokine secretion, phagocytosis, cell-mediated cytotoxicity, and other various antimicrobial functions (49).

2.2.1 Tyrosine-Based Stimulatory and Inhibitory Receptors in Mammals

Recognition and binding of ligands by immunoregulatory receptors results in receptor cross-linking and the transduction of signals via intracellular recruitment and activation of various adaptors and effectors, which is mediated via signalling motifs contained with the cytoplasmic tail (CYT) regions of these proteins. Here, various signalling molecules are recruited, and a wide array of signalling networks and cascades are triggered that activate and regulate innate immune cellular effector response (49). The structures and amino acid-based motif arrangements of the CYT directly influence the types of signalling molecules recruited following receptor activation and, therefore, the kinds of effector immune responses that are produced. Classically, short-tailed immune receptors are putatively stimulatory, inducing effector responses via charged residues within their transmembrane domains that couple with oppositely charged adaptor proteins (e.g., FcRγ and DAP12) (2,50). These adaptors contain

immunoreceptor tyrosine-based activation motifs (ITAM; amino acid sequence: [D/E]xxYxx[L/I]$x_{(6–8)}$Yxx[L/I]) that, upon receptor engagement, are phosphorylated by Src-family kinases (SFK; i.e., Lyn and Fyn) at tyrosine residues located within the ITAM (51). Src-homology 2 (SH2) containing kinases, such as spleen tyrosine kinase (Syk), are then brought into proximity of sites of receptor engagement via their SH2 domain binding to phosphorylated ITAMs. This in turn, allows for Syk to be autophosphorylated and activated, which further leads to the activation of signalling molecules. Proteins such as phospholipase C gamma 1 (PLCγ) can convert phosphatidylinositol 4,5-bisphosphate ($PI(4,5)P_2$) into 1,4,5-trisphosphate (IP3), which initiate calcium mobilization, and diacylglycerol (DAG) for the activation of mitogen-activated protein kinases (MAPK) (52). While the process leads to two separate molecular pathways, both play roles in the activation of cell-mediated responses, such as cytokine production and degranulation. Another molecule that can be involved in ITAM-dependent receptor signalling is phosphoinositide 3-kinase (PI3K). PI3K can phosphorylate ($PI(4,5)P_2$) into ($PI(3,4,5)P_2$), allowing for an anchor point for other signalling molecules containing the pleckstrin homology (PH) domain such as PLCγ and protein kinase B (PKB/Akt), to be localized to the site of receptor engagement (53). Multiple different (and simultaneous) outcomes can result from the specific signalling pathways induced through the engagement of immune receptors. Examples include proinflammatory gene expression, antimicrobial enzyme activation, cytokine secretion, and the activation of the Arp2/3 complex that plays a role in F-actin polymerization and membrane remodelling required for target engulfment via a process called phagocytosis (54).

A group of receptors that contain members with ITAMs in their CYT are known as Fc receptors (FcRs) and are well known for their ability to bind to the Fc region of antibodies to induce proinflammatory responses (19). Members of the immunoglobulin superfamily (IgSF),

this group of receptors are expressed by a wide range of immune cells from both the myeloid and lymphoid lineages (48). Macrophages use FcRs to induce phagocytosis of opsonized targets, while NK cells have been shown to induce antibody-dependent cellular cytotoxicity (ADCC) through the engagement of stimulatory FcγR (i.e., FcγRIII) receptors with opsonized targets such as infected cells expressing viral proteins on their surface (55). In general, FcR receptors are named after the type of antibody that they bind to. The high-affinity IgE receptor, FcεRI, is found on the surface of mast cells and basophils. IgE is primarily localized in the tissue, unlike other isotypes, and is associated with regulating type I hypersensitivity reactions (56). IgA is expressed in a dimeric and monomeric form and is well known for its role in mucosal immune surveillance. While found at low concentrations within serum, IgA is primarily found within mucosal secretions from the gastrointestinal (GI) tract, tears, sweat, and saliva (57). Within the blood, IgA has been known to associate with FcαRI/CD89 on the surface of immune cells to elicit proinflammatory responses such as macrophage phagocytosis, and degranulation of basophils and eosinophils. Alternatively, IgA can be produced by plasma cells as a dimeric form bound by a J chain which attaches to the polymeric (pIgR) receptors on the basolateral side of epithelial cell membranes. IgA is then translocated to the luminal side of the membrane and released as secretory IgA (SIgA), where it is free to bind and neutralize threats before they make it to the epithelial cell layer (58). As touched on briefly above, FcγR is expressed on the surface of immune cells and binds to IgG antibodies, with restrictions to the type of immune cell that express the subtype of FcγR. For example, within the context of human FcRs, FcγRI only exists on macrophages, mast cells, neutrophils and dendritic cells; FcγRIIA is only expressed on myeloid cells while FcγRIIB is expressed on tissue macrophages, dendritic cells, and in low quantities on monocytes and neutrophils (59). FcγRIIIA exists on macrophages and NK cells,

while FcγRIIIB exists on the surface of basophils and neutrophils. FcγRI as well as FcγRIIIA are both activating subtypes of FcγR that require the association of the FcRγ subunit which contains an ITAM within the intracellular region of the protein during cell activation. FcγRIIA as well as FcγRIIC also contain an ITAM motif, however this motif is localized in the tail of the receptors and do not require the recruitment of the adaptor molecule during receptor engagement (60). While the FcR family has a wide range of receptor subsets with the ability to induce cell activation and immune effector responses, immunoregulatory mechanisms are needed to prevent the overstimulation of proinflammatory responses in healthy hosts.

In comparison to putative stimulatory receptors, long CYT receptor-types are associated with multiple different functional outcomes, again, based on their CYT amino acid arrangements. For example, inhibitory receptor-types are one such possible variation that are usually associated with immunoreceptor tyrosine-based inhibitory motifs (ITIM; amino acid sequence: [V/I/S/L]xYxx[L/I/V]) (2). These inhibitory receptor-types help regulate the cellular activation of stimulatory receptors (i.e., ITAM-containing receptors) and typically require colligation with stimulatory receptors to induce their inhibitory effects. Inhibitory receptors-types are involved in multiple means of causing inhibition, including the recruitment of C-terminal Src kinases (Csk) to Csk binding proteins (Cbp) that phosphorylate residues on SFKs, rendering them inoperable (61). Alternatively, inhibition can also be attributed to ITIM tyrosine phosphorylation and recruitment of SHP-1/SHP-2 and inositol phosphatases (SHIP) to tyrosine residues within the ITIM (usually in tandem), which facilitates the dephosphorylation of activated molecules ultimately halting their activity (61,62). A classic example of ITIM-mediated inhibition involves an innate immune response mediated by NK cells, in contrast to the FcγR ITAM-dependent ADCC response. NK cells survey for abnormal cell phenotypes (e.g.,

virally infected or damaged cells) through the engagement of ITIM-containing killer cell immunoglobulin-like receptors (KIR) to germline-encoded MHC class I molecules that exist on the surface of all nucleated cells (62,63). This engagement of ITIM-containing receptors allows for tolerance of normal cells while preferentially killing modified cells with abnormal or reduced MHC class I expression profiles associated with viral infections. The MHC molecule on the surface of healthy cells acts as the ligand for inhibitory-type KIRs, preventing cell-mediated cytotoxicity and killing. Virally infected cells have been known to down-regulate the MHC class I molecule on the surface of infected cells to evade the immune response of cytotoxic T cells (CTLs) (64). This defensive strategy prevents the interaction between the MHC molecule presenting viral peptides and the T cell receptor (TCR) that would result in the induction of cytotoxic effects. In addition to KIRs, other receptor-types are also observed to contain inhibitory motifs. While a range of FcγRs are stimulatory in nature due to the presence of the ITAM within their CYT, the FcγRIIB variant is the only FcγR to date that contains an ITIM within it's CYT (52). This receptor has been shown to dampen the activating signals of other FcγR as well as B cell receptors (BCRs) by colligating together with stimulatory receptors through binding of antibody complexes (65,66). This aggregation of receptors causes the activation threshold of receptor-based signalling to increase, resulting in an overall dampening of cell activation, suppression of B cell antigen presentation, and even apoptosis of B cells due to engagement of FcγRIIB in the absence of BCRs (67).

Specific immunoregulatory receptor-types may also contain an immunoreceptor tyrosine-based switch motif (ITSM; amino acid sequence: TxYxx[V/I]) within their CYT which can also serve to regulate the functions of stimulatory receptors (68). Just like the name suggests, ITSMs have been examined to elicit differing modes of regulation (i.e., inhibition and activation) based

on factors such as cell-type and available signalling molecules. For example, when a chimeric programmed death 1 (PD-1) protein receptor containing an ITSM motif was expressed on the surface of cluster of differentiation 4 (CD4) T cells (69), it was shown that PD-1 blocked T cell activation via the recruitment of SHP-1 and SHP-2 to the ITSM motif (69). In contrast, this motif has also been shown to recruit adaptor molecules such as SH2 domain protein 1A (SH2D1A) and EWS/FLI1 activated transcript 2 (EAT-2) (70), resulting in the activation of PI3K-dependent phagocytosis (68). The presence of specific immunoreceptor tyrosine-based motifs within the CYT of receptors results in specific molecules being recruited and activated during receptor engagement. This results in finetuning of the resulting signalling cascade, thereby influencing downstream signalling components and regulating cellular effector responses.

2.2.2 Overview of Cellular Effector Responses in Innate Immunity

Myeloid cells are a fundamental part of the innate immune system that mediate proinflammatory responses to eliminate foreign entities and maintain homeostasis during primary pathogen challenge. These immune cells are involved in a wide range of cellular effector responses that are conserved across vertebrates and include cytokine secretion, degranulation, and phagocytosis. Granulocytes, as their name suggests, are cells associated with the release of granule-containing antimicrobial products for the killing and neutralization of targets. Tissue-resident mast cell, as well as circulating basophil degranulation, occurs when antigen binds to the IgE/FcεRI complex, resulting in the release of leukotrienes, prostaglandins, and histamine, a central part of the allergy response (56). The most abundant leukocyte in the body, neutrophils, can phagocytose pathogens by engaging PRRs and Fc receptors on their surface. Activated neutrophils can also induce NADPH oxidase to create superoxide and their myeloperoxidase (MPO) to create other reactive oxygen species (71). Hypochlorous acid can also be produced in

the presence of hydrogen peroxide from hydrogen peroxide dismutase. These species produced by neutrophils can merge with the engulfed pathogen leading to its destruction. Alternatively, neutrophils can also create and secrete serine proteases, lysozymes, defensins, and cathepsins for a more directed attack against pathogens within the extracellular environment (72). While appearing in low amounts within the blood, eosinophils and basophils play a role in allergic reactions and the defence against pathogens. Eosinophils produce an extensive repertoire of components within their cationic granules, including eosinophil peroxidase, eosinophil cationic protein, eosinophil-derived neurotoxin, and many others (73).

As mentioned briefly above, NK cells and CTLs survey for virally infected or unhealthy cells via specific receptors (e.g., KIRs and FcR) by engaging non-self pathogen molecules, reduced self markers, or induced self-stress markers to destroy infected or damaged cells. Upon receptor engagement, NK cells adhere to the target cell initiated by integrin proteins (e.g., lymphocyte function-associated antigen 1; LFA-1) while forming the immunological synapse between the two cells (74). Granules formed within the NK cell fuse with the membrane and release the contents into the cleft; perforin can then bind to and form pores within the target cell membrane where granzyme serine proteases are able to enter the cell (75). Granzyme A can induce swift caspase-independent cell death (76) through mechanisms such as the production of reactive oxygen species (ROS), disrupts the mitochondrial electron transport chain (ETC), as well as translocation and release of nucleases into the nucleus (77). Granzyme B's substrate is caspase 3, triggering the induction of the caspase cascade, resulting in apoptosis of the target cell (78).

In addition to releasing granules, NK cells and CTLs can induce cell death through the engagement of death receptors, most notably the FasL transmembrane receptor. This receptor is stored in secretory granules and depends on cellular degranulation to be expressed on the surface of the immune cells (79). FasL engages with CD95 on the surface of target cells and activates the apoptotic signalling cascade; death-inducing signalling complex (DISC) is created and results in the activation of caspase 8 and 10, leading to a full caspase cascade and cell apoptosis (80).

In addition to the previously mentioned neutrophil-mediated phagocytosis and degranulation, other effector responses can be induced by neutrophils to contain pathogens. NETosis is the neutrophil-specific innate immune response characterized by the release of large web-like structures known as neutrophil extracellular traps (NETs) facilitated by the death of the neutrophil (81). Various pathogens induce this antimicrobial response (e.g., *Staphylococcus aureus*, *Listeria monocytogenes*) (82,83) as well as pathogen molecules (e.g., LPS, lipoteichoic acid) (84). Neutrophils, in response to pathogen stimulation, release decondensed chromatin (i.e., DNA and histones) combined with antimicrobial proteins such as MPOs, lysozymes, elastase, and antifungal calgranulin to immobilize and kill pathogens (85). The overall charge of the NETs allows for electrostatic interaction with pathogens resulting in their entrapment and destruction (85).

Inflammation is defined as the immune system's reaction to pathogens and other foreign entities with the goal of pathogen clearance and initiating the repair process characterized by tissue redness, swelling, pain, and heat (86). Cytokines are small proteins that are heavily involved in controlling a significant aspect of cellular processes, including inflammation. For example, Interleukin-1β (IL-1β), tumor necrosis factor-α (TNF-α) and interleukin-6 (IL-6) are

considered proinflammatory cytokines and stimulate the activation of intracellular signalling pathways (i.e., NF-κB, MAPK, Janus kinase (JAK)-signal transducer and activator of transcription; STAT) through the engagement of immune receptor proteins (87). IL-1β and TNF-α have both been associated with cell proliferation and apoptosis, while TNF-α itself has been shown to prime macrophages for the production of nitric oxide and enhance its phagocytic abilities (87). While inflammation is a fundamental part of pathogen clearance, chronic inflammation can result in severe tissue damage, disease progression, and even mortality. As such, the resolution of inflammation must be a well-controlled and coordinated process. Major anti-inflammatory cytokines include (IL)-1 receptor antagonist, IL-4, IL-10, IL-11, and IL-13 (86). While other cytokines have inhibitory effects, they depend on specific contexts and could be classified as either inhibitory or stimulatory (i.e., interferon-α, transforming growth factor β (TGF-β), IL-6). IL-10 is one of the more potent cytokines with anti-inflammatory properties, inhibiting activated macrophages and repressing their ability to release proinflammatory cytokines such as IL-1 and TNF-α (88).

Phagocytosis is the cell-mediated process of ingesting particles greater than 0.5 μm. While phagocytosis in unicellular organisms is used to uptake nutrients, it is a fundamental immunological process spread across vertebrates and invertebrates alike, allowing for the destruction of pathogens, apoptotic cells, and foreign objects as well as regulation of tissue repair (89,90). Phagocytosis is associated with a wide range of cell types and is significant for homeostasis, but only professional phagocytic immune cells can undergo phagocytosis to a high degree of proficiently, including macrophages, dendritic cells, and neutrophils (89). In general, phagocytosis is a temporal event with significant stages that occur during the process. Particles are detected by immune receptors on the surface of the phagocyte, internal activation of cellular

processes leading to the formation of the phagocytic cup, active internalization of the particle, formation of the particle-containing vacuole, and merging of the vacuole with lysosomes to form the phagolysosome for the destruction of the engulfed target (90). Phagocytic receptor-types on the surface of phagocytes can be classified into two main groups: opsonic and non-opsonic receptors. As mentioned above, non-opsonic receptors, such as C-type lectins and scavenger receptors, recognize PAMPS to induce phagocytes to engulf the targets. While TLRs are not part of the non-opsonic group, they contribute to enhancing phagocytic receptors (23). Opsonic receptors bind to and recognize opsonins (i.e., antibodies, compliment) bound to the surface of invading pathogens to induce efficient destruction of the tagged target. As mentioned above, FcγRs recognize IgG complexes resulting in membrane clustering and engulfment while simultaneously activating alternative cellular responses (91).

2.2.3 Functional Plasticity of Immune Proteins

The presence of immunoreceptor tyrosine-based motifs (i.e., ITAM; stimulatory, ITIM inhibitory) within the CYT of immune receptor tails is generally how immune proteins are categorized (2). However, effector responses that are induced from the engagement of ITAM or ITIM-containing immune receptors do not always lead to activation or inhibition classically associated with these motifs. Instead, many receptor-types with ITAM or ITIM signalling motifs display both functional inhibition and activation associated with the same receptor, which is defined as functional plasticity. The binding avidity of ligands to receptor proteins also has been shown to act as a discriminator for the variability of signalling outcomes to regulate innate immune responses. For example, specific ITAM-containing receptors have displayed functional plasticity and are characterized by inhibitory modes of action termed inhibitory ITAM (iITAM). FcαRI can bind to antigen complexes of IgA to activate cellular responses. However, upon

binding non-antigen bound IgA monomers, FcαRI induces potent inhibitory responses through the recruitment and activation of SHP-1 to the ITAM (92). This interaction is fundamental in the control of immune responses by preventing tissue damage and returning immune cells to a resting state (18).

Another mechanism controlling functional plasticity is the presence of functionally competing motifs within the CYT of the same receptor type. For example, FcR-like (FCRL) 5 is an ITAM-like and ITIM motif-containing receptor that is expressed on a subset of B cells (93). When this receptor was co-ligated with the BCR, a reduced wave of calcium influx showed the role of FCRL5 in dampening B cell activation via the BCR. Disrupting the ITAM-like motif of FCRL5 caused a complete shutdown of cellular responses while mutating the tyrosine residue within the ITIM surprisingly led to enhanced calcium flux. The observations of dual potential signalling receptors suggest that the combination of signalling motifs within the CYT may dynamically modulate cell effector responses.

Another case of functional plasticity is shown for the human KIR2DL4 (CD158d), which contains a charged arginine amino acid residue within its transmembrane domain that results in recruitment of ITAM containing adaptors as well as a single ITIM motif within the CYT, reminiscent of inhibitory KIR receptors (94). Overall, the KIR2DL4 ITIM does not seem to play a role in NK-mediated cytotoxic effects, which is inhibited by co-ligation with inhibitory ITIM-containing KIR receptors. However, when the stimulatory ability of KIR2DL4 is disrupted, the receptor can inhibit other stimulatory receptors, possibly by the recruitment of inhibitor molecules SHP-1 and SHP-2 that were shown to bind to the receptor.

Overall, immune receptors are fundamental for cellular control over various effector innate immune responses that contribute to pathogen clearance and homeostasis. While immunoreceptor tyrosine-based motifs within immune proteins give context to signalling pathways used to control effector responses, there is more complexity to this regulation beyond the simple activation and inhibition definition of immune receptors.

2.3 Teleost Immunoregulatory Receptors

In general, innate immune cell effector responses are conserved between fish and mammals; however, the immunoregulatory receptor-types and their associated signalling networks are not as well studied in fish. Functionally, teleost macrophages and B cells have been shown to perform phagocytosis (95), mast cells and neutrophils elicit degranulation (96,97), and fish neutrophils/NK cells induce cell-mediated cytotoxicity (98,99). While these responses in fish are similar to their mammalian counterparts, there are still large gaps in knowledge regarding how fish immunoreceptor networks control these responses. Recently, several fish immunoregulatory families have been discovered due to molecular cloning and the availability of teleost genomes. Their characterization is beginning to provide comparative immunologists further insights into how fish immunoregulatory networks initiate, inhibit, and control potent innate immune cell effector responses.

2.3.1 Immunoglobulin Super Family (IGSF)

The IgSF is an extensive group of cellularly expressed proteins typically defined by the presence of one or more extracellular immunoglobulin-like domains, proteins characterized by an immunoglobulin fold composed of two antiparallel β-sheets with a disulfide bond that is

commonly found within the core to stabilize the structure (48,100). The IgSF consists of many related receptor groups (i.e., leukocyte Ig-like receptors (LILRs), FcRs, FCRLs, and KIRs) that display great diversity between, as well as within, individual groups, a feature that may have arisen as a result of evolutionary pressure to ever-changing pathogen ligands (101). Receptor groups, such as FcRs, that bind similar ligands are typically located clustered together within a number of chromosomes. MHC I binding receptors (e.g., KIRs and LILRs) are found on human chromosome 19q13.4 (102), while Fc binding receptors (e.g., FcRs) are located on chromosome 1q21-23 (103). In many vertebrate model organisms (e.g., mice, birds, amphibians), studies have shown that IgSF members cluster in regions similar to that of human leukocyte receptor complex (LRC) and FcR complexes (104–108). Similar to what was mentioned previously with PRRs, IgSF members are germline-encoded and recognize a repertoire of pathogen molecules, opsonins, host proteins, and a variety of other ligands to fine-tune immune cell effector responses. Both myeloid and lymphoid cell lineages contain receptors from the IgSF with tightly controlled immune effector responses balanced by the presence of both activating and inhibitory receptor-types.

2.3.2 Fish Immunoregulatory Receptors Belonging to the IgSF

Many of the identified immune receptors in teleost fish belong to the IgSF, with some teleost immune receptor groups sharing common features with the mammalian receptor families within the broader superfamily (48). However, further characterization of teleost immune receptors remains obscure due to the lack of identified ligands. In addition, the discovery of fish-specific immune receptors families (e.g., novel immune-type receptors; NITRs) strongly suggests that immune function within teleost is fine-tuned via fish specific mechanisms and cannot be directly compared to mammal immunity (109). However, the characterization of these

fish immune receptors-types has led scientists to make discoveries and comparisons about vertebrate immune regulation.

Similar to section 2.2.1 above, IgA and IgM can be considered polymeric immunoglobulins (pIg) secreted at mucosal barriers to neutralize potential pathogens from entering the host (110). pIgs are secreted into the mucosa by binding to mammalian pIg receptors (pIgRs) on the basolateral side of cells and transcytosed via vesicles. The binding of pIgs to pIgRs requires the joining (J) chain, which links the Fc portions of two antibodies together. Many studies have shown that bony fish contain IgM within the skin and gut mucosa (111). The first pIgR in fish was identified in fugu which shared similar features to those from mammals, birds, and amphibians; however, the pIgR identified in fish contained low amino acid identity in comparison (112). Additional pIgRs were identified in common carp (*Cyprinus carpio L.*), zebrafish, range-spotted grouper (*Epinephelus coioides*), and trout (113–115). Fugu pIgRs are mainly expressed in the thymus, skin, gills, intestine and even in epithelial cells of the intestines and skin (112). Common carp pIgRs are primarily expressed in the liver, spleen, hindgut, and head kidney, while again, being observed in the epithelial cells of the intestines and skin (113). pIgRs, similar to most groups within the IgSF, contain extracellular Ig domains, a TM region, and a CYT having variable arrangements of amino acids. An interesting feature between pIgRs of different animal groups is that the number of Ig domains varies. For example, humans encode five Ig domains (110) while rabbits and bovines encode for three domains (116,117); even shorter still, teleost fish receptors only contain two Ig domains (112–114). Analysis of these features revealed that the D1 domain was responsible for binding pIg through non-covalent interactions and that this feature is conserved amongst mammalian species and species of chickens and *Xenopus* (118–120). Furthermore, the D5 region of pIgR also binds to pIg via

covalent bonds, a feature that is also conserved throughout mammals, birds, and amphibians (118). When examining the short extracellular domain of teleost pIgRs, the D1 is related to mammalian D1 domains while the proximal domain is related to the domains of other vertebrates, suggesting that the D1 domain is indeed required for basic pIg binding (118–120). However, this interaction for teleost fish cannot be confirmed as the D1 domains are not conserved between species, which may explain why there is little homology between mammalian and fish IgRs as stated previously. Another area of uncertainty is that the CYT region of teleost receptors do not match that of other animal species pIgR CYTs (118) although, it has been well known that teleost fish have robust mucosal immune responses that serve as an essential first line of defence in the aquatic environment (113). Thanks in part to cloning and transfection experiments, it is now known that fish polymeric IgM associates with pIgR facilitating the aforementioned mucosal transcytosis (112).

A putative teleost homologue of vertebrate FcR and FCRLs was also discovered during an investigation of available genome databases for channel catfish. IpFcRI is a receptor protein predicted to contain 3 Ig-like domains, although it lacks a transmembrane and CYT region, giving rise to the prediction that this protein is secreted or perhaps associates with adaptor molecules (121). Early protein modelling of IpFcRI suggested that the two distal Ig-like domains shared homology with other FcRs while also containing a putative Ig binding site (121). Quantitative polymerase chain reaction (Q-PCR) of peripheral blood leukocytes (PBL) indicated that granulocytes and lymphocytes expressed IpFcRI; however, it was also shown that tissue and cell type could individually alter the expression of IpFcRI (121). Using a recombinant IpFcRI expressed in an insect cell expression system, IpFcRI was confirmed to be a secreted protein while also being detected in catfish plasma using polyclonal antibodies (121). Even though this

protein is secreted, co-immunoprecipitation (co-IP) experiments revealed that IpFcRI binds to serum-derived fish IgM, indicating that it is a teleost FcμR (121).

NITRs are another receptor family originally discovered in pufferfish but have been identified in other teleosts such as channel catfish, rainbow trout, and zebrafish (109,122). Expression analyses of NITRs reveal that they are expressed in both myeloid and lymphoid cell lines, including catfish NK-like cells, T cells, macrophages, and B cells (122,123). Certain NITRs have also been classified as analogous to KIRs due to their ability to bind to allogeneic B cell targets while being expressed on NK-like cells (124). Typical NITRs possess one to two extracellular Ig domains, which have been characterized to be related to T cell receptors. They also contain a TM region and CYTs with variable lengths containing differing arrangements of signalling motifs (i.e., ITIM-like, ITAM-like, or both). Similar to putative stimulatory receptors, certain NITR-types contain a very short CYT with no signalling motifs but possess a positively charged aspartic residue that has been shown *in vitro* to recruit the adaptor molecule DAP12 to activate PI3K signalling (125).

2.3.3 Channel Catfish (*Ictalurus punctatus*) Leukocyte Immune-Type Receptors (IpLITRs)

Teleost represents a large and diverse group of ray-finned fish that makeup about half of all living vertebrate species (126). This group of boney fish contains an assortment of innate and adaptive immune cells and immune cell receptors similar to that of mammals, as mentioned above. A representative of the group, channel catfish, has been an excellent model to characterize teleost immunity thanks in part to having leukocytes that do not require transformation to survive in culture for long periods, leading to the establishment of lymphoid catfish cell lines (5,48).

TS32.15 and TS32.17 are catfish CTL cell lines that were created through immunizing outbred fish with alloantigen (B cells) (5,48). These cell lines were used to help generate an expressed sequence tag (EST) library, which resulted in the identification of three representatives of a new immune receptor family, IpLITR 1, IpLITR 2 and IpLITR 3. The three new receptors contain a variable number of extracellular Ig domains (four, three, and six, respectively). Looking at their CYT regions, IpLITR 1 includes two ITIMs, an ITIM-like, and an ITSM, suggesting that this receptor engages in inhibitory signalling (5,48). IpLITR 2 and IpLITR 3 have a short CYT attached to a TM region with an imbedded positively charged lysine residue. It was predicted that these two receptors required the recruitment of adaptor molecules to be expressed on the surface of cells to induce putative stimulatory signalling responses (5,48).

As confirmed by analysis of the zebrafish genome, the gene complex encoding IpLITRs is polygenic and polymorphic and is located on multiple separated chromosomes but still shares homology between them (5). Originally it was predicted that the formation of multiple LITR clusters was the product of gene duplication events, but the determination of the functions of these receptors within and between the clusters remains obscure. When comparing LITRs to other vertebrate models, multiple receptor genes are identified from various sources (e.g., birds, amphibians, and mammals) and included receptors-types from the IgSF such as FcRs, FCRLs, and members of the LRC. Teleost receptor-types such as pIgRs, NITRs and IpFcRI were interestingly not closely matched to LITRs during database searches, further cementing LITRs as a definitive receptor family. At the time of discovery and characterization, further analysis of the different Ig domains suggested that the domain distal regions (i.e., D1 and D2) were more closely related to proteins from mammalian FcR and FCRL receptors, while the domain

proximal regions (i.e., D3 and D4) were related to immune protein encoded within the mammalian LRC region (5,48).

To further characterize IpLITRs, expression analysis via northern blotting revealed that LITRs were highly expressed in the hematopoietic pronephros and the mesonephros (IpLITR 1 and IpLITR 2) with low expression in the spleen and heart of channel catfish (5,48). Using RT-PCR, it was found that IpLITR 1 and IpLITR 2 are expressed in a range of tissues, including the spleen, PBLs, kidney, gills, heart, liver, intestine, and thymus. Along with CTLs, IpLITRs were also shown to be expressed in catfish NK-like cells, macrophages, and B cells. Additionally, no expression of IpLITRs was observed in a non-immune cell, ovarian cell line indicating that this receptor family was mainly only involved in immune cell-based regulation. Upregulation of these receptors was also looked at 12 days post-stimulation of PBLs and cytotoxic T cells stimulation, resulting in an increased expression of IpLITR 1 and IpLITR 2 (127).

During RT-PCR testing to examine the expression of the LITR-types within catfish cells, multiple versions of the IpLITRs were observed (5,127). Cloning and sequencing of these expressed transcripts revealed multiple versions of stimulatory and inhibitory IpLITR-types, resulting in around forty sequenced LITR genes. Of those that were identified, a large majority of them were similar to IpLITR 2, containing a variable amount of Ig domains; however, the presence of short CYTs with charged TM regions was indicative of putative stimulatory receptors. Taking a closer look at the Ig domains of the identified IpLITRs, similar arrangements of the distal D1 and D2 regions were observed; however, they contained the most amino acid variability compared to the membrane proximal regions. This gave rise to the idea that, like most receptors within the IgSF, the D1 and D2 domains of the receptors function as the primary ligand

binding region (5,127). Using database comparison as well as homology modelling, it was predicted that representative IpLITRs contained similar key amino acid residues to that of leukocyte immunoglobulin-like receptor B1 (LILRB1) and that certain IpLITR-types could possibly bind to MHC I molecules.

Recent syntenic analysis in our lab was conducted to further examine the evolutionary relationship LITRs have with other mammalian immune receptors. It was shown that IpLITRs cluster together in large groups on chromosomes (e.g., goldfish chromosomes 3, 7, and 40) while also linked to other genes such as the signalling lymphocytic activation molecule (SLAM) family (6). Further analysis of the LITR Ig domains' phylogenetic relationship with mammalian receptors indeed confirmed the connection with the FCRL group. However, unlike previous claims about how proximal domains of IpLITRs shared relation to receptors encoded within the LRC complex, there was no clear evidence for this link between LITRs and mammalian Ig domains. While an LRC-like region was discovered within the zebrafish genome, LITR genes were not found in this region (6).

In summary, the use of the catfish immune cell lines has been instrumental in discovering a new immune receptor family distinct from those previously found. While it is clear that there is a phylogenetic relationship between this receptor family and those from mammals, the overall regulatory functions remain a mystery but provide an excellent model for examining the receptor-based control of cell signalling networks in fish. The following two sections will focus on using a heterologous expression system to study LITRs and a review of newly discovered LITRs in zebrafish.

2.4 LITR-mediated Immunoregulatory Responses

2.4.1 Stimulatory IpLITRs Association with Intracellular Adaptor Molecules

Looking at the putative stimulatory IpLITR 2.6b, an isoform of the previously mentioned IpLITR 2, the presence of a short CYT region with a positively charged lysine residue gave rise to the prediction that this receptor binds to adaptor molecules upon receptor engagement to allow for its surface expression and subsequent stimulatory signalling (128). To test this hypothesis, human embryonic kidney (HEK-293T) cells were co-transfected with a hemagglutinin (HA), N terminally-tagged IpLITR 2.6b in addition to FLAG-tagged negatively charged catfish adaptor proteins (i.e., IpFcRγ, IpFcRγ-L, IpCD3ζ-L, or IpDAP12) which each contain a single ITAM motif within their CYT regions. Using flow cytometry and western blotting, it was shown that IpLITR 2.6b associated with IpFcRγ, IpFcRγ-L and IpCD3ζ-L and its association with IpFcRγ and IpFcRγ-L (not IpCD3ζ-L) resulted in an increase in cell surface expression of IpLITR 2.6b (128). DAP12, an adaptor that is commonly found to associate with other members of the IgSF, contains lysine residues in the TM region (51,129) that did not associate with IpLITR 2.6b (128). To further study IpLITR 2.6b-adaptor interactions and the requirement of residues within the TM regions of the proteins, the positively charged lysine residue within the TM region of IpLITR 2.6b was mutated to either a positively charged arginine or an uncharged alanine residue (128). In addition, the negatively charged aspartic acid residue in the TM region of IpFcRγ-L was also mutated into an alanine. The mutations of the residues within the TM region of IpLITR 2.6b resulted in no disturbance in its ability to associate with the adaptor proteins. Surprisingly, this mutation enabled IpLITR 2.6b to interact with DAP12, which caused augmentation of the surface expression of the receptor. In contrast, the adaptor molecule IpFcRγ-L without the negatively charged aspartic residue could not associate with IpLITR 2.6b. This data suggests that unlike what is reported for mammalian stimulatory receptor-adaptor dynamics (129), IpLITR

2.6b does not need the positive charge within its TM region to bind to and associate with the adaptor IpFcRγ-L, however, the charge in the TM of IpFcRγ-L is crucial for its association with IpLITR 2.6b and its function (128). These experiments also showed that IpLITR 2.6b formed heterodimer complexes with IpFcRγ-L and IpCD3ζ-L, a phenomenon also observed for FcRγ-CD3ζ -dependent signalling transduction in mammals (130). In summary, these experiments confirmed that the putative stimulator receptor IpLITR 2.6b associates with ITAM-containing teleost adaptor molecules and provided new insight regarding the dynamics of this receptor-adaptor interaction.

To functionally determine the signalling capabilities of the IpLITR 2.6b-IpFcRγ-L complex, a chimeric receptor was generated where the extracellular domains of IpLITR 2.6b were fused with the TM and ITAM-containing CYT region of IpFcRγ-L (8). This IpLITR 2.6b/IpFcRγ-L (now referred to as IpLITR 2.6b) chimera was tagged with an N-terminal hemagglutinin (HA) tag, allowing it to be stimulated using anti-HA specific monoclonal antibodies (mAbs), followed by stable transfection and expressed of the chimera in the rat basophilic leukocyte cell line (RBL-2H3). When stimulated using anti-HA mAbs, IpLITR 2.6b was a potent inducer of RBL-2H3-mediated degranulation while mutating the functional tyrosine within the CYT ITAM into a non-functional phenylamine abrogated the response, confirming these responses are ITAM dependent (8). IpLITR 2.6b activation resulted in the phosphorylation of extracellular signal-regulated kinase (ERK) 1/2 protein as well as protein kinase B (Akt), which was, again, absent during the engagement of the mutated ITAM-containing receptor. Pharmacological inhibitors targeting key intracellular signalling molecules caused significant reductions of IpLITR 2.6b-induced degranulation via the disruption of Src family kinases (SFKs), Mitogen activated protein kinase (MAPK) kinase (MEK1 and MEK2),

phosphatidylinositol 3-kinases (PI3K), and protein kinase C (PKC) (8). In contrast, no significant degranulation was inhibited by p38 MAPK and c-Jun N-terminal kinases (JNKs) pathway inhibitors. IpLITR 2.6b transfected cells could also induce an ITAM-dependent mode of phagocytosis when cells were incubated with αHA opsonized 4.5 μm polystyrene beads as targets. This data was the first to show functional IpLITR 2.6b-mediated signalling events and indicated that this stimulatory IpLITR-type used classical kinase-dependent signalling cascades as well as an ITAM-dependent mode of phagocytosis.

Other functional outputs were also examined for further characterization of IpLITR 2.6b. During αHA crosslinking of the receptor, IL-3, IL-4, IL-6, and TNF-α were detected to be secreted using a cytokine screening profile along with increased phosphorylation levels of several signalling molecules downstream of IpLITR 2.6b activation, including ERK 1/2, MEK6, MSK2, Akt2, and ribosomal S6 kinase (RSK)1 (12). These responses were comparable to the stimulation of RBL-2H3 cells to endogenous IgE and suggested that IpLITR 2.6b signalling can induce multiple responses in RBL-2H3 cells.

As mentioned above in section 2.2.1, stimulatory receptors, such as FcRs, are well characterized in mammals and require the association of ITAM-containing adaptors to facilitate the further recruitment of signalling molecules to induce cellular effector responses such as phagocytosis (51). For example, the engagement of FcRs can result in the recruitment of the ITAM-containing adaptor FcRγ which is phosphorylated by SFKs, leading to the recruitment and activation of kinases such as Syk. From here, other downstream signalling molecules can be recruited and activated, including PI3K, Vav, Rho family GTPases (e.g., Ras-related C3 botulinum toxin substrate; Rac1 and cell division control protein 42; Cdc42) resulting in the

activation of F-actin polymerization machinery to induce phagocytic cup formation during the early stages of phagocytosis (131,132). To observe the possible role that certain molecules have on the IpLITR 2.6b-mediated phagocytic response, another pharmacological inhibitor array was conducted during a flow cytometric-based phagocytosis assay (11). Overall the phagocytic response was blocked by inhibition of SFKs, Syk, PI3Ks, Akt, Cdc42, RAC1/2/3, MEK1/2, phosphoinositide-dependent kinase 1 (PDK1), PKC, and F-actin polymerization. Confocal microscopy of IpLITR 2.6b-mediated phagocytosis also confirmed the ability of these receptors to induce an ITAM-dependent phagocytic phenotype reminiscent of what is described for mammals (11,133). This data suggests that IpLITR 2.6b regulates ITAM-dependent phagocytic responses utilizing signalling molecules akin to the known mammalian FcR-mediated phagocytic pathway.

2.4.2 Inhibitory IpLITRs Recruit Protein Tyrosine Phosphatases

As mentioned in section 2.2.1, inhibitory receptor-types typically contain long CYTs embedded with various signalling motifs, such as ITIMs, which attenuate stimulatory immune signalling through receptor recruitment and activation of inhibitory signalling molecules that dampen stimulatory signalling cascades and cellular effector responses (2). To investigate the inhibitory properties of certain putative inhibitory IpLITR-types, receptor chimeras were created through the fusion of the CYTs of IpLITR 1.2a or IpLITR 1.1b with the TM and extracellular domain of human NK receptor KIR2DL3 (134). As the natural ligand for LITRs are unknown, the use of the extracellular domain of KIR2DL3 and its ligand (i.e., HLA-Cw3) became a valuable tool to stimulate IpLITR-mediated signalling artificially. IpLITR 1.2a contains an ITIM along with an ITSM; IpLITR 1.1b, on the other hand, contains two ITIMs (Y_{477} and Y_{499}) and an ITSM (Y_{503}) within the membrane distal region of its CYT, in addition to a membrane proximal

region that does not contain a recognizable signalling motif, although three tyrosine residues (Y_{433}, Y_{453} and Y_{463}) are present (127,134). Following the transient expression of these chimeras in HEK-293 cells, both SHP-1 and SHP-2 were shown to be recruited to each receptor chimera following phosphorylation of tyrosines within their ITIMs, however, the membrane proximal region of IpLITR 1.1b did not recruit any phosphatases (134).

2.4.3 Inhibitory IpLITRs Diminish NK-Mediated Cytotoxicity

The same inhibitory IpLITR chimeric constructs were transfected into mouse NK-like cells to assess the specific effects that putative inhibitory IpLITR-types have on lymphocyte-mediated cytotoxicity (13). Using HLA-Cw3 expressing B cell targets in a cytolysis experiment, the focus of earlier studies was to establish if the putative inhibitory IpLITR CYT regions could inhibit cytotoxicity, and to identify what specific signalling pathways are utilized by these IpLITR-types. The possible signalling role of the membrane proximal region of IpLITR 1.1b was also examined, although it did not contain any ITIMs. Overall, it was shown that the CYT region of IpLITR 1.2a inhibited B cell killing through a SHP-dependent mechanism, however, while the CYT of IpLITR 1.1b was also able to inhibit cytolysis, the ability of the receptor to induce inhibition was not completely reliant on the ITIM recruitment of SHP-1 (13). For example, when chimeras were created and transfected that only contained the membrane proximal (IpLITR $1.1b^{PROXIMAL\ CYT}$) or distal (IpLITR $1.1b^{DISTAL\ CYT}$) regions of IpLITR 1.1b CYT, it was shown that both IpLITR $1.1b^{DISTAL\ CYT}$ and surprisingly $1.1b^{PROXIMAL\ CYT}$ could both inhibit cellular killing responses. While IpLITR $1.1b^{DISTAL\ CYT}$ inhibition of killing was dependent on SHP-1 recruitment, $1.1b^{PROXIMAL\ CYT}$ was not (13). It was determined that $1.1b^{PROXIMAL\ CYT}$ induced inhibition through the presence of a series of amino acids that closely resemble the Csk binding motif consensus sequence, which was confirmed by coimmunoprecipitation. In mammals, Csk is

a kinase that inhibits cellular signalling through the phosphorylation of the negative regulatory site on SFKs, suppressing its catalytic activity (135). To summarize, inhibitory IpLITR types 1.2a and 1.1b suppressed lymphocyte-mediated cytotoxicity through a SHP-dependent mechanism (13). However, IpLITR 1.1b also employs a unique SHP-independent mechanism through the binding of Csk to its membrane proximal region, which showcases that IpLITRs have versatile abilities for the regulation of immune cell effector responses.

2.4.4 Inhibitory IpLITRs Demonstrate Functional Plasticity through Initiation of Phagocytosis

Similar to what was described above for the stimulatory receptor IpLITR 2.6b, the putative inhibitory receptor IpLITR 1.1b construct was also transfected and stably expressed in RBL-2H3 cells to further examine the receptor's ability to regulate immune cell processes (12). Surprisingly, it was shown that engagement of IpLITR 1.1b with the same αHA opsonized 4.5 μm polystyrene bead targets resulted in phosphorylation of signalling molecules, including ERK1/2 and Akt while inducing a phagocytosis response that was independent of the recruitment of ITAM-containing adaptor molecules. When an IpLITR 1.1b construct containing no CYT region was transfected and stimulated, it was observed that while the construct was still expressed on the cell surface, the phagocytic response induced by CYT-containing receptors was abolished, indicating that this response was explicitly caused by its CYT region (12). The calcium chelator EDTA was later introduced to IpLITR 1.1b expressing cells, however, the phagocytic response was unaffected, in contrast to the diminishment seen with the addition of EDTA to the IpLITR 2.6b-expressing cell line. However, inhibition of actin polymerization using Cytochalasin D did halt the response, confirming that IpLITR 1.1b induces an F-actin-dependent mode of phagocytosis (12). In direct comparison to these observations, IpLITR 1.2a

was also shown to induce a phagocytic response, indicating that the ITIMs and the ITSMs within both receptors may be responsible, for not only the inhibitory nature of these receptors, but may also indicate that ITIMs are more versatile in their signalling potential beyond purely being inhibitory. When observing IpLITR-mediated phagocytosis more carefully through microscopy, it was shown that 1.1b caused a unique mode of bead capture and engulfment with the formation of long filopodia-like protrusions emanating from the cell surface to bind to targets; an effect that was not observed for IpLITR 2.6b (11). It was also noted that unlike IpLITR 2.6b-induced phagocytosis, which readily engulfed many bead targets, 1.1b displayed a stalled phagocytic phenotype whereby most beads were only bound to the surface of the cells and not completely internalized. Furthermore, induction of phagocytosis by IpLITR 1.1b was not affected by incubation at sub-ambient temperatures (22°C), which again sets the 1.1b phagocytic phenotype apart from that of IpLITR 2.6b which was unable to consume bead targets below 27ºC. From our previous studies, we have demonstrated that IpLITR 1.1b is a potent inhibitor of stimulatory signalling and cellular effector responses, including NK-like cell-mediated cytotoxicity as well as phagocytosis (13,14). This evidence of IpLITR 1.1 b's ability to induce an ITAM-independent mode of phagocytosis is the first description of a teleost ITIM-containing receptor`s ability to induce functional plasticity (12,131). While our lab has begun to unravel the inner mechanisms controlling this aspect, more research needs to be done to further reveal the conserved and divergent aspects of vertebrate signalling.

2.4.5 Inhibitory IpLITRs Associate with Stimulatory Signalling Machinery to Facilitate Phagocytosis

IpLITR 1.1b has been observed to induce a unique ITAM-independent mode of phagocytosis facilitated by the formation of filopodia-like extensions. Early in our studies of this

model, it was proposed that within the distal region of the CYT of IpLITR 1.1b, the specific tyrosines embedded within the ITIM and ITSM motifs may recruit adaptor proteins to facilitate the signalling cascade for IpLITR 1.1b-mediated phagocytosis (12). The filopodia-like protrusions associated with IpLITR 1.1b are continuously expressed regardless of target availability which may be explained by its role of continuous surveying of the extracellular environment for targets (11). This would suggest that F-actin polymerization machinery are activated at a basal state and that signalling molecules may be continuously associated with IpLITR 1.1b.

As mentioned in section 2.2.1, ITSMs have been implemented to activate and inhibit cellular effector responses (68–70). Activation of signalling responses in cells has been shown to involve SHP-2, which, when recruited to receptor ITIM/ITSM, acts as a scaffold for the binding of molecules such as growth factor receptor-bound 2 (Grb2) (136,137). From here, Grb2 can associate with Grb2-associated binders (Gabs), which can bind to PI3Ks when phosphorylated, leading to further recruitment and activation of molecules for the induction of the phagocytic response (127,137,138). Alternatively, it has also been examined that Syk is able to bind to the CYT of receptors following phosphorylation of two tandem ITIMs to induce stimulatory signalling transduction, as seen with platelet endothelial cell adhesion molecule-1 (PECAM-1) (139). This hypothesis was indeed supported in further pharmacological trials where IpLITR 1.1b-mediated phagocytosis was significantly dampened by SFK, Syk, and F-actin inhibitors (11). As mentioned previously, IpLITR 1.1b inhibited NK-like cell cytotoxicity (13) through phosphorylation and the recruitment of signalling molecules to the membrane distal and proximal regions. It was then proposed that since IpLITR displays such a distinct ITAM-independent mode of phagocytosis, perhaps both the proximal and distal regions of the CYT are

also involved in regulating signalling mechanisms for actin polymerization. With the presence of a consensus sequence for the binding of a non-catalytic region of tyrosine kinase adaptor protein (Nck) within IpLITR 1.1b's proximal CYT region (134), it was additionally proposed that Nck facilitates the binding of the WASp family verprolin-homologous protein-2 (WAVE2) complex resulting in the activation of the F-actin polymerization machinery (140). Co-immunoprecipitation experiments confirmed that the proximal region of IpLITR 1.1b was associated with Nck1, Csk, Grb2, and Vav1 compared to the CYT membrane distal region, which bound to Syk, PI3K and SHP-2 (141). When examining the unique filopodia-like structures produced by IpLITR 1.1b transfected RBL-2H3 cells, it was shown that Nck, but not phosphorylated Syk (pSyk), colocalizes with the protrusions (9). While the functional relevance of these extensions is not fully understood, the observations that they enhance target acquisition would lead to the notion that there is a basal level phosphorylation of IpLITR 1.1b to facilitate Nck binding, which could result in the association of F-actin machinery to form these extensions. It was also important to note that both pSyk and Nck were recruited to sites of bead-cell contact at all stages of the phagocytic process, implying that both molecules are important in both the capture and engulfment mechanisms of phagocytosis.

Overall the association of IpLITR 1.1b with various signalling molecules suggests that while the membrane distal region of IpLITR 1.1b is possibly able to bind to Syk to induce an ITAM-independent mechanism for cellular activation, the membrane proximal region is also important to facilitate these functional outcomes, of which IpLITR 1.1b provides a new model for studying a unique mode of phagocytic control.

2.4.6 IpLITRs-mediated Crosstalk Inhibition of Phagocytosis

The dynamic nature of immune regulation consists of multiple signals converging to fine-tune and establish the most appropriate response against encountered insults. As such, the notion that a single immune receptor-type is responsible for the sole mediation of immune effector responses is unreasonable, however, it is still an important tool to continue to analyze immune receptor signalling mechanisms specifically. As mentioned in section 2.2.1, long-tailed putative inhibitory receptors typically induce their regulation via the colligation with activating receptors (2,61). During co-engagement, inhibitory receptors recruit inhibitory-associated molecules (e.g., SHP-1/2) near stimulatory effectors resulting in an overall dampening of cell signalling cascades. For example, IpLITR 1.1b can illicit an ITIM-dependent and -independent mechanism for the inhibition of NK-like cell killing (13). Catfish immune cells have been previously shown to co-express both putative inhibitory and activating LITR-types with similar amino acid identity within the distal region of the Ig domains between receptors, indicating possible similar ligand binding (127). It was then hypothesized that putative inhibitory and stimulatory IpLITR-types, when co-engaged, could crosstalk to regulate immune effector responses (14). To examine this, AD-293 cells were stably co-transfected with HA-tagged IpLITR 2.6b and FLAG-tagged IpLITR 1.1b. αHA and αFLAG mAbs co-opsonized 4.5 μm fluorescent bead targets were added to cells to co-engage both sets of catfish receptors for crosstalk, which was then analyzed using a flow cytometric phagocytosis assay. These studies found that co-engagement of both receptors led to an overall dampening of the phagocytic response compared to the robust engulfment of targets seen when IpLITR 2.6b is engaged without IpLITR 1.1b. This indicated that IpLITR 1.1b is responsible for inhibiting IpLITR 2.6b-mediated phagocytosis when the receptors are co-engaged to targets (14). Site-directed mutagenesis was then used to create strategic CYT

proximal (IpLITR 1.1b$^{Porx\ CYT}$) and distal (IpLITR 1.1b$^{Distal\ CYT}$) dysfunctional mutant IpLITR 1.1b constructs. When IpLITR 1.1b$^{Distal\ CYT}$ was co-engaged with IpLITR 2.6b, no inhibition was observed, and target beads were engulfed comparable to the phagocytic response seen for the IpLITR 2.6b engaged with targets alone. IpLITR 1.1b$^{Porx\ CYT}$ was able to induce inhibition of IpLITR 2.6b-mediated phagocytosis equivalent to IpLITR 1.1$^{wt\ CYT}$; however, when observed over time, IpLITR 1.1b$^{Porx\ CYT}$ was unable to sustain inhibition and resulted in IpLITR 2.6b-mediated engulfment of targets when cells and beads were incubated together for more extended periods of time (14). It was theorized that similar to characterization studies in mouse NK-like cells (13), Csk was possibly being recruited to the membrane proximal region and playing a role in sustaining IpLITR inhibition (14). Microscopy and co-immunoprecipitation revealed that indeed Csk was being recruited to the membrane proximal region of IpLITR 1.1b. It was also observed that the membrane distal region was able to recruit SHP-2 and was most likely responsible for the attributed inhibition seen. Interestingly, SHP-2 recruitment to IpLITR 1.1b as well as dampening of phosphotyrosine signalling is dependent on the crosslinking of IpLITR 1.1b and IpLITR 2.6b, and that singular engagement of 1.1b did not result in SHP-2 recruitment. It is suggested that perhaps a feedback loop is created for ITAM-associated phagocytosis in that IpLITR 2.6b activation is required for its own inhibition by recruitment of kinases for possible phosphorylation of residues within the ITIM-containing receptor IpLITR 1.1b.

In conclusion, IpLITR 1.1b-mediated control of phagocytosis is dependent on the recruitment of key signalling molecules that can dampen stimulatory signalling during receptor crosstalk. IpLITR 1.1b can also dynamically control inhibition through the recruitment of molecules to specific regions within its CYT, highlighting new mechanisms of teleost-based receptor control of effector immune responses.

2.5 Zebrafish (*Danio rerio*) as a Research Model

Zebrafish has been a model organism in many biology fields and have been used in various research ranging from behavioural perception and cognitions studies in the 1960s (142) to more recent studies in genetics using CRISPR-Cas9 genome editing (143). Regardless of the field of study, rapid generation time, ease of care, a fully annotated genome, and similar tissue and organ structure to mammals make zebrafish an excellent comparative experimental model system (144). This is no exception for immunological studies, as adult zebrafish contain complete immune systems with adaptive and innate immune branches (145). The zebrafish model also offers a separation of the immune system whereby only innate immunity is present early on in embryogenesis, while the adaptive system is fully functional by 4 - 6 weeks post fertilization (wpf). Even in embryos, zebrafish have been shown to possess important innate immune cells similar to mammals. For example, besides containing neutrophils that aid in the resolution of wound inflammation (146), macrophage-like cells have been described to phagocytose bacteria (147). Macrophage cells have been detected in zebrafish as early as erythrocytes and migrate to sites of intravenous injection, where they engulf and destroy large quantities of bacteria. The detection of migrating macrophages within zebrafish has also been observed in infected body cavities isolated from the main blood supply. Similar to mammals, zebrafish macrophages also become activated in the presence of insults, however, only a portion of macrophages were detected to be activated in areas of bacterial infection (147). Many immune genes and proteins of zebrafish are homologous to that of mammals, such as interferon responsive genes (e.g., psmb9, immunity-related GTPases (IRGs), and ifn itself), which were upregulated in the presence of IFN-γ1 and IFN-γ2 (148). Further examination also found that IFN-γ signalling is crucial for the resistance of bacterial infection in zebrafish embryos when a

decrease in the survival of ifn-γ-knockout embryos resulted during *E. coli* and *Yersinia ruckeri* infection.

A wide variety of immune genes and cell types have allowed zebrafish to be an excellent model for studying aspects of innate immunology. This also extends to zebrafish innate immune receptors-types found to contain members related to that of mammalian receptor families as well as novel fish-specific receptor families. Zebrafish have been found to contain approximately twenty-four TLR variants, of which ten are described to be orthologous to certain human TLR members (e.g., TLRs 2-5, 7-9) (149,150). Zebrafish TLR22 is closely related to the toll 9 gene in *Drosophila melanogaster* and is part of a fish-specific subfamily, while TLR21 is found in fish, amphibians, and birds. Of these identified zebrafish receptors, a proportion of them have been described as being possible spliced variants (e.g., TLR 4.1a and 4.1b), while others may be the result of gene duplications (e.g., TLR4.1 and 4.2). Downstream signalling molecules of TLR-induction have also been characterized, including molecules such as MYD88, TRIF, IRF3 and IRF7 within zebrafish (151–153). NITRs are another receptor family that has been studied in zebrafish. As mentioned previously, these fish-specific members of the IgSF contain two Ig domains, a TM region, and tyrosine motif-containing CYT (154). Close to forty NITR genes spread across four receptor subfamilies were found to be encoded within zebrafish linkage group 7 through radiation hybrid panel mapping, a technique used to characterize chromosomes by determining the distance between regions of interest. Regions flanking this cluster share similarities to the genomic regions within mouse chromosome 7 that contains conserved synteny to the LRC encoded region of human chromosome 19q13.3-q13.4 (154). Overall, zebrafish are an excellent model to study aspects of the vertebrate innate immune system thanks to features such as rapid growth, range of immune cells, and presence of immune genes similar to that of

mammals. Zebrafish containing both homologous and teleost-specific immune receptor families also establish zebrafish as a foundational platform for studying the immunoregulatory receptor-mediated control of innate immune cell effector responses.

2.5.1 Zebrafish LITRs

Five putative LITR-types from zebrafish were originally identified from an early assembly of the zebrafish genomes (15). However, it has been estimated that at least 137 LITR-related Ig-like receptor domains are present in the zebrafish genome (155). Subsequent research in our lab further utilized zebrafish as a model to understand the potential role LITRs may play *in vivo*. Initial database searches were conducted using IpLITRs (i.e., IpLITR 1, IpLITR 2 and IpLITR 3) as query sequences for BLASTp searches with top matches being screened for the presence of extracellular Ig domains, TM regions, as well as CYT regions (15). Of the potential zebrafish LITR-types that were identified, four were chosen for further study due to their unique CYT characteristics and were named based on the chromosome they were identified on. For example, DrLITR 1.2 is located on zebrafish chromosome 1 (represented by the 1 before the period) and was the second LITR found on that chromosome (represented by the 2 after the period). Initial screening of receptors described DrLITR 1.2 and DrLITR 1.1 containing three Ig domains, as well as TM and CYT regions containing two contrasting signalling motifs, an ITAM and ITIM. This is a motif arrangement typically unseen in individual immune signalling receptor tails. DrLITR 1.1 was considered a partial sequence due to the absence of a signal peptide and a start codon. DrLITR 15.1 contains three extracellular Ig domains, a TM and a CYT with two tandem ITIM motifs as well as an ITSM (15), reminiscent of the IpLITR 1.1b distal domain (127). DrLITR 23.1 contains four extracellular Ig domains, a short CYT, and a TM region with a positively charged lysine residue (15). To confirm the expression of these DrLITR-types, RT-

PCR was performed, where it was found that all the identified DrLITR-types were expressed in adult zebrafish as well as embryo development. Additionally, sanger sequencing was performed to confirm the structure of DrLITRs compared to database searches. Overall, DrLITR 1.1 and DrLITR 1.2 were similar (>95%) to the identified sequences from BLAST searches while DrLITR 15.1 was found to contain four Ig domains instead of the predicted three domains, and DrLITR 23.1 was found to contain a total of six Ig domains (15). Additional RT-PCR experiments were then performed using zebrafish cDNA extracted from different developmental stages (i.e., 0 hours post fertilization; hpf to 168 hpf), and it was shown that all the reference DrLITR-types were expressed throughout all the life stages of the zebrafish examined. Comparisons of the DrLITR sequences to other mammalian receptor proteins using position-specific iterative (PSI) basic local alignment search tool (BLAST) revealed homology of DrLITRs to FcRLs and to that of IgSF members encoded within the LRC complex, including CEACAMs, SIGLECs and PSGs (15). As previously mentioned in section 2.3.3, IpLITR characterization studies originally found that IpLITRs were also distantly related to FcRs and FcRLs, as well as LRC-encoded receptors (5,127). However, unlike IpLITRs, there was no observed homology of DrLITRs to LRC-encoded LILRs or KIRs (15).

2.5.2 DrLITR Expression Analysis

To examine DrLITR transcriptional activity, each receptor was examined for their expression in various zebrafish life cycle stages of development using qPCR (15). Specifically, zebrafish were intraperitoneally injected with zymosan (i.e., a fungal ligand for TLR2 and Dectin-1), and RNA was extracted at various time intervals to examine DrLITR expression changes during the course of induced inflammation. As a point of comparison for DrLITR gene expression, selected genes of key inflammatory molecules (i.e., IL-8, TNF-α, MPO, TLR22 and

C6) from various components of the innate immune system were chosen as these molecules have been well characterized for their pro-inflammatory functions in addition to identification of zebrafish life cycle stages these inflammatory markers appear during embryogenic development (156). For example, MPO is an enzyme secreted by neutrophils during degranulation to attack and destroy microbes, while gene expression has been reported to be detected within zebrafish embryos as early as 18 hpf (157). During testing, the gene expression of the inflammatory molecules were observed to generally increase slowly over embryonic development, with expression levels peaking around 1 day post fertilization (dpf) (15). This was also seen for the gene expression of DrLITR 15.1; however it was also shown that all of the DrLITRs examined (e.g., DrLITR 1.1, DrLITR 1.2, DrLITR 15.1 and DrLITR 23.1) were expressed as early as 1 hpf. In comparison to the inflammatory genes, as well as DrLITR 15.1 expression, DrLITR 1.1, DrLITR 1.2 and DrLITR 23.1 expression levels peaked prior to 1 dpf and remained relatively low until 168 hpf (15). Interestingly, all DrLITR-type genes were expressed at significantly high levels in unfertilized eggs, indicating that these receptors may be maternally sourced. This suggests that maternal cell cytoplasm containing RNA for specific genes during the embryo's development is passed to the embryo (158). While the full purpose of this action remains unknown, it is suggested that passing possible immune genes (e.g., DrLITRs) may play a role in zebrafish development (15). For example, in the unfertilized eggs of Atlantic cod (*Gadus morhua*), transcripts of maternally sourced antimicrobial components, such as lysozyme and cathelicidin, were found with lysosome activity also detected at this early developmental stage (159). The transfer of these maternally sourced genes may help prime the innate immune system during fish embryo development for exposure to a pathogen-rich extracellular environment.

During inflammation, various immune genes (e.g., TNF-α, IL-1β, and IL-6), and by association proteins encoded by these genes, are both upregulated and downregulated during the course of infection to allow for swift resolution of infections, while also preventing overall host tissue damage (160). Acute expression of inflammatory components aids in rapid immune defence responses of the host, however continuous (i.e., chronic) expression of these factors can lead to autoimmunity and chronic inflammation; therefore, immune gene expression is tightly regulated and often only induced when immune cells encounter microbes and/or damaged tissues. During infections in fish, a significant upregulation of important immune genes such as IL-1β and TNF-α has been shown to occur (161). In addition, common carp infected with the parasitic ciliate *Ichthyophthirius multifiliis* resulted in the upregulation of complement factor B/C2-A as well as C3, however mannose-binding lectin-associated serine proteases were downregulated compared to non-infected carp (162). In our previous studies, zebrafish were intraperitoneally injected with zymosan and monitored for DrLITR transcriptional activity. (15). Looking at the control genes, IL-1β expression was consistent with published results (156) and was significantly up regulated 2, 6, 8, and 12 hours post injection of zebrafish (15). When examining the gene expression of DrLITRs, DrLITR 1.1 was upregulated ~12 hours post injection while DrLITR 1.2 was upregulated at 3, 6, and 12 hours. Interestingly, DrLITR 15.1 was not significantly upregulated post zymosan injection, and DrLITR 23.1 expression was down regulated 24 hours post zymosan injection compared to control receptor expression levels (15). Overall, DrLITR gene expression after injection of zymosan did not follow a distinct pattern of upregulation as was observed for IL-1β. This variable level of expression is perhaps due to the dynamic functional difference between each of the DrLITR-types. For example, it is known that catfish macrophages express IpLITRs (5) and therefore it is possible that during

inflammation, macrophages could be migrating to the zebrafish viscera to assist with the clearing of insults or damaged cells and tissue repair (e.g., phagocytosis). Increased numbers of macrophages expressing DrLITRs may cause varied expression levels rather than DrLITRs being upregulated during inflammatory responses.

In summary, DrLITRs are expressed by zebrafish at very early stages of development and continue to be expressed throughout the organism's life (15). The presence of receptor gene expression in eggs prior to fertilization indicates that they are perhaps maternally sourced, suggesting that these genes play an important role in fish development in early embryogenesis by priming the innate immune system of the embryo for release into pathogen-rich water. DrLITR gene expression patterns due to exposure to zymosan were not similar to each other or to that of pro-inflammatory cytokines during both embryogenesis and within adult zebrafish, which may indicate that receptors within the group may have different functional roles. The non-significant up or downregulation observed for DrLITR 15.1 and the downregulation for DrLITR 23.1 could be a result of specific immune cell-types basely expressing these receptors on their surface. In the process known as efferocytosis, immune cells clear apoptotic cells through cellular engulfment related to phagocytosis (15,163). Coordination of receptors on the surface of immune cells are required to effectively bind to target cells allowing for other receptors to be engaged for the cellular engulfment. Thus, receptors such as DrLITR 15.1 and DrLITR 23.1 that are continuously expressed on the surface of immune cells mediate the binding of the ligand allowing for other receptors (e.g., DrLITR 1.2 and DrLITR 1.1) to bind and engage the target for its engulfment and destruction (15).

2.6 Conclusions

LITRs were discovered over a decade ago within channel catfish and were shown to be co-expressed by myeloid and lymphoid immune cell lines. At the time of discovery, IpLITRs were shown to be related to mammalian receptor-types, including LRC-encoded receptors (e.g., KIRs and LILRs) as well as FcR and FCRL receptor families. However, recent syntenic analysis has cemented their relation to the FcR and FCRLs. Currently, there is no identification of the ligands for LITRs hampering our knowledge of the overall role these receptors may play in teleost immunity. Nevertheless, mammalian expression systems have been essential for studying LITRs' immune cellular networks and controlling innate immune cell effector functions. Specifically, IpLITRs have been shown to regulate cytotoxicity, degranulation, cytokine secretion, and phagocytosis. However, the versatility of LITR signalling is context-dependent displaying very different outcomes when expressed within differing cell types. When examining immunoreceptor tyrosine-based motifs within the CYT of IpLITRs, the tail regions' modularity displays stimulatory and inhibitory properties, synergistically fine-tuning the immune regulation of not only the receptor itself but also other catfish immune receptors through LITR-mediated crosstalk. In addition, the ability of the putative inhibitory receptor IpLITR 1.1b to induce an F-actin-dependent mode of phagocytosis showcases that receptor-based immunoregulation has developed functional plasticity early on in the evolution of signalling pathways among vertebrates.

Increasing evidence of receptor function is beginning to reveal that in specific contexts, ITAM-containing receptors display inhibitory properties while ITIM-containing receptors can also activate signalling pathways. For example, as mentioned previously, the ITIM-containing receptor IpLITR 1.1b can inhibit lymphocyte-mediated cytotoxicity and induce an ITAM-independent mode of phagocytosis through recruitment of classical activating associated

signalling molecules when expressed in certain myeloid cell lines. Rather than simple finite control of cellular responses, interactions of receptors and their integrated signalling motifs act to dynamically fine-tune receptor signalling events. Clearly, the classical definition of inhibitory and stimulatory receptors based solely on the presence of certain signalling motifs is unreliable and requires more extensive study. As such, LITRs displaying unique arrangements of signalling motifs (i.e., IpLITR 1.1b; membrane distal CYT containing two ITIMs, ITSM, proximal region with three tyrosine residues) are an excellent model for the examination of possibly new mechanisms of vertebrate receptor-mediated control of signalling that has already begun to reveal novel immune regulatory mechanism controlling innate immune cell effector responses.

The recent identification of several DrLITR-types has also revealed unique arrangements of immunoreceptor tyrosine-based motifs (i.e., ITAM and ITIM) within their CYTs. The presence of putative functionally contrasting tyrosine motifs within the CYT allows for formulating new hypotheses regarding immunoregulatory receptor signalling mechanisms. To investigate the signalling potential of these new DrLITR receptor-types, my research aims in this thesis are; i) to create wild-type and signalling motif dysfunctional DrLITR constructs to generate DrLITR-expressing AD-293 cell lines, ii) examine the phagocytic potential of DrLITRs using a flow cytometric phagocytosis assay, and iii) examine how the ITIM-augments the phagocytic capacity of DrLITR 1.2. These DrLITRs represent a possible new receptor-based mechanism in which vertebrates can regulate effector responses and may further our insight on immune regulation functional plasticity.

Chapter III

Materials and Methods

3.1 Cell lines, Antibodies & Plasmid Constructs

3.1.1 Cells

AD-293 cells, an adhesion-enhanced version of HEK-293 cells, were cultured in Dulbecco's Modified Eagle Media (DMEM; Sigma-Aldrich, St. Louis, MO) supplemented with 10% heat-inactivated fetal bovine serum (FBS: (Thermo Fisher Scientific, Waltham, MA) 100 units/mL of penicillin + 100 mg/mL of streptomycin (Gibco; Thermo Fisher Scientific) incubated at 37°C, 5% CO_2. For routine passage of cells in a 75cm^2 vented culture flask, once cells had reached ~80% confluency, culture media was decanted, and cells were washed with 5 mL of prewarmed Dulbecco's phosphate-buffered saline (DPBS). DPBS was removed, and cells were then washed with 2mL of 0.05% trypsin + EDTA and incubated at 37°C, 5% CO_2 for 5 minutes. Cells were then resuspended with the addition of 3 mL fresh culture media, aided by careful dislodging of cells with a cell scraper. 600 µL of cell suspension was then transferred to a new vented flask containing 10 mL of fresh culture media.

3.1.2 Antibodies

The following antibodies were used to detect and engage LITR constructs on the surface of AD-293 cells: Mouse α-HA mAb IgG_1 (Invitrogen; Thermo Fisher Scientific, Waltham, MA), Mouse α-FLAG mAb IgG_1 (Invitrogen), Mouse IgG_1 isotype (Invitrogen), AF647 conjugated Rabbit-α-Mouse (H+L) pAb (Invitrogen), PE-conjugated Goat-α-Mouse (H+L) F(ab')2 (Invitrogen).

The following antibodies were used for confocal microscopy: Rabbit α-pSHP2 pAb (Cell Signalling Technology, Danvers, MA), Rabbit α-pSyk pAb (Cell Signalling Technology), AF488 conjugated Goat-α-Rabbit pAb (H+L) (Invitrogen), AF647 conjugated Goat-α-Mouse (H+L) pAb (Invitrogen).

3.1.3 Plasmid Constructs

Zebrafish cDNAs containing DrLITRs (DrLITR 1.2 and DrLITR 15.1) were obtained from a previous graduate student (Hima Gurupalli) (164). Generation of N-terminal hemagglutinin (HA) epitope-tagged pDisplay constructs were generated as described previously (7,8,12,14). Briefly, oligo primers (Table 3.1; IDT) were designed against DrLITR sequences with the addition of flanking restriction sites (SmaI/SalI) and were used in reverse transcriptase PCR (RT-PCR) reactions. RT-PCR reactions were set up as follows; 0.2 μL of Phusion High-Fidelity DNA polymerase (Invitrogen), 1 μg of provided zebrafish cDNA as template, 1 μL of each flanking primer as mentioned above (10 mM), 0.4 μL of 10 mM dNTPs, 4 μL of 5X Phusion HF buffer, nuclease-free H_2O to create a total mixture volume of 20 μL. For all PCR reactions, thermocycler conditions were as follows; denaturation took place at 98°C for 1 minute, followed by 30 round cycles of denaturation at 98°C for 15 seconds, annealing of DNA at 60°C for 30 seconds and extension at 72°C for 1 minute. After cycling, a final extension took place at 72°C for 10 minutes. PCR products were digested with SmaI and SalI restriction enzymes (FastDigest; Thermo Fisher Scientific) and ligated into pDisplay mammalian expression vector (Invitrogen; Thermo Fisher Scientific) that adds HA-tagged epitopes to receptor constructs allowing for the detection and activation of receptors using α-HA monoclonal antibodies (mAb; Invitrogen; Thermo Fisher Scientific). All plasmid constructs were subsequently confirmed for

the presence of ligated products the sequenced at the Molecular Biology Service Unit (MBSU) at the University of Alberta

Signalling deficient mutants were created to study the role that immunoreceptor tyrosine-based activation motif (ITAM) and immunoreceptor tyrosine-based inhibitory motif (ITIM) have on receptor-signalling dynamics within the same cytoplasmic tail region. To create these mutant constructs, pDisplay DrLITR 1.2 ^{wt} was used as a template to generate mutated tyrosine residues within the CYT motif regions. Internal primers (Table 3.1) were designed against DrLITR 1.2 ^{wt} CYT ITAM and ITIM regions to mutate tyrosine (Y) into phenylalanine (F) by replacing a single nucleotide within internal primers to create a missense mutation with the addition of regions of nucleotide overlap between the internal primers to allow for overlap extension during PCR reactions. DrLITR 1.2 $^{ITAM\ ko}$ has two Y`s in the ITAM region of the CYT mutated to F (i.e., DrLITR 1.2 ^{wt} tyrosines 356/368). DrLITR 1.2 $^{ITIM\ ko}$ has Y in the ITIM region of the CYT mutated to F (i.e., DrLITR 1.2 ^{wt} tyrosine 391).

Site-directed mutagenesis was broken up into two parts; creation of the two overlapping PCR products containing the missense mutation and the overlap extension of the two PCR products to create a full-length DNA fragment of the LITR construct. Initially, two sets of PCR reactions were conducted between the forward (Fwd) flanking primer and the reverse (Rvs) internal motif overlap primer and between the Rvs flanking primer and the Fwd internal overlap primer. These PCR reactions were performed as described for RT-PCR above with the additional exception of 50 ng of pDisplay DrLITR 1.2 ^{wt} being used as a template DNA. Following the first part of site-directed mutagenesis, the products went through PCR product purification and were then used as templates for the second part of site-directed mutagenesis. For overlap extension PCR, the reaction was conducted as described above for RT-PCR with the exception that two

PCR products were both used as DNA template (50 ng each) and no primers were used. PCR thermocycler conditions were changed to only run for 10 rounds during the temperature cycling stage. After overlap extension occurred, the original Fwd and Rvs 1.2 ^{wt} flanking primers were added to the reaction and an additional full PCR reaction occurred with no modification to the thermocycler conditions was performed. As described above, mutated constructs were similarly digested (SmaI/SalI) and ligated into pDisplay mammalian expression vector.

3.2 Creation of DrLITR stably expressing AD-293 cell lines

DrLITR-expressing cell lines were established through cellular transfection of AD-293 cells with DrLITR-containing plasmids. Prior to transfection, $2x10^5$ parental AD-293 cells were seeded in 24-well culture plates in DMEM -/- and 10% FBS. The next day 1 µg of each pDisplay construct plasmid DNA (i.e., DrLITR 1.2 ^{wt}, 1.2 $^{ITIM\ ko}$, 1.2 $^{ITAM\ ko}$, 15.1) was added to 2 µL of Turbofect reagent (Fisher Scientific) with the addition of Opti-MEM reduced serum media (Gibco; Thermo Fisher Scientific) to a total volume of 100 µL. Transfection mixtures were vortexed for at lead 15 seconds and incubated at room temperature for 15 minutes. Transfection mixtures were then added dropwise to seeded cells and were grown at 37°C and 5% CO_2 for 48 hrs. Transfected AD-293 cells were selected for by replacing growth media for DMEM supplemented with 800 µg/ml of G418 disulfate salt solution (Sigma-Aldrich) for 1 week.

Viable cells were sorted through FACs sorting to select AD-293 cells stably expressing high levels of DrLITR constructs on their surface (14). Briefly, post-selected cells were washed with DPBS and 0.05% trypsin + EDTA. These cells were then harvested, and ~$1x10^5$ cells were moved to Eppendorf tubes containing 500 µL of sorting buffer (1x DPBS, 0.5% bovine serum albumin; BSA, 2 mM EDTA). Samples were then centrifuged for 2.5 minutes at 500 x g; the supernatant was aspirated, and samples were resuspended in 50 µL sorting buffer containing

primary antibody (0.1 μg of αHA mAb or IgG_1 isotype control). Samples were then incubated on ice for 30 minutes, subsequently washed with 1mL ice-cold sorting buffer, centrifuged for 2.5 minutes at 500 x g, decanted, and were resuspended again with 50 μL of sorting buffer containing 0.25 μg of secondary antibody (PE-conjugated goat-α-mouse F(ab')2). Staining and washing steps, as described above, were repeated, and samples were resuspended in 250 μL of sorting buffer. Samples were then sorted based on their HA-epitope staining expression, and the top 5% of expressing cells were sorted as single-cell clones into a 96-well culture plate using the BD FACS Aria™ III cell sorter. Individual clones were then allowed to grow to confluency and screened for their levels of DrLITR surface expression.

3.3 Examination of construct surface expression through flow cytometry

To examine DrLITRs expression on the surface of AD-293 cell lines, cells were screened for their levels of HA-epitope tagged receptor surface expression similar to what was described in Section 3.2 of this thesis. Briefly, cell lines were grown to ~ 80% confluency and were harvested with 0.05% trypsin + EDTA. ~$1x10^5$ cells were then moved to Eppendorf tubes containing 500 μL of FACS buffer (1x DPBS, 0.5% bovine serum albumin, 2 mM EDTA, 0.05% NaN_3). Samples were then centrifuged for 2.5 minutes at 500 x g; the supernatant was aspirated, and samples were resuspended in 50 μL of FACS buffer containing primary antibody (0.1 μg of αHA mAb or IgG_1 isotype control). Following incubation on ice for 30 minutes, cells were subsequently washed with 1 mL ice-cold sorting buffer, centrifuged for 2.5 minutes at 500 x g, decanted, and were resuspended again with 50 μL of FACS buffer containing 0.25 μg of secondary antibody (PE-conjugated goat-α-mouse F(ab')2). Staining and washing steps, as described above, were repeated, and samples were resuspended in 250 μL of FACS buffer. Analysis was conducted using an Attune Nxt Flow Cytometer (Thermo Fisher Scientific,

Waltham, MA), and stained cells were gated based on FSC-A versus SSC-A parameters to remove cellular debris and large aggregates. FSC-A was gated versus FSC-H to remove doublets, and receptor expression was gated based on the level of PE fluorescent intensity and compared to IgG_1 stained isotype controls.

3.4 Imaging Flow Cytometry Phagocytosis Assays to Examine DrLITR-mediated Phagocytosis

3.4.1 Establishment of Optimal Conditions for DrLITR-mediated Phagocytosis by Comparing Protein A vs Protein G-coated Beads

To establish optimal conditions for DrLITR-mediated phagocytosis, antibody-specific binding to both protein A and protein G was examined using flow cytometric phagocytosis assays (14). Briefly, 4.5 μm yellow-green (YG) beads (Polysciences, Warrington, PA) were pre-absorbed with either protein A or protein G (Sigma-Aldrich) and opsonized with 2 μg/mL of α-HA mAb or with 2 μg/mL of IgG_1 isotype control. One day prior to experiments, $3x10^5$ IpLITR 2.6b and DrLITR (i.e., 1.2 ^{wt}, 1.2 $^{ITIM\ ko}$, 1.2 $^{ITAM\ ko}$, 15.1) stably expressing AD-293 cells were seeded in a 24-well cell culturing plate in normal growth media (DMEM, 10% FBS, 400 μg/mL G418) and allowed to adhere to the culture plate overnight. On the day of the experiments, growth media was removed from the cells and replaced with 500 μL prewarmed phagocytosis buffer (1:1 ratio of 1xDPBS with 2 mg/mL bovine serum albumin (BSA) and Opti-MEM). $9x10^5$ opsonized YG beads were added to each sample as phagocytic targets with bead-cell interactions synchronized through centrifugation at 100 x g for 1 min, then incubated at 37°C for 15 minutes. The phagocytosis buffer was removed, and samples were washed with DPBS, followed by the addition of 200 μL of ice-cold phagocytosis buffer with 0.5 μg of secondary antibody AF647 conjugated rabbit-α-mouse pAb to differentiate surface-bound bead events from phagocytic bead

events. Samples were then incubated at 4°C for 30 minutes, the antibody mixture was removed, and cells were washed with DPBS. Samples were harvested with 0.05% trypsin + EDTA and moved to Eppendorf tubes, then centrifuged at 500 x g for 2.5 minutes before the supernatant was aspirated. To remove non-specifically bound bead targets from cells, samples were resuspended with 200 µL of ice-cold 0.05% trypsin + EDTA and incubated on ice for 10 minutes. 1 mL of ice-cold phagocytosis buffer was added to samples, followed by centrifugation at 500 x g for 2.5 minutes. Samples were aspirated, and pellets were resuspended in 25 µL of DPBS + 1% paraformaldehyde (PFA) and were analyzed on the ImageStream mkII (Amnis; Luminex, Austin, TX). Briefly, 5000 cell events were collected, and data was analyzed using the IDEAS® v6.2 software (Amnis); connected component masking (14,165) was used to accurately differentiate between cells with phagocytosed beads or cells with only surface-bound beads.

Specifically, to resolve bead positioning relative to the cell, a secondary antibody stain (AF647) was added to samples which recognize the primary antibodies on the surface of the bead targets. As such, beads that were fully internalized would not be stained, as the secondary antibody would be unable to cross the plasma membrane. IDEAS® software allowed for accurate discrimination of bead positioning through a series of masks based on fluorescence, as described in (165). Connected component masks were set up to analyze relative bead size (i.e., large beads were classified as component 1, smaller beads were classified as component 2, etc). Only cells containing three or less beads were gated as analysis of cells with four beads and higher were reported to interfere with accurate analysis of fluorescence. Further masks were set up to analyze each detected event by measuring the relative levels of fluorescence of both green (YG beads) and red (AF647) fluorescence. With this analysis, cell-bead interactions were then defined based on the presence or absence of the 647 fluorescence; cells that contained bead(s)

that associated with red fluorescence were classified as surface-bound, while cells that contained at least one bead absent of the red fluorescence was defined as phagocytic.

3.4.2 Establishment of Optimal Conditions for DrLITR-mediated Phagocytosis by Comparing Concentration of mAbs on Opsonized Bead Targets.

To establish optimal conditions for DrLITR-mediated phagocytosis, phagocytic targets were opsonized with varying antibody concentrations to allow for the greatest resolution in phagocytic phenotype between DrLITR constructs analyzed through imaging flow cytometry. Briefly, 4.5 μm YG beads were pre-absorbed with protein G and opsonized with varying concentrations of α-HA mAb (i.e., 1 μg/mL, 0.5 μg/mL, 0.25 μg/mL) or with 1 μg/mL of IgG_1 isotype control. A phagocytosis assay was conducted as described in section 3.4.1 with the exception of DrLITR (i.e., 1.2 ^{wt}, 1.2 $^{ITIM\ ko}$, 1.2 $^{ITAM\ ko}$, 15.1) cell lines incubated with $9x10^5$ bead targets with varying mAb concentrations for 0, 15 and 30 minutes.

3.4.3 Establishment of Optimal Conditions for DrLITR-mediated Phagocytosis by Comparing Bead-Cell Incubation Times

To observe optimal conditions for DrLITR-mediated phagocytosis, bead-cell interactions were observed on a time scale to visualize differences in the phagocytic phenotype between DrLITR constructs. A phagocytic, flow cytometric assay was conducted similarly to section 3.4.1 with the exception of cell samples incubated at differing times (0 minutes, 5 minutes, 10 minutes, 15 minutes) with 4.5 μm bead targets preabsorbed with protein G and opsonized with 1 μg/mL α-HA mAb.

3.4.4 Examining DrLITR-based Target Binding Abilities

The ability of receptor-expressing cells to bind to phagocytic targets during recovery from suboptimal temperatures was observed through imaging flow cytometry to further resolve the phagocytic phenotype between DrLITR constructs. AD-293 cells ($3x10^5$) expressing DrLITRs (i.e., 1.2 ^{wt}, 1.2 $^{ITIM\ ko}$) were seeded in a 24-well cell culturing plate in normal growth media and allowed to adhere to the culture plate overnight. On the day of the experiments, the growth media was removed from the cells and replaced with 500 µL ice-cold phagocytosis buffer. Cells were incubated for 30 minutes at 4°C before the addition of $9x10^5$ 4.5 µm YG beads preabsorbed with protein G and opsonized with 1 µg/mL α-HA mAb or with 1 µg/mL of IgG_1. Following centrifugation of samples at 100 x g for 1 minute, samples were incubated for a further 30 minutes at 4°C. Cells were then moved to a 37°C incubator and allowed to warm up at specific time intervals (i.e., 0, 2, 4, 8, 16 minutes; 16 minutes for IgG_1 coated beads). Samples were then counter-stained, processed, and analyzed as described in section 3.4.1.

3.4.5 Pharmacological Assessment of DrLITR-mediated Phagocytosis

Pharmacological inhibitors targeting common intracellular signalling molecules were tested using imaging flow cytometry to examine the possible role and recruitment of specific signalling molecules likely required for DrLITR-mediated phagocytosis. AD-293 cells ($3x10^5$) expressing IpLITR 2.6b and DrLITR (i.e., 1.2 ^{wt}, 1.2 $^{ITIM\ ko}$) were seeded in a 24-well cell culturing plate 1 day before experimentation. The following day, cell media was removed, and samples were washed with DPBS. A phagocytosis buffer containing a high dose (HD) and a low dose (LD) of various pharmacological inhibitors (Table 3.2.) was added, and samples were incubated at 37°C for 1 hour. As a vehicle control, samples were also incubated for 1 hour with 0.5% DMSO. Without removing drug-inoculated phagocytosis buffer, $9x10^5$ YG beads

opsonized with either 1 μg/mL of α-HA mAb, 0.4 μg/mL of α-HA mAb + 2.5 μg/mL of isotype IgG_1, or with 1 μg/mL of IgG_1 isotype control, were added to seeded cell samples and synchronized through centrifugation at 100 x g for 1 minute. To further assess the effects of the drug NSC 87877 on LITR-mediated phagocytosis, a cell line co-expressing IpLITR 2.6b-1.1b was also seeded in 24 well cell culture plates and preincubated with HD and LD of NSC 87877 (or 0.5% DMSO). To engage both LITRs for receptor-mediated cross talk, 2.6b-1.1b expressing cells were incubated $9x10^5$ YG beads opsonized with 0.4 μg/mL of α-HA mAb + 2.5 μg/mL of α-FLAG mAb and centrifuged for 1 minute at 100 x g. Samples were then processed and analyzed as described in section 3.4.1.

3.5 Confocal Microscopy Examination of Signalling Molecule Recruitment during DrLITR-mediated Phagocytosis

3.5.1 Examining the Recruitment of pSHP-2 and pSyk to the Phagocytic Cup during DrLITR-mediated Phagocytosis

To examine the recruitment and involvement of signalling molecules to the phagocytic cup during DrLITR-mediated phagocytosis, a fluorescence confocal microscopy-based phagocytosis assay was performed. Briefly, $2x10^5$ IpLITR (i.e., 2.6b-1.1b) and DrLITR (i.e., 1.2^{wt}, $1.2^{ITIM\ ko}$, $1.2^{ITAM\ ko}$) stably expressing AD-293 cells were seeded on top of microscope cover slips in a 24-well cell culturing plate and allowed to adhere overnight. Growth media was removed from the cells and replaced with 500 μL prewarmed phagocytosis buffer. $6x10^5$ non-fluorescent (NF) polystyrene beads (Polysciences) were opsonized with either 1 μg/mL of α-HA mAb to stimulate DrLITR constructs, 0.4 μg/mL of α-HA mAb + 2.5 μg/mL of α-FLAG mAb for the crosslinking of IpLITR constructs, or 0.4 μg/mL of α-HA mAb + 2.5 μg/mL of IgG_1 isotype control to independently activate IpLITR 2.6b. Opsonized beads were added to each

sample as phagocytic targets with bead-cell interactions synchronized through centrifugation at 100 x g for 1 minute, then incubated at 37°C for 8 minutes. Cells were subsequently fixed with 4% PFA for 10 minutes and were stained both extracellularly and intracellularly via immunofluorescence (9,10,14). Samples adhered to coverslips were transferred to parafilm containing 0.5 µg/mL of AF647 conjugated goat-α-mouse secondary pAbs diluted in 50 µL of antibody staining buffer (ASB; DPBS with 1% BSA and 0.05% NaN_3). Samples were then incubated at 4°C for 30 minutes, moved back into 24-well culture plates and washed with ASB before the addition of 1x permeabilization buffer (Biolegend, San Diego, CA) and incubated at room temperature for an additional 15 minutes. Samples on cover slips were once again moved to parafilm containing 50 µL of cell staining buffer (CSB; Biolegend) with a 1:50 dilution of either rabbit α-pSHP2 pAb or rabbit α-pSyk pAb. After an additional 30 minutes at room temperature, samples were washed with CSB and moved a final time onto parafilm with 50 µL of CSB containing 2µg/mL of AF488 conjugated goat-α-mouse secondary pAb for a final 30 minutes at room temperature. Samples were washed one final time with CSB and mounted onto microscope slides with ProLong Gold Antifade (Thermo Fisher Scientific) and allowed to set for 12 hours at room temperature. Samples were visualized with a Laser Scanning Confocal Microscope (LSM; Zeiss LSM 710, 63x objective 1.2 oil plan-Apochromat) with bead-cell event images collected and analyzed through Zen Lite (Zeiss, Oberkochen, Germany) analysis software. To measure mean fluorescent intensities (MFI) of pSHP-2 and pSyk recruitment during LITR-mediated phagocytosis of bead targets, a representative line was drawn across phagocytic cup formation with intensities of fluorescence for both the signalling molecules and the bead counter stain measured across the representative line using both Zen Lite and ImageJ (NIH) software. To further measure consistent MFI values of pSHP-2 recruitment within the phagocytic

cup formation, at least 50 bead-cell interactions per sample were measured for their mean area of fluorescence (MAF) within a zone of interest at bead-cell interfaces analyzed through Zen Lite software.

3.6 Statistical Analysis

Means of multiple groups were compared together by ANOVA followed by post-hoc Tuckey analysis to determine statistical significance between groups of samples (denoted by alphabetically assigned letters; Prism 6, GraphPad, San Diego, CA). To determine the significance differences between two groups, a non-parametric t-test was used (Mann-Whitney; denoted by asterisks; Prism 6, GraphPad, San Diego, CA).

Table 3.1. PCR primers used in this thesis.

Primer Name	Sequence 5' – 3'
DrLITR 1.2 SmaI Fwd [a]	TCCCCCGGGTACTCAAAAACTGCAATAT
DrLITR 1.2 SalI Rvs [a]	GCGTCGACGAAATAAGTCAAGATGTGAC
DrLITR 1.2 $^{ITIM\ ko}$ **Overlap Fwd** [b]	GTGAAGATGATGGTTCCACATTTTTTAATATTGATC
DrLITR 1.2 $^{ITIM\ ko}$ **Overlap Rvs** [b]	TGTGGAACCATCATCTTCACGGTCGTCTG
DrLITR 1.2 $^{ITAM\ ko}$ **Overlap Fwd** [b]	GACCCCAATTCCAGATGCTCTGAGTTCGACACA
DrLITR 1.2 $^{ITAM\ ko}$ **Overlap Rvs** [b]	TCTGGAATTGGGGTCAAGGGCCATGAAGGGATC
DrLITR 15.1 SmaI Fwd [a]	TCCCCCGGGTTCAATCCAACAGAAGTAAA
DrLITR 15.1 SalI Rvs [a]	GCGTCGACTCATTGAGGCACCTGAGAATA
pDisplay Fwd [c]	TAATACGACTCACTATAGGGA
pDisplay Rvs [c]	ATCCTCTTCTGAGATGAGTTT

[a] Primers used to amplify 1.2 sequences for ligation into pDisplay plasmids. [b] Primers used for overlap extension mutation of specific signalling motifs within the CYT of 1.2 ^{wt}. [c] Primers used for the amplification of pDisplay-ligated sequences for sequencing and conformation.

Table 3.2. Pharmacological inhibitors, molecular targets, and doses tested

Drug	Intracellular Target	High Dose (μM)	Low Dose (μM)
PP2	Src-family tyrosine kinases	10	1
ER 27319	Syk kinase	250	25
Wortmannin	PI3K, PLK1, MLCK	10	1
NSC 87877	SHP-2, SHP-1, PTP1B	3.2	0.32
Cytochalasin D	Actin polymerization	25	N/A

Chapter IV

Examination of DrLITR-mediated Control of the Phagocytic Response

4.1 Introduction

Phagocytosis is an actin-dependent cellular engulfment process of extracellular particles greater than 0.5 μm (89). Typically, the process is initiated by the engagement of surface-bound phagocytic immune receptor-types that recognize specific ligands resulting in the phosphorylation of tyrosine residues within ITAM-containing CYT motifs, recruitment of intracellular signalling molecules, induction of intracellular signalling, activation of actin polymerization machinery, membrane remodelling, and finally internalization of the target. For example, following the binding of IgG-ligand complexes, human FcγR associates with the ITAM-containing adaptor FcRγ (51). SFKs located in close proximity to these motif-containing receptors phosphorylate tyrosine residues within ITAMs, allowing for the recruitment of the SH2 domain-containing molecule Syk. This kinase is then activated by SFK-mediated phosphorylation resulting in signalling cascade propagation and, eventually, the stimulation of the actin polymerase machinery (89).

Our lab has extensively studied LITRs as a teleost immune receptor model system for understanding the regulation and control of innate immune effector responses. Two contrasting IpLITR-types have been well studied in their control over immune effector responses, emphasizing their ability to regulate phagocytosis. Specifically, IpLITR 2.6b is a stimulatory receptor-type that induces an ITAM-dependent mode of phagocytosis (8,11,12,14). This

phenotype has been well described for mammalian receptor models (e.g., FcRs) and is facilitated by the phosphorylation of tyrosine residues found within the ITAM for the recruitment of stimulatory molecules such as Syk (51). Subsequent recruitment and activation of downstream signalling molecules results in F-actin-driven engulfment of targets. The putative inhibitory receptor IpLITR 1.1b was shown to induce a novel ITAM-independent mode of phagocytosis when transfected into RBL-2H3 cells (9–12). However, unlike IpLITR 2.6b, this LITR-type induced a stalled capture and engulfment phenotype facilitated by long filopodia-like protrusions from the membrane (10,11). When both IpLITR 2.6b and IpLITR 1.1b were co-transfected into a mammalian non-immune cell line (AD-293), IpLITR 2.6b was again able to induce an ITAM-dependent mode of phagocytosis in these cells, however, IpLITR 1.1b was not able to generate any mode of phagocytosis (14). When both receptors were co-engaged, IpLITR 1.1b significantly cross-inhibited the signalling potential and phagocytic response of IpLITR 2.6b through a SHP-2-dependent mechanism. Interestingly, the ability of IpLITR 1.1b to sustain inhibition was mediated through the recruitment of Csk to its membrane proximal CYT region.

Recently, we have identified several new LITR-types within the genome of the zebrafish (*Danio rerio*) (15). These LITR-types were upregulated as early as 1 hour post fertilization in zebrafish embryos with some LITRs upregulated following zymosan exposures. Interestingly, DrLITR 1.2 and DrLITR 1.1 contain a unique arrangement of tandem ITAM and ITIM signalling motifs within their CYT region. This arrangement within the same receptor-type is unusual as these motifs are typically associated with separate stimulatory (i.e., ITAM) and inhibitory (i.e., ITIM) receptor-types (19). Co-engagement of inhibitory and stimulatory receptor-types on the same cell results in crosstalk regulation allowing for fine-tuning of immune responses by creating thresholds for activation. To date, there is no information on the impact of having both

an ITAM and an ITIM within the same CYT of an individual immunoregulatory receptor-type. The novel arrangements of immunoreceptor tyrosine-based motifs within the CYT of these DrLITRs brings into question the specific roles these receptors play in mediating cellular effector responses and suggests a possible role in receptor-based functional plasticity. For example, perhaps the engagement and activation of these receptor-types results in the recruitment of both ITAM and ITIM-specific signalling molecules to the receptor tails. While ITAM-specific kinases (e.g., Syk) can induce stimulatory activation by phosphorylating important signalling molecules resulting in a signalling cascade, the localization of ITIM-specific phosphatases, such as SHP-2 or SHIP1/2, may result in dephosphorylating signalling molecules and other protein domains localized to the receptor tails. Thus, a decreased activation level can be achieved compared to receptors that only contain an ITAM within its CYT, resulting in an overall dampened cellular effector response.

The specific objectives of this chapter were to use a previously established mammalian expression model system to study DrLITR receptor-types and to use this system to investigate the roles of both the ITAM and ITIM motifs within the context of same receptor CYT of DrLITR 1.2 through the aforementioned imaging flow cytometric phagocytosis assay. I hypothesized that DrLITR 1.2 ^{wt} would have an intermediate phagocytic capacity compared to DrLITR 1.2 $^{ITIM\ ko}$ when engaged by target beads, while DrLITR 1.2 $^{ITAM\ ko}$ and DrLITR 15.1 would be unable to initiate phagocytosis. The presence of the ITAM suggests that DrLITR 1.2 can recruit essential signalling molecules such as Syk to induce signalling cascades needed for phagocytosis. As such, the absence of a functional ITAM within both DrLITR 1.2 $^{ITAM\ ko}$ and DrLITR 15.1 suggests that these receptors cannot activate the necessary machinery for the engulfment of targets. In addition, the presence of the ITIM within DrLITR 1.2 ^{wt} may play a role in receptor

inhibitory crosstalk whereby recruited inhibitory molecules (i.e., SHP-2) may result in an increase in the activation threshold of the receptor. Regulation and fine-tuning of receptor-based immune responses are determined by the overall sum of inhibitory and stimulatory signalling. Engagement of stimulatory signalling must overcome inhibitory signals to induce the intended effector response. The presence and activation of inhibitory signalling increase activation thresholds and are crucial in preventing overstimulation of receptors and cellular responses which can lead to autoimmune disease. For example, disrupting the inhibitory receptor FcγRIIB in murine models results in increased Ig release, systemic anaphylaxis, and elevated immune complex-mediated inflammation (19). Therefore the presence of an ITIM within an ITAM-containing receptor may play a role in regulating the intensity of receptor signalling capabilities. By making construct mutants deficient in important signalling motifs within the receptors' CYT (i.e., ITAM and ITIM), direct comparisons can be made by observing the change in the cells' ability to associate and engulf targets.

Overall, my results show that DrLITRs and mutant constructs were stably expressed on the surface of AD-293 cells and that, as predicted, the putative inhibitory receptor DrLITR 15.1 was unable to induce phagocytosis. My results also show that, as expected, DrLITR 1.2 generated an ITAM-dependent mode of phagocytosis when engaged by bead targets. Unexpectedly, the phagocytic response is also dependent on the ITIM motif for the full functional phagocytic potential of DrLITR 1.2.

4.2 Results

4.2.1 DrLITR Construct-Expressing AD-293 Cell Lines

To examine DrLITR-mediated signalling, I created wild-type (wt) and signalling deficient mutant constructs and then generated DrLITR-expressing AD-293 cells. The DrLITR 1.2 ^{wt} CYT contains an ITAM with two functional tyrosine residues as well as an ITIM with one tyrosine residue (Fig. 4.1A). DrLITR 1.2 $^{ITIM\ ko}$ contains the same structure as DrLITR 1.2 ^{wt}, however, the tyrosine within the ITIM has been mutated to phenylalanine (i.e., ITIM ko; Y/**F** ^{391}; Fig. 4.1B). DrLITR 1.2 $^{ITAM\ ko}$ is also similar to DrLITR 1.2 ^{wt} but contains two phenylalanines in place of the two tyrosines within the ITAM (i.e., ITAM ko; Y/**F** ^{356} and Y/**F** ^{368}; Fig. 4.1C). DrLITR 15.1 contains a CYT with two ITIM motifs and an ITSM motif (Fig. 4.1D).

Schematic cell-expressing representations of each receptor construct (i.e., DrLITR 1.2 ^{wt}, DrLITR 1.2 $^{ITIM\ ko}$, DrLITR $^{ITAM\ ko}$, DrLITR 15.1) are shown in Figure 4.2A. Each construct contains a hemagglutinin (HA) tag on the N-terminus followed by Ig domains (D1, D2, etc.), TM regions, and CYT segments with the indicated immunoreceptor tyrosine-based motifs and associated tyrosines or phenylalanines (Fig. 4.2A). To examine the cell surface expression of each construct, clones were stained with either primary αHA mAb (grey shading) or isotype control IgG_1 (no shading) followed by PE-conjugated secondary pAb and visualized for their relative fluorescence levels using flow cytometry to establish the relative expression levels of receptors on the surface of cells (Fig. 4.2B). The x-axis represents the fluorescence intensity associated with the expression level of DrLITR constructs on the surface of the cell vs. number of cell events (y-axis) measured (Fig. 4.2B).

4.2.2 Image Flow Cytometric Analysis of DrLITR-mediated Phagocytosis

To examine if DrLITR constructs are activated by the bead-based phagocytosis assay and to determine the optimal experimental conditions for this assay, YG beads were preabsorbed with either protein A or with protein G prior to the addition of 2 μg/mL of αHA or with 2 μg/mL of isotype IgG_1. Cells were then incubated for 15 minutes with opsonized targets and analyzed for their phagocytic activity. Specifically, cells were considered phagocytic if they contained at least one completely internalized bead (black bars) but not phagocytic if they had one or more attached beads (grey bars) on their cell surface with the absence of any completely engulfed beads. IpLITR 2.6b-expressing cells were also analyzed for their phagocytic capacity as a positive control to compare results to that of a bonafide ITAM-dependent mode of phagocytosis. When incubated with protein A preabsorbed YG beads, DrLITR 1.2 ^{wt} displayed 74.6% phagocytic activity that was statistically similar ($p \leq 0.05$) to IpLITR 2.6b with 77.9% of cells being phagocytic (Fig. 4.3A). Both DrLITR 1.2 $^{ITAM\ ko}$ and DrLITR 15.1 had significantly decreased values of phagocytosis at 12.6% and 7.1%, respectively, while DrLITR 1.2 $^{ITIM\ ko}$ had an intermediate level phagocytic response at 44.8% that was significantly different ($p \leq 0.05$) from receptors facilitating high (DrLITR 1.2 ^{wt} and IpLITR 2.6b) and low (DrLITR 1.2 $^{ITIM\ ko}$ and DrLITR 15.1) levels of phagocytosis (Fig. 4.3A). DrLITR 1.2 ^{wt}, DrLITR 1.2 $^{ITIM\ ko}$, DrLITR $^{ITAM\ ko}$, DrLITR 15.1 and IpLITR 2.6b were also all assessed for their ability to associate with beads with values of 34.8%, 47.8%, 13.0%, 15.5% and 41.8% respectively (Fig. 4.3A). In the context of this assay, association with beads refers to all cell events that contain at least one fluorescent bead, regardless of its position relative to the cell membrane (i.e., phagocytosed and cell surface-bound). Association was compared to cell events that did not interact, bind, or phagocytose a target as a measure for receptor sensitivity to target engagement as well as binding

avidity of receptors to targets. In this assay, trypsin was used to remove non-specifically bound beads on the surface of cells, therefore, surface-bound events were assumed to be receptor-specific binding of target beads that have not yet been fully internalized by the cell.

When receptor construct-expressing cells were incubated with YG beads preabsorbed with protein G, their overall phagocytic and bead associations were greater than that shown using the protein A absorbed beads. Specifically, DrLITR 1.2 ^{wt}, DrLITR 1.2 $^{ITIM\ ko}$, and IpLITR 2.6b all had significantly similarly high rates of phagocytosis at 89.3%, 91.4% and 87.9%, respectively (Fig. 4.3B). In addition, DrLITR $^{ITAM\ ko}$ and DRLITR 15.1 again showed low rates of phagocytosis at 5.4% and 7.8%, respectively (Fig 4.3B). When looking at the association of protein G preabsorbed beads, DrLITR 1.2 ^{wt}, DrLITR 1.2 $^{ITIM\ ko}$, DrLITR $^{ITAM\ ko}$, DrLITR 15.1 and IpLITR 2.6b had 65.5%, 67.3%, 47.9%, 50.9% and 59.4%, respectively (Fig. 4.3B).

4.2.3 Optimization of YG Bead αHA mAb Concentrations for DrLITR-mediated Phagocytosis

To further optimize phagocytosis assay conditions and to resolve phagocytic differences between the constructs, DrLITR-expressing cells were temporally examined for their phagocytic activities at 0, 15, and 30 minutes using YG target beads opsonized with varying concentrations of αHA mAb (0.25 μg/mL, 0.5 μg/mL, and 1 μg/mL) or with 1 μg/mL of IgG1 isotype control. Prior to antibody opsonization, YG targets were preabsorbed with protein G, as it was determined that protein G allowed for the highest binding affinity for the IgG_1 subclass of antibodies, thereby increasing receptor engagement with less overall antibody concentration. Immediately following exposure of the cells to the beads (0 minutes), little phagocytosis was observed when DrLITR 1.2 ^{wt} was engaged with αHA mAb opsonized bead targets regardless of

mAb concentration (Fig. 4.4A). This trend was observed for all construct-expressing cells ranging from 2.4% - 6.4% of phagocytosis, which represents the assay background (Fig. 4.4). After 15 minutes, DrLITR 1.2 ^{wt}-expressing cells phagocytosed 39.7% of beads coated with 0.25 µg/mL αHA mAb (Fig. 4.4A). As the concentration of αHA mAb increased (0.5 µg/mL and 1 µg/mL), so did the number of phagocytic cells (65.7% and 79.8%, respectively; Fig. 4.4A). In comparison, the trend seen for the 30-minute incubation of DrLITR 1.2 ^{wt}-expressing cells with beads follows a similar pattern to the 15-minute incubations but resulted in an overall increase in the proportion of phagocytic cells (67.5%, 88.2% and 92.4%, respectively; Fig. 4.4A). When cells were incubated with IgG-coated beads at 0, 15 or 30 minutes, only background levels of phagocytosis were observed, ranging from 5.4% - 8.6%. This pattern was observed for all constructs when the IgG1 isotype control opsonized beads were used as targets regardless of incubation times (range of 4.4% - 16.8%; Fig. 4.4). When DrLITR 1.2 $^{ITIM\ ko}$ was engaged with YG bead targets with increasing levels of αHA mAb a similar pattern of increasing levels of phagocytosis was observed at 15 minutes as well as 30 minutes incubation similar to DrLITR 1.2 ^{wt} (Fig. 4.4B). In comparison, DrLITR $^{ITIM\ ko}$ had a decreased level of phagocytosis which correlated to ~0.5x decrease in levels of phagocytosis compared to DrLITR 1.2 ^{wt} (compare Fig. 4.4A and Fig. 4.4B). Both DrLITR $^{ITAM\ ko}$ and DrLITR 15.1 had similarly low patterns of phagocytosis to each other regardless of antibody concentration or incubation times with target beads ranging from 3.2% - 9.8% phagocytosis for DrLITR 1.2 $^{ITAM\ ko}$ (Fig. 4.4C) and 3.3% - 20.1% phagocytosis for DrLITR 15.1 (Fig. 4.4D).

4.2.4 Temporal Analysis of DrLITR-mediated phagocytosis

DrLITR construct-expressing cells were then examined over a temporal scale to further resolve phagocytic differences between constructs and to observe optimal phagocytosis

conditions. Construct-expressing cells were incubated with YG beads opsonized with 1 μg/mL of αHA mAb for 0, 5, 10, or 15 minutes. Samples were also incubated with 1 μg/mL of isotype IgG_1 as a control. The phagocytic capacity of DrLITR 1.2 ^{wt}-expressing cells increased over the time of incubation with opsonized targets. The proportion of phagocytic cells, however, stayed relatively low initially at 3.0% with no incubation time with targets and 4.0% after only 5 minutes of incubation (Fig. 4.5A). This drastically increased at the 10-minute mark, where 44.0% of cells engulfed targets, which further increased to 70.1% after 15 minutes. Very few cells contained phagocytosed IgG_1 opsonized beads at the highest incubation time (15 minutes), and this was seen for every construct-expressing cell line ranging from 4.2% - 4.8% of cells phagocytosing IgG_1 coated beads (Fig. 4.5). The proportion of total DrLITR 1.2 ^{wt}-expressing cells binding to beads resulted in a similar increasing pattern over increasing incubation time with targets (Fig. 4.5A). Unlike DrLITR 1.2 ^{wt} phagocytic capacity, there was an increased proportion of bead-bound cells at 20.5% at 5 minutes of incubation with beads. This again increased to 25.2% at 10 minutes and 39.3% at 15 minutes. Similar to the pattern above, DrLITR 1.2 $^{ITIM\ ko}$-expressing cells also displayed a gradual increase of phagocytic cells at 4.3%, 4.3%, 20.5% and 40.4%, respectively (Fig. 4.5B). Again, DrLITR 1.2 $^{ITIM\ ko}$-expressing cells displayed a relative 50% decrease in the phagocytic capacity compared to the proportion of phagocytic cells for DrLITR 1.2 ^{wt} (compare Fig. 4.5A and Fig. 4.5B). Differing from DrLITR 1.2 ^{wt}, a large proportion (44.3%) of DrLITR 1.2 $^{ITIM\ ko}$-expressing cells associated with beads prior to incubation (Fig. 4.5B). This proportion increased in association with incubation time up to 57.2% after 15 minutes. Once again, very few cells were engulfed by DrLITR 1.2 $^{ITAM\ ko}$-expressing cells (Fig. 4.5C) or by DrLITR 15.1-expressing cells (Fig. 4.5D) regardless of the time cells were incubated with opsonized beads ranging from 3.3% - 5.1% and 3.2% - 4.0%,

respectively. However, when looking at the bead associations for the two receptor constructs, DrLITR 1.2 $^{ITAM\ ko}$-expressing cells bound a moderate amount of bead targets at 17.8%, 19.7%, 25.8% and 20.9%, respectively (Fig. 4.5C). This trend was similar for DrLITR 15.1-expressing cells as 11.6%, 13.3%, 19.6% and 19.9% of cells bound beads (Fig. 4.5D). At 15 minutes of incubation with protein G preabsorbed, 1 μg/mL of αHA mAb opsonized beads, constructs displayed similar differences for phagocytic capacity between receptors as reported previously for protein A coated beads at a higher mAb concentration (2 μg/mL). Specifically, the proportion of DrLITR 1.2 ^{wt} containing cells that were able to phagocytose beads was significantly higher ($p \leq 0.05$) than that for any DrLITR construct under the same conditions (Fig. 4.5E). Again, DrLITR 1.2 $^{ITIM\ ko}$ showed an intermediate phagocytic response significantly lower than that of DrLITR 1.2 ^{wt} but still higher than that of both DrLITR 1.2 $^{ITAM\ ko}$ and DrLITR 15.1 whose phagocytic capacities were the lowest (Fig. 4.5E).

4.2.5 ITIM Knockout DrLITRs Display Increased Bead-Binding and Decreased Phagocytic Phenotype during Recovery from Cold Incubation

Following the observations made on the differing phagocytic phenotypes between DrLITR 1.2 ^{wt} and DrLITR 1.2 $^{ITIM\ ko}$, further investigation of the specific differential bead-cell associated responses was conducted using a modified cold-binding assay. Specifically, construct-expressing cells were preincubated at 4°C before and after the addition of YG bead targets. Cells were then warmed by incubating at 37°C for 0, 2, 4, 8, and 16 minutes and examined for their ability to associate and phagocytose beads. By cooling cells to sub-ambient temperatures and measuring bead binding during warming, observations can be made about overall receptor binding affinity to bead targets. Comparisons can then be made between each construct's ability to engage the phagocytic machinery as it slowly becomes available during incubation at 37°C.

DrLITR 1.2 ^{wt} expressing cells had low levels of bead binding (11.5%) when incubated at 4°C in the absence of any warming in comparison to IgG1 isotype control coated beads (6.5%) warmed for 15 minutes (Fig. 4.6A). The bead association stayed relatively low from 2 minutes to 8 minutes (15.9%, 17.7% and 14.5%) but increased at 16 minutes of warming to 33.9% of cells binding targets. The phagocytic capacity of DrLITR 1.2 ^{wt} mimicked its bead association; low levels of cells containing phagocytosed beads were observed from 0 minutes to 8 minutes ranging from 2.2% - 5.5% of cells phagocytosing targets (Fig. 4.6B). After 16 minutes of incubation, the phagocytic cell proportion of DrLITR 1.2 ^{wt} increased dramatically to 58.4% (Fig. 4.6B). DrLITR 1.2 $^{ITIM\ ko}$ was significantly different from DrLITR 1.2 ^{wt}. For example, while bead association from 0 minutes of incubation to 8 minutes reflected a similar slight linear increase, 30.8% of DrLITR 1.2 $^{ITIM\ ko}$-expressing cells associated with beads prior to any incubation and continued to increase (31.2%, 32.4% 35.4% and 36.7%) through to the entire 16 minutes of warming (Fig. 4.6C). DrLITR 1.2 $^{ITIM\ ko}$ -expressing cells had a similar phagocytic capacity during the warming of the cells from 0 to 8 minutes ranging from 3.0% - 4.7% (Fig. 4.6D). In contrast with DrLITR 1.2 ^{wt} and as seen previously with other phagocytosis experiments, DrLITR 1.2 $^{ITIM\ ko}$ had an overall low proportion of cells phagocytosing targets after 16 minutes of warming (Fig. 4.6D).

4.3 Discussion

In this chapter, my main objective was to examine the role of ITAM and ITIM motifs in tandem for controlling DrLITR 1.2-mediated phagocytosis. To this end, I created signalling motif-deficient mutant constructs and established DrLITR-expressing AD-293 cell lines which were analyzed using a flow cytometric phagocytosis assay. My results show that while DrLITR

1.2 ^{wt} can generate a potent ITAM-dependent phagocytic response, the ITIM motif potentially modulates ligand binding and is required for the full phagocytic potential of the receptor. This reveals potentially new information regarding the functional roles of ITIMs that are classically defined as inhibitory.

The previous establishment of a mammalian heterologous expression system within our lab allowed us to examine the phagocytic phenotypes of IpLITRs and to further study the underlying signalling networks that control immune effector responses (5,8). Additionally, utilizing imaging flow cytometric analysis has led to increased resolution of opsonized YG bead target positioning relative to receptor-expressing cells during phagocytosis, further defining the signalling capacity of tyrosine-based receptor functions. My thesis work takes advantage of this system, which has already helped us characterize IpLITR immunoregulation, including the IpLITR 1.1b-mediated crosstalk inhibition of IpLITR 2.6b (5). This allowed for an excellent platform to study newly discovered DrLITR-types, identify their phagocytic phenotypes, and to further study the functional purpose of tandem contrasting signalling motifs within the same receptor CYT (i.e., ITAM and ITIM).

Of the DrLITRs that were originally found in zebrafish, DrLITR 15.1 was reminiscent of the previously studied IpLITR 1.1b. Specifically, DrLITR 15.1 contains two tandem ITIMs as well as an ITSM, like the structure of the membrane distal region of IpLITR 1.1b. This classified DrLITR 15.1 as a putative inhibitory receptor-type and indicated that this receptor might need to be co-ligated with a stimulatory receptor to see any DrLITR 15.1-mediated control over phagocytic responses. DrLITR 15.1 was an ideal construct for comparing induction of phagocytosis and to confirm the previous observations made in our lab that inhibitory-type

receptors are not able to induce a phagocytic response in AD-293 cells (14). This is in contrast to IpLITR 1.1b-expressing RBL-2H3 cells that were able to induce an ITAM-independent mode of phagocytosis (9–12). When DrLITR 1.2 ^{wt}-expressing cells were engaged with bead targets, a very robust phagocytic response was observed that was comparable to the phenotype seen for the ITAM-containing chimeric receptor IpLITR 2.6b/IpFcRγ-L. Consistent with previous data, IpLITR 2.6b has been shown to induce potent cellular responses, including phagocytosis, when transfected and activated in various mammalian cell lines (8,11,14). Specifically, IpLITR 2.6b has been used in previously mentioned IpLITR crosstalk studies in AD-293 cells as the main potent inducer of the phagocytic response, where co-ligation with IpLITR 1.1b resulted in the overall dampening of phagocytosis (5). As such, IpLITR 2.6b was utilized as a reference for comparing DrLITR-mediation over phagocytic responses to an ITAM-dependent mode of phagocytosis. While phagocytosis was expected to occur during the induction of DrLITR 1.2 ^{wt}, the overall level was surprising as it was predicted that the ITIM within the CYT of DrLITR 1.2 ^{wt} would potentially abrogate this functional outcome resulting in an overall reduced level of phagocytosis in comparison to the ITIM knockout variant. As expected, DrLITR 1.2 $^{ITAM\ ko}$-expressing cells had a complete reduction in phagocytic capacity compared to the wild-type construct regardless of changing experimental factors (i.e., time, mAb concentration), highlighting that DrLITR 1.2 ^{wt}, like other stimulatory receptors (e.g., FcγR, Dectin-1, and IpLITR 2.6b), requires a functional ITAM motif to elicit phagocytosis (1,4–6). However, knocking out the ITIM within DrLITR 1.2 did not increase the phagocytic capacity of receptor-expressing cells as predicted. Rather, the proportion of phagocytosing DrLITR 1.2 $^{ITIM\ ko}$ expressing cells was surprisingly almost half the amount seen for wild-type DrLITR 1.2. This effect was unexpected but consistently observed when experimental conditions of the

phagocytosis assay were modified. By comparing the phagocytic capacities seen between DrLITR 1.2 ^{wt} and DrLITR 1.2 $^{ITIM\ ko}$, it appears as though the ITIM is required for full functional activity of DrLITR 1.2 ^{wt}. Overall, my results illustrate the first functional characterization of teleost immune receptors with tandem ITAM and ITIM motifs. I have shown that these receptors induce potent ITAM-dependent modes of phagocytosis, and interestingly, while not required for the phagocytic response, the ITIM is involved in the full phagocytic potential of the receptor. This model suggests new avenues of signalling mechanisms that will be explored later in this thesis.

Experiments investigating the phagocytic phenotypes of DrLITR 1.2 ^{wt} and its mutant counterparts (i.e., DrLITR 1.2 $^{ITIM\ ko}$ and DrLITR 1.2 $^{ITAM\ ko}$) were also performed under different experimental conditions, including i) establishment of optimal antibody concentrations for bead opsonization, ii) temporal assessment of DrLITR-mediated phagocytosis, and iii) effects of reduced temperature on target binding. I optimized the conditions for YG bead targets used to engage DrLITR constructs in two ways. The first was the use of two different antibody-binding proteins (i.e., protein A and protein G), which are preabsorbed to the surface of YG beads that allow for antibodies to be associated directly to bead targets. Protein A and G are bacterial virulence factors that exist on the cell wall of bacteria to escape the immune system of infected hosts (166). These proteins bind to the Fc portion of antibodies to prevent opsonization of the bacteria and prevent cell-mediated immune responses (e.g., phagocytosis). While both antibody-binding proteins are found on the surface of bacteria, they contain separate affinities for certain isotype classes of antibody as well as being specific for certain antibodies sourced from different animal species. For example, Protein A is found on *Staphylococcus aureus* and has high binding affinity for guinea pig IgG_1 while binding weakly to mouse IgG_1 (166). Alternatively, protein G

is found on certain *Streptococcal* species and has high binding affinity to mouse IgG_1 and weak binding to chicken IgG (167). These proteins have been isolated and utilized for their specific binding capacity of antibodies; in the context of the phagocytosis assay, polystyrene YG beads are preabsorbed with protein A or G to bind antibodies to the surface of bead targets for the engagement of receptor constructs (9,10,14,165,166). The second way bead targets were optimized was by examining increasing concentrations of αHA mAb opsonized to the surface of beads. Both experimental methods tested DrLITR binding avidity to target beads directly or indirectly through antibody binding and receptor engagement. Avidity is defined by the overall strength of the interactions between the receptor and associated ligands through the affinity of the direct bond made and the number of total interactions between the receptors and ligands (168). Typically, increased receptor-ligand avidity leads to an increase in receptor-associated signalling and thereby allowing for a more intense, rapid cellular effector response. However, certain receptor interactions lead to differential signalling responses based on receptor-ligand avidity. For example, the receptor FcαRI associates with the ITAM-containing adaptor molecule FcRγ when engaged with IgA (18). Large immune complexes composed of multiple IgA molecules and ligands results in stronger receptor avidity, where the ITAM can become phosphorylated by SFKs, leading to Syk recruitment and subsequent recruitment and activation of further signalling molecules for the induction of cellular effector responses such as phagocytosis, ADCC, and cytokine release. Upon engagement of monomeric IgA, the FcαRI takes on a different role whereby low valency binding of the ligand leads to Syk-based recruitment of SHP-1, which dampens phosphorylation signalling and leads to an overall inhibition of cell activation (18). As such, avidity binding was examined for DrLITR constructs to targets to observe the full range of signalling potentials for these receptors. My results showed

that both DrLITR 1.2 ^{wt} and DrLITR 1.2 $^{ITIM\ ko}$ unsurprisingly increased phagocytic capacity with increasing levels of mAb. While using the higher mAb affinity protein G molecule on YG beads also led to an overall increase in phagocytic capacity of both receptors, interestingly the response of DrLITR 1.2 $^{ITIM\ ko}$ was comparable to DrLITR 1.2 ^{wt}.

This similarity of phagocytic capacity for both DrLITR 1.2 ^{wt} and DrLITR 1.2 $^{ITIM\ ko}$ indicated that perhaps high avidity engagement of DrLITR 1.2 $^{ITIM\ ko}$ receptors to targets results in induction of stimulatory signalling that becomes indistinguishable from DrLITR 1.2 ^{wt}. This suggests that perhaps ITAM-containing receptors (e.g., DrLITR 1.2 $^{ITIM\ ko}$) are able to generate a large signalling potential (and, by association, a greater cellular response output) during strong ligand engagement that diminishes as the ligand binding decreases. In contrast, perhaps the presence of the tandem ITIM within the ITAM-containing receptor (i.e., DrLITR 1.2 ^{wt}) enhances signalling at all levels of ligand binding, thereby not requiring as much engagement to overcome the activation threshold, but still reaches a signalling maximum comparable to ITAM only-containing receptors during high binding avidity to ligands. Regarding the total target binding between the receptors, knocking out the ITIM of DrLITR 1.2 resulted in an increase in the number of cells bound to targets. This was not expected for a receptor whose ability to phagocytose targets was seemingly diminished by the absence of a tyrosine-based signalling motif. This combination of evidence suggests that perhaps the presence of the ITIM within the same CYT of an ITAM modulates receptor interactions by increasing the overall sensitivity of the receptor to its associated ligands. As a result, immune cell activation and effector responses would require reduced ligand binding to facilitate intended effector responses, creating a more sensitive and efficient mechanism for the induction of responses like phagocytosis. Receptor modulation of sensitivity has been described; for example, CD19 is a co-receptor for BCRs,

where through the binding of C3d-opsonized antigens, CD19 facilitates increased antibody production, DNA synthesis, and enhanced release of Ca^{2+} for cell signalling (10). When comparing the structure of DrLITR 1.2 and the presence of an ITAM and ITIM within the receptor tail, FCRL5 is a receptor with similar structural features containing both an ITIM as well as an ITAM-like sequence within the CYT of the receptor (93). This ITAM-like motif differs from the conventional ITAM by containing a glutamic acid in place of an aliphatic residue at the +3 position of the second tyrosine residue. FCRL5 crosslinking on the surface of B cells to the BCR resulted in the overall dampening of calcium signalling as well as tyrosine phosphorylation compared to the engagement of the BCR alone. When the tyrosine residues within the ITAM were mutated to dysfunctional phenylalanine, complete dampening of calcium flux occurred. However, ITIM mutations resulted in a bolstering of calcium release as well as enhanced activation of ERK. This information suggests that the ITIM can modulate the cell effector responses and signalling capabilities of receptors compared to the differential response observed when the ITAM variant of the dual signalling motif receptor is examined.

The incubation of cells at sub-ambient temperatures decreases cell membrane fluidity and diminishes the cell signalling transduced by the engagement of the receptors as many of the receptor signalling components, as well as the receptors themselves, are directly associated with the membrane (169). As a result, the binding interactions between receptors and the target is largely due to receptor-target avidity. Gradually warming the construct-expressing cells interacting with targets also allows for observations of how the phagocytic machinery is coordinated as signalling mechanisms slowly become available during warming to 37°C. Warming allows cell membranes to regain fluidity while signalling molecules and receptors can begin to associate and engage with one another. Subtle differences can arise through the

influence of different conditions to which the receptor-containing cells and bead targets are subjected. This may highlight the importance that these signalling motifs have on immune effector responses and coordinated signalling events. For example, it was shown that IpLITR 1.1b induced a phagocytic response at temperatures as low as 22°C compared to IpLITR 2.6b, where the response was dampened at any temperature below 27°C (11). To further elucidate IpLITR 1.1b-mediated phagocytosis and the underlying mechanisms controlling this response, pharmacological inhibitors of common signalling molecules associated with ITAM-dependent phagocytosis were utilized (11). It was found that the ITAM-containing receptor IpLITR 2.6 was affected by inhibitors blocking certain signalling molecules such as PI3K, Cdc42, PDK1 and PKC. In contrast, the phagocytic response induced by IpLITR 1.1b was only affected by SFK, Syk, and F-actin polymerization blockers. It was suggested then that the phagocytic response observed by IpLITR 1.1b required a minimal number of signalling molecules to stimulate the actin polymerization machinery. This would help explain why the formation of filopodia-like protrusions induced by IpLITR 1.1b did not require ligand binding. Following cooling of receptor expressing cells at 4°C, the phagocytic capacity of both DrLITR 1.2 ^{wt} and DrLITR 1.2 $^{ITIM\ ko}$ receptors showed no significant increase until 16 minutes of warming where it appears that most of the phagocytic machinery is available or beginning to become available during receptor engagement. Additionally, like previous data, DrLITR 1.2 $^{ITIM\ ko}$ cells displayed a reduced phagocytic capacity compared to DrLITR 1.2 ^{wt}. When observing receptor binding of targets, DrLITR 1.2 ^{wt} and DrLITR 1.2 $^{ITIM\ ko}$ had very different binding patterns. While it appeared that DrLITR 1.2 ^{wt} binding to targets was fairly similar to its phagocytic capacity (i.e., increased after 16 minutes of warming), a large number of DrLITR 1.2 $^{ITIM\ ko}$ -expressing cells were able to bind to targets even prior to any warming, which only resulted in a slight increase in binding as

warming time increased. Taken together, it appears that the absence of the ITIM motif within DrLITR 1.2 increases the binding capacity of the receptor and even allows for increased binding at suboptimal temperatures.

While these observations of DrLITR-mediated control reveal interesting new information on how possible signalling dynamics can fine-tune phagocytosis, it should be noted that these results rely on the overexpression of DrLITRs in a well-characterized mammalian cell line (i.e., AD-293). However, this non-immune epithelioid cell line has been successfully utilized in other studies to characterize immune receptor-types. Within our own lab, the efficacy of the AD-293 system became apparent when observations of IpLITR 2.6b-mediated phagocytosis was described to be phenotypically similar to that of our previous studies of IpLITR 2.6b within the myeloid cell line RBL-2H3. In other crosstalk studies that utilized another heterologous expression system, chimeric FcγRIIA receptors (extracellular domain of FcγRI and CYT of FcγRIIA) were expressed along side FcγRIIB to specifically study the crosstalk interactions between the two receptors while also eliminating unintended interactions with other receptors that exist on hematopoietic cells (170). The responses observed using the overexpression of these receptors within this model allow for a conserved response of an ITAM-dependent mode of phagocytosis within a non-phagocytic cell line. Therefore, examination of the signalling dynamics controlling these responses can be directly associated with receptors that initiate the induction of these conserved signalling pathways.

In summary, I have optimized a mammalian heterologous expression system previously used in our lab, to study the function of ITAM and ITIM in tandem within the CYT of a single immune receptor and examined their effects on controlling phagocytosis. I have demonstrated

that this unique motif arrangement induces a potent ITAM-dependent mode of phagocytosis during the engagement of receptor targets comparable to that of other ITAM-containing receptors (1,6), which is consistent with our previous finding on IpLITR 2.6b ability to induce phagocytosis (2,5,11). My results also indicated for the first time that the ITIM within the receptor tail modulates the signalling capacity of the receptor by increasing its ability to phagocytose targets while reducing the receptor's target binding capabilities. Overall, this data suggests new possible mechanisms by which teleost immunoregulatory receptors are able to enhance their signalling capabilities. Specifically, classically defined inhibitory motifs in the context of a flanking ITAM within the same receptor CYT synergistically increases the signalling capability of the receptor. This may suggest that the ITIM can recruit signalling molecules associated with inhibition that contribute to the stimulatory signalling cascade and subsequent cellular effector responses observed. Chapter V in this thesis will examine important signalling molecules recruited to the motifs within the receptor tails, as well as downstream activation of further signalling molecules responsible for coordinating the phagocytic response. These topics will be assessed through confocal fluorescence microscopy as well as the pharmacological inhibition of signalling molecules during the induction of phagocytosis.

A.

DrLITR 1.2 wt

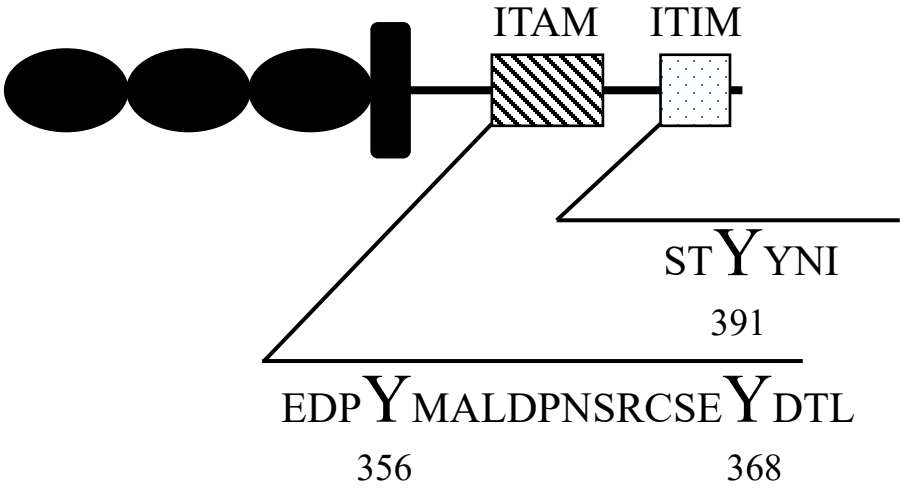

B.

DrLITR 1.2 ITIM ko

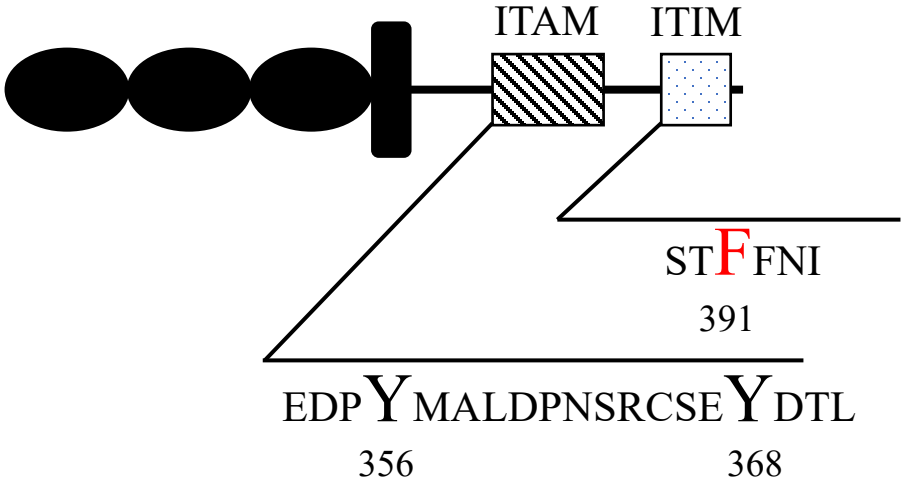

C.

DrLITR 1.2 **ITAM ko**

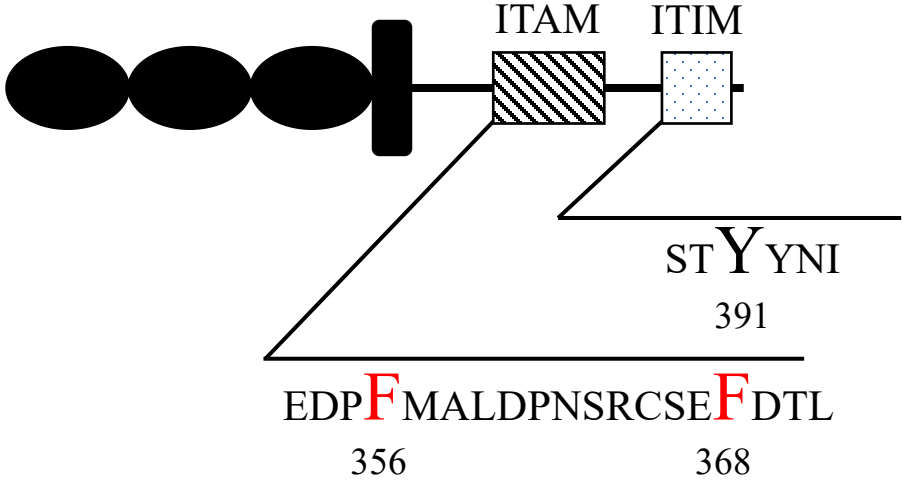

D.

DrLITR 15.1

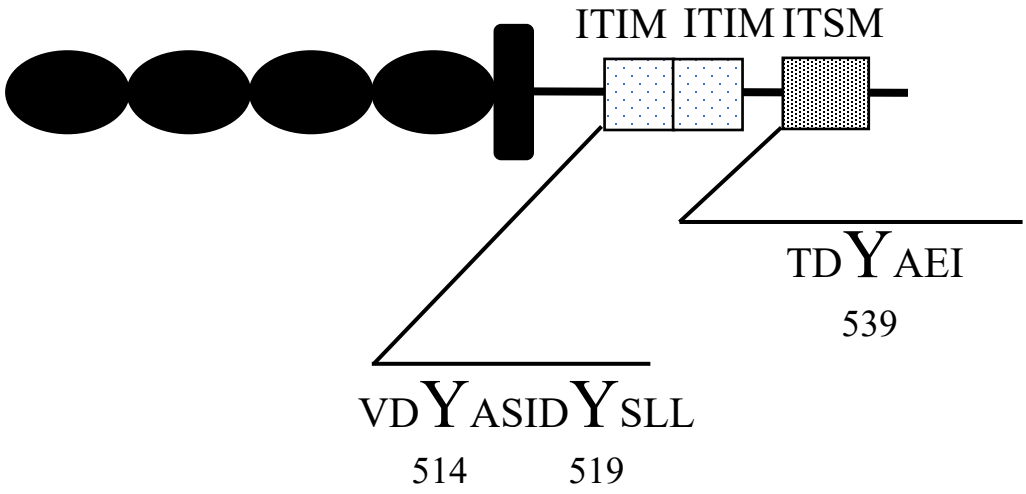

Figure 4.1. Comparison of DrLITR CYT immunoreceptor tyrosine-based motifs between transfected constructs. Receptors depicted here represent generated constructs used in this thesis. DrLITR 1.2 ^{wt} (**A**) contains 3 tyrosine residues as part of the receptors ITAM and ITIM within the same CYT. Through site-directed mutagenesis, 1.2 $^{ITIM\ ko}$ (**B**) was created through the substitution of the tyrosine within the ITIM (Y_{391}) of 1.2 ^{wt} with phenylalanine (F_{391}) to establish ITIM dysfunctional mutants. In a similar fashion, to create an ITAM-deficient version of the receptor, 1.2 $^{ITAM\ ko}$ (**C**) was established by also substituting tyrosines (Y_{514} and Y_{519}) within the ITAM to phenylalanines (F_{514} and F_{519}). DrLITR 15.1 (**D**) contains 4 tyrosine residues, 2 of which are embedded in 2 overlapping ITIM motifs followed by an ITSM motif.

A.

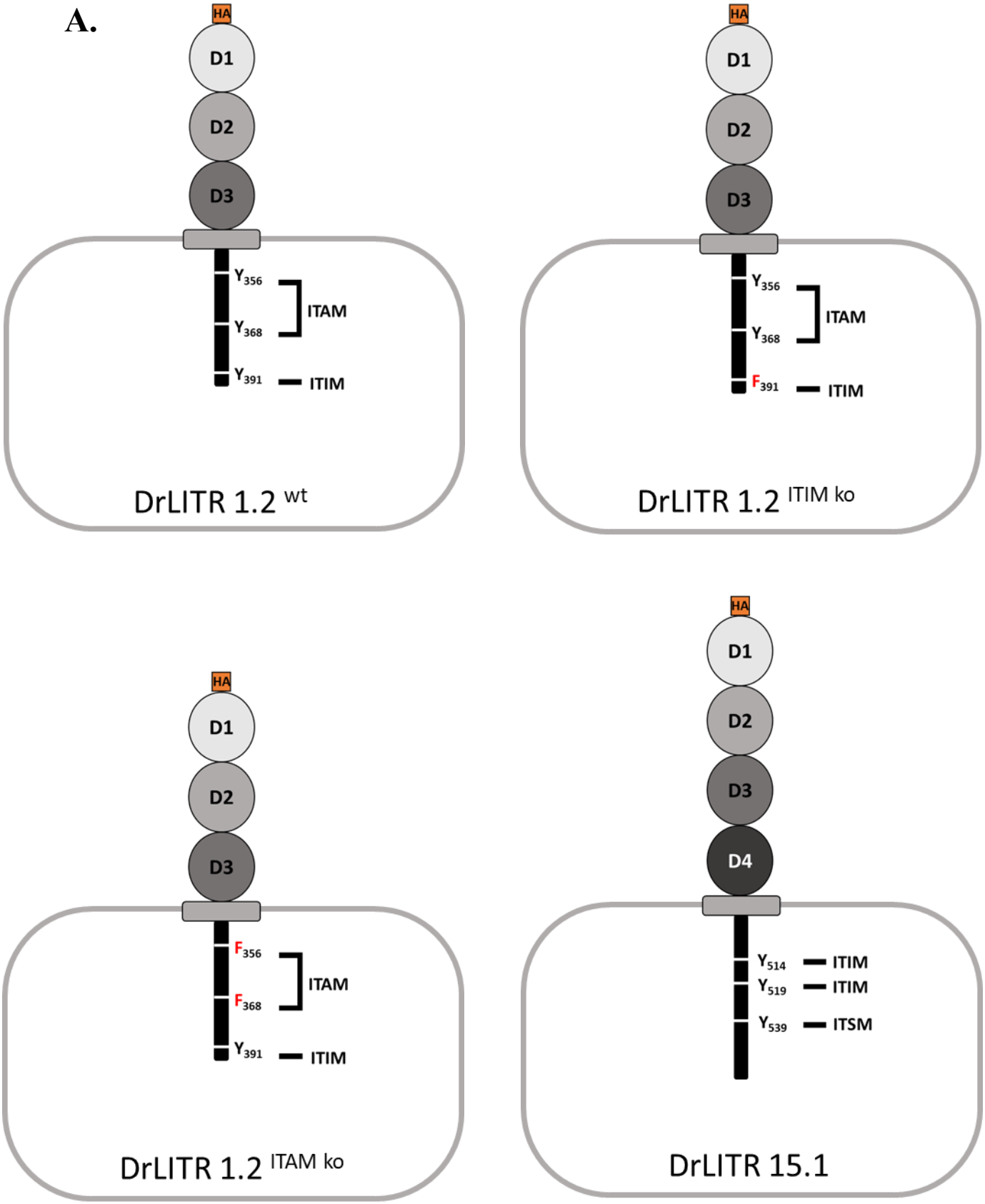
HA
D1
D2
D3
D4
Y_{356}
Y_{368}
Y_{391}
ITAM
ITIM
F_{356}
F_{368}
F_{391}
Y_{514}
Y_{519}
Y_{539}
ITSM
DrLITR 1.2 wt
DrLITR 1.2 ITIM ko
DrLITR 1.2 ITAM ko
DrLITR 15.1

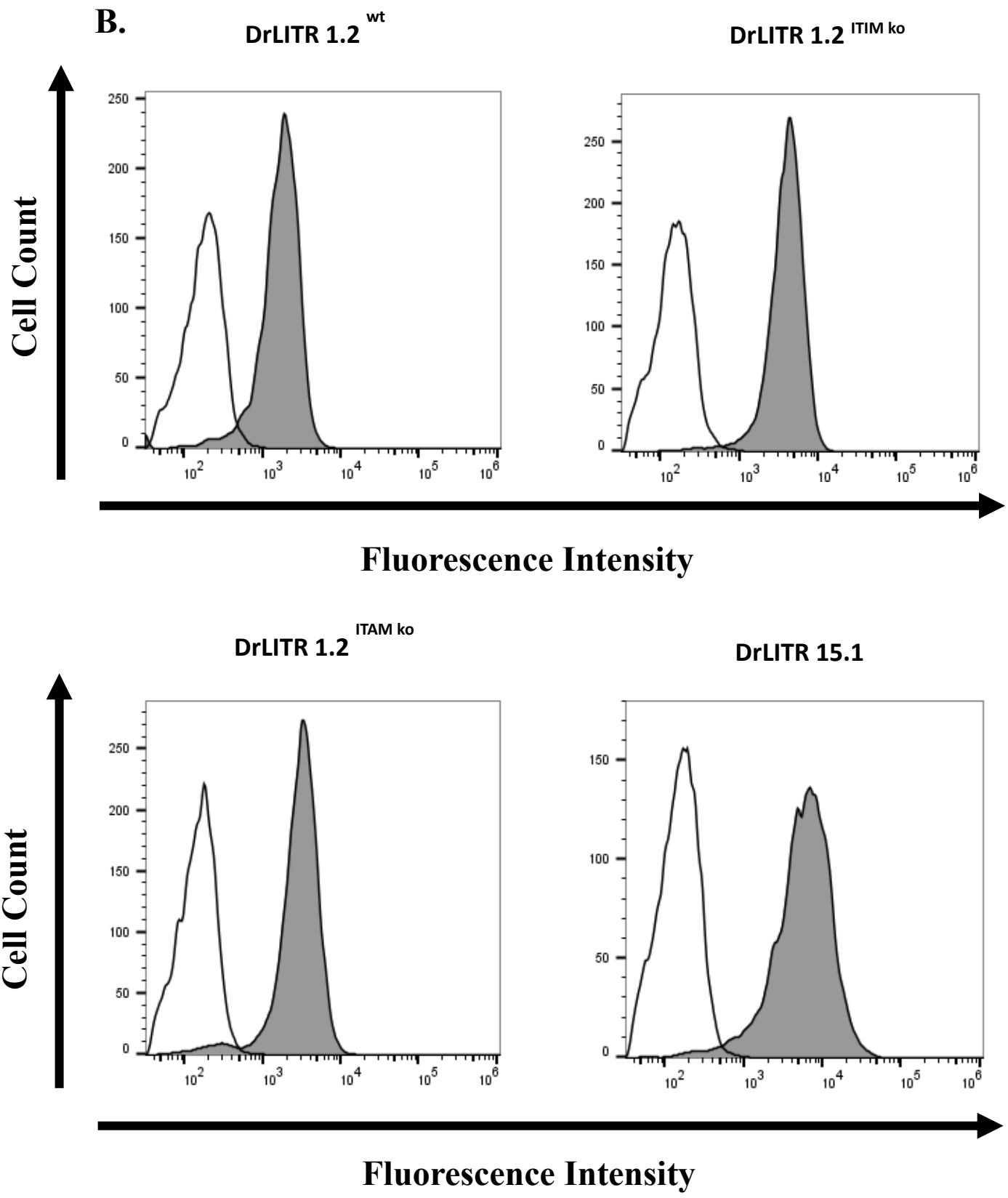
B.
DrLITR 1.2 wt
DrLITR 1.2 ITIM ko
DrLITR 1.2 ITAM ko
DrLITR 15.1
Cell Count
Fluorescence Intensity
Cell Count
Fluorescence Intensity

Figure 4.2. Cell-surface expression profiles and receptor schematics of generated DrLITR constructs stably transfected into AD-293 cells. Schematic representation of DrLITR constructs transfected into AD-293 cells (**A**). Images depict protein receptors containing a hemagglutinin (HA) tag on the N-terminus of the receptor, followed by immunoglobulin domains (D1, D2, etc.), a transmembrane region, and a cytoplasmic tail (CYT) region. DrLITR 1.2 ^{wt} contains an immunoreceptor tyrosine-based activation motif (ITAM) in tandem to an immunoreceptor tyrosine-based inhibitory motif (ITIM) within the same CYT. DrLITR 15.1 contains 2 overlapping ITIM motifs within its CYT, followed by an immunoreceptor tyrosine-based switch motif (ITSM). DrLITR (1.2 ^{wt}, 15.1) constructs from zebrafish (*Danio rerio*) embryo cDNA library were amplified via PCR and sub-cloned into pDisplay eukaryotic expression vector using SmaI/SalI digestion enzymes. Additionally, mutant constructs (1.2 $^{ITIM\ ko}$, 1.2 $^{ITAM\ ko}$) were generated through site-directed mutagenesis and overlap extension PCR to mutate motif functional tyrosines (Y) into dysfunctional phenylamines (F). Parental AD-293 cells were transfected with the expression vector, underwent antibiotic selection, and were cloned after FACS sorting. Cell clones for each DrLITR construct were then primarily stained with mouse αHA mAb and secondarily stained with goat-α-mouse conjugated PE. Samples were visualized for their DrLITR protein surface expression (**B**) with the Attune NxT flow cytometer (ThermoFisher). Cell events were gated initially based on FSC-A versus SSC-A parameters to remove debris and large cellular clumps, then FSC-A was gated versus FSC-H to remove doublets. PE fluorescence intensity was analyzed as a histogram for cellular events where αHA stained cells (grey shading) were compared to IgG_1 isotype control stained cells (no shading).

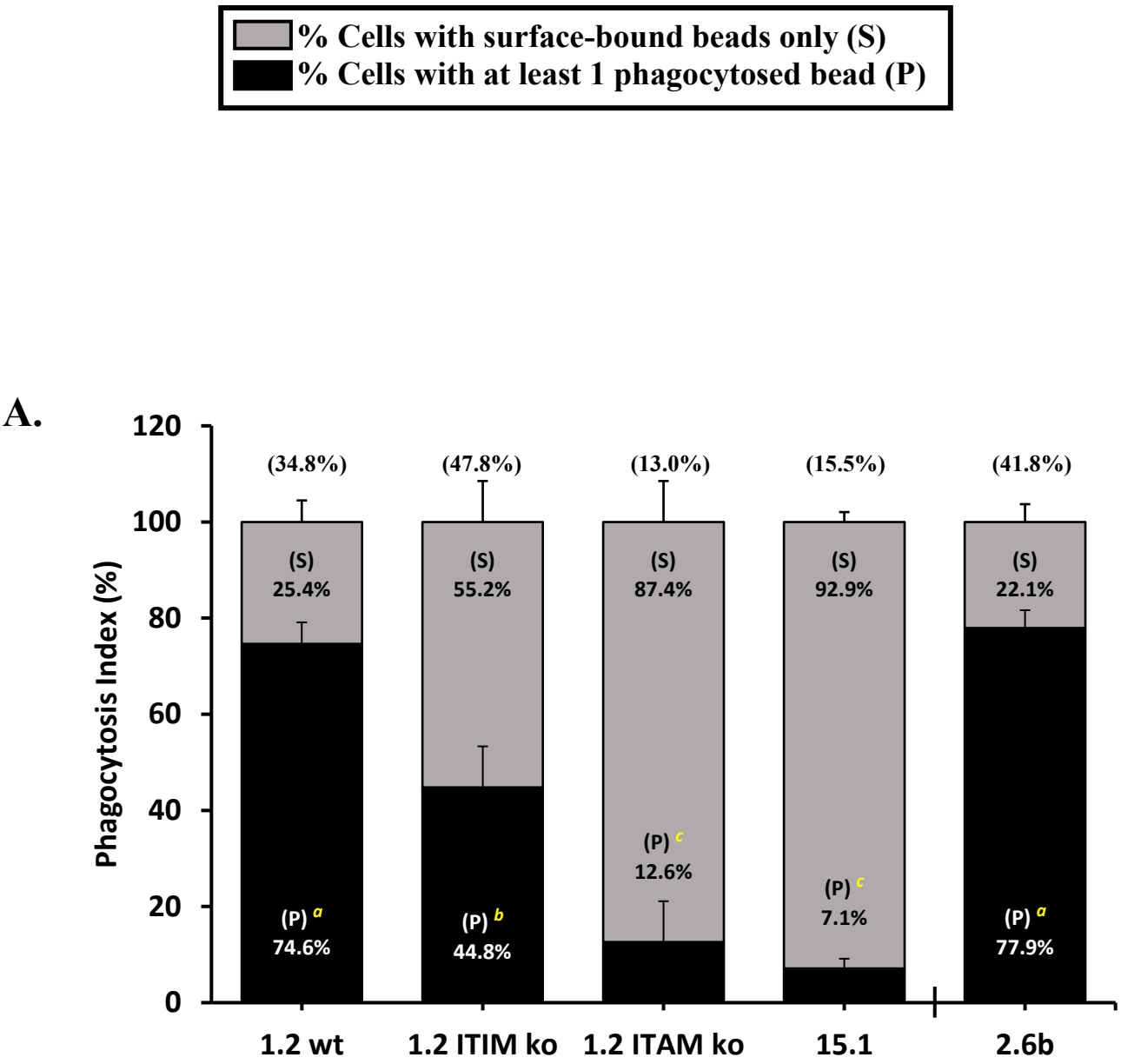
% Cells with surface-bound beads only (S)
% Cells with at least 1 phagocytosed bead (P)
A.
Phagocytosis Index (%)
120
100
80
60
40
20
0
(34.8%)
(47.8%)
(13.0%)
(15.5%)
(41.8%)
(S) 25.4%
(S) 55.2%
(S) 87.4%
(S) 92.9%
(S) 22.1%
(P) a 74.6%
(P) b 44.8%
(P) c 12.6%
(P) c 7.1%
(P) a 77.9%
1.2 wt
1.2 ITIM ko
1.2 ITAM ko
15.1
2.6b

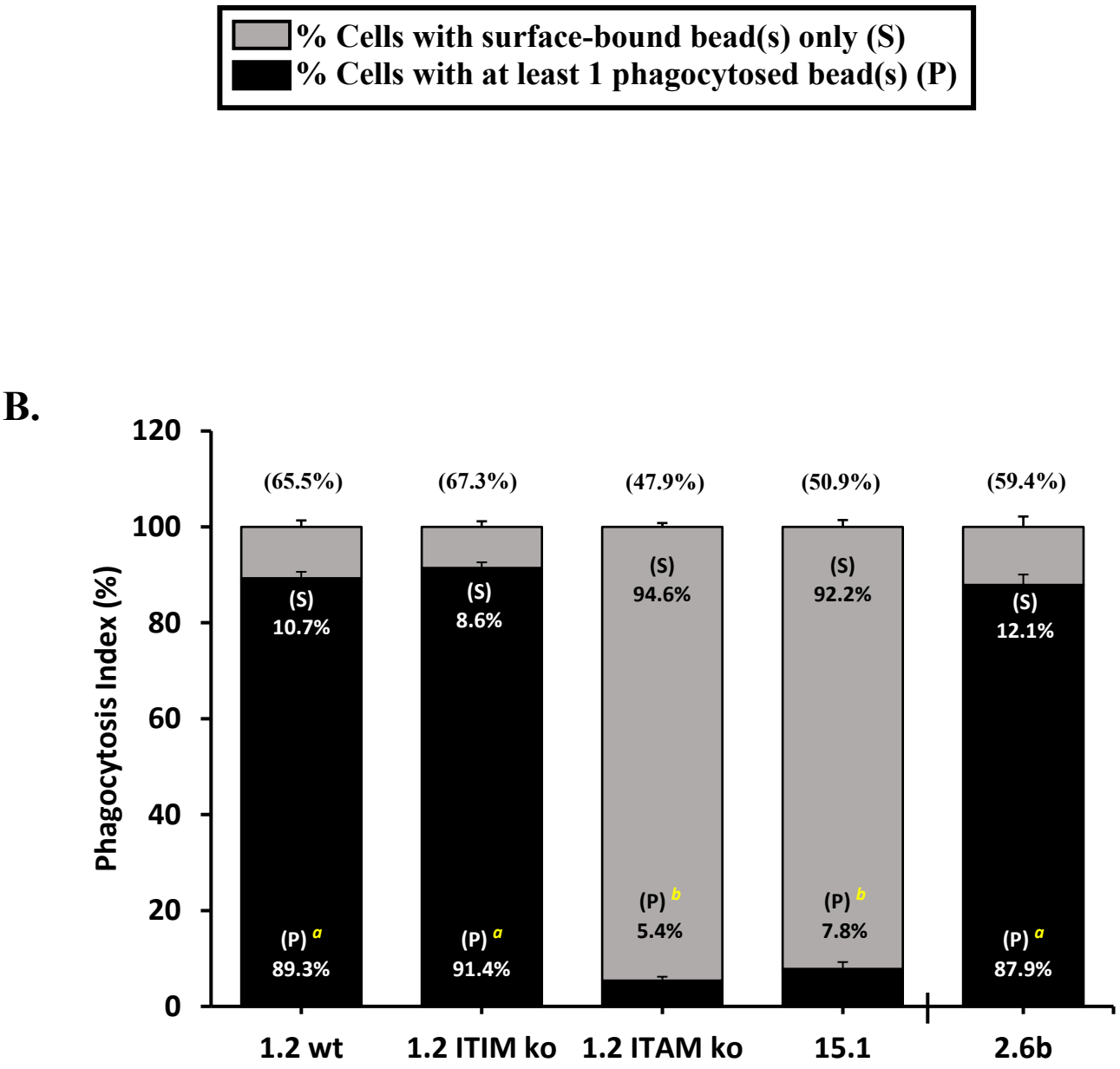
% Cells with surface-bound bead(s) only (S)
% Cells with at least 1 phagocytosed bead(s) (P)
B.
Phagocytosis Index (%)
120
100
80
60
40
20
0
(65.5%)
(67.3%)
(47.9%)
(50.9%)
(59.4%)
(S) 10.7%
(P) a 89.3%
(S) 8.6%
(P) a 91.4%
(S) 94.6%
(P) b 5.4%
(S) 92.2%
(P) b 7.8%
(S) 12.1%
(P) a 87.9%
1.2 wt
1.2 ITIM ko
1.2 ITAM ko
15.1
2.6b

Figure 4.3. Phagocytosis assays reveal subtle differences and similarities between LITR-types and mutant constructs through imaging flow cytometry. 3 x 10^5 AD293 cells stably expressing DrLITR wild-type (1.2 ^{wt} and 15.1), mutant (1.2 $^{ITIM\ ko}$ and 1.2 $^{ITAM\ ko}$) or IpLITR (2.6b) constructs were incubated with 4.5µm YG beads (9 x 10^5), coated in protein A (**A**) or protein G (**B**) followed by opsonization with αHA mAb (2µg/mL), for 15 minutes at 37°C. Samples were then counter-stained and subsequently analyzed using the ImageStream X Mark II. Events were classified as phagocytic (P; black bars) with at least 1 bead being internalized or surfaced bound (S; grey bars) with only surface attached beads. Samples were normalized, and the % values were calculated as # of surface-bound events or # of phagocytic events / # of all bead-associated events. Each bar represents the mean ± SEM of total cells associated with beads from 3 independent experiments. The bracketed % value above each bar represents the proportion of cells associated with beads. Sample data groups were analyzed using a one-way ANOVA and Tukey test (Prism 6, GraphPad, La Jolla, CA, USA). Bars containing different letters (*a, b*, or *c*) represent statistical significance ($p \leq 0.05$) between phagocytosis (%) means.

A.

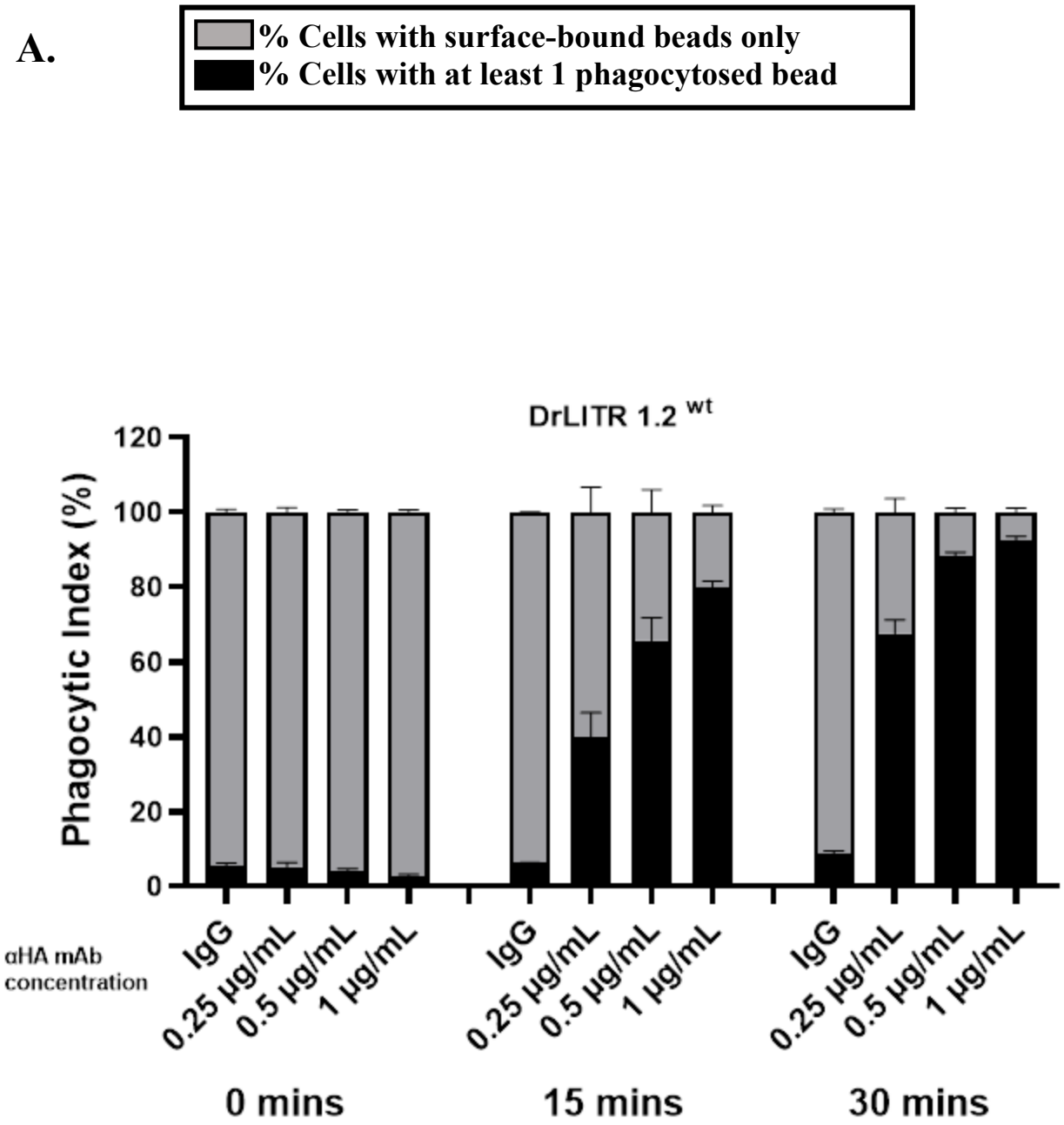
% Cells with surface-bound beads only
% Cells with at least 1 phagocytosed bead
DrLITR 1.2 wt
Phagocytic Index (%)
120
100
80
60
40
20
0
αHA mAb concentration
IgG
0.25 µg/mL
0.5 µg/mL
1 µg/mL
IgG
0.25 µg/mL
0.5 µg/mL
1 µg/mL
IgG
0.25 µg/mL
0.5 µg/mL
1 µg/mL
0 mins
15 mins
30 mins

B.

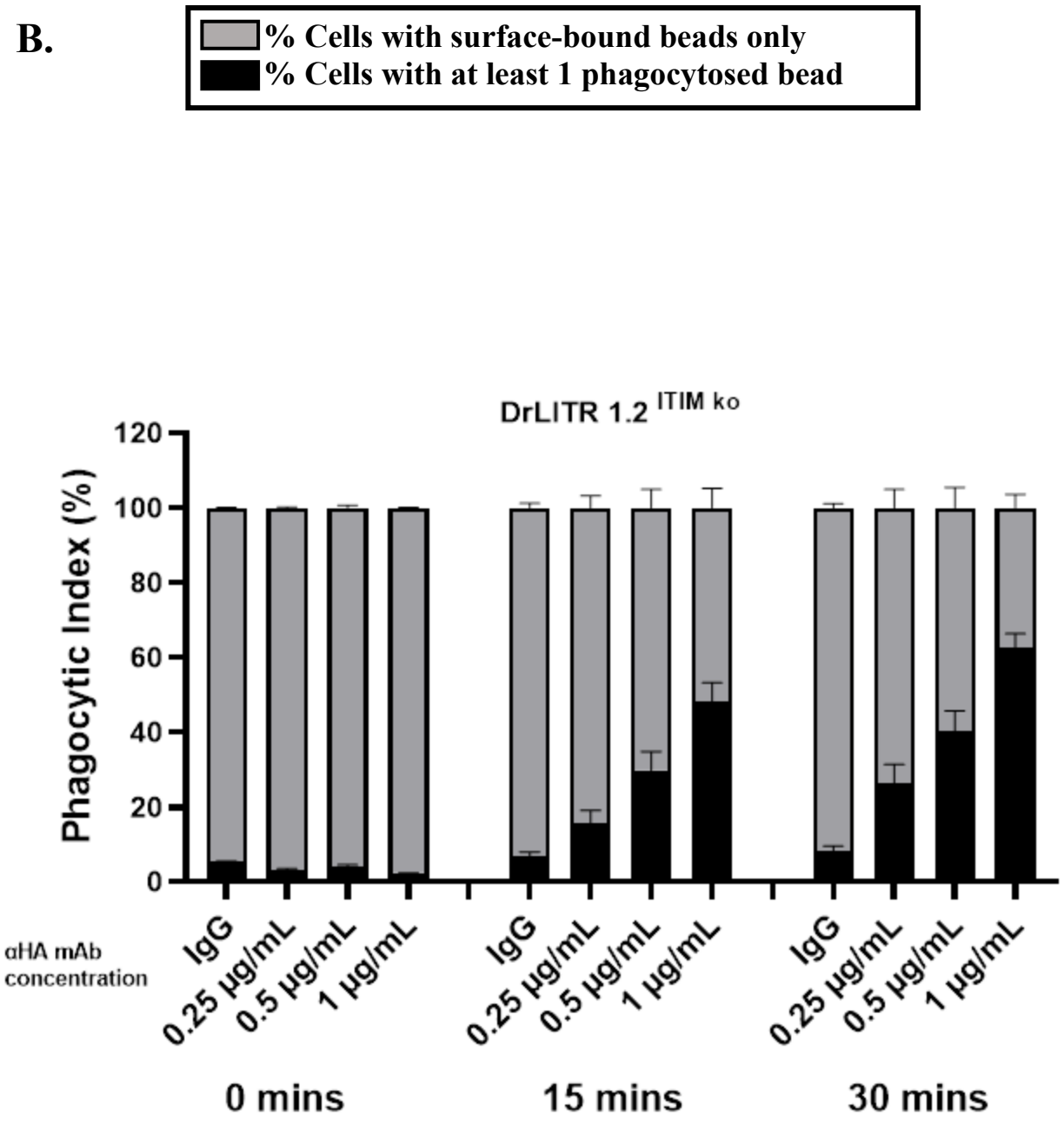
% Cells with surface-bound beads only
% Cells with at least 1 phagocytosed bead
DrLITR 1.2 ITIM ko
Phagocytic Index (%)
120
100
80
60
40
20
0
αHA mAb concentration
IgG
0.25 µg/mL
0.5 µg/mL
1 µg/mL
0 mins
15 mins
30 mins

C.

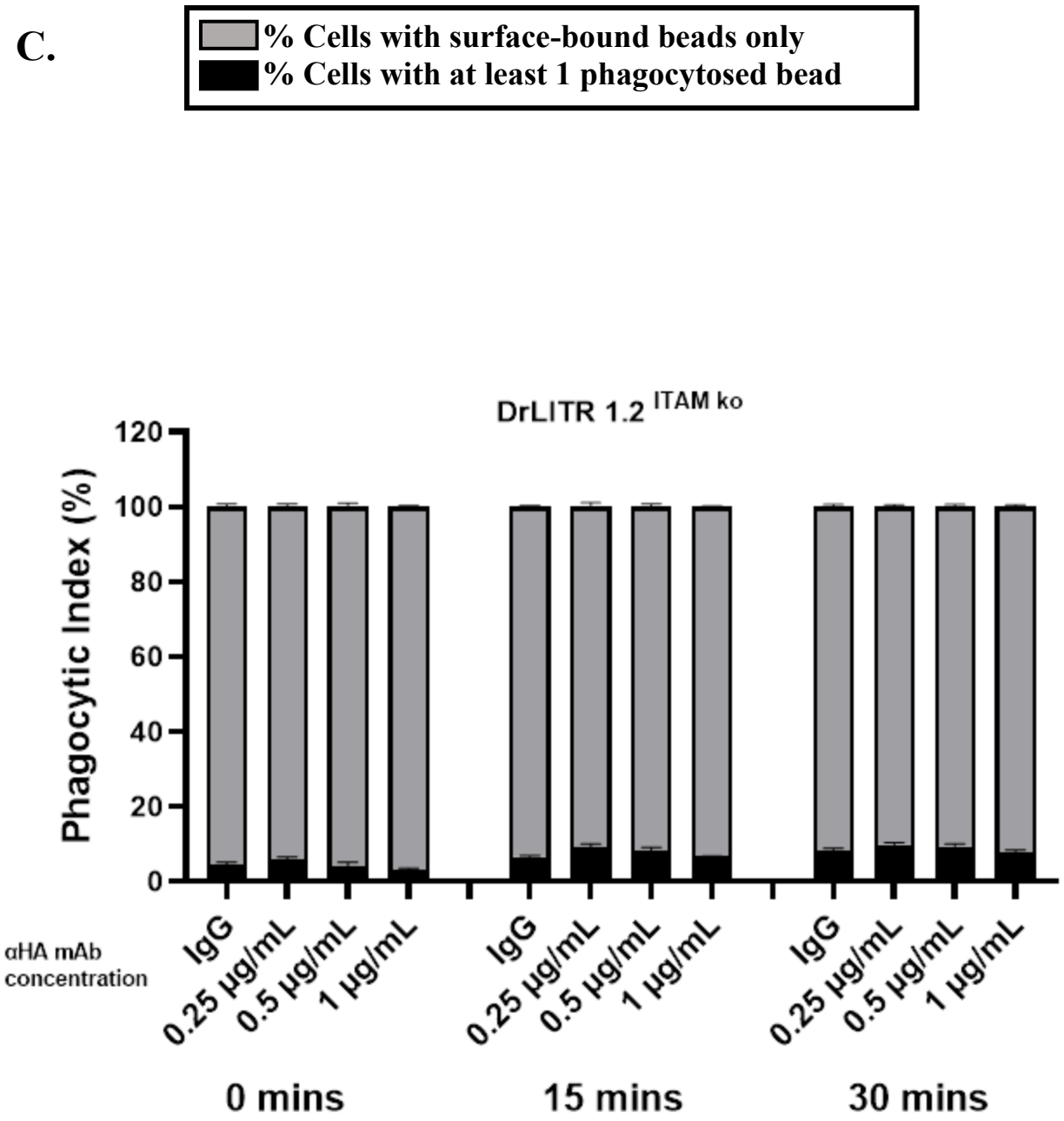
% Cells with surface-bound beads only
% Cells with at least 1 phagocytosed bead
DrLITR 1.2 ITAM ko
Phagocytic Index (%)
120
100
80
60
40
20
0
αHA mAb concentration
IgG
0.25 µg/mL
0.5 µg/mL
1 µg/mL
0 mins
15 mins
30 mins

D.

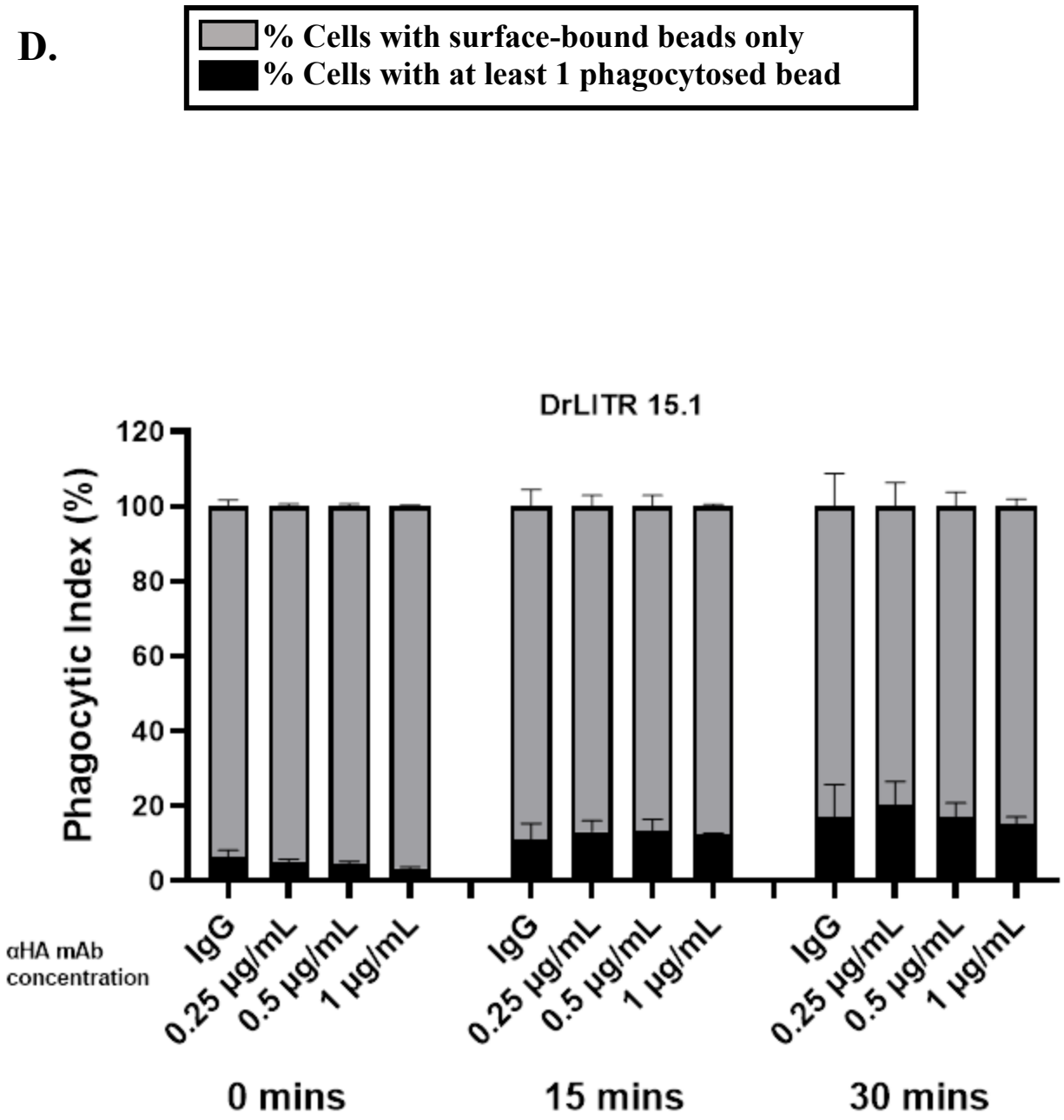
% Cells with surface-bound beads only
% Cells with at least 1 phagocytosed bead
DrLITR 15.1
Phagocytic Index (%)
120
100
80
60
40
20
0
αHA mAb concentration
IgG
0.25 µg/mL
0.5 µg/mL
1 µg/mL
IgG
0.25 µg/mL
0.5 µg/mL
1 µg/mL
IgG
0.25 µg/mL
0.5 µg/mL
1 µg/mL
0 mins
15 mins
30 mins

Figure 4.4. Concentration optimization of αHA mAb on YG microsphere targets for optimal DrLITR-based phagocytosis conditions. 3 x 10^5 AD-293 cells stably expressing DrLITR constructs, 1.2 ^{wt} (**A**), 1.2 $^{ITIM\ ko}$ (**B**), 1.2 $^{ITAM\ ko}$ (**C**), and 15.1 (**D**) constructs were incubated with 4.5μm YG beads (9 x 10^5) opsonized with varying levels of mAb αHA (1, 0.5, and 0.25μg/mL) for 0, 15 and 30 minutes at 37°C (or isotype control IgG_1 (1μg/mL) opsonized YG beads) before being counter-stained and subsequently analyzed using the ImageStream X Mark II. Events were classified as phagocytic (P; black bars) with at least 1 bead being internalized or surfaced bound (S; grey bars) with only surface attached beads. Samples were normalized, and the % values were calculated as # of surface-bound events or # of phagocytic events / # of all bead-associated events. Each bar represents the mean ± SEM of total cells associated with beads from 3 separate experiments.

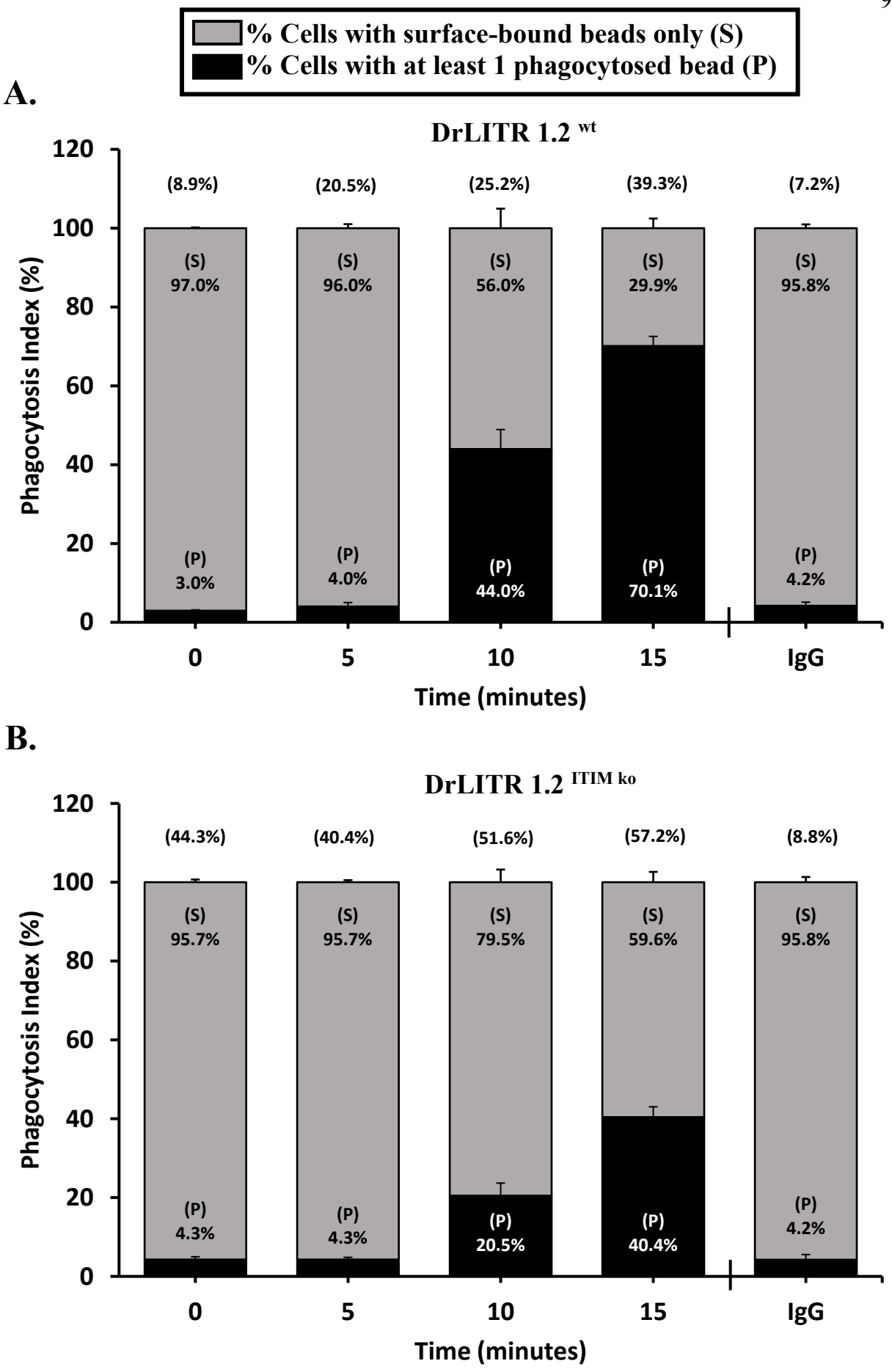
% Cells with surface-bound beads only (S)
% Cells with at least 1 phagocytosed bead (P)
A.
DrLITR 1.2 wt
Phagocytosis Index (%)
120
100
80
60
40
20
0
(8.9%)
(20.5%)
(25.2%)
(39.3%)
(7.2%)
(S) 97.0%
(S) 96.0%
(S) 56.0%
(S) 29.9%
(S) 95.8%
(P) 3.0%
(P) 4.0%
(P) 44.0%
(P) 70.1%
(P) 4.2%
0
5
10
15
IgG
Time (minutes)
B.
DrLITR 1.2 ITIM ko
Phagocytosis Index (%)
120
100
80
60
40
20
0
(44.3%)
(40.4%)
(51.6%)
(57.2%)
(8.8%)
(S) 95.7%
(S) 95.7%
(S) 79.5%
(S) 59.6%
(S) 95.8%
(P) 4.3%
(P) 4.3%
(P) 20.5%
(P) 40.4%
(P) 4.2%
0
5
10
15
IgG
Time (minutes)

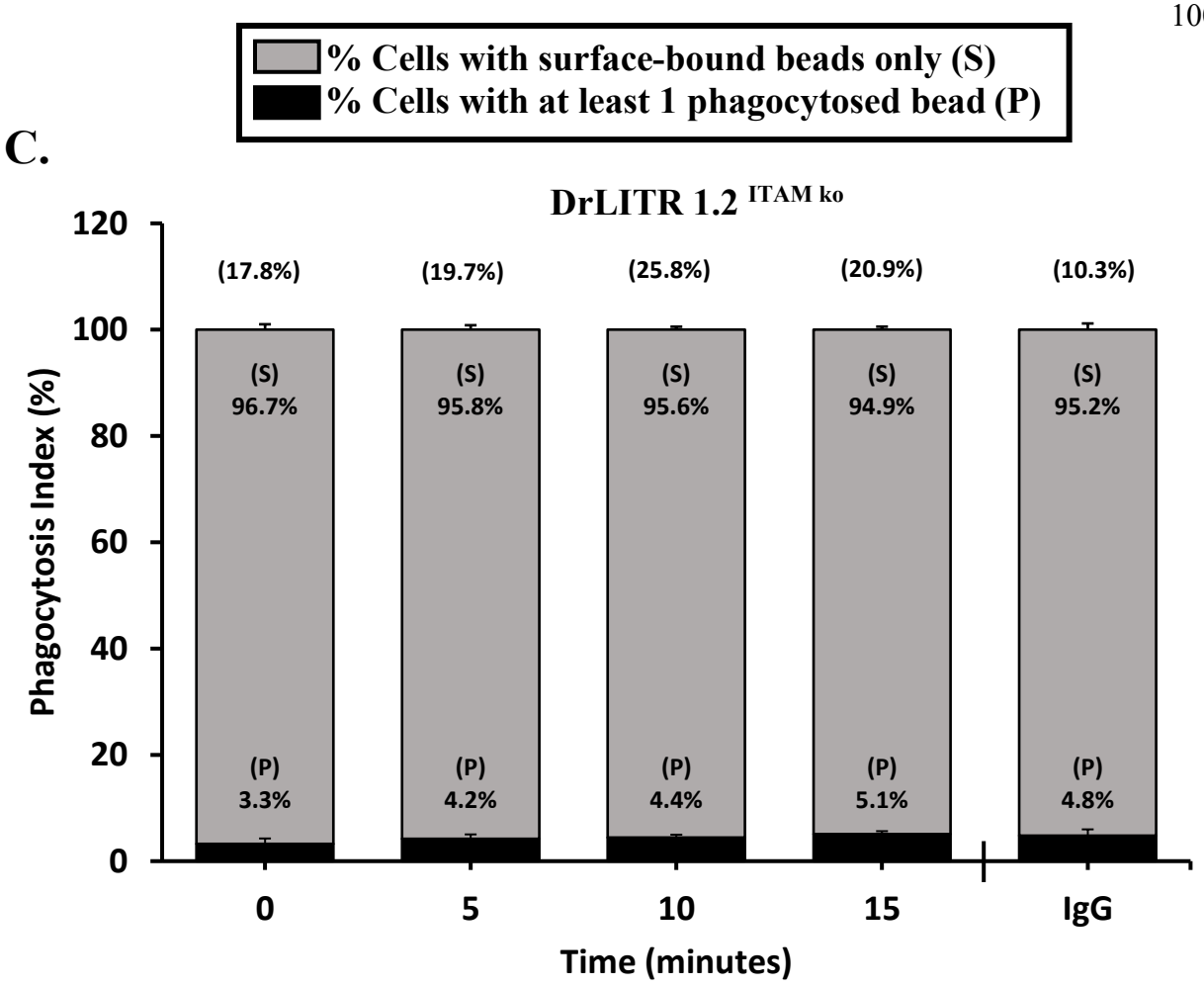
% Cells with surface-bound beads only (S)
% Cells with at least 1 phagocytosed bead (P)
C.
DrLITR 1.2 ITAM ko
Phagocytosis Index (%)
120
100
80
60
40
20
0
(17.8%)
(19.7%)
(25.8%)
(20.9%)
(10.3%)
(S) 96.7%
(S) 95.8%
(S) 95.6%
(S) 94.9%
(S) 95.2%
(P) 3.3%
(P) 4.2%
(P) 4.4%
(P) 5.1%
(P) 4.8%
0
5
10
15
IgG
Time (minutes)

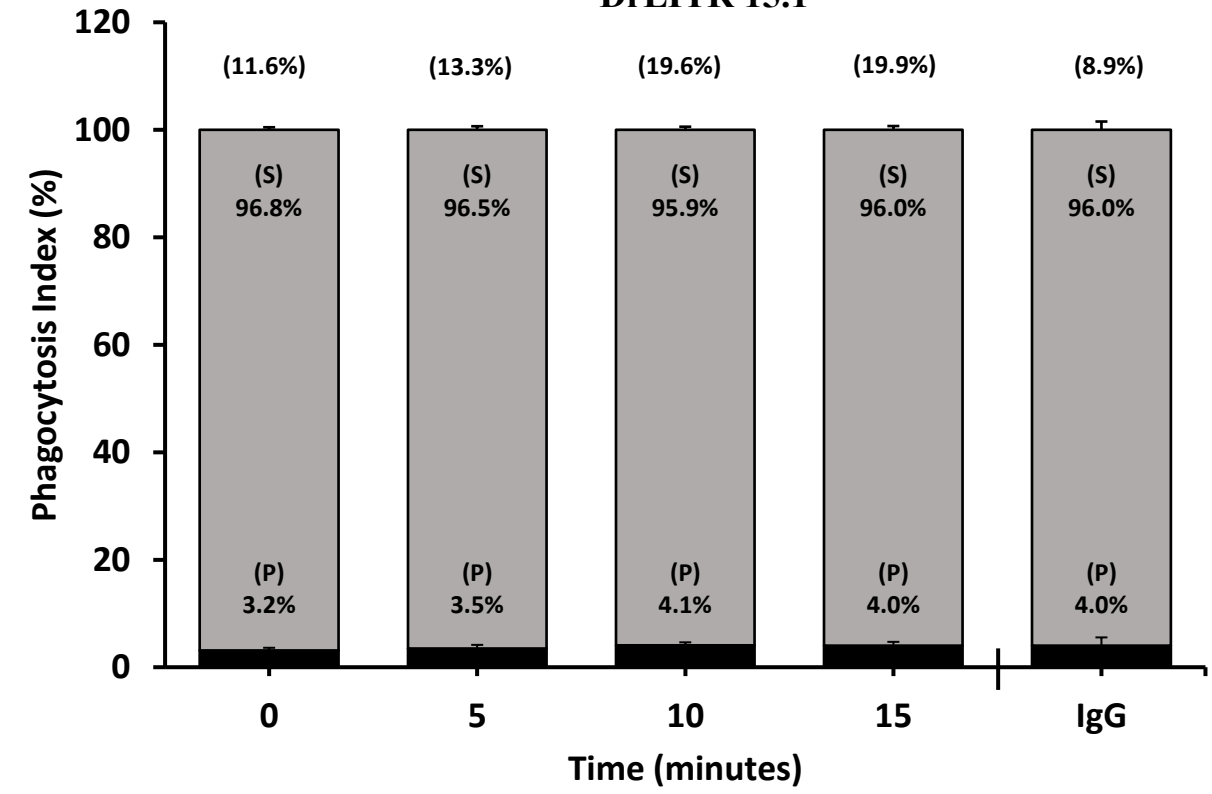
D.
DrLITR 15.1
Phagocytosis Index (%)
120
100
80
60
40
20
0
(11.6%)
(13.3%)
(19.6%)
(19.9%)
(8.9%)
(S) 96.8%
(S) 96.5%
(S) 95.9%
(S) 96.0%
(S) 96.0%
(P) 3.2%
(P) 3.5%
(P) 4.1%
(P) 4.0%
(P) 4.0%
0
5
10
15
IgG
Time (minutes)

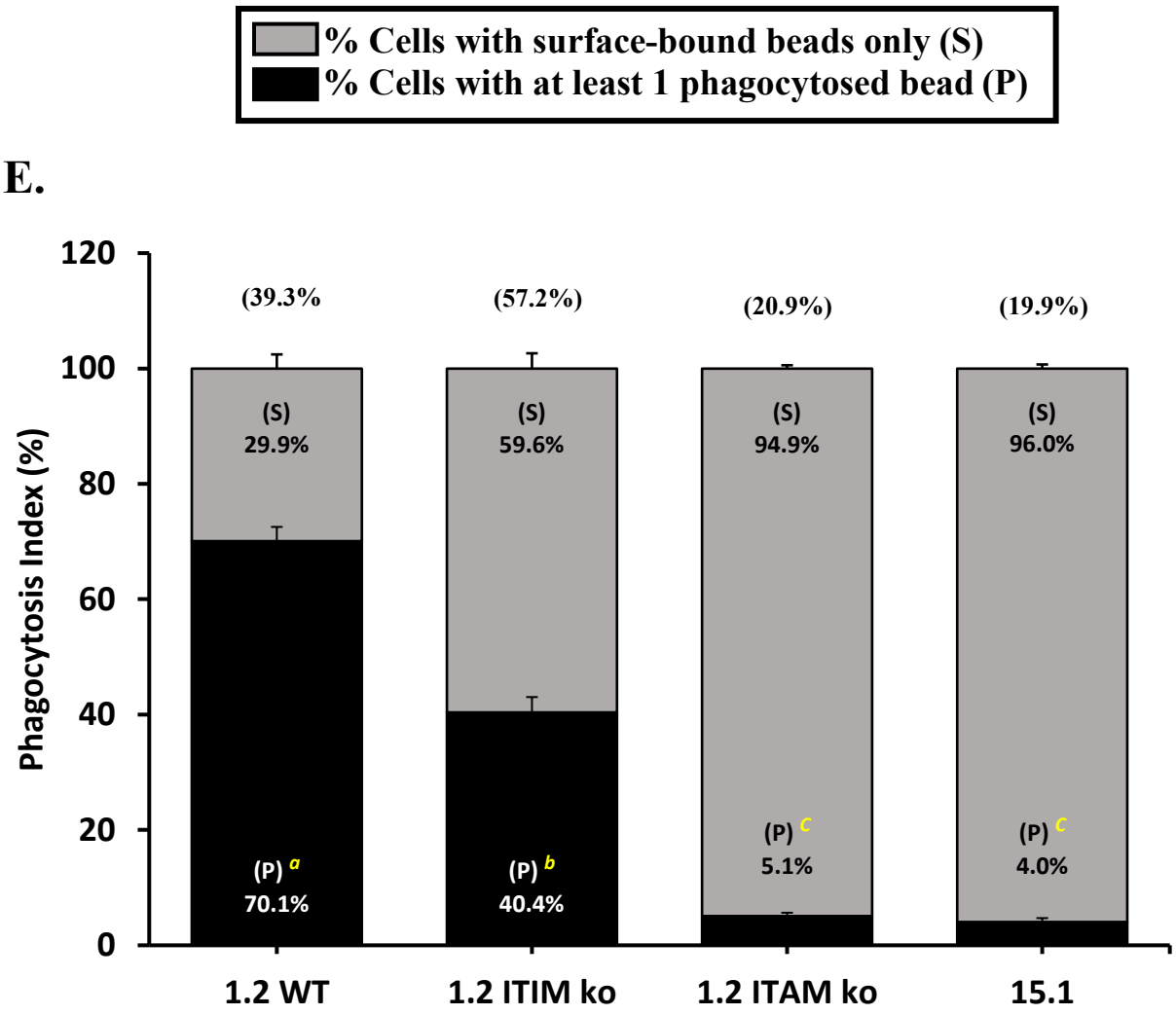

Figure 4.5. Temporal-based analysis of DrLITR-mediated phagocytosis through imaging flow cytometry. 3 x 10^5 AD293 cells stably expressing DrLITR 1.2 ^{wt} (**A**), 1.2 $^{ITIM\ ko}$ (**B**), 1.2 $^{ITAM\ ko}$ (**C**), and 15.1 (**D**) constructs were incubated with mAb αHA (1µg/mL) opsonized 4.5µm YG beads (9 x 10^5) for 0, 5, 10, and 15 minutes at 37°C (or isotype control IgG_1 (1µg/mL) opsonized YG beads for 15 minutes) before being counter-stained and subsequently analyzed using the ImageStream X Mark II. For additional analysis, the 15-minute bead incubation values (**E**) for each construct were conglomerated and compared to each other. Events were classified as either being phagocytic (P; black bars) with at least 1 bead being internalized or surfaced bound (S; grey bars) with only surface attached beads. Samples were normalized, and the % values were calculated as # of surface-bound events or # of phagocytic events / # of all bead-associated events. Each bar represents the mean ± SEM of total cells associated with beads from 3 separate experiments. The bracketed % value above each bar represents the proportion of cells associated with beads. Sample data groups were analyzed using a one-way ANOVA and Tukey test (Prism 6, GraphPad, La Jolla, CA, USA). Bars containing different letters (*a, b,* or *c*) represent statistical significance ($p \leq 0.05$) between phagocytosis (%) means.

A.

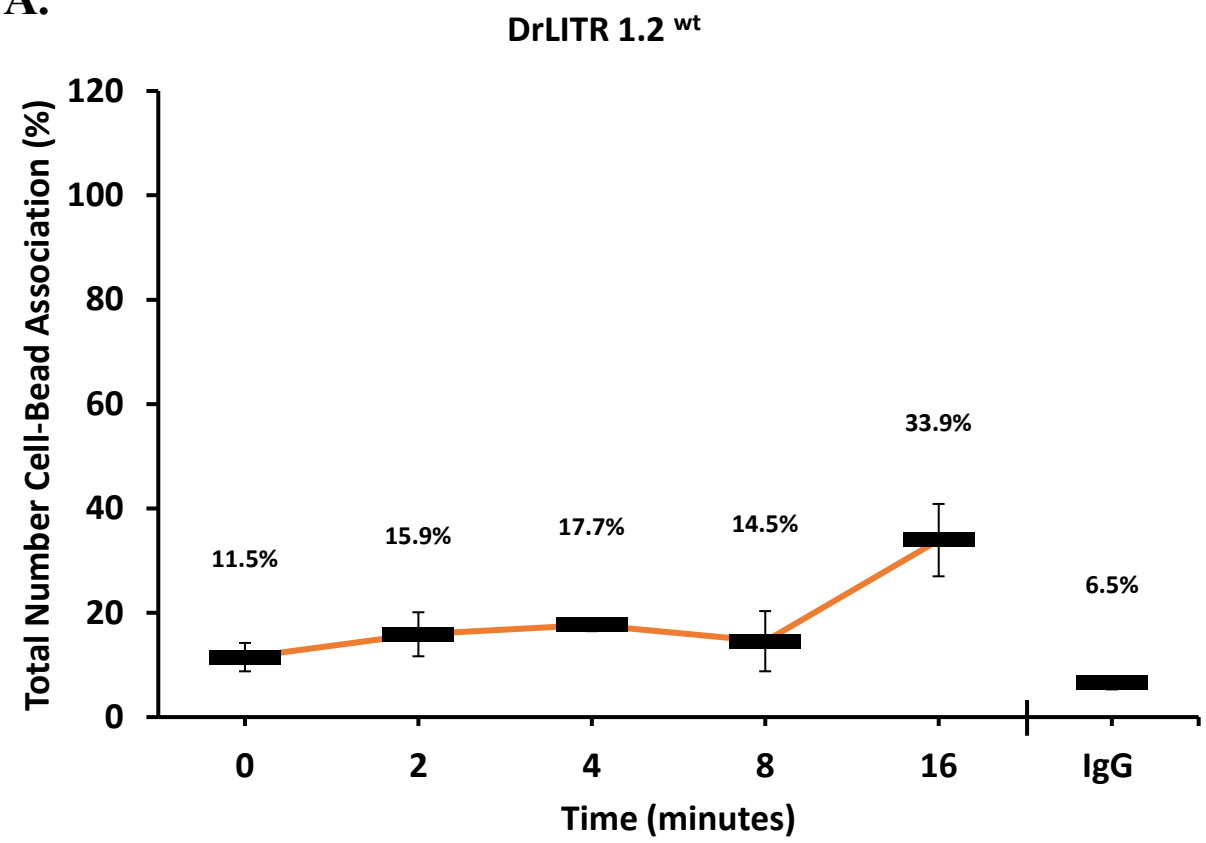
DrLITR 1.2 wt
Total Number Cell-Bead Association (%)
120
100
80
60
40
20
0
11.5%
15.9%
17.7%
14.5%
33.9%
6.5%
0
2
4
8
16
IgG
Time (minutes)

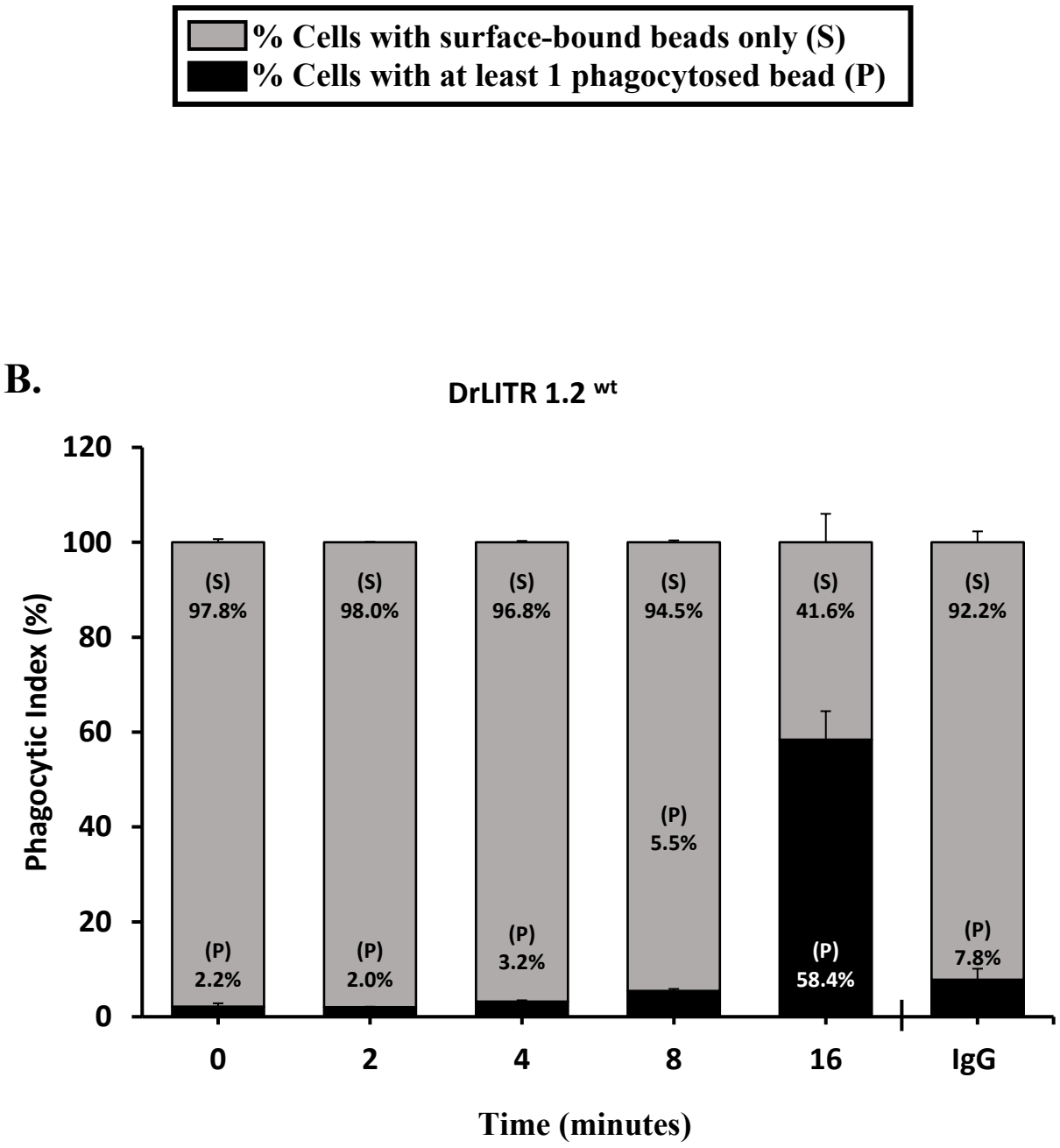
% Cells with surface-bound beads only (S)
% Cells with at least 1 phagocytosed bead (P)
B.
DrLITR 1.2 wt
Phagocytic Index (%)
120
100
80
60
40
20
0
(S) 97.8%
(P) 2.2%
(S) 98.0%
(P) 2.0%
(S) 96.8%
(P) 3.2%
(S) 94.5%
(P) 5.5%
(S) 41.6%
(P) 58.4%
(S) 92.2%
(P) 7.8%
0
2
4
8
16
IgG
Time (minutes)

C.

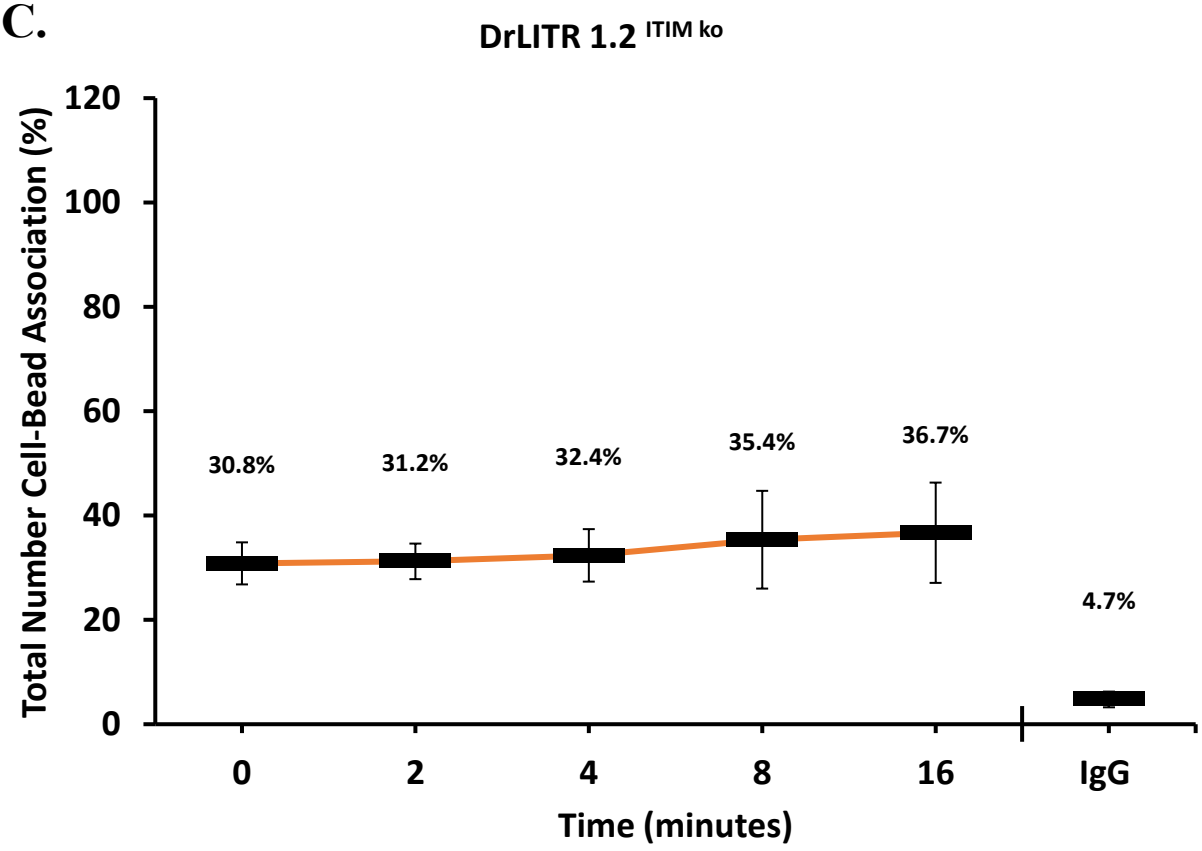
DrLITR 1.2 ITIM ko
Total Number Cell-Bead Association (%)
120
100
80
60
40
20
0
30.8%
31.2%
32.4%
35.4%
36.7%
4.7%
0
2
4
8
16
IgG
Time (minutes)

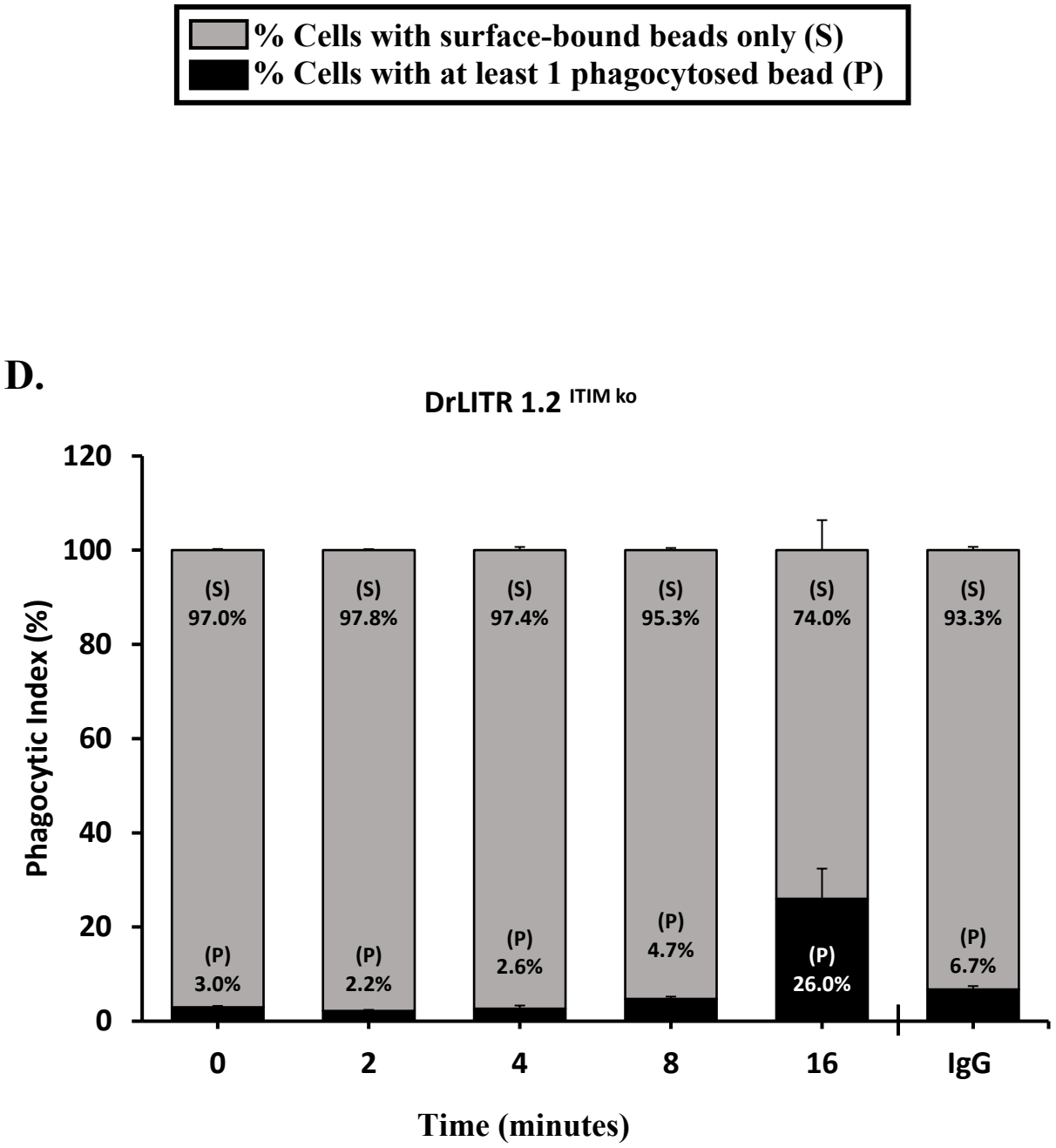
% Cells with surface-bound beads only (S)
% Cells with at least 1 phagocytosed bead (P)
D.
DrLITR 1.2 ITIM ko
Phagocytic Index (%)
120
100
80
60
40
20
0
(S) 97.0%
(P) 3.0%
(S) 97.8%
(P) 2.2%
(S) 97.4%
(P) 2.6%
(S) 95.3%
(P) 4.7%
(S) 74.0%
(P) 26.0%
(S) 93.3%
(P) 6.7%
0
2
4
8
16
IgG
Time (minutes)

Figure 4.6. Knockout mutant displays contrasting binding and phagocytic phenotype during recovery from cold incubation. 3 x 10^5 AD-293 cells stably expressing DrLITR 1.2 ^{wt} and 1.2 $^{ITIM\ ko}$ constructs were preincubated for 30 minutes at 4°C followed by the addition of 4.5μm YG beads (9 x 10^5) opsonized with αHA mAb (1μg/mL) and left to incubate for a further 30 minutes at 4°C. Samples were then allowed to warm at differing increments by moving them to 37°C for 0, 2, 4, 8 and 16 minutes. As an isotype control, cells were alternatively given IgG_1 (1μg/mL) coated YG beads, incubated at 4°C then warmed at 37°C for 16 minutes. Samples were then counter-stained and subsequently analyzed using the ImageStream X Mark II. Cells associated with bead targets from 1.2 ^{wt} (**A**) or 1.2 $^{ITIM\ ko}$ (**B**) samples were calculated as the # of cell-bead-associated events / # total cell events. In addition, events from 1.2 ^{wt} (**C**) or 1.2 $^{ITIM\ ko}$ (**D**) were classified as either being phagocytic (P; black bars) with at least 1 bead being internalized or surfaced bound (S; grey bars) with only surface attached beads. Samples were normalized, and the % values were calculated as # of surface-bound events or # of phagocytic events / # of all cell-bead-associated events. Each bar and line bar represents the mean ± SEM from 3 independent experiments.

Chapter V

Examining Recruitment of pSHP-2 and Stimulatory Signalling Effectors during DrLITR 1.2-mediated Phagocytosis

5.1 Introduction

In chapter IV, my results showed that DrLITR 1.2 ^{wt} induced an ITAM-dependent mode of phagocytosis when engaged with opsonized bead targets, however, the phagocytic activity was significantly reduced when the ITIM within the CYT was functionally knocked out. It was also shown that target binding to DrLITR 1.2 $^{ITIM\ ko}$-expressing cells increased in comparison to the binding of targets to DrLITR 1.2 ^{wt}-expressing cells and even facilitated enhanced target binding at sub-ambient temperatures. Taken together, these observations suggest that the ITIM motif within DrLITR 1.2 is required to facilitate the receptor's full phagocytic potential and is likely directly involved in the downstream signalling mechanisms of DrLITR 1.2 ITAM-dependent control over target binding and engulfment processes.

The requirement of the ITAM within the CYT of DrLITR 1.2 for the induction of phagocytosis suggests that this receptor may be similar to that of classical stimulatory receptor-types such as the mammalian FcRs (51). Initial engagement of the receptors by ligands results in SFKs phosphorylating tyrosine residues embedded within the ITAM of the receptor CYT (51,89,90). This then creates a docking site by which early signalling kinases, such as Syk, can be recruited via their SH2 domains. This association with the receptor causes Syk to become activated (by SFKs or autophosphorylation), resulting in further phosphorylation and activation of other downstream signalling components (e.g., PI3K and PLCγ), leading to regulation of F-actin polymerization and cell membrane remodelling for the engulfment of bound receptor

ligands. Since the phagocytic response requires a functional ITAM within the CYT of DrLITR 1.2, it can be hypothesized that the engulfment of targets is initiated by the engagement of receptors leading to the recruitment of proximal signalling molecules (SFKs and Syk), facilitating activation of intermediate signalling components (PI3K), resulting in the induction of distal phagocytic machinery (F-actin polymerization) commonly associated with the control of ITAM-dependent phagocytosis. Thus pharmacological inhibition of these components during the phagocytic process should result in a significant abrogation of DrLITR 1.2-mediated phagocytosis. The use of small molecule inhibitory drugs has been utilized in our lab for pharmacological profiling of the ITAM-dependent and ITAM-independent signalling pathways of both IpLITR 2.6b and the IpLITR 1.1b phagocytosis, respectively (11). For example, drug inhibition of the signalling components SFK, Syk, PI3K, Akt, Cdc42, RAC1/2/3, MEK1/2, PDK1 and F-actin polymerization all dampened the phagocytic response observed during engagement of IpLITR 2.6b receptors in RBL-2H3 cells. However, it was found that only inhibition of SFK, Syk, and F-actin polymerization resulted in a decrease of phagocytosis observed for IpLITR 1.1b. This data suggested that the mechanisms utilized by IpLITR 1.1b differed from that of IpLITR 2.6b, requiring a smaller set of signalling components for the inductions of IpLITR 1.1b-mediated phagocytosis.

Since a reduction of phagocytosis was previously observed as a result of mutating the ITIM within the CYT of DrLITR 1.2, it is likely that the direct recruitment of signalling molecules to this motif somehow facilitates the enhancement of signalling downstream of receptor engagement. ITIM-containing receptors are classically associated with inhibition via the recruitment of SH2-domain-containing tyrosine phosphatases such as SHP-1, SHP-2, and SHIP (19,89). These enzymes facilitate the hydrolysis of phosphate groups resulting in signalling

molecule inactivation and/or inability to associate with other signalling molecules and domains, overall dampening effector responses. As mentioned previously, increasing data on ITIM-containing receptors is beginning to reveal that aside from their classical inhibitory roles, these receptors are also involved in the induction of stimulatory signalling. For example, PECAM-1 contains tandem ITIMs within its CYT that have been shown to recruit Syk (139). Approximately 22 amino acids separate the tyrosines within the ITIMs at a distance greater than the ~12 amino acids typical ITAM tyrosines are separated by. However, it was shown that the phosphorylation of both tyrosines exhibits ITAM-like properties and are required for the association with Syk, leading to Syk phosphorylation aiding in macrophage proliferation and preventing aggregation of cells. In a similar context, our lab's previous studies have also showcased that the ITIM-containing receptor IpLITR 1.1b induces an ITAM-independent mode of phagocytosis in myeloid cells facilitated by the catalytic activity of both Src and Syk kinases (9–11). In addition to the functional plasticity of signalling motifs, signalling molecules classically associated with specific motifs are not restricted to facilitate strict inhibition or activation. For example, SHP-2 can also function as an adaptor molecule in a phosphatase-independent mechanism by associating with Gab2, which contains tyrosine motifs, a PH domain, as well as a proline-rich region for binding of SH3 and SH2 domain-containing molecules such as PI3K and PLCγ (171). Stimulated platelet-derived growth factor receptor (PDGF-R) has also been shown to bind SHP-2 to a tyrosine residue within the CYT of the receptor, causing SHP-2 itself to become phosphorylated and allowing for Grb-2 binding directly to SHP-2 (172). This association with SHP-2 leads to further activation of downstream molecules such as Ras, a key regulator of cell proliferation, growth, and migration (6). This SHP-2 complexing with Grb2 as well as Gab2 is also observed during T lymphocyte stimulation with IL-2, where mutations

preventing the recruitment of SHP-2 resulted in controlled activation of ERK (171). Interestingly, the phosphatase enzymatic activity of SHP-2 is also documented to contribute to the stimulatory induction of cell signalling. For example, SHP-2 is required in RTK signalling by dephosphorylating the transmembrane glycoprotein PAG/Cbp (173). This protein directly associates with Csk, localizing it close to SFKs within the cell, allowing Csk to dampen SFK activity by phosphorylating inhibitory C-terminal tyrosines. The activity of SHP-2 indirectly bolsters SFK activation, and in contrast, SHP-2 deficiency has led to hyperphosphorylation of SFK C-terminal tyrosines and also decreased PLCγ and Ras activation. Overall, both lines of evidence for SHP-2-based cell activation suggest two models (i.e., phosphatase-independent and phosphatase-dependent) are possible regarding the ITIM-enhancement of DrLITR 1.2-mediated phagocytosis. Therefore, it is hypothesized that DrLITR 1.2 recruits SHP-2 to its ITIM motif during the phagocytosis of bead targets. It is also hypothesized that if SHP-2 was recruited, it plays a role in the enhancement of the DrLITR 1.2-mediated phagocytic response observed compared to the ITIM knockout variant. It is also predicted that if pSHP-2 is indeed recruited during phagocytosis, it is possible to decern whether the enzymatic activity of the phosphatase plays a role in this response through pharmacological inhibition of SHP-2 and measuring the level of phagocytosis that changes from blocking this potential pathway by utilizing the phagocytosis assay established in chapter IV.

The objective of this thesis chapter was to begin to examine the signalling dynamics associated with DrLITR 1.2 control over the phagocytic response. To test my hypothesis that SHP-2 is recruited and involved in fine-tuning DrLITR-mediated phagocytosis, fluorescence confocal microscopy was used to examine the recruitment of phosphorylated SHP-2 (pSHP-2) to phagocytic cups formed by DrLITR 1.2-expressing cells engulfing bead targets. In addition, a

pharmacological profile was conducted on DrLITR 1.2 to examine further the potential involvement of SHP-2 and molecules commonly associated with ITAM-dependent phagocytosis. My results indicate that pSHP-2 is recruited during DrLITR-mediated phagocytosis and that its augmentation of phagocytosis may be independent of phosphatase activity. Additionally, my results also show that the signalling network as well as the signalling components (i.e., SFK, Syk, PI3K and F-actin polymerization) utilized by DrLITR 1.2 reflects that of an ITAM-containing receptor. This data provide new insights into the mechanistic control over cellular effector responses by an ITAM and ITIM-containing receptor.

5.2 Results

5.2.1 Confocal Examination of pSHP-2 and pSyk Recruitment during DrLITR 1.2-mediated Phagocytosis

Confocal fluorescence microscopy was performed to assess the recruitment of pSHP-2 to the CYT of DrLITR 1.2. Specifically, DrLITR 1.2 ^{wt}, DrLITR 1.2 $^{ITIM\ ko}$, and DrLITR 1.2 $^{ITAM\ ko}$-expressing cells were incubated with αHA mAb opsonized NF beads. As controls, IpLITR 2.6b and IpLITR 1.1b co-expressing cells were incubated with either αHA mAb + αFLAG mAb or αHA mAb + IgG_1 co-opsonized beads. Extracellularly exposed areas of bead targets were stained with IgG-conjugated AF647 (red) to decern between internalized targets that were protected from staining by the cellular membrane. Cells were internally stained for signalling molecules of interest (i.e., pSHP-2 or pSyk) using primary pAb and secondary IgG-conjugated AF488 (green). Analysis of bead targets that were partially engulfed by the cells were represented by a red half-ring fluorescence where an active phagocytic process was occurring. Representative microscopy images (Fig. 5.1) show the fluorescence of stained molecules of interest (top panel; green),

counterstained exposed bead targets (middle panel; green) and a merge between the two fluorescence channels (bottom panel; red + green). Cross-linking of both IpLITR 2.6b and IpLITR 1.1b with the same bead target resulted in the recruitment of pSHP-2 to the phagocytic synapse (i.e., areas around the target that contained minimal amounts of red bead counter stain) represented by the green fluorescence (Fig. 5.1A). In comparison, engagement of IpLITR 2.6b alone did not result in the recruitment of pSHP-2. DrLITR 1.2 ^{wt} engagement also resulted in the recruitment of pSHP-2 to the bead-cell interface, however, DrLITR 1.2 containing a dysfunctional ITIM (i.e., DrLITR 1.2 $^{ITIM\ ko}$) did not. In addition, receptors containing a dysfunctional ITAM motif also displayed an absence of pSHP-2 recruitment and had reduced numbers of phagocytic events when compared to the other receptor construct-expressing cells (data not shown). In addition to pSHP-2 recruitment, IpLITR 2.6b, DrLITR 1.2 ^{wt}, and DrLITR 1.2 $^{ITIM\ ko}$ all recruited pSyk to the phagocytic synapse when engaged by bead targets, while DrLITR 1.2 $^{ITAM\ ko}$ did not (Fig.5.1B).

To further assess the recruitment of pSHP-2 to the receptor CYT during LITR-mediated phagocytosis and to quantify the level of fluorescence, microscopy images were measured for the mean fluorescence intensity (MFI) across targets during cellular engulfment. For each figure, a reference arrow was drawn across a bead target where the level of fluorescence for both pSHP-2 (left panel; green) as well as bead counterstain (middle panel; red) was measured within the merged fluorescence image (Fig. 5.2; right panel; green + red). The measured fluorescence of pSHP-2 (green line) and the bead counter stain (red line) across the reference arrow were then plotted on a histogram. Targets of interest are indicated (*) and were chosen for their pattern of decreased fluorescence of bead stain at the bead-cell interface indicating the target was being engulfed. Figure 5.2A shows co-opsonized beads being engulfed at the time of sample

preparation by IpLITR 2.6b and IpLITR 1.1b co-expressing cells indicated by the absence of bead counterstain fluorescence on the side of the target interacting with the cell (Fig. 5.2A; 6.75 μm, ~450 MFI). This was inverse for the level of pSHP-2 fluorescence examined in the same region (~1875 MFI). The area of the extracellularly exposed bead had prominent levels of bead counterstain fluorescence (2.25 μm; ~1905 MFI) with low levels of pSHP-2 (~375 MFI). When IpLITR 2.6b was engaged alone by targets, engulfment of beads still took place as indicated by the single high peak of bead fluorescence (Fig. 5.2B; 2.52 μm, ~3500 MFI), however, intracellular recruitment of pSHP-2 at the bead-cell interface did not occur (7.02 μm, ~800 MFI). Examination of wild-type DrLITR 1.2 (i.e., DrLITR 1.2 ^{wt}) during bead target engagement also led to phagocytosis of the target (Fig. 5.2C; 2.20 μm, ~2800 MFI), while recruiting elevated levels of pSHP-2 to the phagocytic synapse (6.75 μm, ~2400 MFI). In comparison, DrLITR 1.2 $^{ITIM\ ko}$ engulfment of targets (2.20 μm, ~2450 MFI) did not result in the recruitment of intracellular pSHP-2 (Fig. 5.2D, 6.70 μm, ~500 MFI). In all measured samples, the areas of extracellularly exposed beads had no recruitment of pSHP-2, as indicated by little to no overlap of bead fluorescence. In contrast, high fluorescence of pSHP-2 was seen at the intracellular portion of the target, where no bead stain was measured.

The mean fluorescence intensities of pSHP-2 at the bead-cell synapse was measured for fifty separate phagocytic events for IpLITR 2.6b crosslinked with IpLITR 1.1b, IpLITR 2.6b engaged alone, DrLITR 1.2 ^{wt} and DrLITR 1.2 $^{ITIM\ ko}$. Consistent with what was observed above, the cross-linking of IpLITR 2.6b with IpLITR 1.1b resulted in the recruitment of pSHP-2 (Fig. 5.3; ~1360 MFI) to the phagocytic synapse at significantly higher levels ($p \leq 0.001$) than that of single engagement of IpLITR 2.6b to targets (~570 MFI). Similarly, engagement of DrLITR 1.2 ^{wt} to bead targets also resulted in high pSHP-2 fluorescence (~1250 MFI) that was significantly

($p \leq 0.001$) decreased when the ITIM was knocked out (~530 MFI). Overall, this data suggests that co-engagement of IpLITR 2.6b with IpLITR 1.1b results in the recruitment of pSHP-2 to the phagocytic synapse. Additionally, my results show that DrLITR 1.2 can also recruit pSHP-2 during phagocytosis and is dependent on the presence of a functional ITIM within the receptor CYT.

Further examination of the phagocytic synapse for the recruitment of pSyk was conducted similarly to what was mentioned above for pSHP-2 fluorescence examination. Briefly, the fluorescence of pSyk (green) and bead counterstain (red) was measured on a reference arrow that crossed a bead target undergoing phagocytosis (Fig. 5.4). Targets being engulfed by IpLITR 2.6b-expressing cells resulted in the recruitment of pSyk (Fig. 5.4A; green line, 6.4 μm, ~2950 MFI) to the phagocytic synapse opposite to the extracellularly exposed side of the target as indicated by the single bead-stained peak (red line; 1.9 μm, ~3500 MFI). This was also seen for targets being engulfed by DrLITR 1.2 ^{wt} and DrLITR 1.2 $^{ITIM\ ko}$ co-expressing cells where pSyk recruitment resulted in high measured fluorescence at the bead-cell interface at ~3500 MFI (Fig. 5.4B; 6.7 μm) and ~2800 MFI (Fig. 5.4C; 6.5 μm), respectively. However, mutation of the ITAM motif within DrLITR 1.2 (i.e., DrLITR 1.2 $^{ITAM\ ko}$) led to an overall reduction of recruited pSyk to the bead-cell interface where low fluorescence was measured (Fig. 5.4D; 6.6 μm, ~1020 MFI). Similar to pSHP-2 examination, there was little to no measured merged fluorescence between exposed beads and recruitment of pSyk at areas of high fluorescence intensity. In summary, IpLITR 2.6b, along with DrLITR 1.2, are able to recruit pSyk to the phagocytic synapse during the phagocytosis of bead targets. In addition, DrLITR 1.2-mediated recruitment of pSyk is dependent on a functional ITAM within the receptor CYT.

5.2.2 Pharmacological Examination of DrLITR-mediated Phagocytosis

To investigate the potential mechanisms involved in DrLITR-controlled signalling, pharmacological inhibitors of signalling molecules and phagocytic machinery components were examined for their effects on DrLITR-mediated phagocytosis. In addition to pharmacological profiling, separate YG targets were given to samples that were opsonized with either a higher or lower concentration of αHA mAb to observe how receptor-target binding avidity affects the induction of signalling components for phagocytosis. Finally, an enzymatic inhibitor of SHP-2 activity was also used to decern the potential role SHP-2 plays in bolstering DrLITR 1.2-mediated phagocytosis. Molecules chosen for pharmacological inhibition were selected based on components associated with ITAM-dependent phagocytosis as well as previous pharmacological studies done in our lab on IpLITR 2.6b and IpLITR 1.1b-mediated phagocytosis (11). Inhibitors used in this thesis are listed in Table 3.2, which displays drug names, their intracellular molecular target(s), and the concentrations used at high dose (HD; μM) and low dose (LD; μM) levels. Figure 5.5 shows the inhibition of phagocytosis (y-axis) due to the addition of the indicated pharmacological inhibitors (x-axis) added to samples and was analyzed using the imaging flow cytometric phagocytosis assay explored in chapter IV.

Inhibitory profiles between LITR-expressing cells show similar trends in the reduction of phagocytosis. For example, IpLITR 2.6b, DrLITR 1.2 ^{wt}, and DrLITR 1.2 $^{ITIM\ ko,}$ when engaged with low αHA mAb opsonized targets, were most affected by Cytochalasin D (actin polymerization; 84% - 90% inhibition), Wortmannin (PI3K; 67% - 80% inhibition), and PP2 (Src kinases; 22% - 73% inhibition; Fig. 5.5A, 5.5B, and 5.5C). However, PP2 appeared more effective at inhibiting phagocytosis associated with DrLITR 1.2 $^{ITIM\ ko}$ (67%) compared to DrLITR 1.2 ^{wt} (22%; compare Fig. 5.5B vs Fig. 5.5C). NSC 87877 (SHP-2) also affected all

three LITR construct-expressing cells lines similarly with no significant ($p \geq 0.05$) inhibition of phagocytosis, though it is noted that in all three cases, there appears to be a slight increase in phagocytosis rather than any inhibition, ranging from -3% to -10% inhibition (Fig. 5.5A, 5.5B, and 5.5C). While DrLITR 1.2 ^{wt} appeared to be affected by ER 27319 (Syk) with inhibition of 16%, only inhibition of DrLITR 1.2 $^{ITIM\ ko}$ (26%) and IpLITR 2.6b-mediated phagocytosis (41%) by the drug was significantly ($p \leq 0.05$) different from the vehicle control. A ten-fold reduction in the concentration of pharmacological inhibitors resulted in a large decrease in overall inhibition for all three constructs for both PP2 (range from -2% to 9%) and ER 27319 (range from -5% to -3%), Wortmannin at low dosage still resulted in significantly high inhibition of phagocytosis (range from 42% - 58%) between all three construct expressing cells (Fig. 5.5A, 5.5B, and 5.5C).

The same panel of pharmacological inhibitors was also used to block IpLITR 2.6b, DrLITR 1.2 ^{wt}, and DrLITR 1.2 $^{ITIM\ ko}$-expressing cells incubated with high αHA mAb opsonized targets to better examine the role binding avidity may play in signal transduction and to resolve differences between LITR constructs further. As was seen when using the low mAb opsonized targets, phagocytosis of high mAb opsonized beads for all three construct-expressing cells mainly were affected by Cytochalasin D treatment (> 95% inhibition; Fig. 5.5D, 5.5E, and 5.5F). In addition, Wortmannin (PI3K blocker) significantly inhibited phagocytosis of the three constructs compared to the vehicle control, although the level of inhibition observed was higher when engaged with low mAb targets. Specifically, inhibition due to Wortmannin treatment for IpLITR 2.6b cells went from 67% with low mAb targets and was significantly different ($p \leq 0.05$) to the 48% inhibition seen with high mAb targets (compare Fig. 5.5D and Fig. 5.5A). The change seen with DrLITR 1.2 $^{ITIM\ ko}$ cells treated with Wortmannin was also significantly

different ($p \leq 0.05$) and went from 80% inhibition with low mAb targets to 54% with high mAb beads (compare Fig. 5.5C and Fig. 5.5F). The pharmacological inhibition of Src family kinases (PP2) also displayed differences in the dampening of phagocytosis between constructs engulfing low vs high mAb opsonized targets. PP2 (SFK blocker)-based inhibition of phagocytosis for IpLITR 2.6b-expressing cells changed dramatically when low mAb targets (72%) were used in comparison to high mAb beads (11%; compare Fig. 5.5D and Fig. 5.5A). A relatively smaller change in PP2 (SFKs)-induced inhibition was also seen for DrLITR 1.2 $^{ITIM\ ko}$-expressing cells (67% to 43%), although the differences seen were not significant ($p \geq 0.05$; compare Fig. 5.5C and Fig. 5.5F). The use of ER 27319 (Syk blocker) had a greater inhibitory effect on IpLITR 2.6b-expressing cells when engaged with low mAb targets (41%) rather than high mAb targets (26%), however, unlike what was observed for low mAb beads, the inhibition of phagocytosis of high mAb targets measured was not statistically significant from that of the vehicle control ($p \leq 0.05$; compare Fig. 5.5D and Fig. 5.5A). Unlike how greater inhibition was observed when switching to low mAb opsonized bead targets for certain drugs, the use of ER 27319 on DrLITR 1.2 $^{ITIM\ ko}$-expressing cells resulted in an increase in the level of inhibition from the engagement of low mAb targets (26%) to high mAb targets (32%), which was statistically significant compared to the DMSO vehicle control (compare Fig. 5.5C and Fig. 5.5F). Interestingly, in comparison to the other LITR constructs (i.e., IpLITR 2.6b and DrLITR 1.2 $^{ITIM\ ko}$), DrLITR 1.2 ^{wt} displayed very little measured differences in drug-based inhibition of phagocytosis between low mAb targets and high mAb targets for Wortmannin (74% and 81%), PP2 (22% and 28%), and for ER 27319 (16% and 18%), although inhibition of low mAb targets with ER 27319 was significant ($p \leq 0.05$) against DMSO vehicle control unlike what was seen for the inhibition of engulfment of low mAb targets (compare Fig. 5.5B and Fig. 5.5E). Similarly to what was

observed previously with low mAb opsonized beads, a 10-fold reduction in drug concentration resulted in a large decrease in inhibition for PP2 (range from 1% to 3% inhibition), ER 27319 (range from 2% to 5% inhibition), and Wortmannin (range from 11% - 40% inhibition; Fig. 5.5D, 5.5E, and 5.5F). Once again, regardless of construct, the concentration of drug, or amount of αHA on the surface of targets, no significant ($p \geq 0.05$) increase in inhibition was attributed to the addition of NSC 87877 (ranging from -4% and 1% inhibition).

Finally, to establish a control for the potential phosphatase activity of SHP-2 when recruited to DrLITR 1.2, NSC 87877 (SHP-2 inhibitor) was utilized on IpLITR co-expressing cells. Specifically, the co-engagement of both IpLITR 2.6b and IpLITR 1.1b is required for crosstalk inhibition of IpLITR 2.6b-induced phagocytosis in a SHP-2-mediated process (14). Thus the addition of NSC 87877 would potentially restore the phagocytosis induced by IpLITR 2.6b, by inhibiting the enzymatic activity of SHP-2 recruited by IpLITR 1.1b, under the assumption that SHP-2 phosphatase activity is responsible for the inhibition measured. As per Figure 5.5G, there was no significant increase in the levels of phagocytosis when cells were exposed to both high (3%) and low concentrations (7%) of NSC 87877 during phagocytosis of co-opsonized bead targets.

5.3 Discussion

My main objective in this thesis chapter was to examine the molecular signalling mechanisms controlling DrLITR 1.2-mediated phagocytosis with a special interest in the recruitment of signalling molecules to the ITIM within the receptor CYT. In addition, the identification of molecule regulators commonly associated with ITAM-mediated phagocytosis were examined to solidify this receptor as a stimulatory immunoregulatory protein. Here I show

that upon cellular engulfment of targets, DrLITR 1.2 recruits pSHP-2 to the phagocytic synapse in an ITIM-dependent manner. I also show that, similar to ITAM-containing phagocytic receptors such as IpLITR 2.6b, DrLITR 1.2 can recruit pSyk to the synapse as well. Additionally, pharmacological profiling suggests DrLITR 1.2 utilizes signalling regulators of phagocytosis commonly seen for other immunoregulatory receptor-types.

Phagocytic phenotypic investigation of DrLITR 1.2 within a heterologous expression system was examined in chapter IV and led to observations that DrLITR 1.2 induced an ITAM-dependent phagocytic response employed by this receptor when engaged with opsonized bead targets. As a result, it was first hypothesized that DrLITR 1.2 utilized signalling components (i.e., SFK, Syk, PI3K and F-actin polymerization) commonly associated with the ITAM-dependent phagocytic pathway seen in other receptor-types such as FcRs and IpLITR 2.6b (11,51,89). Additionally, since the presence of the ITIM facilitated an enhanced phagocytic capacity of DrLITR 1.2, it was hypothesized that the ITIM could recruit ITIM-associated signalling molecules, such SHP-2, during the phagocytic process and that the recruitment of these signalling molecules enhanced the phagocytic capacity of the receptor. The next logical step in investigating DrLITR-mediated phagocytosis was to elucidate the specific signalling molecules involved in this response, however, while the use of imaging flow cytometry was ideal for high throughput analysis of LITR-mediated phagocytosis, it was unable to be used for the detailed examination of signalling molecule recruitment during phagocytosis. Therefore fluorescence confocal microscopy was used to begin to examine signalling molecule recruitment to the phagocytic synapse. Confocal analysis of DrLITR 1.2 during the engulfment of beads allowed for a more thorough and detailed screening of cells interacting with targets. In the same principle as the imaging flow phagocytic assay, bead counterstain was used to distinguish bead

targets as well as the progression of phagocytosis via stages of bead engulfment. Surface-bound beads fully exposed to the extracellular environments appeared as a red ring, while completely engulfed targets were protected from the antibody stain that was unable to pass the cell membrane. Cells of interest were depicted as a half ring of fluorescence which indicated that the target bead was being phagocytosed at the time of sample processing as the portion of the bead exposed to the extracellular environment would be counterstained, leaving the internal portion of the target undergoing engulfment, unstained and protected due to being captured by the plasma membrane. As such, a phagocytic synapse between the DrLITR-containing cell and the target could be visualized by comparing the elevated level of bead extracellular counterstain fluorescence that did not overlap with the fluorescence of intracellularly stained cell signalling molecules of interest. Information on the possible signalling components utilized for coordinated signalling during DrLITR 1.2 receptor engagement could then be deduced by examining molecule recruitment to the bead-cell interface where engagement of the receptor to the target leads to the induction of the signalling cascade associated with receptor-type (i.e., at the phagocytic synapse)

As mentioned in chapter IV, DrLITR 1.2 induces a robust phagocytic phenotype when engaged by targets that is dependent on the presence of a functional ITAM. In the context of ITAM-containing (or ITAM adaptor molecule recruiting) stimulatory receptors, dual tyrosine residues within the ITAM become phosphorylated by SFKs, whereby SH2 domain-containing kinases, like Syk, are able to bind and become activated by phosphorylation (51,89,90). pSyk is then able to continue and phosphorylate other signalling molecules critical for the start of a signalling cascade and induction of cell effector responses (e.g., phagocytosis). Syk is involved in the signalling pathways of many receptor types, including phagocytosis by CR3, Dectin-1, and

FcγR receptor engagement (16,17). Thus, as a crucial initial signalling molecule for phagocytosis, I wanted to examine the potential of DrLITR 1.2 to recruit pSyk via its ITAM to begin investigating the potential signalling molecules and pathways utilized by this immune receptor-type, and to draw comparisons to other ITAM-containing immunoregulatory receptors. Consistent with what was shown in our previous studies, the ITAM-containing receptor IpLITR 2.6b recruits pSyk to the phagocytic synapse between receptor-expressing cells and bead targets engaging receptor constructs (9). In direct comparison, DrLITR 1.2 was able to similarly recruit pSyk to the synapse, directly supporting previous observations that DrLITR 1.2-induces an ITAM-dependent mode of phagocytosis. This was also observed regardless of DrLITR 1.2 containing a functional or dysfunctional ITIM, again reaffirming the previous observations that the inhibitory aspect of the ITIM did not reduce the phagocytic capacity of the receptor. Overall, this information helps solidify the classification that DrLITR 1.2 is similar to other stimulatory ITAM-containing receptor types by recruiting the same initial molecules that propagate the response.

Since previous data showed that DrLITR 1.2 induced a potent ITAM-dependent mode of phagocytosis with the recruitment of the ITAM-associated signalling molecule Syk, it seemed unlikely that a possible inhibitory molecule such as SHP-2 could be co-recruited to the phagocytic synapse. However, the differential phagocytosis capacities observed between DrLITR 1.2 ^{wt} and DrLITR 1.2 $^{ITIM\ ko}$ suggested that ITIM-associated molecules (e.g., SHP-2) facilitate the differences seen. As mentioned before, ITIMs are classically associated with inhibitory receptor-types. Upon receptor triggering, tyrosine residues within the ITIM become phosphorylated and promote the recruitment of phosphatases (i.e., SHP-1, SHP-2, SHIP1, SHIP2) via their SH2 domains (62). Recruited and phosphorylated (i.e., activated) phosphatases

(e.g., pSHP-2) are then able to dephosphorylate signalling molecules and other proteins in close proximity to the site of receptor engagement, overall dampening cell signalling and inhibiting cellular effector responses. This was observed in our lab when the ITAM-containing receptor IpLITR 2.6b was co-transfected into the same AD-293 cell line as the ITIM-containing receptor IpLITR 1.1b. Upon co-engagement of both receptors with the same bead targets, receptor crosstalk resulted in overall inhibition of the phagocytic response that was seen when IpLITR 2.6b was engaged alone (14). The use of confocal microscopy during this receptor crosstalk event also revealed that pSHP-2 was localized to the bead-cell interface and that any tyrosine mutations within the membrane distal region (i.e., ITIM-containing region) of IpLITR 1.1b prevented recruitment of pSHP-2. As such, co-engagement of IpLITR 2.6b and IpLITR 1.1b was ideal for observing the recruitment of pSHP-2 to the phagocytic synapse compared to the engagement of DrLITR 1.2 constructs during confocal analysis. Consistent with our lab's previous studies, co-engagement of the IpLITRs resulted in substantial pSHP-2 recruitment during phagocytosis, and that singular engagement of IpLITR 2.6b did not as the ITIM-containing receptor was not stimulated. As predicted, DrLITR 1.2 was able to recruit pSHP-2 to the phagocytic synapse in an ITIM-dependent manner, and that there was a significant decrease of pSHP-2 fluorescence when the ITIM was knocked out. This information supports predictions that the pSHP-2 could play a supporting role in mediating control over the phagocytosis seen for DrLITR 1.2 ^{wt} whereby knocking out the ITIM results in dampening of the response. My results show that DrLITR 1.2, consistent with other ITAM-containing receptors, is able to recruit pSyk to the phagocytic synapse in an ITAM-dependent manner during engagement with bead targets. My work also shows, interestingly, that this receptor recruits pSHP-2 to the synapse that is dependent on a functional ITIM upon engagement. Overall these results suggest that not only

does the ITAM within DrLITR 1.2 dominate the functional phagocytic output of the receptor, but it is able to do so light of the fact that the putative inhibitory molecule pSHP-2 is recruited to ITIM that enhances the phagocytic response.

Immunoregulatory receptor signalling networks are extremely complex and may differ not only among receptor-types but also between cells on which the receptors are expressed. For example, the dual motif (i.e., ITAM-like and ITIM) containing receptor FCRL5 is expressed on the surface of B cells. Co-ligation of this receptor significantly inhibited BCR activation and the resulting Ca^{2+} signalling when expressed in MZ B cells (93). However, similar B1 B cell line experiments did not disrupt BCR signalling. It was suggested that the differences observed may be due to MZ B cells containing higher intrinsic levels of SHP-1, basal calcium flux, and overall tyrosine phosphorylation that result in stronger signalling transduction during FCRL5 engagement. As such, employing pharmacological inhibitors of signalling molecules associated with a wide range of receptor signalling pathways allowed for a generalist screen of the potential mediators that DrLITR 1.2 utilizes during the control of phagocytosis. Previous use of drugs in our lab were used to characterize the signalling networks of IpLITR 1.1b. When this receptor was expressed in myeloid cells (i.e., RBL-2H3), it induced a unique ITAM-independent mode of phagocytosis that was only affected by inhibitors of Syk, SFK, and F-actin polymerization (11). In comparison, the phagocytic response from the ITAM-containing receptor IpLITR 2.6b was inhibited by drugs targeting Syk, SFK, F-actin polymerization, PI3K, PDK1, Cdc42, Rac, and PKCs. Similarly, I wanted to use drug-based inhibition assays using DrLITR 1.2-expressing cells to characterize the components involved in signalling regulation. However, the previous use of pharmacological inhibitors on phagocytosis was based on IpLITRs expressed in RBL-2H3 cells (11). Therefore, I first observed the effects of these drugs on IpLITR 2.6b-expressing AD-293

cells to, i) observe if pharmacological inhibition of common signalling molecules translate across cell lines for the same receptor-type, and ii) to optimize drug concentrations to establish significant inhibition of IpLITR 2.6b. Initial drug concentrations were set based on what was previously reported for RBL-2H3-expressing IpLITR 2.6b (11). Apart from increasing drug concentrations of Wortmannin and ER 27319, all pharmacological inhibitors tested were effective at inhibiting IpLITR 2.6b-mediated phagocytosis within AD-293 cells. In addition to the established concentrations of drugs, a 10x reduction in the concentrations were also examined on phagocytosis to observe a drug dose dependency on inhibition, in which all drugs on all receptor-types displayed.

Consistent with what was reported in RBL-2H3 cells (11), pharmacological inhibition of Src family kinases, Syk, PI3K, and F-actin polymerization all contributed to the inhibition of IpLITR 2.6b-mediated phagocytosis in AD-293 cells. In part, these mediators represent the key components of the phagocytic machinery described in the FcR-mediated phagocytic pathway, whereby proximal (SFKs and Syk), intermediate (PI3K), and distal (F-actin polymerization) components are well studied in mammals for their functions in phagocytosis (51,89,90). The observations made that both DrLITR 1.2 ^{wt} and DrLITR 1.2 $^{ITIM\ ko}$ were affected by all the pharmacological inhibitors do support the hypothesis that DrLITR 1.2 utilizes common signalling factors (i.e., SFK, Syk, PI3K, and F-actin polymerization) of the ITAM-dependent phagocytic signalling pathway. While it was unsurprising that DrLITR 1.2-mediated signalling involved these molecules in its control over phagocytosis, it was interesting to observe how inhibitors such as PP2 (SFK) and ER 27319 (Syk) were more effective against DrLITR 1.2 ^{wt}, while Wortmannin inhibited phagocytosis for both constructs relatively the same. Although ER 27319 (Syk inhibitor) did not significantly inhibit phagocytosis of DrLITR 1.2 ^{wt} when engaged

with low mAb opsonized beads, phagocytic inhibition of DrLITR 1.2 ^{wt} with low mAb targets, as well as confocal microscopy all suggest that DrLITR 1.2 does in fact associate with Syk, although it is interesting that DrLITR 1.2 $^{ITIM\ ko}$ is more affected by the inhibition of the Syk inhibitor. The differences between the two constructs suggest that the ITIM may play a role in stabilizing or ensuring that the signalling mechanisms attributed by the receptor are induced. Perhaps the ITIM, in this case, results in the recruitment of signalling molecules that stabilize or enhance the initial signalling components, thereby ensuring that DrLITR 1.2 is able to induce its signalling capacity and overall lowering the receptor activation threshold. For example, in both the proposed phosphatase-dependent (Fig. 5.6A) and phosphatase-independent (Fig. 5.6B) models, recruitment of SHP-2 to the ITIM within the tail of DrLITR 1.2 may result in overall bolstering of early signalling components by either enhancing SFK and Syk activation (phosphatase-dependent) or by acting as scaffolding for signalling components to be localized to areas of kinase activity (phosphatase-independent). In either case, this could result in less reliance of both SFKs and Syk activity to induce the phagocytosis phenotype seen, thereby limiting the effect these pharmacological inhibitors induce on DrLITR 1.2-mediated phagocytosis. While this proposed mechanism is inherently unique, there is evidence that SHP-2 is able to provide support to other signalling molecules post-receptor engagement. Specifically, phosphoproteomic studies have examined that drug inhibition of SHP-2 during EGFR stimulation resulted in a large decrease in the phosphorylation of certain molecules (137). The addition of an allosteric SHP-2 inhibitor resulted in a decrease in the phosphorylation of Gab1, Gab2, as well as SHP-2 itself within MDA-MB-268, EGFR-overexpressed cell line. Point mutations within the functional domains of SHP-2 determined that the SH2 domains of SHP-2, not the catalytic sites, are responsible for the prevention of dephosphorylation of

phosphotyrosine sites (pY) 659 on the adaptor protein Gab1 and pY643 on Gab2. The authors suggested that SHP-2 takes on a scaffolding role in the protection of pY sites by shielding them from dephosphorylation by other phosphatases (137). There is also further evidence that SHP-2 plays additional roles in other signalling pathway regulation involving phosphatase activity. Inhibition of SHP-2 results in the increased phosphorylation of the inhibitory residue pY209 on Grb2, preventing the association of Son of Sevenless **(**Sos) and activation of Ras. Similarly, PI3K subunits accumulate inhibitory phosphorylation of tyrosines within the inner subunits (PI3KR1 and PI3KR2) when SHP-2 is inhibited, thereby suppressing kinase activity (137). Overall, the data suggest that while DrLITR 1.2 utilizes common signalling components of the ITAM-dependent phagocytic machinery, the ITIM within the same CYT may continue to modulate the signalling capacity of the receptor by enhancing early signalling machinery.

The binding avidity of receptors to targets influences the strength of downstream signalling and cellular effector responses (174,175). Typically the more ligand that is present and bound results in the activation of more receptors, thereby influencing signalling molecules that are activated, leading to an enhanced cellular effector response. It was unsurprising that the engagement of both IpLITR 2.6b and DrLITR 1.2-expressing cells with bead targets opsonized with lower αHA mAb in the presence of pharmacological inhibitors resulted in overall greater inhibition of phagocytosis. Since high mAb opsonized bead targets could engage more receptor constructs on the cell's surface, increased levels of intracellular molecule activation may require increased levels of drugs to obtain previous levels of inhibition of phagocytosis measured with the engagement of low mAb targets. However, what was interesting is that once again, DrLITR 1.2 ^{wt} displayed a differing response, in comparison to DrLITR 1.2 $^{ITIM\ ko}$ and IpLITR 2.6b, to the change of mAb concentration on the surface of bead targets. While drug inhibitors were less

effective against DrLITR 1.2 $^{ITIM\ ko}$ and IpLITR 2.6b when engaged with higher mAb targets, the level of phagocytic inhibition observed for DrLITR 1.2 ^{wt} during exposure to drugs appeared to remain the same regardless of the mAb concentration on targets. While this observation was unexpected, it does bring back the idea that the ITIM may enhance and possibly protect the signalling capabilities of the receptor. As mentioned in chapter IV, the differential response observed when DrLITR 1.2 ^{wt} and DrLITR 1.2 $^{ITIM\ ko}$ cells are engaged with bead targets suggests the possibility that the ITIM functions to increase the sensitivity of the receptor during target engagement. In this scenario, DrLITR 1.2 ^{wt,} when engaged by both high and low mAb opsonized beads, induces a high phagocytic capacity. Aided by the recruitment of SHP-2 to the functional ITIM, it could then result in an enhanced or protective capacity for the proximal (SFKs and Syk) signalling components of the phagocytic response, shielded by the pharmacological effects.

My observations on the differing phagocytic capacities of DrLITR 1.2-expressing cells and the ITIM knockout variant on bead targets gave rise to the hypothesis that DrLITR 1.2 was able to recruit SHP-2 via the ITIM region within the CYT and that SHP-2 facilitates this differential response. Confocal analysis showed the recruitment of pSHP-2 to the phagocytic synapse during DrLITR-mediated phagocytosis and that a functional ITIM was required for the response. This gave rise to another hypothesis that SHP-2 could act as a scaffold in a phosphatase-independent (Fig. 5.6B) model for the recruitment of other adaptor and signalling molecules, such as interactions with Grb2 and Gab2, for the localization of kinases such as PI3K for downstream facilitation of effector responses (i.e., phagocytosis) (171,172). However, it was also predicted that SHP-2 could have a phosphatase-dependent (Fig. 5.6A) mode of increasing cell activation, such as preventing recruitment and activity of Csk by dephosphorylating

PAG/Cbp, thereby preventing phosphorylated inhibition of SFKs (173). My results showed that inhibiting the enzymatic activity of SHP-2 with pharmacological inhibitors resulted in no change to how wild-type DrLITR 1.2 facilitated phagocytosis. This gave an indication that perhaps SHP-2 does indeed function as a scaffold protein rather than utilizing phosphatase activity when recruited to the ITIM within DrLITR 1.2 during phagocytosis. However, it should be noted that unlike what was expected, SHP-2 activity was not inhibited with the addition of the drug during IpLITR 2.6b and IpLITR 1.1b crosstalk. It was characterized that IpLITR 1.1b facilitates its inhibitory effect on IpLITR 2.6b through the recruitment of SHP-2 (14), therefore it was predicted that the addition of the phosphatase drug would restore the phagocytic ability of IpLITR 2.6b. As this was unexpectedly not the case, it cannot be said for certain that competitive enzymatic inhibitor NSC 87877 was sufficient to determine whether SHP-2, in the context of DrLITR 1.2, functioned as a scaffold rather than a phosphatase during DrLITR 1.2-mediated phagocytosis. In addition, previous studies on IpLITR crosstalk inhibition of phagocytosis did not characterize whether the enzymatic activity of SHP-2 specifically resulted in the inhibition of IpLITR 2.6b phagocytosis (14). Rather, ITIM-knockout variants of IpLITR 1.1b were generated and co-engaged with IpLITR 2.6b, whereby it was determined that the ITIM, and subsequently the recruitment of SHP-2, resulted in the inhibition observed. Further experimentation would be required to conclude whether SHP-2 acts in a phosphatase-independent or dependent manner during DrLITR 1.2-mediated phagocytosis.

In this thesis chapter, I used the established DrLITR 1.2 construct-expressing cell lines to test the hypothesis that DrLITR 1.2 utilizes signalling molecules associated with the ITAM-dependent phagocytic response seen for other stimulatory receptors. In addition, I also hypothesized that DrLITR 1.2 is able to recruit pSHP-2 through its CYT-containing ITIM during

the engulfment of targets and that pSHP-2 facilitates the differential phagocytic response observed between DrLITR 1.2 ^{wt} and DrLITR 1.2 $^{ITIM\ ko}$. My results indicate that DrLITR 1.2, through the presence of its ITIM, recruits pSHP-2 to the phagocytic synapse during the phagocytosis of bead targets. I also showed that DrLITR 1.2 involves common phagocytic signalling components (e.g., SFK, Syk, PI3K, and F-actin polymerization) consistent with IpLITR 2.6b-mediated phagocytosis as well as mammalian FcR signalling networks (11,51,89). To explain DrLITR 1.2 relationship with SHP-2 during phagocytosis, I have proposed a phosphatase-independent and phosphatase-dependent model for how SHP-2 may contribute to DrLITR 1.2-mediated phagocytosis. The ITIM within the ITAM-containing receptor DrLITR 1.2 enhances the overall phagocytic response induced by DrLITR 1.2 while also appearing to reduce the ability of the receptor to bind to targets. The ITIM was also shown to recruit pSHP-2 to the phagocytic synapse while involving signalling molecules associated with an ITAM-dependent response. It is proposed that SHP-2 may act as a scaffolding protein in the phosphatase-independent model by associating with adaptor molecules (e.g., Grb2 and Gab2), thereby localizing other signalling molecules such as kinases (e.g., PI3K) to enhance the signalling potential of the receptor. Additionally, it is also proposed that SHP-2, when recruited to the ITIM within DrLITR 1.2, could utilize its enzymatic activity to dephosphorylate regulatory molecules (e.g., Csk), increasing kinase activity. Overall, I have described a new method by which teleost immunoregulatory receptors may finetune signalling dynamics to control immune cell effector functions.

A.

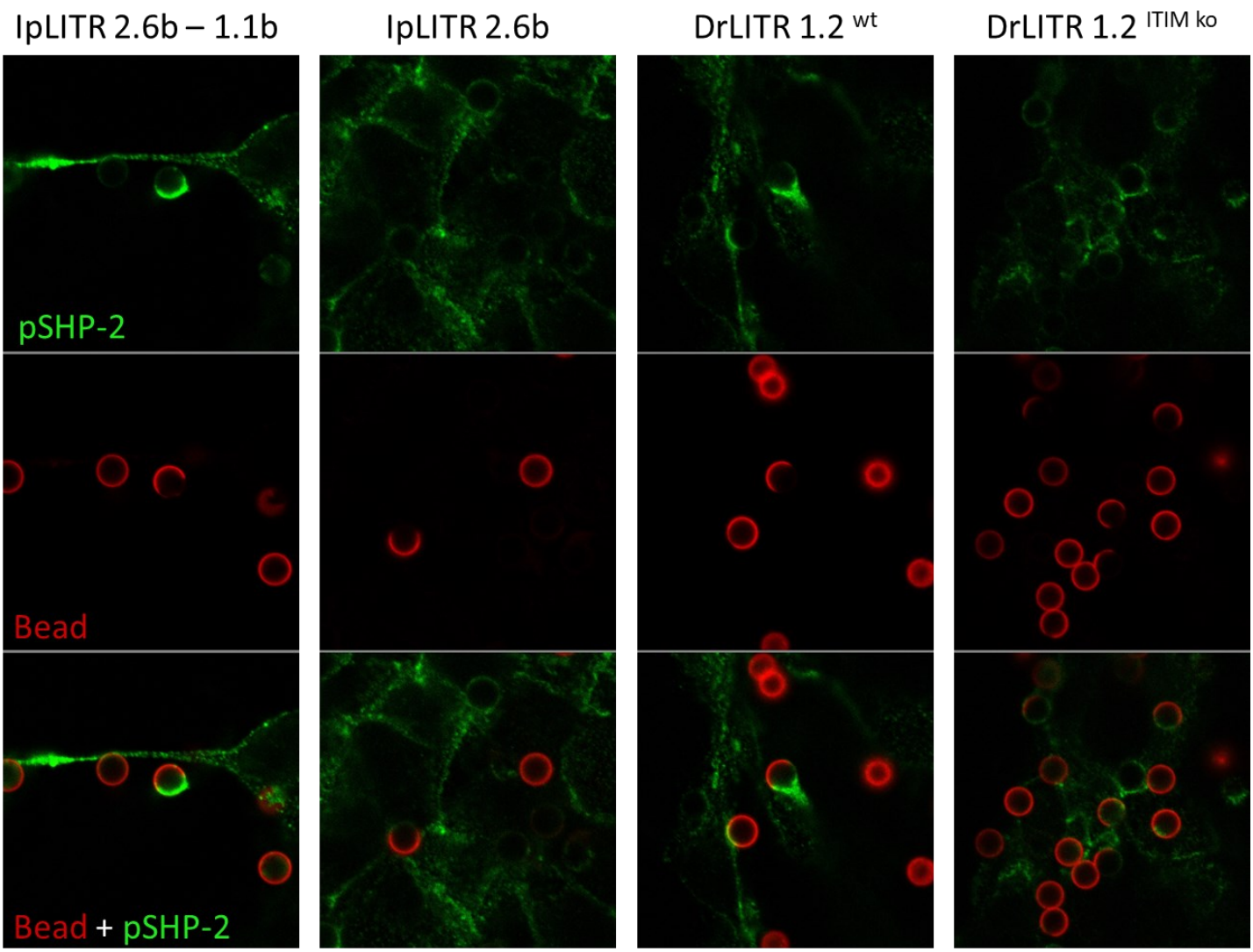
IpLITR 2.6b – 1.1b
IpLITR 2.6b
DrLITR 1.2 wt
DrLITR 1.2 ITIM ko
pSHP-2
Bead
Bead + pSHP-2

B.

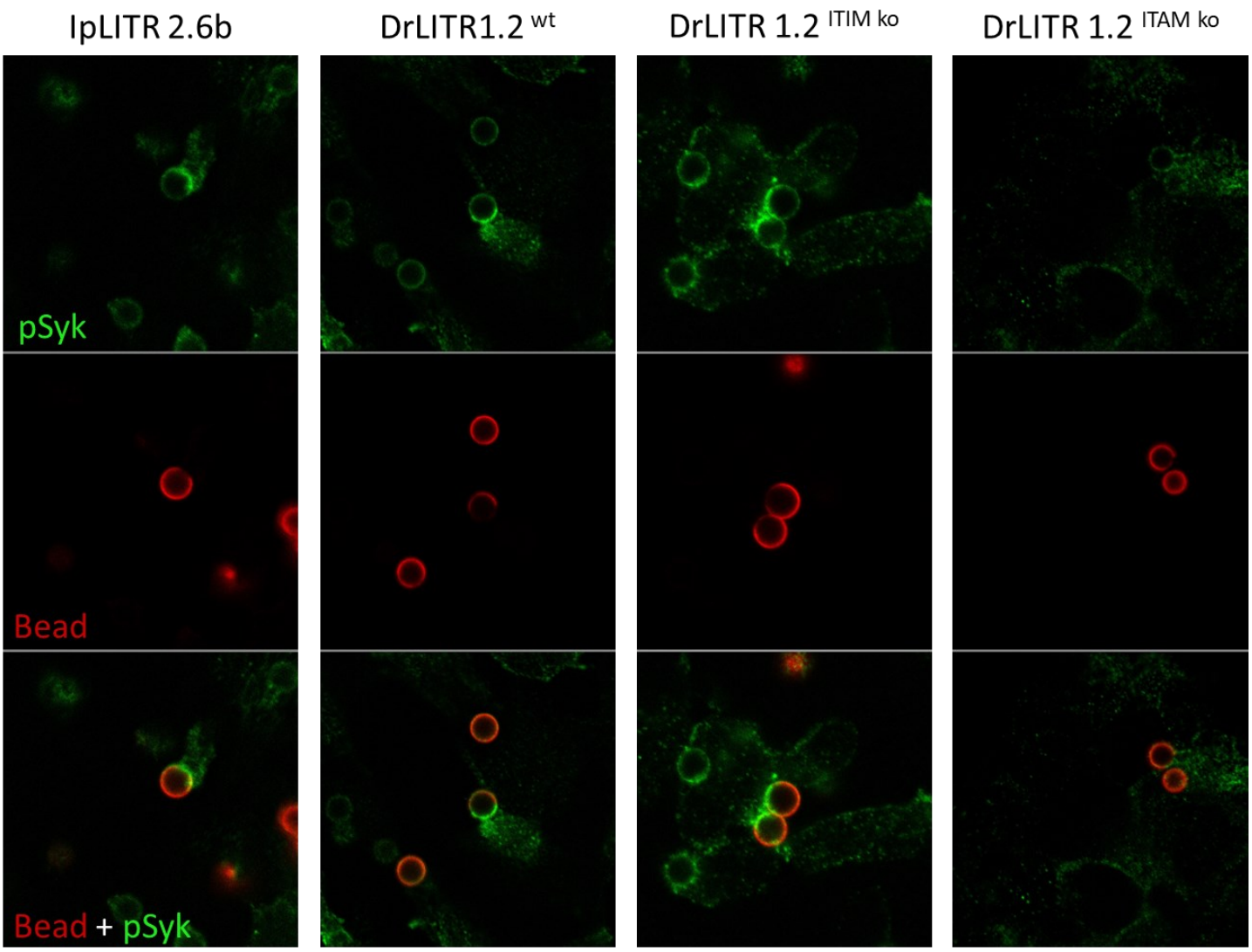
IpLITR 2.6b
DrLITR1.2 wt
DrLITR 1.2 ITIM ko
DrLITR 1.2 ITAM ko
pSyk
Bead
Bead + pSyk

Figure 5.1. Signalling molecule recruitment to the phagocytic synapse through confocal microscopy. AD-293 cells (2 x 10^5) expressing IpLITR and DrLITR constructs were seeded overnight on glass coverslips. Samples were then incubated with mAb-opsonized 4.5μm non-fluorescent beads (6 x 10^5) for 8 minutes at 37°C and subsequently fixed with 4% PFA for 10 minutes. αHA mAb + αFLAG mAb co-opsonized beads were used to co-engage IpLITR 2.6b-1.1b, αHA mAb + IgG_1 co-opsonized beads were used to engage IpLITR 2.6b, and αHA mAb opsonized beads were used to engage DrLITR 1.2 ^{wt} and 1.2 $^{ITIM\ ko}$ constructs. Beads were counterstained using rabbit-α-mouse pAb conjugated with AF647 (**Red**), and cells were then permeabilized. Intracellular pSHP-2 (**A**) or pSyk (**B**) molecules were probed first with rabbit-α-pSHP-2 pAb or with rabbit-α-pSyk pAb followed by incubation with goat-α-rabbit Ab (AF488 conjugated; **Green**). Samples were visualized using a Zeiss LSM 710 confocal microscope at 63x objective. Representative images from each sample show pSHP-2 staining (**Green**) in the first panel, extracellularly exposed and counterstained beads (**Red**) in the second panel, and merged fluorescence in the third panel (Ziess Zen Lite; Oberkochen, Baden-Württemberg, Germany).

IpLITR 2.6b-1.1b

A.

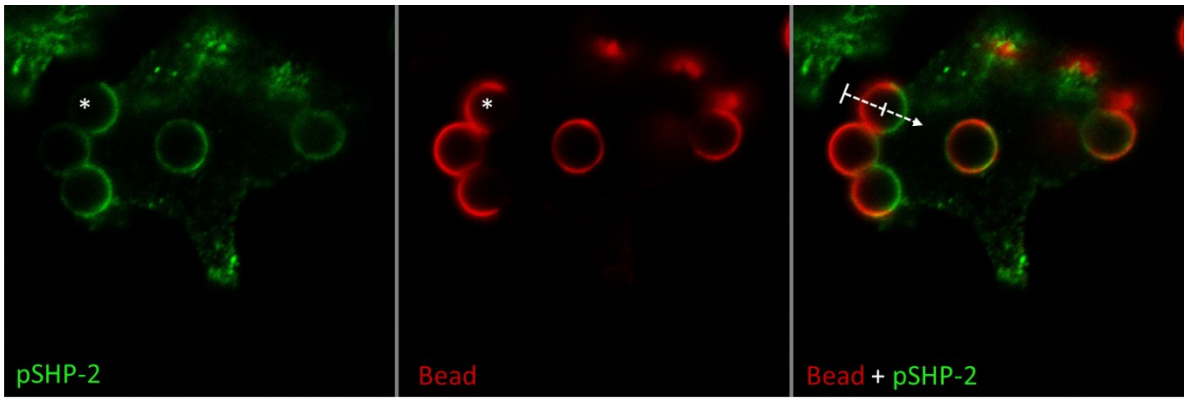

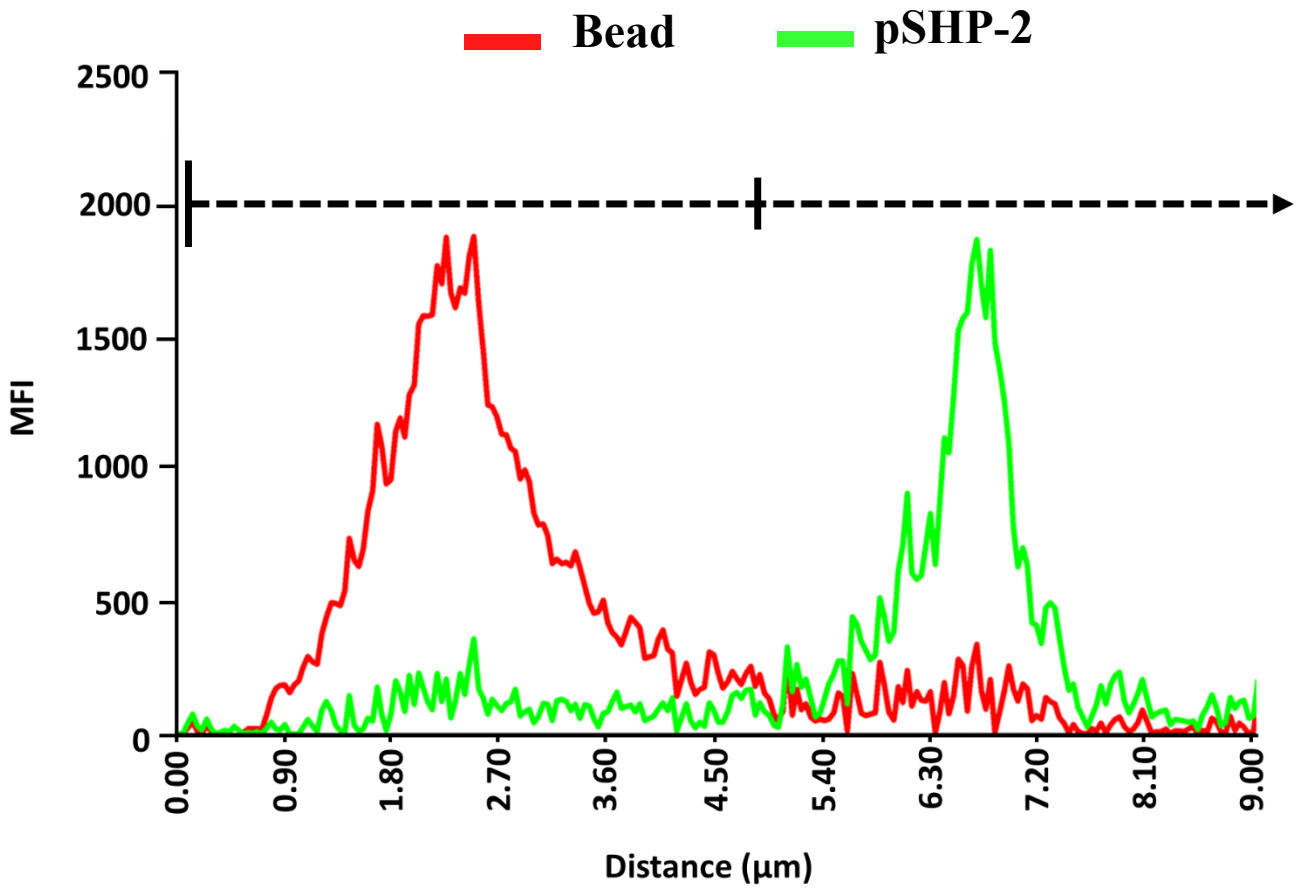

IpLITR 2.6b

B.

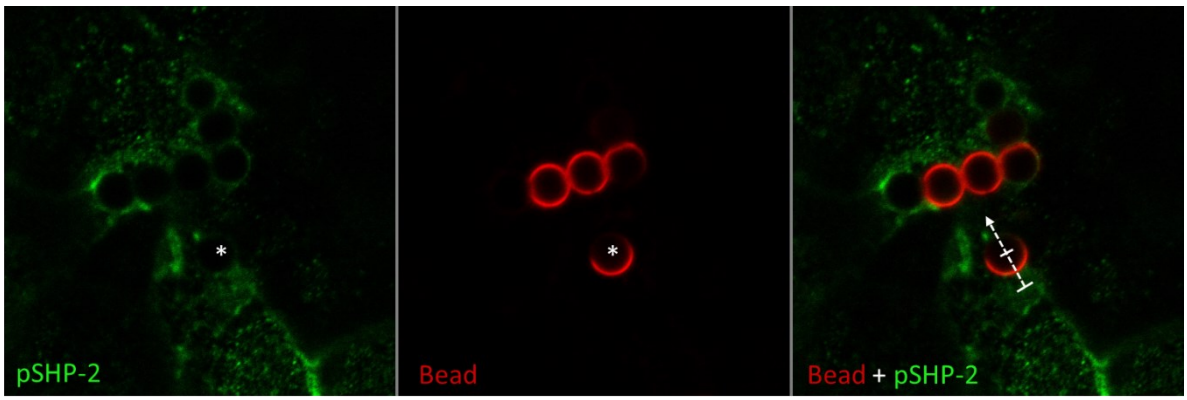
pSHP-2
Bead
Bead + pSHP-2

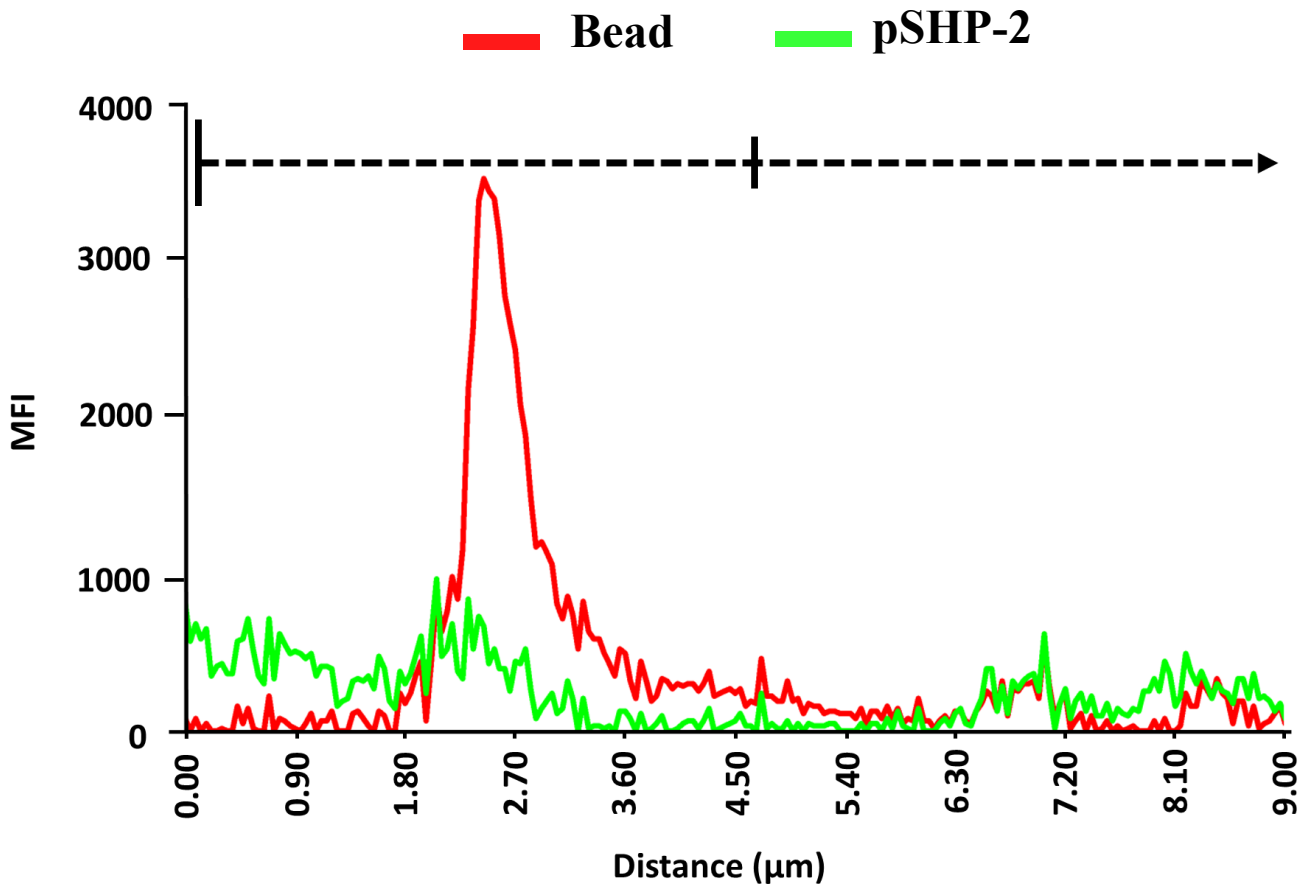
Bead
pSHP-2
4000
3000
2000
1000
0
MFI
0.00
0.90
1.80
2.70
3.60
4.50
5.40
6.30
7.20
8.10
9.00
Distance (µm)

DrLITR 1.2 ^{wt}

C.

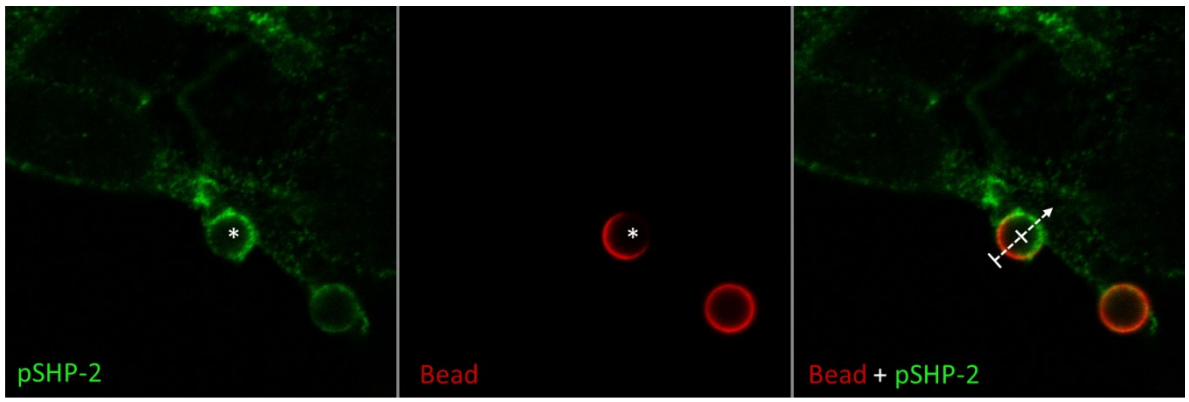

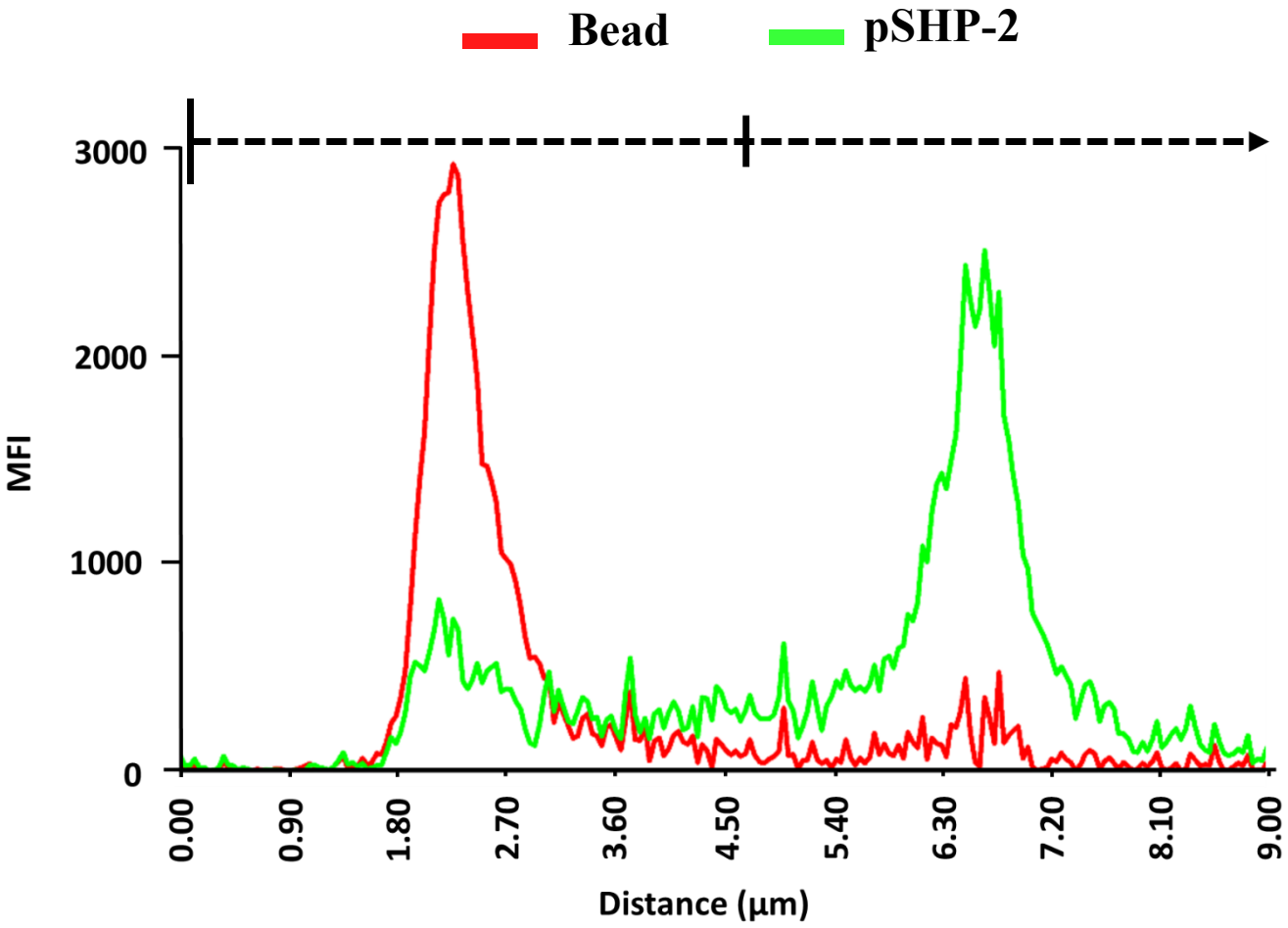

DrLITR 1.2 $^{ITIM\ ko}$

D.

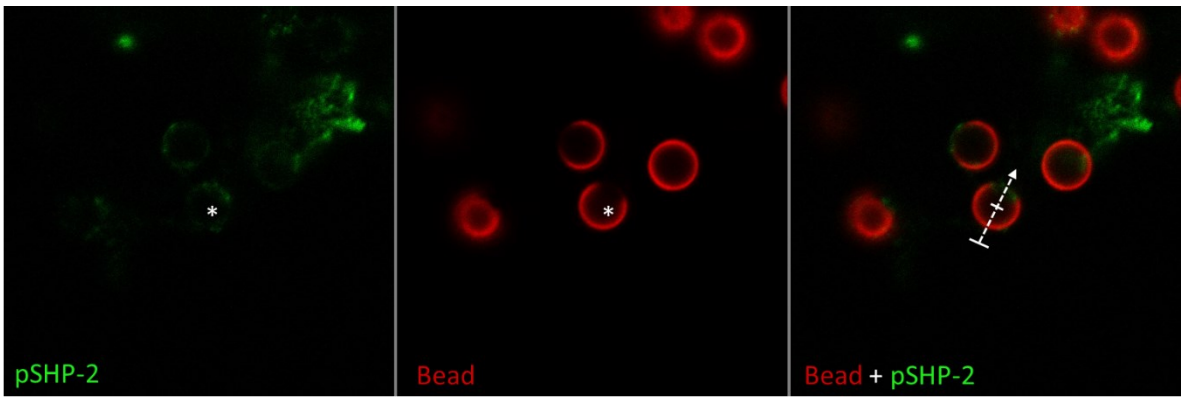

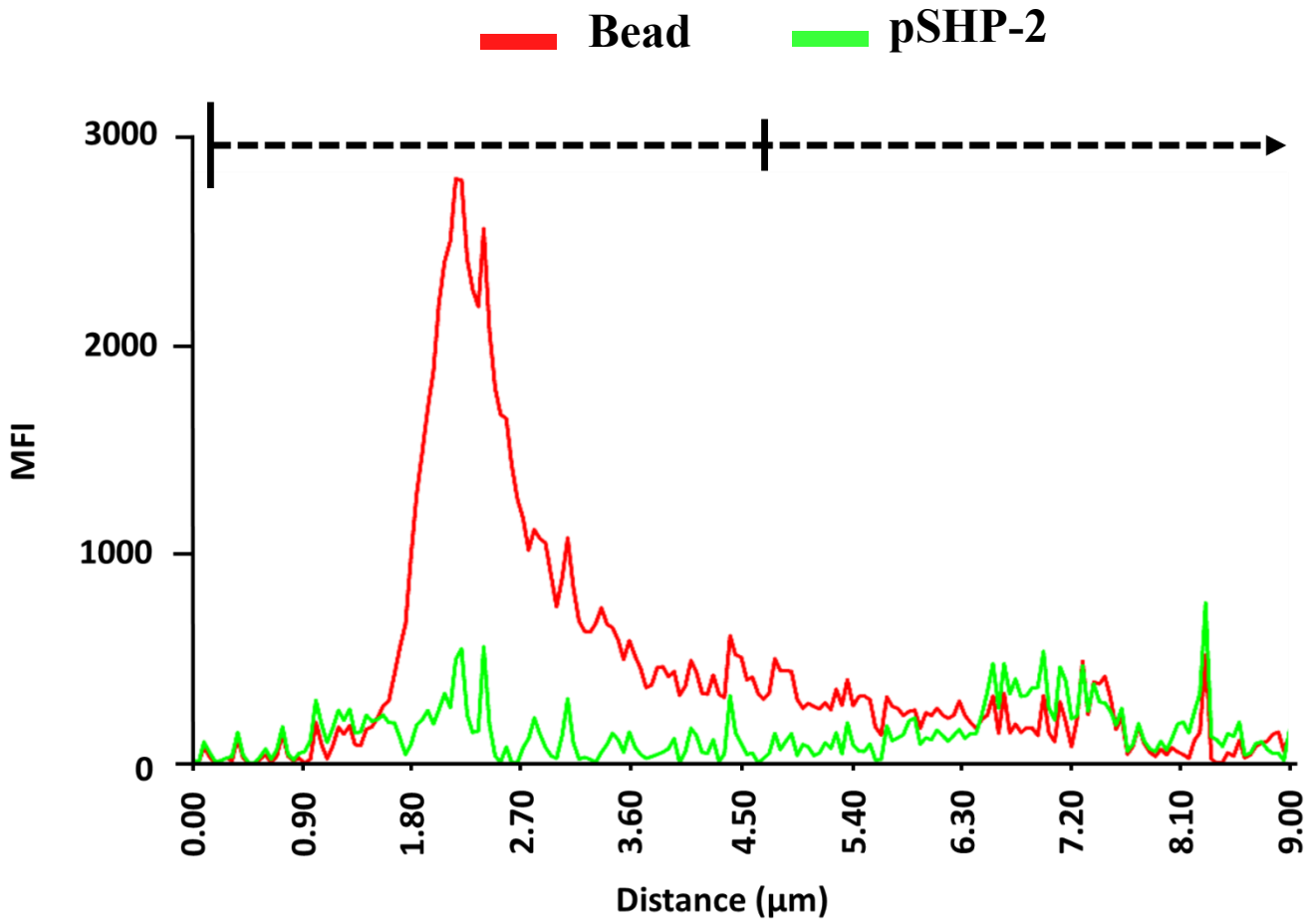

Figure 5.2. Confocal microscopy of pSHP-2 recruitment to the bead-cell phagocytic synapse. AD-293 cells (2 x 10^5) expressing IpLITR and DrLITR constructs were seeded overnight on glass coverslips. Samples were then incubated with mAb-opsonized 4.5μm non-fluorescent beads (6 x 10^5) for 8 minutes at 37°C and subsequently fixed with 4% PFA for 10 minutes. αHA mAb + αFLAG mAb co-opsonized beads were used to co-engage IpLITR 2.6b-1.1b (**A**), αHA mAb + IgG_1 co-opsonized beads were used to engage IpLITR 2.6b (**B**), and αHA mAb opsonized beads were used to engage DrLITR 1.2 ^{wt} (**C**) and 1.2 $^{ITIM\ ko}$ (**D**) constructs. Beads were counterstained using rabbit-α-mouse pAb conjugated with AF647 (**Red**), and cells were then permeabilized. Intracellular pSHP-2 molecules were probed first with rabbit-α-pSHP-2 pAb, followed by incubation with goat-α-rabbit Ab (AF488 conjugated; **Green**). Samples were visualized using a Zeiss LSM 710 confocal microscope at 63x objective. Representative images from each sample show pSHP-2 staining (**Green**) in the first panel, extracellularly exposed and counterstained beads (**Red**) in the second panel, and merged fluorescence in the third panel. Asterix (*) marks the bead-associated phagocytic event of interest between all three panels. Mean fluorescence intensity graphs represent a quantitative assessment of fluorescence intensities of the phagocytic event as measured across the dashed arrow (Zeiss Zen Lite; Oberkochen, Baden-Württemberg, Germany) by calculating MFI (y-axis) of exposed beads (**red line**) and pSHP-2 staining (**green line**) using ImageJ software (Bethesda, Maryland, USA).

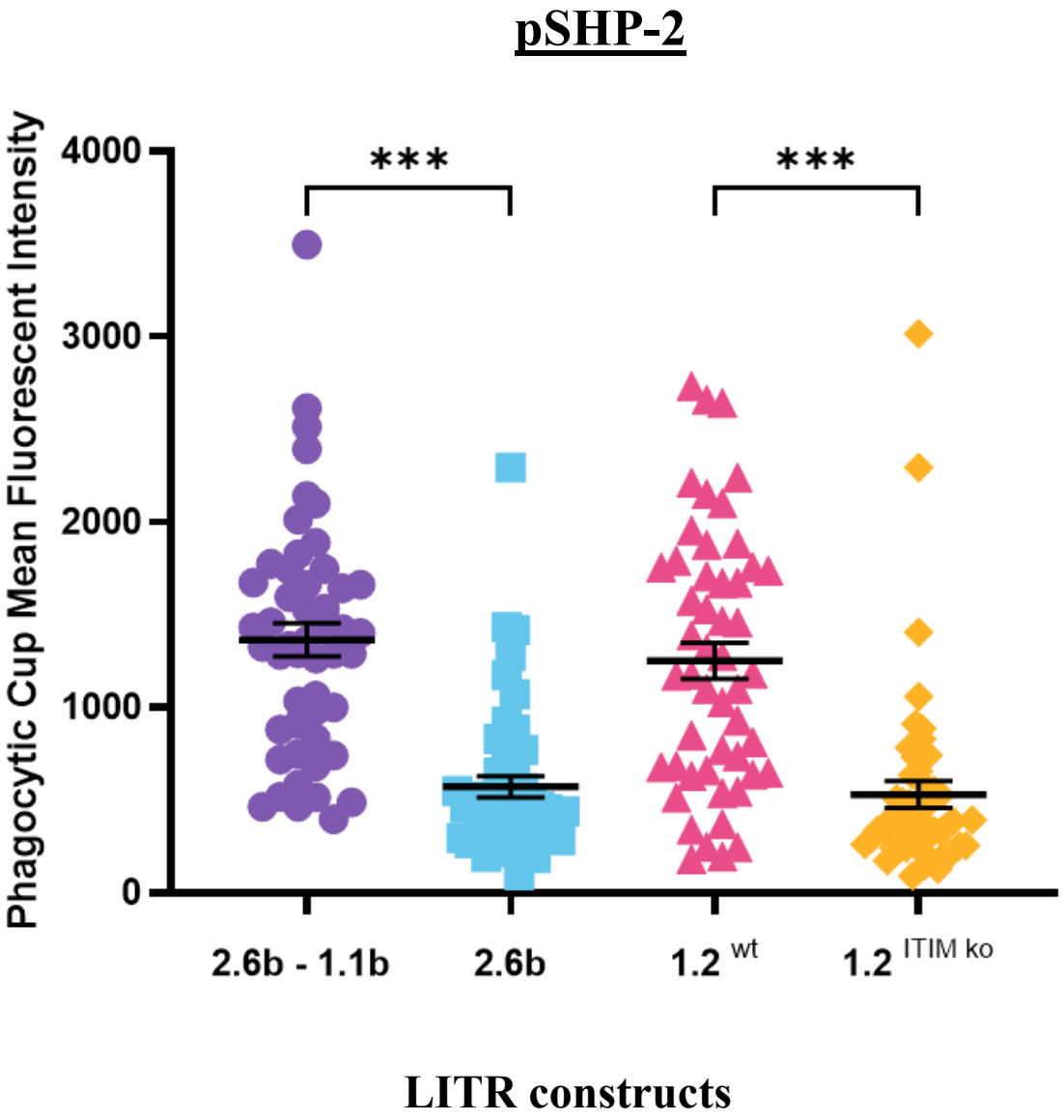
pSHP-2
Phagocytic Cup Mean Fluorescent Intensity
4000
3000
2000
1000
0
***
***
2.6b - 1.1b
2.6b
1.2 wt
1.2 ITIM ko
LITR constructs

Figure 5.3. MFI analysis of pSHP-2 recruitment during LITR phagocytosis. AD-293 cells (2 x 10^5) expressing IpLITR and DrLITR constructs were seeded overnight on glass coverslips. Samples were then incubated with Ab-opsonized 4.5μm non-fluorescent beads (6 x 10^5) for 8 minutes at 37°C and subsequently fixed with 4% PFA for 10 minutes. αHA mAb + αFLAG mAb co-opsonized beads were used to co-engage IpLITR 2.6b-1.1b, αHA mAb + IgG_1 co-opsonized beads were used to engage IpLITR 2.6b, and αHA mAb opsonized beads were used to engage DrLITR 1.2 ^{wt} and 1.2 $^{ITIM\ ko}$ constructs. Beads were counterstained using rabbit-α-mouse pAb conjugated with AF647, and cells were then permeabilized. Intracellular pSHP-2 molecules were probed first with rabbit-α-pSHP-2 pAb, followed by incubation with goat-α-rabbit pAb conjugated with AF488. Samples were visualized using a Zeiss LSM 710 confocal microscope at 63x objective. For quantification of pSHP-2 recruitment, the mean area of fluorescence (MAF) was measured (Zeiss Zen Lite; Oberkochen, Baden-Württemberg, Germany) at the phagocytic cup of 50 events from three independent experiments. Graphs depict the measured events of each experimental group represented by the mean fluorescence intensity (MFI) ± SEM. Sample data groups were analyzed using a non-parametric t-test (Mann-Whitney; Prism 6, GraphPad, La Jolla, CA, USA). Asterisks *, **, ***, represent statistical significance at $p \leq 0.033$, $p \leq 0.002$ and $p \leq 0.001$, respectively, between experimental groups.

IpLITR 2.6b

A.

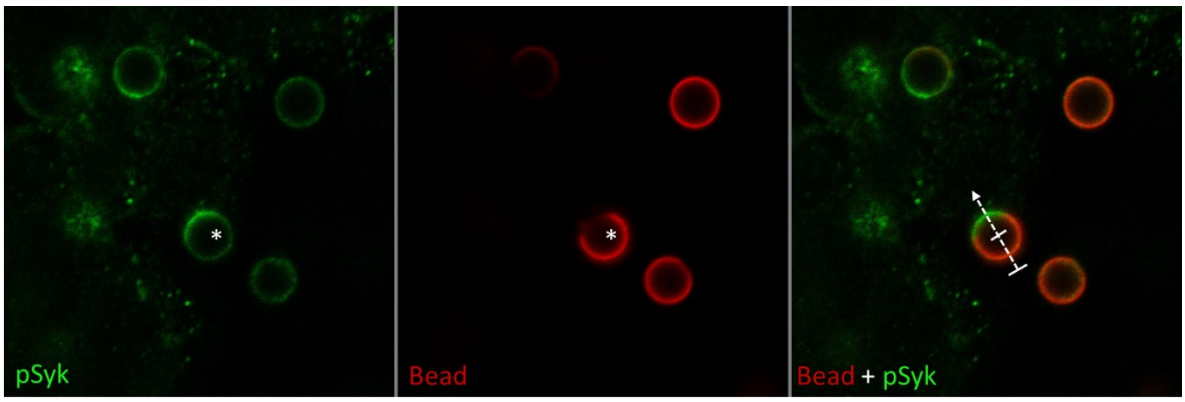
pSyk
Bead
Bead + pSyk

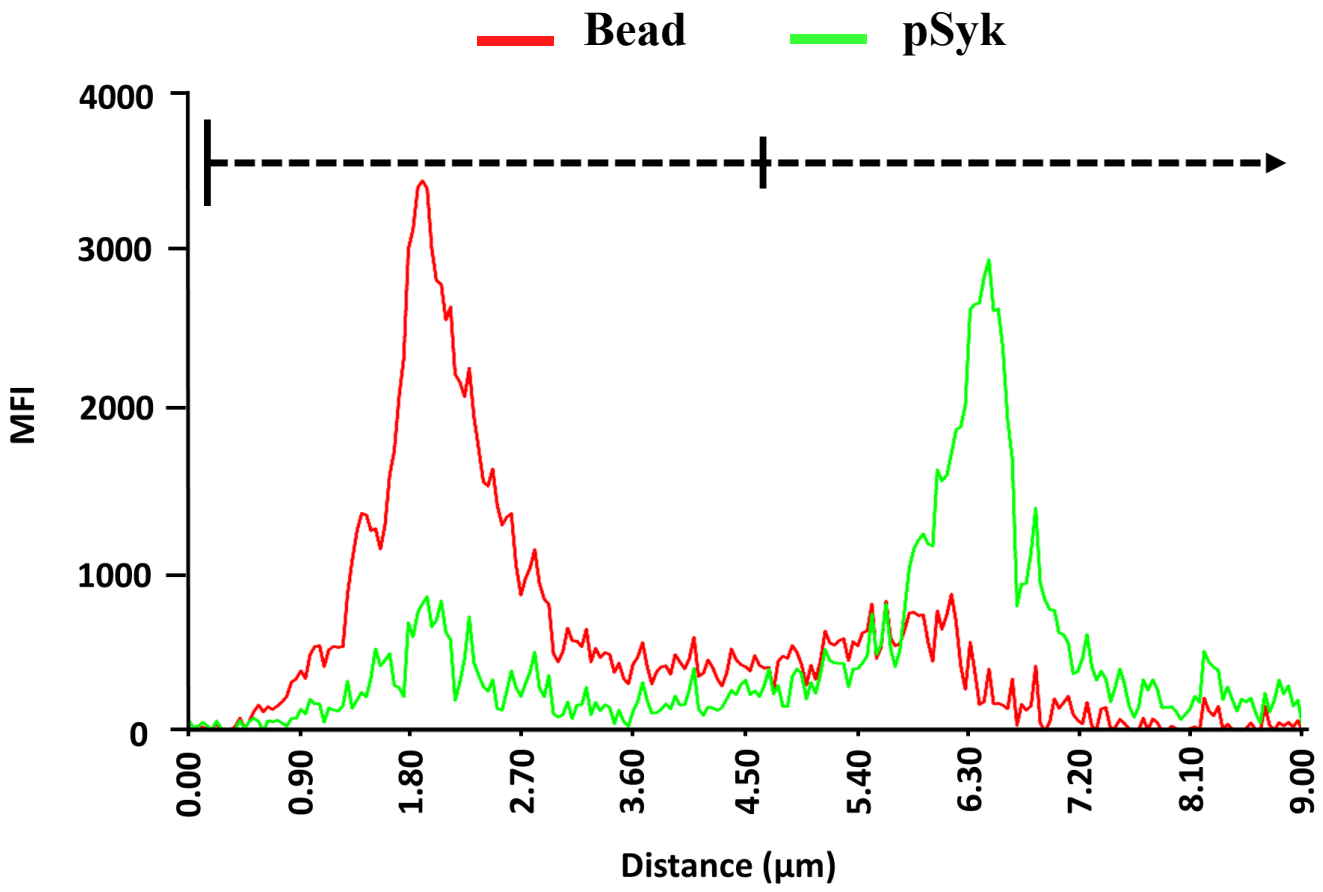
Bead
pSyk
4000
3000
2000
1000
0
MFI
0.00
0.90
1.80
2.70
3.60
4.50
5.40
6.30
7.20
8.10
9.00
Distance (µm)

B.

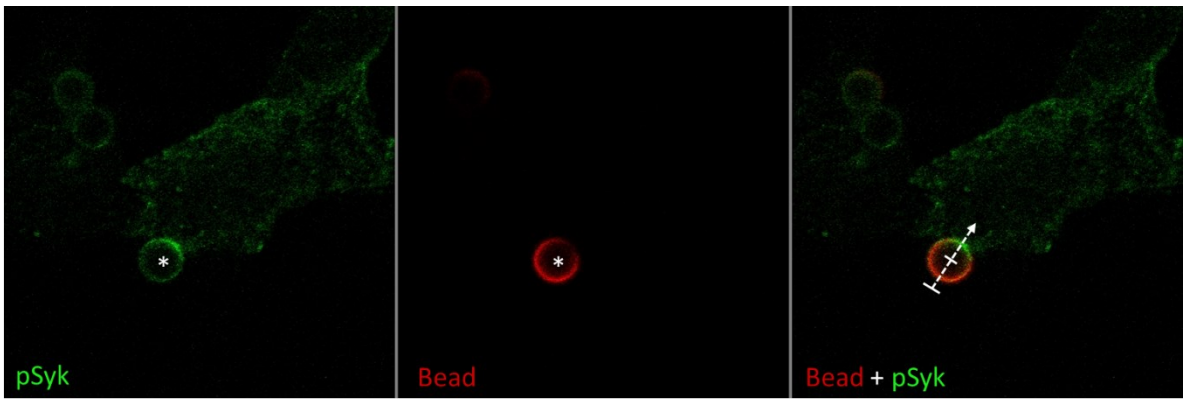
DrLITR 1.2 wt
pSyk
Bead
Bead + pSyk

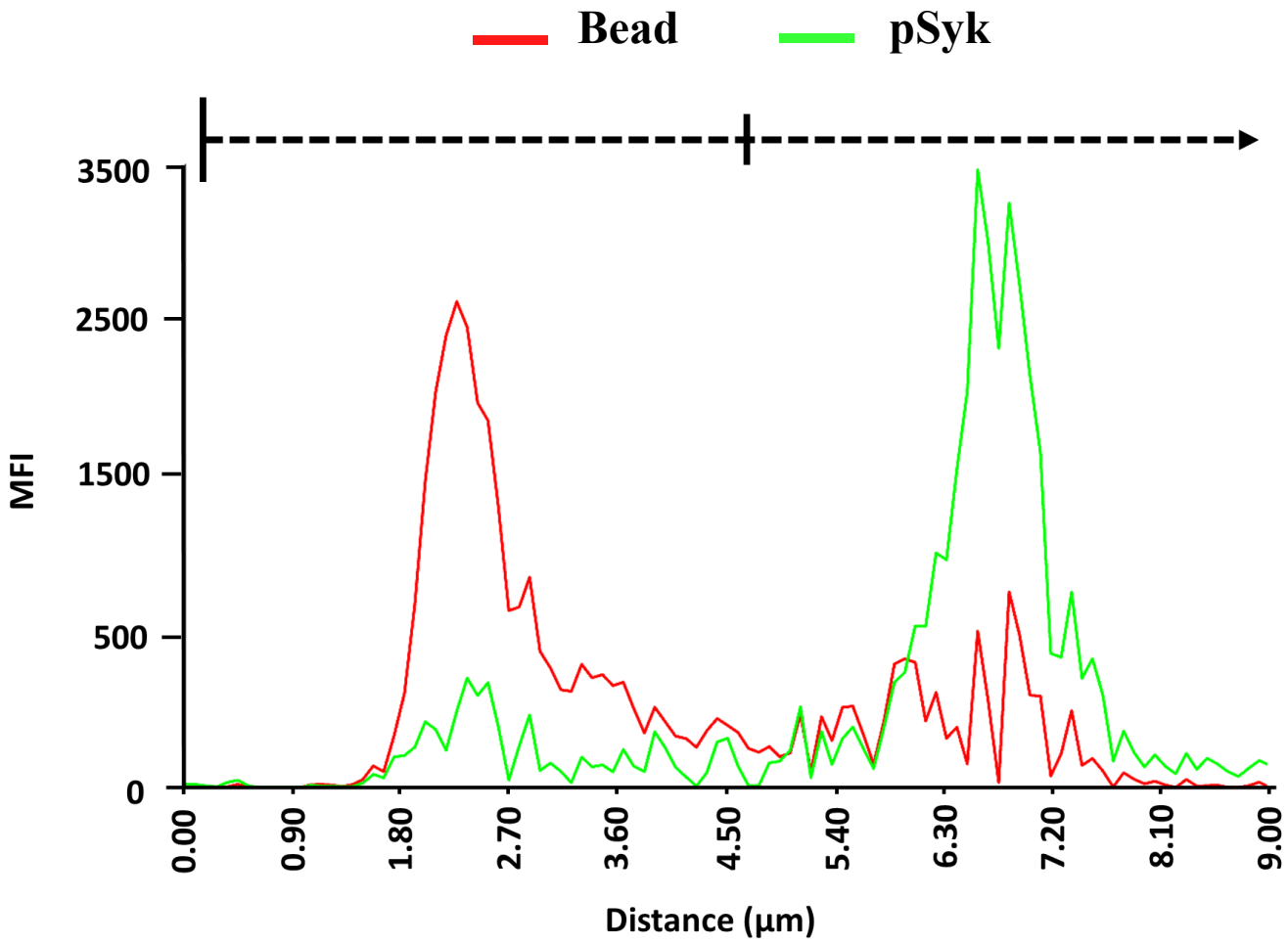
Bead
pSyk
MFI
3500
2500
1500
500
0
0.00
0.90
1.80
2.70
3.60
4.50
5.40
6.30
7.20
8.10
9.00
Distance (µm)

DrLITR 1.2 ITIM ko

C.

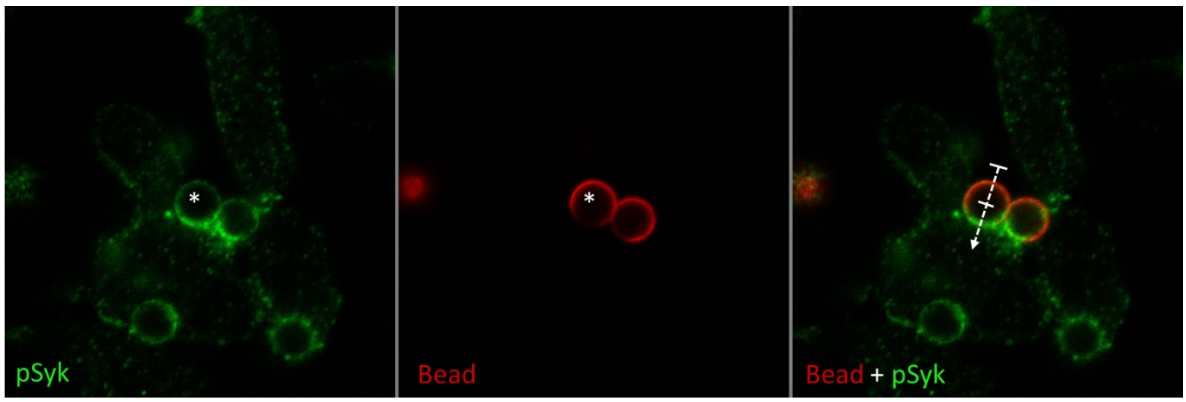

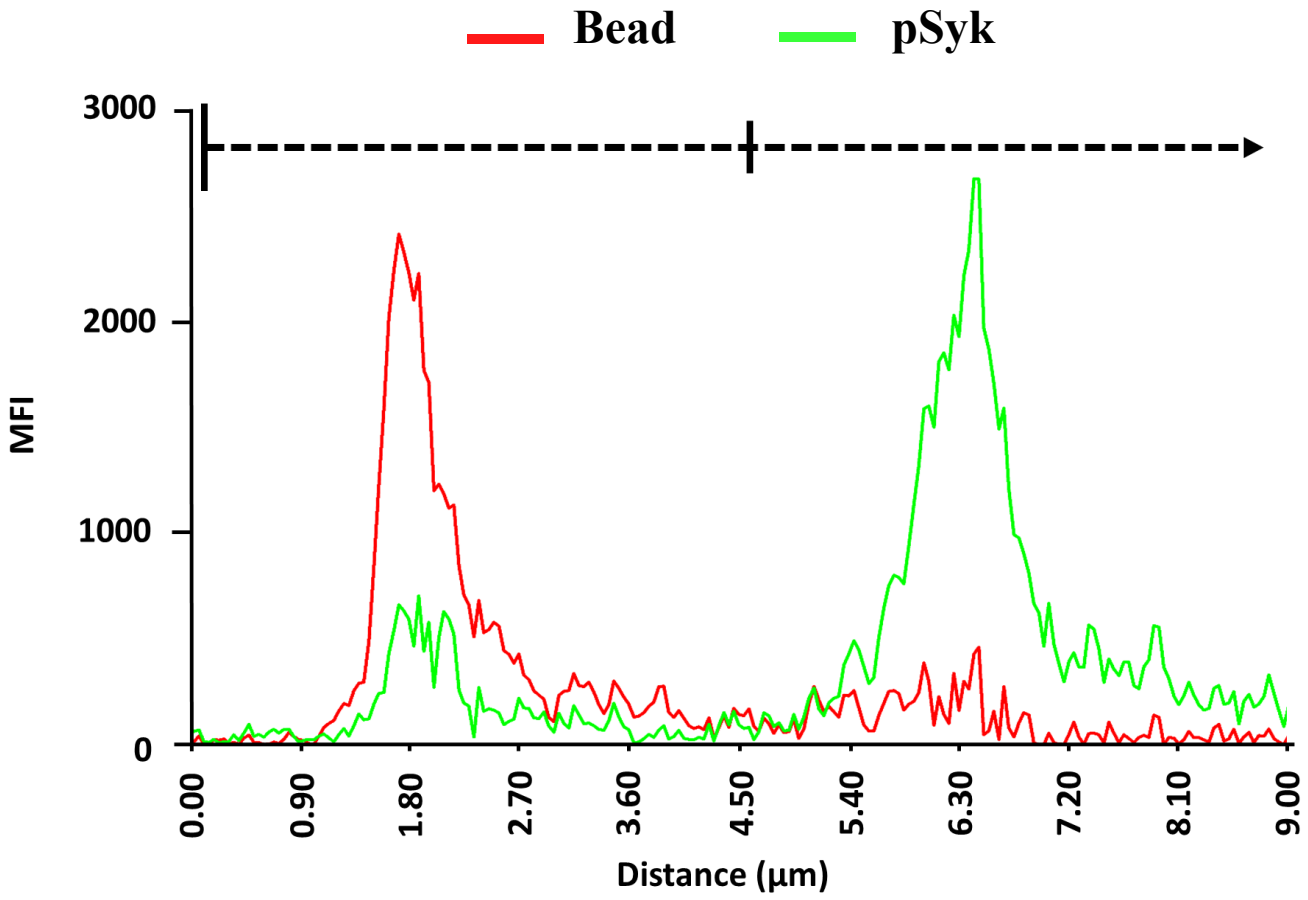

D.

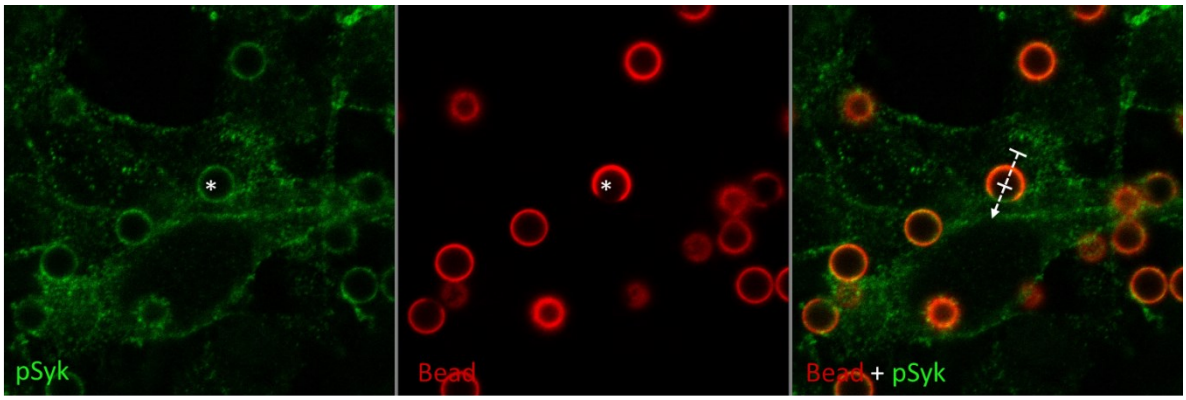
DrLITR 1.2 ITAM ko
pSyk
Bead
Bead + pSyk

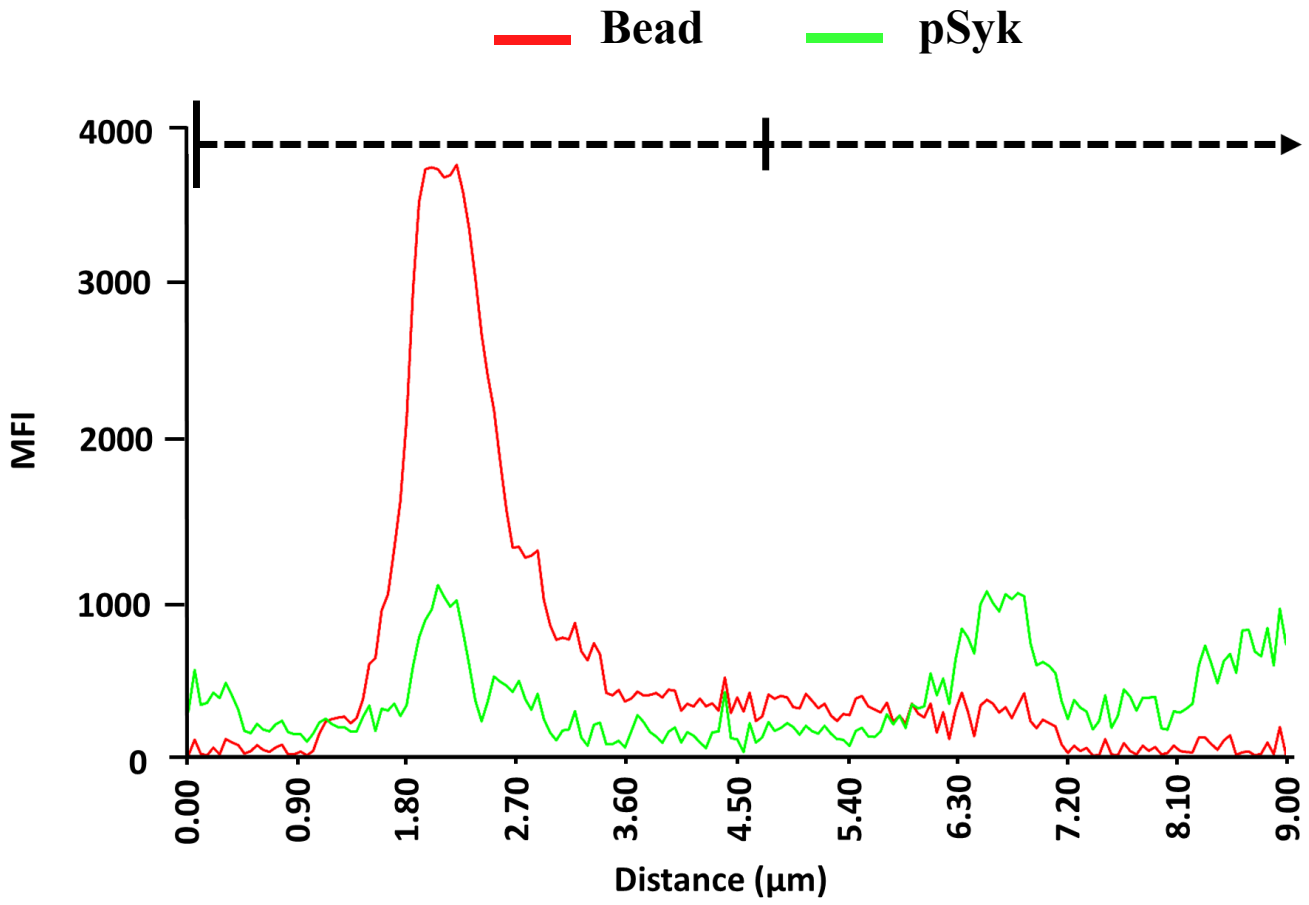
Bead
pSyk
MFI
4000
3000
2000
1000
0
0.00
0.90
1.80
2.70
3.60
4.50
5.40
6.30
7.20
8.10
9.00
Distance (µm)

Figure 5.4. Confocal microscopy of pSyk recruitment to the bead-cell phagocytic synapse. AD-293 cells (2 x 10^5) expressing IpLITR 2.6b (**A),** DrLITR 1.2 ^{wt} (**B**), 1.2 $^{ITIM\ ko}$ (**C**), and 1.2 $^{ITAM\ ko}$ (**D**) constructs were seeded overnight on glass coverslips. Samples were then incubated with αHA mAb opsonized 4.5μm non-fluorescent beads (6 x 10^5) for 8 minutes at 37°C and subsequently fixed with 4% PFA for 10 minutes. Beads were counterstained using rabbit-α-mouse pAb conjugated with AF647 (**Red**), and cells were then permeabilized. Intracellular pSyk molecules were probed first with rabbit-α-pSyk pAb, followed by incubation with goat-α-rabbit Ab (AF488 conjugated; **Green**). Samples were visualized using a Zeiss LSM 710 confocal microscope at 63x objective. Representative images from each sample show pSyk staining (**Green**) in the first panel, extracellularly exposed and counterstained beads (**Red**) in the second panel, and merged fluorescence in the third panel. Asterix (*) marks the bead-associated phagocytic event of interest between all three panels. Mean fluorescence intensity graphs represent a quantitative assessment of fluorescence intensities of the phagocytic event as measured across the dashed arrow (Zeiss Zen Lite; Oberkochen, Baden-Württemberg, Germany) by calculating MFI (y-axis) of exposed beads (**red line**) and pSyk staining (**green line**) using ImageJ software (Bethesda, Maryland, USA).

Low αHA mAb Concentration

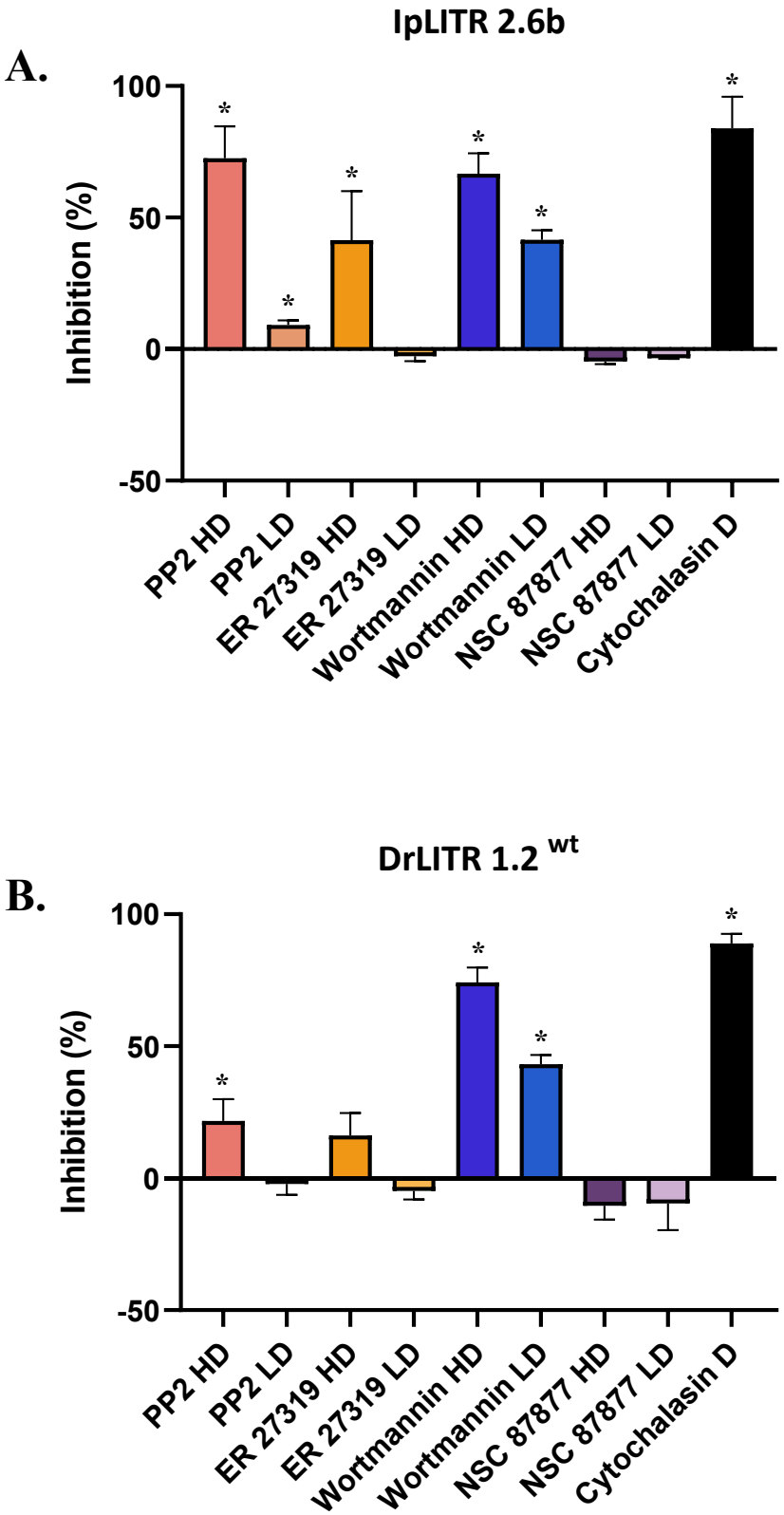

Low αHA mAb Concentration

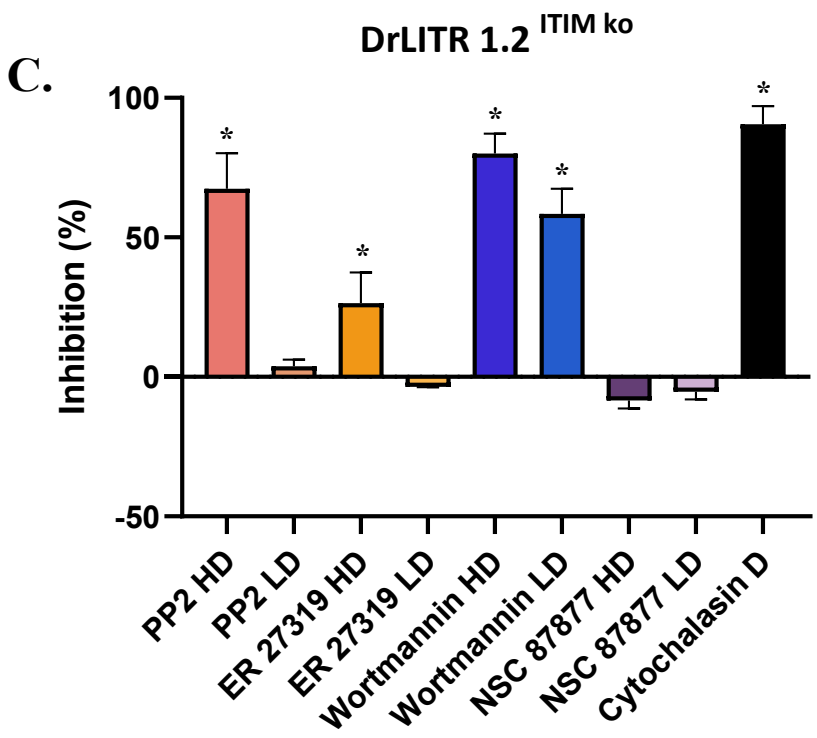

High αHA mAb Concentration

D.

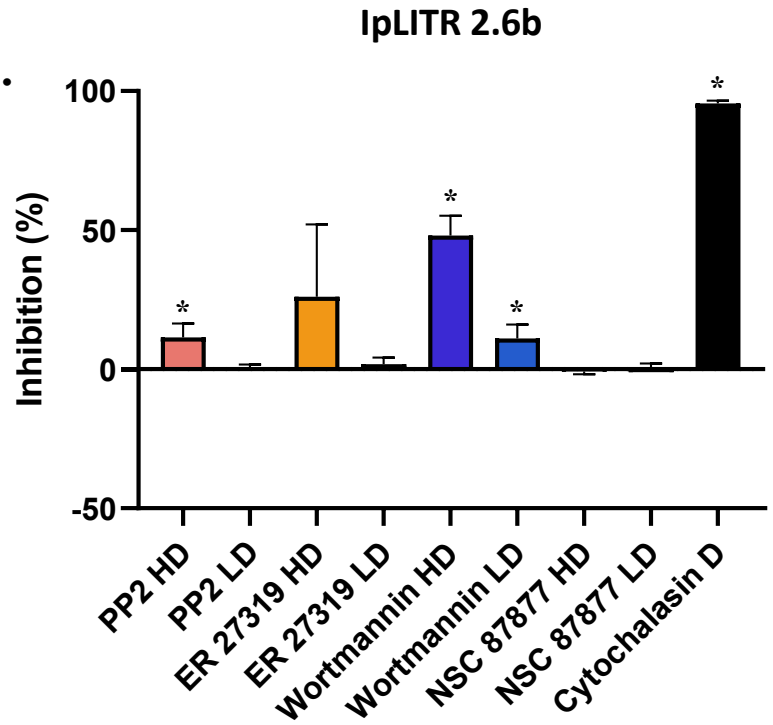

E.

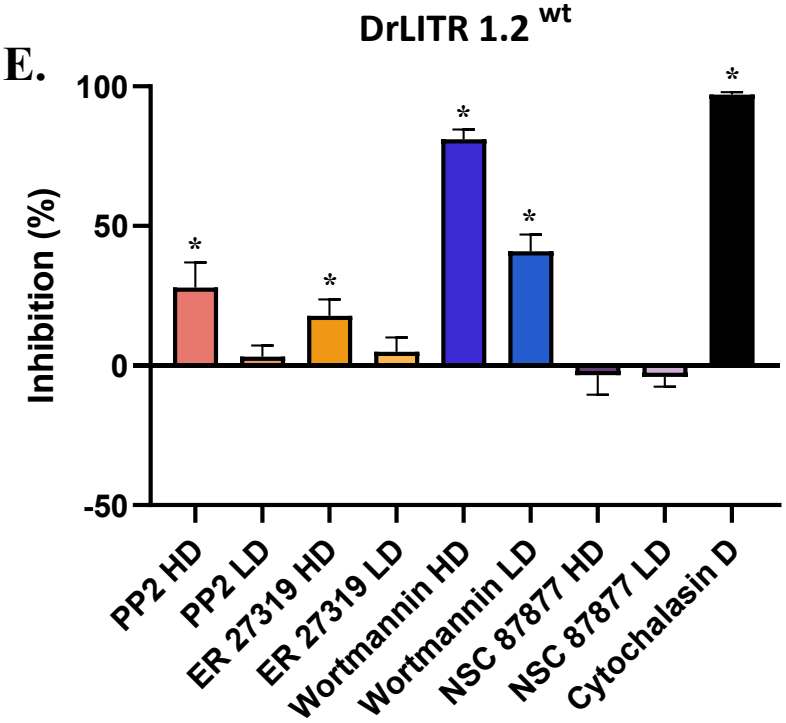

High αHA mAb Concentration

F.

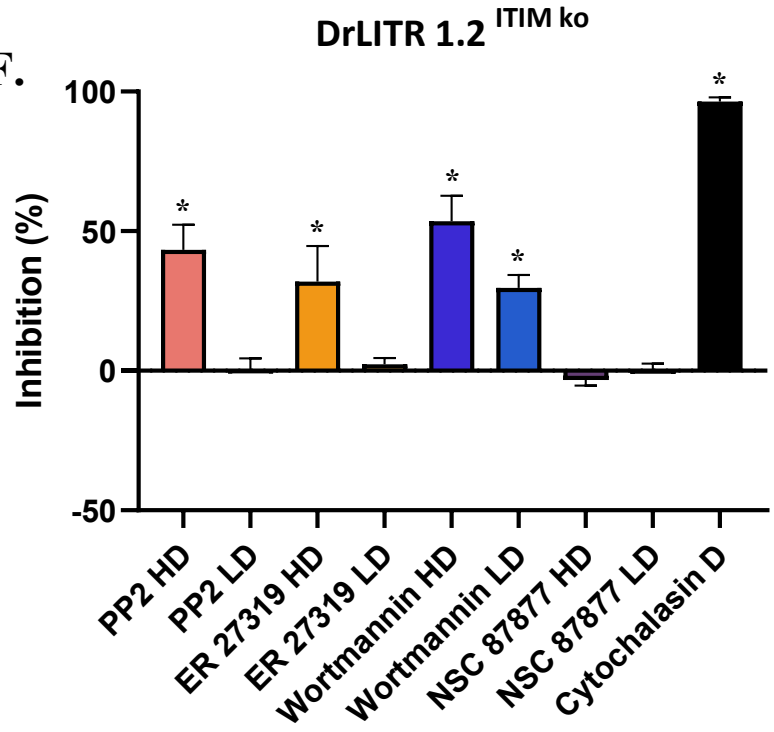

αHA mAb + αFLAG mAb

G.

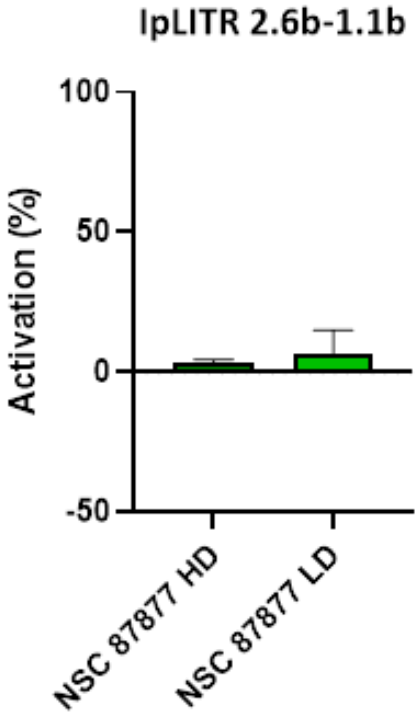

Figure 5.5. Pharmacological inhibition during phagocytosis indicates DrLITR 1.2's ability to utilize ITAM-associated signalling molecules. 3 x 10^5 AD-293 cells stably expressing IpLITR 2.6b-1.1b (**A**, **D**), DrLITR 1.2 ^{wt} (**B**, **E**), and 1.2 $^{ITIM\ ko}$ (**C**, **F**), constructs were preincubated for 1 hour with differing pharmacological blockers at high dosages (HD) and low dosages (LD) or with 0.5% DMSO vehicle control. Without removing drug inoculated media, samples were incubated with 4.5µm YG beads (9 x 10^5) opsonized with either 0.4 µg/mL mAb αHA + 2.5 µg/mL IgG_1 (**A**, **B**, **C**) or with 1 µg/mL mAb αHA (**D**, **E**, **F**) for 15 minutes at 37°C. Samples were then counter-stained and subsequently analyzed using the ImageStream X Mark II, with samples classified as being either phagocytic or surface-bound for YG bead targets. Inhibition was calculated as (1 - %phagocytosis experimental group / %phagocytosis vehicle control group). To measure phagocytic increase due to drug activity, additional seeded IpLITR 2.6b-1.1b cells were also preincubated with NSC 87877 doses or with 0.5% DMSO vehicle control and given YG beads opsonized with 0.4 µg/mL mAb αHA + 2.5 µg/mL mAb αFLAG (**G**). Samples were processed as explained above, and activation was calculated as ((%phagocytosis experimental group - %phagocytosis vehicle control group) / (1 - %phagocytosis vehicle control group)). Each bar represents the mean ± SEM of total cells associated with beads from 3 separate experiments. Sample data groups were analyzed using a t-test (Prism 6, GraphPad, La Jolla, CA, USA). Asterisks (*) represent statistical significance ($p \leq 0.05$) between the analyzed sample and vehicle control data.

A.

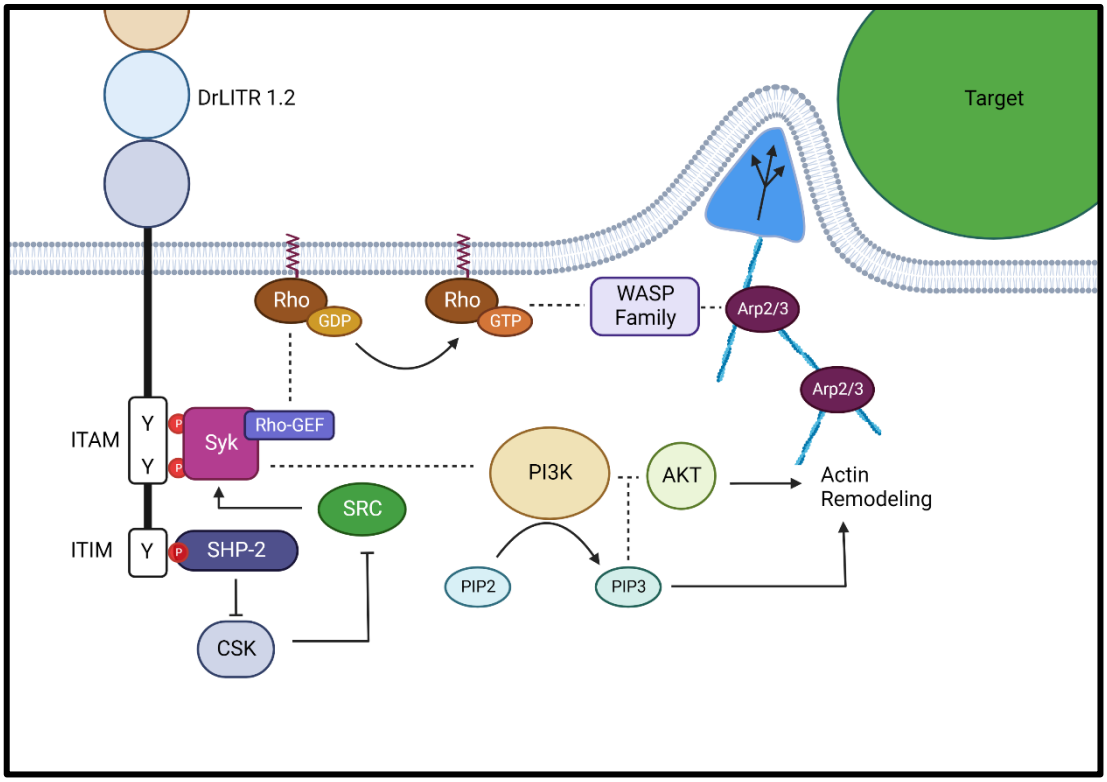
DrLITR 1.2
Target
Rho
GDP
Rho
GTP
WASP
Family
Arp2/3
Arp2/3
ITAM
Y
Y
Syk
Rho-GEF
PI3K
AKT
Actin
Remodeling
SRC
ITIM
Y
SHP-2
PIP2
PIP3
CSK

B.

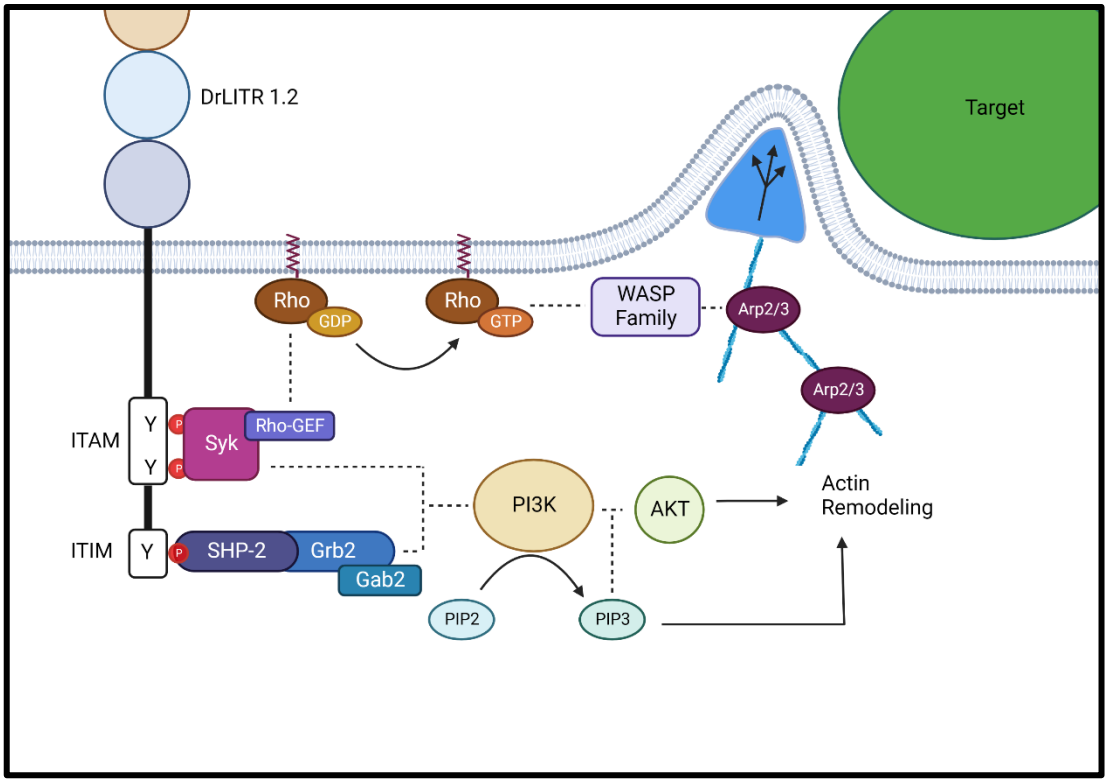
DrLITR 1.2
Target
Rho
GDP
Rho
GTP
WASP
Family
Arp2/3
Arp2/3
ITAM
Y
Y
Syk
Rho-GEF
PI3K
AKT
Actin
Remodeling
ITIM
Y
SHP-2
Grb2
Gab2
PIP2
PIP3

Figure 5.6. Proposed signalling pathway for DrLITR 1.2-based control of ITIM-mediated phagocytosis. DrLITR 1.2 ^{wt} -based control of phagocytosis initially results in the recruitment and activity of spleen tyrosine kinase (Syk) and Src family kinases (SFK) at immunoreceptor tyrosine-based activation motifs (ITAM) within the intracellular tail region of the receptor. Activated Syk is crucial for the initial propagation of downstream signalling responsible for cellular responses (i.e., phagocytosis) through the direct binding of molecules such as guanine nucleotide exchange factors (GEFs) and phosphatidylinositol-3-kinase (PI3K). GEFs regulate Ras homologous (Rho) GTPases which in turn are able to bind to and activate WASP – Wave family proteins leading to the activation of the Arp 2/3 complex and, finally, actin polymerization. In the proposed phosphatase-dependent model (**A**), tyrosine phosphorylation of the tandem immunoreceptor tyrosine-based activation motifs (ITIM) by SFKs results in the recruitment of SHP-2 where phosphatase activity dampens the recruitment and activation of C-terminal Src kinase (Csk). Dampening of Csk activity can increase Src kinase activity as Src family kinases are an enzymatic target for Csk, resulting in phosphorylation of c-terminal tyrosine to become phosphorylated, which causes SFKs to take on an inactive form. The increased activity of Src allows, in turn, for an increase in the activation of tyrosine residues within receptor tail motifs as well as an increase in the activation and recruitment of Syk, resulting in a bolstering of the Syk-dependent signalling cascade. In the phosphatase-independent model (**B**) SHP-2 is recruited to the ITIM within the receptor tail but is proposed to act as a scaffold for the direct binding and complexing of growth factor receptor-bound protein 2 (Grb2) and Grb2-associated-binding protein 2 (Gab2). This complex can directly bind to PI3K, allowing the protein to be close to Syk, further supporting the overall Syk-dependent signalling cascade. Figures created with BioRender.com.

Chapter VI

General Discussion and Future Directions

6.1 Summary of Findings

Previous characterization of IpLITRs have been used to understand mechanisms of immunoregulatory receptor-mediated control of innate immune cell effector responses utilizing a heterologous expression system. For example, IpLITR 2.6b activated ITAM-dependent degranulation and phagocytosis when transfected and stimulated in myeloid cells (RBL-2H3) (8,10–12,176). In contrast, the putative inhibitory receptor IpLITR 1.1b was shown to abrogate the effects of NK cell-mediated cytotoxicity using both an expected ITIM-dependent and an unexpected ITAM-independent mechanisms (13). Furthermore, when transfected in RBL-2H3 cells and induced by opsonized bead-targets, IpLITR 1.1b displayed a novel ITAM-independent mode of phagocytosis characterized by the formation of filopodia-like membrane protrusions (12,177). When IpLITR 1.1b and IpLITR 2.6b were co-transfected together in the same cell line (AD-293) and engaged with co-opsonized targets, receptor-mediated crosstalk resulted in a clear reduction in the phagocytic ability of IpLITR 2.6b with different regions of the IpLITR 1.1b CYT playing distinct roles in sustaining and initializing the inhibitory response (14). Taken together, these lines of evidence highlight the versatility of IpLITR-mediated immunoregulatory control of cell signalling networks as well as the functional plasticity of receptors with both inhibitory and stimulatory properties.

In recent studies, our lab has identified multiple new LITR-types within the genome of the zebrafish (*Danio rerio*) (15). Characterization of these DrLITRs revealed that a specific

subset were comparable to that of classical inhibitory and stimulatory innate immune receptors based on the presence of ITIIMs within the receptor CYT or charged residues suggesting possible recruitment of ITAM-containing adaptor molecules. Additionally, identification of DrLITRs that contained novel arrangements of immunoreceptor tyrosine-based motifs were discovered that suggest possible new mechanisms by which teleosts regulate cell receptor-based signalling networks. Specifically, the identification of DrLITR 1.2 containing opposing tandem signalling motifs (i.e., ITAM and ITIM) within the same receptor CYT brought to question the role the ITIM plays in controlling receptor-based signalling. The presence of a bonafide ITAM within the receptor CYT suggested that this receptor could induce a phagocytic response when transfected into cells and engaged with bead targets through the recruitment of signalling molecules classically associated with other ITAM-containing receptors (e.g., CR3, FcγR, and Dectin-1) (16,17). However, the addition of an ITIM in the CYT also implied that the recruitment of ITIM-specific molecules could dampen the signalling capabilities of this receptor as well as the cellular effector functions. My results in this thesis demonstrate for the first time that DrLITR 1.2 can induce a potent ITAM-dependent mode of phagocytosis whereby the presence of the ITIM enhances the full phagocytic potential. I also show that aside from utilizing similar signalling molecules described in the mammalian FcR ITAM-mediated signalling pathway, DrLITR 1.2 recruits classically defined inhibitory molecules to sites of target engulfment. My thesis work provides new evidence for how immunoregulatory receptors can modulate their signalling capacities and also offers further evidence that putative inhibitory immunoregulatory mechanisms can function to activate cellular signalling.

Our lab has utilized mammalian heterologous expression systems to characterize IpLITRs in the context of immunoregulatory signalling and receptor-based effector responses (14,165). I

took advantage of this system by expressing N-terminally HA-tagged DrLITR constructs on the surface of AD-293 cells. In conjunction with the wildtype DrLITR 1.2 receptor containing both an ITAM and an ITIM within the receptor CYT, motif dysfunctional mutant constructs were created to test the hypothesis that the ITIM dampens DrLITR 1.2-mediated signalling. Within the context of the receptor signalling paradigm, the co-engagement of separate inhibitory receptor-types with stimulatory receptors facilitates the dampening of the overall signalling capabilities of the stimulatory receptor (2,14,19,52,89). This, in turn, allows for a greater activation threshold that needs to be overcome to activate signalling and cellular effector responses, preventing overstimulation and sustained inflammation. This is demonstrated in our previous studies where the putative inhibitory ITIM-containing receptor IpLITR 1.1b was co-engaged with the stimulatory ITAM-containing receptor IpLITR 2.6b using co-opsonized bead targets (14). When observing the response through a phagocytic flow cytometric assay, results showed an overall dampening of the phagocytic response when IpLITR receptors were cross-linked compared to stimulation of IpLITR 2.6b alone. Based on this information and by employing the same phagocytic assay to my newly created DrLITR 1.2 expressing AD-293 cell lines, it was predicted that the ITIM within the CYT of DrLITR 1.2 could potentially recruit inhibitory-associated signalling molecules during DrLITR 1.2-mediated phagocytosis. Consequently, localizing inhibitory molecules to an ITAM-containing receptor could possibly increase the activation threshold of the receptor, thus dampening the observed phagocytic response, and bypassing the need for the stimulatory receptor to be co-ligated with an inhibitory receptor type. My results in chapter IV showed that unlike what was predicted, DrLITR 1.2 ^{wt}-expressing cells had a potent ITAM-dependent phagocytic response when engaged with opsonized bead targets. In comparison, its phagocytic response was significantly decreased when the ITIM motif within

DrLITR 1.2 was functionally knocked out. In addition to this data, it was observed that while DrLITR 1.2 $^{ITIM\ ko}$-expressing cells had a reduced phagocytic capacity compared to its wildtype counterpart, the ITIM knockout construct bound to a greater amount of target beads at both ambient and sub-ambient temperatures. Taken together, this line of evidence suggests that the ITIM motif within DrLITR 1.2 can modulate the phagocytic response induced by the ITAM-containing DrLITR 1.2. Overall, this data also represents a unique functional description for teleost immunoregulatory receptors containing ITAM and ITIM motifs within their CYT.

In chapter V, I further examined the downstream signalling mechanisms coordinating the DrLITR 1.2-mediated phagocytic response. As DrLITR 1.2-expressing cells induced an ITAM-dependent mode of phagocytosis, I hypothesized that DrLITR 1.2 utilized signalling components reminiscent of the FcR and IpLITR 2.6b ITAM-dependent pathways for controlling phagocytosis (51,89,177). To this end, I used the phagocytic assay and pharmacological inhibitors previously used to inhibit IpLITR 2.6b-mediated phagocytosis within RBL-2H3 cells (177). Drugs that were chosen inhibited crucial signalling molecules that represented the proximal (SFK and Syk), intermediate (PI3K) and distal (F-actin polymerization) signalling components of the FcR and IpLITR 2.6b ITAM-dependent phagocytic signalling pathways (51,89,177). As previously reported in RBL-2H3 cells, inhibitors of SFKs, Syk, PI3K, and F-actin polymerization all significantly dampened the phagocytic response induced by the engagement of IpLITR 2.6b-expressing AD-293 cells. In addition, these inhibitors were also effective against both DrLITR 1.2 ^{wt} and DrLITR 1.2 $^{ITIM\ ko}$, however, it appeared that drug inhibition was more affective against DrLITR 1.2 ^{wt} compared to DrLITR 1.2 $^{ITIM\ ko}$. Interestingly, it was also observed that drug inhibition of these signalling molecules was more effective at dampening the phagocytic response induced by IpLITR 2.6b and DrLITR 1.2 $^{ITIM\ ko}$ compared to that seen for DrLITR 1.2

^{wt}. The use of phagocytic targets opsonized with high levels of mAb also revealed that DrLITR 1.2 ^{wt} was not influenced by receptor binding avidity during drug inhibition. These observations, along with phagocytic data on how the ITIM increases the phagocytic capacity of DrLITR 1.2, strongly suggest that the ITIM within the CYT contributes to enhancing and potentially protecting the signalling capabilities of DrLITR 1.2 during bead engulfment.

The presence of the ITIM within the CYT of the ITAM-containing receptor DrLITR 1.2 brings to question the possible signalling capabilities of this unique teleost receptor. Classically, long-tailed inhibitory receptors contain ITIMs within their CYT regions that, during receptor engagement, lead to the phosphorylation of their tyrosine residues and subsequent recruitment of inhibitory-associated phosphatase signalling molecules such as SHP-1, SHP-2, SHIP1, and SHIP2 (2). The differential phagocytic activities observed between DrLITR 1.2 ^{wt} and DrLITR 1.2 $^{ITIM\ ko}$-expressing cells suggests that possible recruited signalling mediators to the ITIM may play a role in modulating the phagocytic response. Thus, it was hypothesized that the ITIM within DrLITR 1.2 could facilitate the recruitment of SHP-2 during phagocytosis of opsonized bead targets. In addition, it was predicted that if indeed SHP-2 was recruited, it could modulate and enhance the overall signalling and phagocytic capacity of the receptor as it has been shown that SHP-2 is able to facilitate enhanced receptor-based signalling in both a phosphatase-independent (171) and phosphatase-dependent (173) mechanism. To test the first part of the hypothesis, confocal microscopy was used to examine the phagocytic engulfment process of the bead targets at the phagocytic synapse. Engagement of LITR receptors on the surface of cells triggers intracellular signalling resulting in F-actin polymerization and membrane remodelling for the engulfment of bead targets. The phagocytic synapse formed between the cell and target was then fluorescently probed to visualize the recruitment of these crucial signalling mediators

localized to the receptors on the membrane of the phagocytic cell. My results show, consistent with what was previously described (14), co-engagement of IpLITR 2.6b with IpLITR 1.1b resulted in receptor crosstalk and the recruitment of pSHP-2 to the phagocytic synapse that is absent when only IpLITR 2.6b is engaged by targets alone. In agreement with my hypothesis, I also confirmed that DrLITR 1.2 recruits pSHP-2 to the phagocytic synapse, requiring a functional ITIM within the receptor CYT region.

To test the second part of the hypothesis that SHP-2 may enhance the phagocytic response seen for DrLITR 1.2 ^{wt} compared to DrLITR 1.2 $^{ITIM\ ko}$, a competitive pharmacological inhibitor against the enzymatic activity of SHP-2, was used. My results showed that the SHP-2 inhibitor did not significantly affect the phagocytic activity of DrLITR 1.2. It should be noted that while it was determined previously in our lab that the ITIMs within IpLITR 1.1b were crucial for crosstalk inhibition as well as the recruitment of SHP-2 during crosstalk, there was no direct evidence that the enzymatic activity of SHP-2 or SHP-2 itself was responsible for IpLITR-mediated crosstalk inhibition (14). Therefore, it cannot be concluded that SHP-2 phosphatase activity was responsible for the differential phagocytic response seen between DrLITR 1.2 ^{wt} and DrLITR 1.2 $^{ITIM\ ko}$. Thus, future studies should focus on identifying whether SHP-2 is involved in the enhanced phagocytic response observed for DrLITR 1.2 ^{wt}. In addition, other studies have suggested that the phosphatase activity of SHP-2 may not contribute to the response observed.

While SHP-2 is classically associated with inhibitory regulation of receptor-based signalling, the receptor PDGF-R, upon stimulation, can recruit and bind to SHP-2, ultimately resulting in downstream signalling leading to Ras activation (172). As per the proposed phosphatase-dependent model (Fig. 5.6B) for how SHP-2 enhances DrLITR 1.2-mediated

signalling, phosphorylation of SHP-2 by kinases, create a docking site allowing other adaptor molecules, such as Grb2 and Gab2, to be recruited near the receptor as well as other signalling components. This is also shown to be the case during stimulation of T lymphocytes with IL-2 whereby the SHP-2, Grb2, and Gab2 complex facilitates the recruitment and binding of other downstream stimulatory signalling molecules such as PI3K and PLCγ (171). The phosphatase activity of SHP-2 is also credited with activating cell signalling. The proposed phosphatase-dependent model (Fig. 5.6A) for SHP-2-mediated signalling enhancement of DrLITR 1.2 phagocytosis suggests that the dephosphorylation of the Csk binding protein PAG/Cbp by SHP-2 can prevent the localization of Csk to areas of SFK activity, preventing phosphorylation of inhibitory residues on SFKs as seen in RTK signalling (135,173). Based on this information, as well as evidence that DrLITR 1.2 can recruit pSHP-2 to the bead-cell interface during phagocytosis, I predicted that SHP-2, when recruited to the ITIM, bolsters the phagocytic response in either a phosphatase-dependent (described previously) or a phosphatase-independent model. In both cases, stimulation of DrLITR 1.2 is expected to result in the phosphorylation of tyrosine residues within both the ITAM and ITIM. Syk is then recruited to the ITAM, facilitating further activation and stimulation of downstream effectors, leading to the activation of the F-actin polymerization machinery for membrane remodelling and engulfment of engaged targets. In the case of the phosphatase-independent model, SHP-2 would be recruited to the phosphorylated ITIM, whereby it can become phosphorylated itself by local kinases. This then creates a site for the recruitment of adaptor molecules, such as Grb2 and Gab2, for further recruitment of signalling molecules such as PI3K. The recruitment of SHP-2 to the ITIM within DrLITR 1.2 is similar in the phosphatase-dependent model, however, the enzymatic activity of SHP-2, when recruited to the ITIM, may result in dephosphorylation of tyrosines causing

regulatory kinases, such as Csk, to be inactive at sites of receptor engagement. Preventing Csk from eliciting its inhibitory activity on SFKs may then allow for enhanced SFK activity, such as activation of kinases (e.g., Syk) or phosphorylating receptor signalling motifs. In both cases, the increase in activity of kinases localized to the receptor could allow for an enhancement of signalling transduction, increased signalling molecule activation, and consequently, lowering the possible activation threshold of the receptor.

The findings in this thesis represent the first functional characterization of ITAM and ITIM motifs in tandem within the same cytoplasmic tail region of a teleost immunoregulatory receptor. My data shows that DrLITR 1.2 elicits a robust ITAM-dependent phagocytic response within mammalian AD-293 cells, reminiscent of other classical stimulatory receptors. I also show that not only is the ITIM required for the full phagocytic capacity of the receptor, but SHP-2 is recruited to sites of target phagocytosis. Overall, my data presents a new model for how immunoregulatory receptors fine-tune cellular signalling networks and provides new insights into how classically defined inhibitory signalling mechanisms may also play roles in augmenting immune cell effector responses.

6.2 Future Directions

6.2.1 Identification of Effector Molecules Recruited during DrLITR 1.2-mediated Phagocytosis

In my experiments, I have shown that DrLITR 1.2 recruits pSHP-2 to the phagocytic synapse, however, there is still a lack of evidence that pSHP-2 contributes to the phagocytic phenotypes observed. In addition, pharmacological inhibition of SHP-2 displayed no effect on IpLITR 1.1b-mediated crosstalk inhibition of IpLITR 2.6b-induced phagocytosis. As mentioned

in chapter V, the inhibitory receptor IpLITR 1.1b, when co-engaged with the stimulatory receptor IpLITR 2.6, induced crosstalk inhibition of the phagocytic response (14). It was determined that IpLITR 1.1b could not initiate this inhibition in the absence of functional ITIMs within its CYT distal region and that pSHP-2 was subsequently recruited during receptor crosstalk. However, my results showed that the introduction of the competitive enzymatic inhibitor NSC 87877 was unable to restore IpLITR 2.6b-mediated phagocytosis by inhibiting the phosphatase/enzymatic activity of SHP-2. It should also be noted that the phosphatase activity of SHP-2 was not exclusively determined to be the reason that IpLITR-mediated crosstalk occurs. Based on this information, both the phosphatase-independent and phosphatase-dependent models for how SHP-2 bolsters the phagocytic capacity of DrLITR 1.2 cannot be determined as the inhibitory activity of NSC 87877 was not confirmed in these experiments.

To confirm the association of SHP-2 to the ITIM within DrLITR 1.2, co-immunoprecipitation (co-Ip) assays could be performed after DrLITR 1.2-mediated phagocytosis is engaged. Not only could this further determine that SHP-2 associates directly with DrLITR 1.2 during receptor engagement, but other signalling molecules important for the transduction of DrLITR 1.2-mediated phagocytosis could be identified. For example, adaptor molecules such as Grb2 and Gab2 could be probed with molecule-specific antibodies during western blotting to determine if SHP-2 does, in fact, act as a scaffold in support of the phosphatase-independent model of how SHP-2 modulated DrLITR 1.2 phagocytosis. In addition, utilizing other pharmacological inhibitors targeting SHP-2 may also provide better insight into the role of this phosphatase protein in DrLITR 1.2-mediated phagocytosis. Specifically, SHP099 is an allosteric pharmacological inhibitor that not only inhibits the phosphatase enzymatic activity of SHP-2 but also prevents SH2-mediated binding to pY motifs. Previous studies have used this drug to

prevent the binding of SHP-2 to adaptor molecules, revealing that the binding of SHP-2 itself is able to protect tyrosine phosphorylation sites on adaptor signalling molecules such as Gab1 and Gab2 (137). While this wouldn't determine whether the phosphatase activity of SHP-2 is involved, it would allow for further conclusions to be made that SHP-2 is indeed associated with the augmentation of DrLITR 1.2-mediated phagocytosis.

6.2.2 DrLITR 1.2-mediated Crosstalk with DrLITR 15.1

Within the context of immune responses, coordinated signalling induction from the engagement of multiple immunoregulatory receptors to the same ligand allows for fine-tuning of responses. Multiple receptors on the surface of immune cells that are engaged by common ligands can localize together to recruit a variety of signalling molecules (i.e., crosstalk) to influence the overall response generated. Assays that examine the induction of a single immune receptor-type, while providing important information about the control of cellular signalling, do not reflect the full complexity of signalling regulation when multiple receptors are engaged. FcRs that recognize and engage antibody complexes crosstalk with other surface-bound receptors such as TLRs, to induce the production of pro-inflammatory cytokines (178). Within our own studies, the stimulatory receptor IpLITR 2.6b was expressed on the same cell line (AD-293) as the putative inhibitory receptor IpLITR 1.1b (14). During receptor crosstalk by engaging both IpLITR constructs with co-opsonized beads, it was observed that not only was the phagocytic capacity of IpLITR 2.6b reduced by IpLITR 1.1b, but distinct CYT regions of 1.1b coordinated differing aspects of the inhibitory response. Early observations made during the discovery of the DrLITRs constructs described DrLITR 15.1 as putatively inhibitory (15). This receptor contains two ITIMs as well as an ITSM within the receptor CYT and resembles the membrane distal region of IpLITR 1.1b, hence the classification as a putative inhibitory-type

receptor. Within this thesis, only initial testing was conducted on DrLITR 15.1, until as predicted, the receptor was not able to engage the necessary machinery to induce a significant phagocytic response. The inhibitory effects of DrLITR 15.1 are not yet confirmed and would require the co-engagement with a stimulatory receptor that was transfected into the same cell line, similar to what was performed during the IpLITR crosstalk studies (14). Thus, DrLITR 15.1 could be potentially co-transfected into the same cell line as DrLITR 1.2 ^{wt} and DrLITR 1.2 $^{ITIM\ ko}$ to answer the question; what role does the ITIM within DrLITR 1.2 play during receptor mediated crosstalk with DrLITR 15.1? Preliminary co-transfection experiments were performed to generate N-terminal HA-tagged DrLITR 15.1 transiently expressing cells with N-terminal FLAG tagged DrLITR 1.2 ^{wt} or DrLITR 1.2 $^{ITIM\ ko}$ constructs. Co-engagement with αHA mAb and αFLAG mAb co-opsonized beads were then introduced and phagocytosis was examined similarly to what was described previously in this thesis. Preliminary data showed that crosstalk inhibition of the phagocytic response by DrLITR 15.1 was greater when co-engaged with DrLITR 1.2 $^{ITIM\ ko}$ compared to the little to no inhibition examined for co-engagement with DrLITR 1.2 ^{wt} (data not shown). This suggests that the presence of the ITIM within DrLITR 1.2 prevents crosstalk inhibition by DrLITR 15.1 during phagocytosis. This theme that the ITIM within DrLITR 1.2 protects and enhances the signalling capability of the receptor to induce phagocytosis proposed in this thesis is again observed in the context of crosstalk inhibition. Thus pursuing the creation of stably co-expressing DrLITRs on the surface of AD-293 cells would serve to create a basis for understanding this possible model of ITIM-mediated protection of signalling potentials.

6.2.3 DrLITR-mediated Signalling in Immune Cells

One of the major caveats to the experiments that were conducted in this thesis was that immunoregulatory receptors were expressed in a non-immune cell line (AD-293). While the expression of LITRs in AD-293 cells allowed our lab to make important conclusions on immunoregulatory receptor potentials, receptor-based control was limited to the intrinsic properties of the cells that they were expressed in. AD-293 cells are not basely phagocytic, however, phagocytosis itself is an ancient cellular process utilizing cytoskeleton components that all cells contain. Thus, introducing a potent stimulatory receptor that engages these cellular components allows for a non-immune cell to induce phagocytosis when engaged. While this property was beneficial, especially for a cell line that is easily transfectable with proteins of interest, utilizing AD-293 cells limited us to essentially rely on phagocytosis as the sole means for examining the control of signalling responses. It would then be interesting to examine other inflammatory signals that DrLITRs control when transfected into other immune cell lines that are capable of outputting other immune effector responses allowing for additional observations to be made about receptor-based signalling. For example, previous studies in our lab used the myeloid rat basophilic leukemia cell line (RBL-2H3) for characterizing IpLITRs. Including phagocytosis (8,10,11), it was shown that IpLITR 2.6b induced cytokine secretion (12) as well as degranulation in these immune cells (8). The availability of immune cell effector responses is not the only advantage of using an immune cell line. Transfection of the putative inhibitory receptor IpLITR 1.1b within RBL-2H3 cells allowed our lab to examine a novel ITAM-independent mode of phagocytosis that was absent when transfected into AD-293 cells. Differing cellular signalling molecules as well as other signalling components due to the change in transfected cell type, can result in drastically differing receptor-based responses. For example, higher availability of SHP-

1 and increased basal calcium levels were thought to be the reason MZ B cells were inhibited when the BCR was co-engaged with transfected FCRL5 (93). In comparison, B1 B cells colligation of FCRL5 to the BCR resulted in no inhibition of the B cell responses. Following these two lines of evidence, transfection of DrLITR 1.2 constructs into an immune cell line could possibly reveal differing mechanisms for controlling the immune response that could not be observed in AD-293 cells.

Additionally, utilizing a fish cell line for the transfection of DrLITRs would also allow for examination of immunoregulation by these receptors in a context more closely resembling where these receptors exist *in vivo*, thus potentially revealing the true function of these receptors within teleost fish. For example, publicly available protocols detail the extraction, culturing, and transfection of zebrafish primary cells (179). Zebrafish embryos are sterilized, dechorionated, and separated into single cells 2 dpf. Cells can then be cultured in poly-L-lysine-coated cell culture plates, where cells can be cultured for several days, similar to other differentiated primary cell cultures. In addition, these extracted cells are also able to be transfected with plasmid DNA via electroporation, where microcopy showcased that GFP fluorescence was visible 1 day after transfecting cells.

6.3 Concluding Remarks

The use of LITRs as a model system has allowed for our lab to understand new insights into vertebrate immunoregulation. Categorization of immune receptor function has been classically determined by the presence of specific immunoreceptor tyrosine-based motifs within their CYT regions. However, an ever-growing list of evidence for immunoregulatory receptors suggests that this simple categorization of either being stimulatory or inhibitory requires

extensive re-examination. Our lab has showcased that the ITIM-containing receptor IpLITR 1.1b was able to induce an ITAM-independent mode of phagocytosis when transfected into a mammalian myeloid cell line. However, the re-examination of this receptor in a non-immune cell line highlighted this receptor's ability to dampen the signalling capacity induced by a stimulatory receptor as well as the resulting phagocytic response. Recent discoveries in our lab have revealed a new set of LITR-types in zebrafish that contain classical stimulatory and inhibitory motifs within the same receptor tail. The presence of these tandem opposing motifs within DrLITR 1.2 brought to question the specific purpose they might play in immunoregulation and controlling cellular effector responses. My results show for the first time that teleost immunoregulatory receptors with an ITAM and ITIM display potent phagocytic responses that utilize components of the classical ITAM-mediated signalling pathway. Furthermore, I also show that the ITIM can recruit the inhibition-associated signalling molecule SHP-2 to the phagocytic synapse and that the ITIM is required for the full phagocytic capacity of DrLITR 1.2. Overall, the information in this thesis further highlights the complexities of vertebrate immunoregulation while revaluating our classical definitions of inhibitory signalling mechanisms.

REFERENCES

1. Fei C, Pemberton J, Lillico D, Zwozdesky M, Stafford J. Biochemical and Functional Insights into the Integrated Regulation of Innate Immune Cell Responses by Teleost Leukocyte Immune-Type Receptors. Biology. 2016 Mar 8;5(1):13.

2. Billadeau DD, Leibson PJ. ITAMs versus ITIMs: striking a balance during cell regulation. J Clin Invest. 2002 Jan 15;109(2):161–8.

3. Uribe C, Folch H, Enriquez R, Moran G. Innate and adaptive immunity in teleost fish: a review. Veterinární Medicína. 2011 Nov 11;56(No. 10):486–503.

4. Alberts B, Johnson A, Lewis J, Raff M, Roberts K, Walter P. Innate Immunity. Mol Biol Cell 4th Ed [Internet]. 2002 [cited 2022 Nov 5]; Available from: https://www.ncbi.nlm.nih.gov/books/NBK26846/

5. Stafford JL, Bengtén E, Du Pasquier L, McIntosh RD, Quiniou SM, Clem LW, et al. A novel family of diversified immunoregulatory receptors in teleosts is homologous to both mammalian Fc receptors and molecules encoded within the leukocyte receptor complex. Immunogenetics. 2006 Sep;58(9):758–73.

6. Wang J, Belosevic M, Stafford JL. Identification of distinct LRC- and Fc receptor complex-like chromosomal regions in fish supports that teleost leukocyte immune-type receptors are distant relatives of mammalian Fc receptor-like molecules. Immunogenetics. 2021 Feb;73(1):93–109.

7. Mewes J, Verheijen K, Montgomery BCS, Stafford JL. Stimulatory catfish leukocyte immune-type receptors (IpLITRs) demonstrate a unique ability to associate with adaptor signalling proteins and participate in the formation of homo- and heterodimers. Mol Immunol. 2009 Dec;47(2–3):318–31.

8. Cortes HD, Montgomery BC, Verheijen K, García-García E, Stafford JL. Examination of the stimulatory signalling potential of a channel catfish leukocyte immune-type receptor and associated adaptor. Dev Comp Immunol. 2012 Jan;36(1):62–73.

9. Lillico DME, Pemberton JG, Niemand R, Stafford JL. Selective recruitment of Nck and Syk contribute to distinct leukocyte immune-type receptor-initiated target interactions. Cell Signal. 2020 Feb;66:109443.

10. Lillico DME, Pemberton JG, Stafford JL. Selective Regulation of Cytoskeletal Dynamics and Filopodia Formation by Teleost Leukocyte Immune-Type Receptors Differentially Contributes to Target Capture During the Phagocytic Process. Front Immunol. 2018 Jun 28;9:1144.

11. Lillico DME, Zwozdesky MA, Pemberton JG, Deutscher JM, Jones LO, Chang JP, et al. Teleost leukocyte immune-type receptors activate distinct phagocytic modes for target acquisition and engulfment. J Leukoc Biol. 2015 Aug;98(2):235–48.

12. Cortes HD, Lillico DME, Zwozdesky MA, Pemberton JG, O'Brien A, Montgomery BCS, et al. Induction of Phagocytosis and Intracellular Signalling by an Inhibitory Channel Catfish Leukocyte Immune-Type Receptor: Evidence for Immunoregulatory Receptor Functional Plasticity in Teleosts. J Innate Immun. 2014;6(4):435–55.

13. Montgomery BC, Cortes HD, Burshtyn DN, Stafford JL. Channel catfish leukocyte immune-type receptor mediated inhibition of cellular cytotoxicity is facilitated by SHP-1-dependent and -independent mechanisms. Dev Comp Immunol. 2012 May;37(1):151–63.

14. Fei C, Zwozdesky MA, Stafford JL. A Fish Leukocyte Immune-Type Receptor Uses a Novel Intracytoplasmic Tail Networking Mechanism to Cross-Inhibit the Phagocytic Response. Int J Mol Sci. 2020 Jul 21;21(14):5146.

15. Gurupalli H. Identification and Molecular Characterization of Zebrafish (Danio rerio) Leukocyte Immune-Type Receptors (DrLITRs) [MSc, Thesis]. University of Alberta; 2020.

16. Tohyama Y, Yamamura H. Protein tyrosine kinase, syk: a key player in phagocytic cells. J Biochem (Tokyo). 2009 Mar;145(3):267–73.

17. Mócsai A, Ruland J, Tybulewicz VLJ. The SYK tyrosine kinase: a crucial player in diverse biological functions. Nat Rev Immunol. 2010 Jun;10(6):387–402.

18. Ben Mkaddem S, Rossato E, Heming N, Monteiro RC. Anti-inflammatory role of the IgA Fc receptor (CD89): from autoimmunity to therapeutic perspectives. Autoimmun Rev. 2013 Apr;12(6):666–9.

19. Takai T. Fc Receptors and Their Role in Immune Regulation and Autoimmunity. J Clin Immunol. 2005 Jan 1;25(1):1–18.

20. Kurtz J. Memory in the innate and adaptive immune systems. Microbes Infect. 2004 Dec;6(15):1410–7.

21. Palm AKE, Henry C. Remembrance of Things Past: Long-Term B Cell Memory After Infection and Vaccination. Front Immunol [Internet]. 2019 [cited 2022 Nov 5];10. Available from: https://www.frontiersin.org/articles/10.3389/fimmu.2019.01787

22. Nimmerjahn F, Ravetch JV. Analyzing Antibody–Fc-Receptor Interactions. In: Ewbank J, Vivier E, editors. Innate Immunity [Internet]. Totowa, NJ: Humana Press; 2008 [cited 2022 Nov 5]. p. 151–62. (Methods in Molecular Biology™). Available from: https://doi.org/10.1007/978-1-59745-570-1_9

23. Iwasaki A, Medzhitov R. Control of adaptive immunity by the innate immune system. Nat Immunol. 2015 Apr;16(4):343–53.

24. Riera Romo M, Pérez-Martínez D, Castillo Ferrer C. Innate immunity in vertebrates: an overview. Immunology. 2016 Jun;148(2):125–39.

25. Vijay K. Toll-like receptors in immunity and inflammatory diseases: Past, present, and future. Int Immunopharmacol. 2018 Jun;59:391–412.

26. Nie L, Cai SY, Shao JZ, Chen J. Toll-Like Receptors, Associated Biological Roles, and Signalling Networks in Non-Mammals. Front Immunol [Internet]. 2018 [cited 2022 Nov 5];9. Available from: https://www.frontiersin.org/articles/10.3389/fimmu.2018.01523

27. Roh JS, Sohn DH. Damage-Associated Molecular Patterns in Inflammatory Diseases. Immune Netw. 2018 Aug 13;18(4):e27.

28. Gong T, Liu L, Jiang W, Zhou R. DAMP-sensing receptors in sterile inflammation and inflammatory diseases. Nat Rev Immunol. 2020 Feb;20(2):95–112.

29. McClure R, Massari P. TLR-Dependent Human Mucosal Epithelial Cell Responses to Microbial Pathogens. Front Immunol [Internet]. 2014 [cited 2022 Nov 5];5. Available from: https://www.frontiersin.org/articles/10.3389/fimmu.2014.00386

30. Delneste Y, Beauvillain C, Jeannin P. Natural immunity - Structure and function of Toll-like receptors Innate immunity: structure and function of TLRs. médecine/sciences. 2007 Jan 1;23(1):67–74.

31. Ivashkiv LB, Donlin LT. Regulation of type I interferon responses. Nat Rev Immunol. 2014 Jan;14(1):36–49.

32. Sen GC, Sarkar SN. Transcriptional signalling by double-stranded RNA: role of TLR3. Cytokine Growth Factor Rev. 2005 Feb 1;16(1):1–14.

33. Molteni M, Gemma S, Rossetti C. The Role of Toll-Like Receptor 4 in Infectious and Noninfectious Inflammation. Mediators Inflamm. 2016;2016:6978936.

34. Isolation of an endotoxin–MD-2 complex that produces Toll-like receptor 4-dependent cell activation at picomolar concentrations [Internet]. [cited 2022 Nov 4]. Available from: https://www.pnas.org/doi/10.1073/pnas.0306906101

35. Lu YC, Yeh WC, Ohashi PS. LPS/TLR4 signal transduction pathway. Cytokine. 2008 May;42(2):145–51.

36. Matsui T, Amagai M. Dissecting the formation, structure and barrier function of the stratum corneum. Int Immunol. 2015 Jun 1;27(6):269–80.

37. Lillywhite HB. Water relations of tetrapod integument. J Exp Biol. 2006 Jan 15;209(2):202–26.

38. Kueneman JG, Parfrey LW, Woodhams DC, Archer HM, Knight R, McKenzie VJ. The amphibian skin-associated microbiome across species, space and life history stages. Mol Ecol. 2014;23(6):1238–50.

39. Muniz LR, Knosp C, Yeretssian G. Intestinal antimicrobial peptides during homeostasis, infection, and disease. Front Immunol. 2012 Oct 9;3:310.

40. Rakers S, Niklasson L, Steinhagen D, Kruse C, Schauber J, Sundell K, et al. Antimicrobial Peptides (AMPs) from Fish Epidermis: Perspectives for Investigative Dermatology. J Invest Dermatol. 2013 May 1;133(5):1140–9.

41. Huopalahti R, European Cooperation in the Field of Scientific and Technical Research (Organization), European Science Foundation, editors. Bioactive egg compounds. Berlin ; New York: Springer; 2007. 298 p.

42. Akinbi HT, Epaud R, Bhatt H, Weaver TE. Bacterial Killing Is Enhanced by Expression of Lysozyme in the Lungs of Transgenic Mice. J Immunol. 2000 Nov 15;165(10):5760–6.

43. Shishido SN, Varahan S, Yuan K, Li X, Fleming SD. Humoral innate immune response and disease. Clin Immunol Orlando Fla. 2012 Aug;144(2):142–58.

44. Killick J, Morisse G, Sieger D, Astier AL. Complement as a regulator of adaptive immunity. Semin Immunopathol. 2018 Jan;40(1):37–48.

45. Dunkelberger JR, Song WC. Complement and its role in innate and adaptive immune responses. Cell Res. 2010 Jan;20(1):34–50.

46. Uszewski MK, Farries TC, Lublin DM, Rooney IA, Atkinson JP. Control of the Complement System. Dixon FJ, editor. Adv Immunol. 1996 Jan 1;61:201–83.

47. Li D, Wu M. Pattern recognition receptors in health and diseases. Signal Transduct Target Ther. 2021 Aug 4;6(1):1–24.

48. Montgomery BC, Cortes HD, Mewes-Ares J, Verheijen K, Stafford JL. Teleost IgSF immunoregulatory receptors. Dev Comp Immunol. 2011 Dec;35(12):1223–37.

49. Charles A Janeway J, Travers P, Walport M, Shlomchik MJ. Receptors of the innate immune system. Immunobiol Immune Syst Health Dis 5th Ed [Internet]. 2001 [cited 2022 Dec 21]; Available from: https://www.ncbi.nlm.nih.gov/books/NBK27129/

50. Pan YG, Yu YL, Lin CC, Lanier LL, Chu CL. FcεRI γ-Chain Negatively Modulates Dectin-1 Responses in Dendritic Cells. Front Immunol [Internet]. 2017 [cited 2022 Nov 18];8. Available from: https://www.frontiersin.org/articles/10.3389/fimmu.2017.01424

51. Hamerman JA, Ni M, Killebrew JR, Chu CL, Lowell CA. The expanding roles of ITAM adapters FcRγ and DAP12 in myeloid cells. Immunol Rev. 2009 Nov;232(1):42–58.

52. Ben Mkaddem S, Benhamou M, Monteiro RC. Understanding Fc Receptor Involvement in Inflammatory Diseases: From Mechanisms to New Therapeutic Tools. Front Immunol [Internet]. 2019 [cited 2022 Nov 7];10. Available from: https://www.frontiersin.org/articles/10.3389/fimmu.2019.00811

53. Yang J, Nie J, Ma X, Wei Y, Peng Y, Wei X. Targeting PI3K in cancer: mechanisms and advances in clinical trials. Mol Cancer. 2019 Feb 19;18(1):26.

54. Velle KB, Fritz-Laylin LK. Arp2/3 complex-mediated actin assembly drives microtubule-independent motility and phagocytosis in the evolutionarily divergent amoeba Naegleria. bioRxiv. 2020 May 15;2020.05.12.091538.

55. Mavilio D, Hosmalin A, Scott-Algara D. Chapter Thirty-Six - Natural killer cells and human immunodeficiency virus. In: Lotze MT, Thomson AW, editors. Natural Killer Cells [Internet]. San Diego: Academic Press; 2010 [cited 2022 Nov 7]. p. 481–97. Available from: https://www.sciencedirect.com/science/article/pii/B9780123704542000363

56. Charles A Janeway J, Travers P, Walport M, Shlomchik MJ. The production of IgE. Immunobiol Immune Syst Health Dis 5th Ed [Internet]. 2001 [cited 2022 Nov 7]; Available from: https://www.ncbi.nlm.nih.gov/books/NBK27117/

57. Snoeck V, Peters IR, Cox E. The IgA system: a comparison of structure and function in different species. Vet Res. 2006 May;37(3):455–67.

58. Bakema JE, van Egmond M. The human immunoglobulin A Fc receptor FcαRI: a multifaceted regulator of mucosal immunity. Mucosal Immunol. 2011 Nov;4(6):612–24.

59. Bruhns P. Properties of mouse and human IgG receptors and their contribution to disease models. Blood. 2012 Jun 14;119(24):5640–9.

60. Ra C, Jouvin MHE, Blank U, Kinet JP. A macrophage Fey receptor and the mast cell receptor for lgE share an identical subunit. 1989;341:3.

61. Tourdot BE, Brenner MK, Keough KC, Holyst T, Newman PJ, Newman DK. Immunoreceptor Tyrosine-based Inhibitory Motif (ITIM)-mediated Inhibitory Signalling is Regulated by Sequential Phosphorylation Mediated by Distinct Nonreceptor Tyrosine Kinases: A Case Study Involving PECAM-1. Biochemistry. 2013 Apr 16;52(15):2597–608.

62. Motoda K, Takata M, Kiura K, Nakamura I, Harada M. SHP-1/immunoreceptor tyrosine-based inhibition motif-independent inhibitory signalling through murine natural killer cell receptor Ly-49A in a transfected B-cell line. Immunology. 2000 Jul;100(3):370–7.

63. Campbell KS, Purdy AK. Structure/function of human killer cell immunoglobulin-like receptors: lessons from polymorphisms, evolution, crystal structures and mutations. Immunology. 2011 Mar;132(3):315–25.

64. Alberts B, Johnson A, Lewis J, Raff M, Roberts K, Walter P. T Cells and MHC Proteins. Mol Biol Cell 4th Ed [Internet]. 2002 [cited 2022 Nov 7]; Available from: https://www.ncbi.nlm.nih.gov/books/NBK26926/

65. Muta T, Kurosaklt T, Misulovint Z, Sanched M, Nussenzweigt MC, Ravetch JV. A 13-amino-acid motif in the cytoplasmic domain of FcyRIIB modulates B-cell receptor signalling. 1994;368:4.

66. Smith KGC, Clatworthy MR. FcγRIIB in autoimmunity and infection: evolutionary and therapeutic implications. Nat Rev Immunol. 2010 May;10(5):328–43.

67. Pearse RN, Kawabe T, Bolland S, Guinamard R, Kurosaki T, Ravetch JV. SHIP Recruitment Attenuates FcγRIIB-Induced B Cell Apoptosis. Immunity. 1999 Jun 1;10(6):753–60.

68. Sidorenko SP, Clark EA. The dual-function CD150 receptor subfamily: the viral attraction. Nat Immunol. 2003 Jan;4(1):19–24.

69. Chemnitz JM, Parry RV, Nichols KE, June CH, Riley JL. SHP-1 and SHP-2 associate with immunoreceptor tyrosine-based switch motif of programmed death 1 upon primary human T cell stimulation, but only receptor ligation prevents T cell activation. J Immunol Baltim Md 1950. 2004 Jul 15;173(2):945–54.

70. Lm S, Sv M, Ag B, Om Z, Tj Y, Ke N, et al. CD150 association with either the SH2-containing inositol phosphatase or the SH2-containing protein tyrosine phosphatase is regulated by the adaptor protein SH2D1A. J Immunol Baltim Md 1950 [Internet]. 2001 May 1 [cited 2022 Nov 11];166(9). Available from: https://pubmed.ncbi.nlm.nih.gov/11313386/

71. Winterbourn CC, Kettle AJ, Hampton MB. Reactive Oxygen Species and Neutrophil Function. Annu Rev Biochem. 2016 Jun 2;85:765–92.

72. Borregaard N, Cowland JB. Granules of the Human Neutrophilic Polymorphonuclear Leukocyte. Blood. 1997 May 15;89(10):3503–21.

73. Abu-Ghazaleh RI, Dunnette SL, Loegering DA, Checked JL, Kita H, Thomas LL, et al. Eosinophil granule proteins in peripheral blood granulocytes. J Leukoc Biol. 1992;52(6):611–8.

74. Prager I, Watzl C. Mechanisms of natural killer cell-mediated cellular cytotoxicity. J Leukoc Biol. 2019;105(6):1319–29.

75. Simone CB, Henkart P. Permeability changes induced in erthrocyte ghost targets by antibody-dependent cytotoxic effector cells: evidence for membrane pores. J Immunol. 1980 Feb 1;124(2):954–63.

76. Beresford PJ, Xia Z, Greenberg AH, Lieberman J. Granzyme A Loading Induces Rapid Cytolysis and a Novel Form of DNA Damage Independently of Caspase Activation. Immunity. 1999 May 1;10(5):585–95.

77. Martinvalet D, Dykxhoorn DM, Ferrini R, Lieberman J. Granzyme A Cleaves a Mitochondrial Complex I Protein to Initiate Caspase-Independent Cell Death. Cell. 2008 May 16;133(4):681–92.

78. Fischer U, Jänicke RU, Schulze-Osthoff K. Many cuts to ruin: a comprehensive update of caspase substrates. Cell Death Differ. 2003 Jan;10(1):76–100.

79. Bossi G, Griffiths GM. Degranulation plays an essential part in regulating cell surface expression of Fas ligand in T cells and natural killer cells. Nat Med. 1999 Jan;5(1):90–6.

80. Peter ME, Krammer PH. The CD95(APO-1/Fas) DISC and beyond. Cell Death Differ. 2003 Jan;10(1):26–35.

81. Vorobjeva NV, Chernyak BV. NETosis: Molecular Mechanisms, Role in Physiology and Pathology. Biochem Biokhimiia. 2020;85(10):1178–90.

82. Pilsczek FH, Salina D, Poon KKH, Fahey C, Yipp BG, Sibley CD, et al. A Novel Mechanism of Rapid Nuclear Neutrophil Extracellular Trap Formation in Response to Staphylococcus aureus. J Immunol. 2010 Dec 15;185(12):7413–25.

83. Munafo DB, Johnson JL, Brzezinska AA, Ellis BA, Wood MR, Catz SD. DNase I Inhibits a Late Phase of Reactive Oxygen Species Production in Neutrophils. J Innate Immun. 2009;1(6):527–42.

84. von Köckritz-Blickwede M, Goldmann O, Thulin P, Heinemann K, Norrby-Teglund A, Rohde M, et al. Phagocytosis-independent antimicrobial activity of mast cells by means of extracellular trap formation. Blood. 2008 Mar 15;111(6):3070–80.

85. Yang H, Biermann MH, Brauner JM, Liu Y, Zhao Y, Herrmann M. New Insights into Neutrophil Extracellular Traps: Mechanisms of Formation and Role in Inflammation. Front Immunol [Internet]. 2016 [cited 2022 Nov 11];7. Available from: https://www.frontiersin.org/articles/10.3389/fimmu.2016.00302

86. Zhang JM, An J. Cytokines, Inflammation and Pain. Int Anesthesiol Clin. 2007;45(2):27–37.

87. Grayfer L, Belosevic M, Grayfer L, Belosevic M. Cytokine Regulation of Teleost Inflammatory Responses [Internet]. New Advances and Contributions to Fish Biology. IntechOpen; 2012 [cited 2022 Nov 9]. Available from: https://www.intechopen.com/state.item.id

88. Moore KW, O'Garra A, Malefyt RW, Vieira P, Mosmann TR. Interleukin-10. Annu Rev Immunol. 1993;11(1):165–90.

89. Uribe-Querol E, Rosales C. Phagocytosis: Our Current Understanding of a Universal Biological Process. Front Immunol. 2020;11:1066.

90. Rosales C, Uribe-Querol E. Phagocytosis: A Fundamental Process in Immunity. BioMed Res Int. 2017;2017:9042851.

91. Rosales C. Fcγ Receptor Heterogeneity in Leukocyte Functional Responses. Front Immunol [Internet]. 2017 [cited 2022 Nov 8];8. Available from: https://www.frontiersin.org/articles/10.3389/fimmu.2017.00280

92. Blank U, Launay P, Benhamou M, Monteiro RC. Inhibitory ITAMs as novel regulators of immunity. Immunol Rev. 2009 Nov;232(1):59–71.

93. Zhu Z, Li R, Li H, Zhou T, Davis RS. FCRL5 exerts binary and compartment-specific influence on innate-like B-cell receptor signalling. Proc Natl Acad Sci. 2013 Apr 2;110(14):E1282–90.

94. Faure M, Long EO. KIR2DL4 (CD158d), an NK Cell-Activating Receptor with Inhibitory Potential. J Immunol. 2002 Jun 15;168(12):6208–14.

95. Esteban M, Cuesta A, Chaves-Pozo E, Meseguer J. Phagocytosis in Teleosts. Implications of the New Cells Involved. Biology. 2015 Dec 4;4(4):907–22.

96. Sfacteria A, Brines M, Blank U. The mast cell plays a central role in the immune system of teleost fish. Mol Immunol. 2015 Jan 1;63(1):3–8.

97. Havixbeck JJ, Barreda DR. Neutrophil Development, Migration, and Function in Teleost Fish. Biology. 2015 Dec;4(4):715–34.

98. Kurata O, Okamoto N, Ikeda Y. Neutrophilic granulocytes in carp, Cyprinus carpio, possess a spontaneous cytotoxic activity. Dev Comp Immunol. 1995 Jul 1;19(4):315–25.

99. Yoshida SH, Stuge TB, Miller NW, Clem LW. Phylogeny of lymphocyte heterogeneity: Cytotoxic activity of channel catfish peripheral blood leukocytes directed against allogeneic targets. Dev Comp Immunol. 1995 Jan 1;19(1):71–7.

100. Horstkorte R, Fuss B. Chapter 9 - Cell Adhesion Molecules. In: Brady ST, Siegel GJ, Albers RW, Price DL, editors. Basic Neurochemistry (Eighth Edition) [Internet]. New York: Academic Press; 2012 [cited 2022 Nov 15]. p. 165–79. Available from: https://www.sciencedirect.com/science/article/pii/B9780123749475000092

101. Abbott JD, Ball G, Boumpas D, Bridges SL, Chatham W, Curtis J, et al., editors. Immunoglobulin superfamily receptors. In: Rheumatology and Immunology Therapy [Internet]. Berlin, Heidelberg: Springer; 2004 [cited 2022 Nov 12]. p. 453–453. Available from: https://doi.org/10.1007/3-540-29662-X_1424

102. Carrington M, Norman P, Carrington M, Norman P. The KIR Gene Cluster. National Center for Biotechnology Information (US); 2003.

103. Davis RS, Wang YH, Kubagawa H, Cooper MD. Identification of a family of Fc receptor homologs with preferential B cell expression. Proc Natl Acad Sci U S A. 2001 Aug 14;98(17):9772–7.

104. Martin A, Kulski J, Witt C, Pontarotti P, Christiansen F. Leukocyte Ig-like receptor complex (LRC) in mice and men. Trends Immunol. 2002 Mar 1;23:81–8.

105. Nikolaidis N, Klein J, Nei M. Origin and evolution of the Ig-like domains present in mammalian leukocyte receptors: insights from chicken, frog, and fish homologues. Immunogenetics. 2005 Apr;57(1–2):151–7.

106. Verbeek JS, Hirose S, Nishimura H. The Complex Association of FcγRIIb With Autoimmune Susceptibility. Front Immunol [Internet]. 2019 [cited 2022 Nov 15];10. Available from: https://www.frontiersin.org/articles/10.3389/fimmu.2019.02061

107. Guselnikov SV, Ramanayake T, Erilova AY, Mechetina LV, Najakshin AM, Robert J, et al. The Xenopus FcR family demonstrates continually high diversification of paired receptors in vertebrate evolution. BMC Evol Biol. 2008 May 16;8(1):148.

108. Viertlboeck BC, Schmitt R, Hanczaruk MA, Crooijmans RPMA, Groenen MAM, Göbel TW. A novel activating chicken IgY FcR is related to leukocyte receptor complex (LRC) genes but is located on a chromosomal region distinct from the LRC and FcR gene clusters. J Immunol Baltim Md 1950. 2009 Feb 1;182(3):1533–40.

109. Yoder JA, Turner PM, Wright PD, Wittamer V, Bertrand JY, Traver D, et al. Developmental and tissue-specific expression of NITRs. Immunogenetics. 2010 Feb;62(2):117–22.

110. Mostov KE, Friedlander M, Blobel G. The receptor for transepithelial transport of IgA and IgM contains multiple immunoglobulin-like domains. Nature. 1984 Mar;308(5954):37–43.

111. Di Conza JJ, Halliday WJ. Relationship of catfish serum antibodies to immunoglobulin in mucus secretions. Aust J Exp Biol Med Sci. 1971 Oct;49(5):517–9.

112. Hamuro K, Suetake H, Saha NR, Kikuchi K, Suzuki Y. A Teleost Polymeric Ig Receptor Exhibiting Two Ig-Like Domains Transports Tetrameric IgM into the Skin. J Immunol. 2007 May 1;178(9):5682–9.

113. Rombout JHWM, van der Tuin SJL, Yang G, Schopman N, Mroczek A, Hermsen T, et al. Expression of the polymeric Immunoglobulin Receptor (pIgR) in mucosal tissues of common carp (Cyprinus carpio L.). Fish Shellfish Immunol. 2008 May 1;24(5):620–8.

114. Feng LN, Lu DQ, Bei JX, Chen JL, Liu Y, Zhang Y, et al. Molecular cloning and functional analysis of polymeric immunoglobulin receptor gene in orange-spotted grouper (Epinephelus coioides). Comp Biochem Physiol B Biochem Mol Biol. 2009 Nov 1;154(3):282–9.

115. Zhang YA, Salinas I, Li J, Parra D, Bjork S, Xu Z, et al. IgT, a primitive immunoglobulin class specialized in mucosal immunity. Nat Immunol. 2010 Sep;11(9):827–35.

116. Kühn LC, Kraehenbuhl JP. The membrane receptor for polymeric immunoglobulin is structurally related to secretory component. Isolation and characterization of membrane secretory component from rabbit liver and mammary gland. J Biol Chem. 1981 Dec 10;256(23):12490–5.

117. Kulseth MA, Krajci P, Myklebost O, Rogne S. Cloning and Characterization of Two Forms of Bovine Polymeric Immunoglobulin Receptor cDNA. DNA Cell Biol. 1995 Mar;14(3):251–6.

118. Kaetzel CS. The polymeric immunoglobulin receptor: bridging innate and adaptive immune responses at mucosal surfaces. Immunol Rev. 2005;206(1):83–99.

119. Braathen R, Hohman VS, Brandtzaeg P, Johansen FE. Secretory Antibody Formation: Conserved Binding Interactions between J Chain and Polymeric Ig Receptor from Humans and Amphibians. J Immunol. 2007 Feb 1;178(3):1589–97.

120. Coyne RS, Siebrecht M, Peitsch MC, Casanova JE. Mutational analysis of polymeric immunoglobulin receptor/ligand interactions. Evidence for the involvement of multiple complementarity determining region (CDR)-like loops in receptor domain I. J Biol Chem. 1994 Dec 16;269(50):31620–5.

121. Stafford JL, Wilson M, Nayak D, Quiniou SM, Clem LW, Miller NW, et al. Identification and Characterization of a FcR Homolog in an Ectothermic Vertebrate, the Channel Catfish (*Ictalurus punctatus*). J Immunol. 2006 Aug 15;177(4):2505–17.

122. Evenhuis J, Bengtén E, Snell C, Quiniou SM, Miller NW, Wilson M. Characterization of additional novel immune type receptors in channel catfish, Ictalurus punctatus. Immunogenetics. 2007 Aug 1;59(8):661–71.

123. Yoder JA. Form, function and phylogenetics of NITRs in bony fish. Dev Comp Immunol. 2009 Feb 1;33(2):135–44.

124. Jp C, Rn H, At M, Dd E, Kn W, Ja HP, et al. A bony fish immunological receptor of the NITR multigene family mediates allogeneic recognition. Immunity [Internet]. 2008 Aug 15 [cited 2022 Nov 10];29(2). Available from: https://pubmed.ncbi.nlm.nih.gov/18674935/

125. Wei S, Zhou JM, Chen X, Shah RN, Liu J, Orcutt TM, et al. The zebrafish activating immune receptor Nitr9 signals via Dap12. Immunogenetics. 2007 Oct;59(10):813–21.

126. Volff JN. Genome evolution and biodiversity in teleost fish. Heredity. 2005 Mar;94(3):280–94.

127. Stafford JL, Bengtén E, Du Pasquier L, Miller NW, Wilson M. Channel catfish leukocyte immune-type receptors contain a putative MHC class I binding site. Immunogenetics. 2007 Jan;59(1):77–91.

128. Mewes J, Verheijen K, Montgomery BCS, Stafford JL. Stimulatory catfish leukocyte immune-type receptors (IpLITRs) demonstrate a unique ability to associate with adaptor signalling proteins and participate in the formation of homo- and heterodimers. Mol Immunol. 2009 Dec;47(2–3):318–31.

129. Feng J, Call ME, Wucherpfennig KW. The Assembly of Diverse Immune Receptors Is Focused on a Polar Membrane-Embedded Interaction Site. PLOS Biol. 2006 Apr 25;4(5):e142.

130. Kinet JP. The γ-ξ dimers of Fc receptors as connectors to signal transduction. Curr Opin Immunol. 1992 Feb 1;4(1):43–8.

131. Lillico DME, Zwozdesky MA, Pemberton JG, Deutscher JM, Jones LO, Chang JP, et al. Teleost leukocyte immune-type receptors activate distinct phagocytic modes for target acquisition and engulfment. J Leukoc Biol. 2015 Aug;98(2):235–48.

132. Park H, Cox D. Cdc42 regulates Fc gamma receptor-mediated phagocytosis through the activation and phosphorylation of Wiskott-Aldrich syndrome protein (WASP) and neural-WASP. Mol Biol Cell. 2009 Nov;20(21):4500–8.

133. Zhang Y, Hoppe AD, Swanson JA. Coordination of Fc receptor signalling regulates cellular commitment to phagocytosis. Proc Natl Acad Sci U S A. 2010 Nov 9;107(45):19332–7.

134. Montgomery BCS, Mewes J, Davidson C, Burshtyn DN, Stafford JL. Cell surface expression of channel catfish leukocyte immune-type receptors (IpLITRs) and recruitment of both Src homology 2 domain-containing protein tyrosine phosphatase (SHP)-1 and SHP-2. Dev Comp Immunol. 2009 Apr;33(4):570–82.

135. Okada M. Regulation of the Src Family Kinases by Csk. Int J Biol Sci. 2012 Nov 1;8(10):1385–97.

136. Li C, Iosef C, Jia CYH, Han VKM, Li SSC. Dual functional roles for the X-linked lymphoproliferative syndrome gene product SAP/SH2D1A in signalling through the signalling lymphocyte activation molecule (SLAM) family of immune receptors. J Biol Chem. 2003 Feb 7;278(6):3852–9.

137. Vemulapalli V, Chylek LA, Erickson A, Pfeiffer A, Gabriel KH, LaRochelle J, et al. Time-resolved phosphoproteomics reveals scaffolding and catalysis-responsive patterns of SHP2-dependent signalling. Cooper JA, Mayer BJ, editors. eLife. 2021 Mar 23;10:e64251.

138. Li W, Nishimura R, Kashishian A, Batzer AG, Kim WJ, Cooper JA, et al. A new function for a phosphotyrosine phosphatase: linking GRB2-Sos to a receptor tyrosine kinase. Mol Cell Biol. 1994 Jan;14(1):509–17.

139. Wang J, Wu Y, Hu H, Wang W, Lu Y, Mao H, et al. Syk protein tyrosine kinase involves PECAM-1 signalling through tandem immunotyrosine inhibitory motifs in human THP-1 macrophages. Cell Immunol. 2011;272(1):39–44.

140. Pils S, Kopp K, Peterson L, Delgado Tascón J, Nyffenegger-Jann NJ, Hauck CR. The Adaptor Molecule Nck Localizes the WAVE Complex to Promote Actin Polymerization during CEACAM3-Mediated Phagocytosis of Bacteria. PLoS ONE. 2012 Mar 20;7(3):e32808.

141. Zwozdesky MA, Fei C, Lillico DME, Stafford JL. Imaging flow cytometry and GST pulldown assays provide new insights into channel catfish leukocyte immune-type receptor-mediated phagocytic pathways. Dev Comp Immunol. 2017 Feb;67:126–38.

142. Kalueff AV, Gebhardt M, Stewart AM, Cachat JM, Brimmer M, Chawla JS, et al. Towards a Comprehensive Catalog of Zebrafish Behavior 1.0 and Beyond. Zebrafish. 2013 Mar;10(1):70–86.

143. de Vrieze E, de Bruijn SE, Reurink J, Broekman S, van de Riet V, Aben M, et al. Efficient Generation of Knock-In Zebrafish Models for Inherited Disorders Using CRISPR-Cas9 Ribonucleoprotein Complexes. Int J Mol Sci. 2021 Aug 30;22(17):9429.

144. Veldman MB, Lin S. Zebrafish as a Developmental Model Organism for Pediatric Research. Pediatr Res. 2008 Nov;64(5):470–6.

145. Novoa B, Figueras A. Zebrafish: model for the study of inflammation and the innate immune response to infectious diseases. Adv Exp Med Biol. 2012;946:253–75.

146. Mathias JR, Perrin BJ, Liu TX, Kanki J, Look AT, Huttenlocher A. Resolution of inflammation by retrograde chemotaxis of neutrophils in transgenic zebrafish. J Leukoc Biol. 2006;80(6):1281–8.

147. Herbomel P, Thisse B, Thisse C. Ontogeny and behaviour of early macrophages in the zebrafish embryo. Development. 1999 Sep 1;126(17):3735–45.

148. Sieger D, Stein C, Neifer D, van der Sar AM, Leptin M. The role of gamma interferon in innate immunity in the zebrafish embryo. Dis Model Mech. 2009 Dec;2(11–12):571–81.

149. Jault C, Pichon L, Chluba J. Toll-like receptor gene family and TIR-domain adapters in Danio rerio. Mol Immunol. 2004 Jan 1;40(11):759–71.

150. Li Y, Li Y, Cao X, Jin X, Jin T. Pattern recognition receptors in zebrafish provide functional and evolutionary insight into innate immune signalling pathways. Cell Mol Immunol. 2017 Jan;14(1):80–9.

151. Purcell MK, Smith KD, Aderem A, Hood L, Winton JR, Roach JC. Conservation of Toll-like receptor signalling pathways in teleost fish. Comp Biochem Physiol Part D Genomics Proteomics. 2006 Mar 1;1(1):77–88.

152. Fan S, Chen S, Liu Y, Lin Y, Liu H, Guo L, et al. Zebrafish TRIF, a Golgi-Localized Protein, Participates in IFN Induction and NF-κB Activation1. J Immunol. 2008 Apr 15;180(8):5373–83.

153. Hu W, van Steijn L, Li C, Verbeek FJ, Cao L, Merks RMH, et al. A Novel Function of TLR2 and MyD88 in the Regulation of Leukocyte Cell Migration Behavior During Wounding in Zebrafish Larvae. Front Cell Dev Biol . 2021 [cited 2022 Nov 28];9. Available from: https://www.frontiersin.org/articles/10.3389/fcell.2021.624571

154. Yoder JA, Mueller MG, Wei S, Corliss BC, Prather DM, Willis T, et al. Immune-type receptor genes in zebrafish share genetic and functional properties with genes encoded by the mammalian leukocyte receptor cluster. Proc Natl Acad Sci. 2001 Jun 5;98(12):6771–6.

155. Rodríguez-Nunez I, Wcisel DJ, Litman GW, Yoder JA. Multigene families of immunoglobulin domain-containing innate immune receptors in zebrafish: Deciphering the differences. Dev Comp Immunol. 2014 Sep 1;46(1):24–34.

156. Oyarbide U, Rainieri S, Pardo M a. Zebrafish (Danio rerio) Larvae as a System to Test the Efficacy of Polysaccharides as Immunostimulants. Zebrafish. 2012 Jun;9(2):74–84.

157. Berman JN, Kanki JP, Look AT. Zebrafish as a model for myelopoiesis during embryogenesis. Exp Hematol. 2005 Sep 1;33(9):997–1006.

158. Wylie C. Germ Cells. Cell. 1999 Jan 22;96(2):165–74.

159. Seppola M, Johnsen H, Mennen S, Myrnes B, Tveiten H. Maternal transfer and transcriptional onset of immune genes during ontogenesis in Atlantic cod. Dev Comp Immunol. 2009 Nov 1;33(11):1205–11.

160. Galley H, Webster N. The immuno-inflammatory cascade. Br J Anaesth. 1996 Aug 1;77:11–6.

161. Gonçalves AF, Neves JV, Coimbra J, Rodrigues P, Vijayan MM, Wilson JM. Cortisol plays a role in the high environmental ammonia associated suppression of the immune response in zebrafish. Gen Comp Endocrinol. 2017 Aug 1;249:32–9.

162. Gonzalez SF, Buchmann K, Nielsen ME. Complement expression in common carp (Cyprinus carpio L.) during infection with Ichthyophthirius multifiliis. Dev Comp Immunol. 2007 Jan 1;31(6):576–86.

163. Doran AC, Yurdagul A, Tabas I. Efferocytosis in health and disease. Nat Rev Immunol. 2020 Apr;20(4):254–67.

164. Gurupalli H. Identification and Molecular Characterization of Zebrafish (Danio rerio) Leukocyte Immune-Type Receptors (DrLITRs) [Thesis, MSc]. University of Alberta; 2020.

165. Fei C, Lillico DME, Hall B, Rieger AM, Stafford JL. Connected component masking accurately identifies the ratio of phagocytosed and cell-bound particles in individual cells by imaging flow cytometry: Component Masking to Study Phagocytosis. Cytometry A. 2017 Apr;91(4):372–81.

166. Goding JW. Use of staphylococcal protein A as an immunological reagent. J Immunol Methods. 1978 Apr 1;20:241–53.

167. Akerström B, Brodin T, Reis K, Björck L. Protein G: a powerful tool for binding and detection of monoclonal and polyclonal antibodies. J Immunol. 1985 Oct 1;135(4):2589–92.

168. Zhang H, Williams PS, Zborowski M, Chalmers JJ. Binding affinities/avidities of antibody–antigen interactions: Quantification and scale-up implications. Biotechnol Bioeng. 2006;95(5):812–29.

169. Los DA, Murata N. Membrane fluidity and its roles in the perception of environmental signals. Biochim Biophys Acta BBA - Biomembr. 2004 Nov 3;1666(1):142–57.

170. Chan KR, Zhang SLX, Tan HC, Chan YK, Chow A, Lim APC, et al. Ligation of Fc gamma receptor IIB inhibits antibody-dependent enhancement of dengue virus infection. Proc Natl Acad Sci. 2011 Jul 26;108(30):12479–84.

171. Arnaud M, Mzali R, Gesbert F, Crouin C, Guenzi C, Vermot-Desroches C, et al. Interaction of the tyrosine phosphatase SHP-2 with Gab2 regulates Rho-dependent activation of the c-fos serum response element by interleukin-2. Biochem J. 2004 Sep 1;382(Pt 2):545–56.

172. Bennett AM, Tang TL, Sugimoto S, Walsh CT, Neel BG. Protein-tyrosine-phosphatase SHPTP2 couples platelet-derived growth factor receptor beta to Ras. Proc Natl Acad Sci. 1994 Jul 19;91(15):7335–9.

173. Zhang SQ, Yang W, Kontaridis MI, Bivona TG, Wen G, Araki T, et al. Shp2 regulates SRC family kinase activity and Ras/Erk activation by controlling Csk recruitment. Mol Cell. 2004 Feb 13;13(3):341–55.

174. Jenkins MR, Tsun A, Stinchcombe JC, Griffiths GM. The strength of T cell receptor signal controls the polarization of cytotoxic machinery to the immunological synapse. Immunity. 2009 Oct 16;31(4):621–31.

175. Oostindie SC, Lazar GA, Schuurman J, Parren PWHI. Avidity in antibody effector functions and biotherapeutic drug design. Nat Rev Drug Discov. 2022;21(10):715–35.

176. Lillico DME, Pemberton JG, Stafford JL. Trypsin differentially modulates the surface expression and function of channel catfish leukocyte immune-type receptors. Dev Comp Immunol. 2016 Dec;65:231–44.

177. Lillico DME, Zwozdesky MA, Pemberton JG, Deutscher JM, Jones LO, Chang JP, et al. Teleost leukocyte immune-type receptors activate distinct phagocytic modes for target acquisition and engulfment. J Leukoc Biol. 2015 Aug;98(2):235–48.

178. Hoepel W, Newling M, Vogelpoel LTC, Sritharan L, Hansen IS, Kapsenberg ML, et al. FcγR-TLR Cross-Talk Enhances TNF Production by Human Monocyte-Derived DCs via IRF5-Dependent Gene Transcription and Glycolytic Reprogramming. Front Immunol. 2019 Apr 8;10:739.

179. Russo G, Lehne F, Pose Méndez SM, Dübel S, Köster RW, Sassen WA. Culture and Transfection of Zebrafish Primary Cells. J Vis Exp JoVE. 2018 Aug 17;(138):57872.